AN ABSTRACT OF THE DISSERTATION OF

Hilda J. Tromp-van Meerveld for the degree of Doctor of Philosophy in Forest Engineering presented on March 19, 2004.
Title: Hillslope Hydrology: From Patterns to Processes

Abstract approved:

Jeffrey J. McDonnell

This dissertation re-examines the now standard perceptual model of hillslope hydrological response to rainfall, which includes the growth of a saturated wedge at the soil-bedrock interface or impeding layer. It also challenges the notion of bedrock impermeability and the assumption that the pattern of subsurface stormflow is determined by the soil moisture pattern. The results presented in this dissertation challenge the status quo model and show that at the Panola Mountain research hillslope, subsurface storm flow is a threshold-function of precipitation. This threshold is a result of a disconnection between transient saturated areas and the slope base during small to medium size storms (< 55 mm). Water must fill bedrock depressions before it can flow further downslope. Once filled, connectivity between subsurface saturated areas and the slope base is established and subsurface flow initiates. Transient saturation does not have the form of a saturated wedge but starts first in the shallow soil areas. The pattern of transient saturation does not resemble the pre-event soil moisture pattern but is a function of soil depth and bedrock micro-topography. Flow through bedrock is a major component of the hillslope water balance. Soil moisture distribution across the slope shows two distinct states: wet and dry. Soil moisture in the shallow soil areas of the hillslope limits transpiration during the late growing season but transpiration is not soil moisture limited on deeper soil sections. Overall, these findings represent a new perceptual model of hillslope hydrological response during and between rainfall events.

Hillslope Hydrology: From Patterns to Processes

by
Hilda J. Tromp-van Meerveld

A DISSERTATION

submitted to

Oregon State University

In partial fulfillment of
the requirements for the
degree of

Doctor of Philosophy

Presented March 19, 2004
Commencement June 2004

Doctor of Philosophy dissertation of Hilda J. Tromp-van Meerveld presented on March 19, 2004.

APPROVED:

_____

Major Professor, representing Forest Engineering

_____

Head of the Department of Forest Engineering

_____

Dean of the Graduate School

I understand that my dissertation will become part of the permanent collection of Oregon State University libraries. My signature below authorizes release of my dissertation to any reader upon request.

_____

Hilda J. Tromp-van Meerveld, Author

ACKNOWLEDGEMENTS

First of all, I would like to thank my major professor Jeff McDonnell for his guidance, encouragement and insightful comments during the past four years. I also would like to thank my committee members B.J. Bond, J.S. Selker, J.P. Wigington, and D. Myrold for their helpful comments. I would like to thank Jake Peters and Brent Aulenbach for their support for this project, their help with the database and their help in the field and our useful discussions. I also would like to thank Doug Burns and Jim Freer for the initial construction of the trench. If they had not constructed the trench, this dissertation may have looked very different. I would like to thank the Panola Mountain State Conservation Park rangers for letting us use the park as a research site, making it possible for us to live on the site and for being great neighbors during our stay in Georgia.

Kevin, Willem, Kellie, Markus, Jan, Brian and Nick, I enjoyed working and sharing an office with you. You all influenced my thinking greatly. Taro and Yuko, I enjoyed your visit to our lab. Thank you very much for the discussions on pipeflow and hillslope hydrological processes. Hannah, thank you for our discussions on modeling and science in general. Georgianne, thank you for introducing me to the world of sapflow sensors.

Last but certainly not least, I would like to thank my family and friends. Mom and dad, thank you very much for all your love and support. Martin, thank you very much for being a great field assistant but mostly for your love and for supporting me.

TABLE OF CONTENTS

TABLE OF CONTENTS (Continued)

TABLE OF CONTENTS (Continued)

TABLE OF CONTENTS (Continued)

LIST OF FIGURES

LIST OF FIGURES (Continued)

LIST OF FIGURES (Continued)

LIST OF FIGURES (Continued)

LIST OF FIGURES (Continued)

LIST OF FIGURES (Continued)

LIST OF TABLES

1 Introduction

1.1 Introduction

Subsurface storm flow is a dominant runoff producing mechanism in many upland environments around the world (Bonell, 1998). In addition to controlling water quantity, subsurface stormflow processes are fundamental to flushing of labile nutrients and base cations to aquatic systems (e.g. Creed et al., 1996; Burns, 1998; Hill et al., 1999; Burt and Park, 1999; Welsch, 2001; Anderson and Dietrich, 2001), landslide initiation (Iverson, 2000; Montgomery et al., 2002) and lateral redistribution of water at the small catchment scale (Western et al., 1999) and large watershed scale (Wigmosta et al., 1994).

The classic conceptual model for subsurface stormflow generation is shown schematically in Figure 1.1. This model has become imbedded in hydrology text books (e.g. Hornberger et al., 1998; Ward and Robinson, 2000) and hydrological models (e.g. Wigmosta et al., 1994). The main tenet of the standard conceptualization is that water ponds at the soil-bedrock interface or at a soil horizon contact due to the permeability contrast between the soil layers. This creates transient subsurface saturation, which in turn results in lateral subsurface flow (e.g. Whipkey, 1965; Weyman, 1973; McDonnell, 1990; Peters et al., 1995; Tani, 1997; Buttle and Turcotte, 1999; McGlynn et al., 2002). The transient subsurface saturated area has the form of a saturated wedge that expands upslope from a trench face (or stream bank) with increasing precipitation and then contracts as a result of drainage (Whipkey, 1965; Dunne and Black, 1970; Weyman 1973; Atkinson, 1978). While vertical and lateral flow is often dominated by preferential flow enhancement, pre-event water dominates subsurface flow (Sklash et al., 1986; McDonnell, 1990; Anderson et al., 1997). Total subsurface stormflow (Western and Grayson, 1998) and the pattern of subsurface stormflow across the hillslope (Anderson and Burt, 1978) are generally assumed to be determined by soil moisture content. Indices of soil moisture are thought to represent topographically driven subsurface stormflow (Western et al., 2004). The now standard conceptual model described in Figure 1.1 has been flow-centric and focused at the event time scale. An implicit assumption has been that subsurface flow responses are linear or at least continuous.

Recent commentary in the broad hydrologic literature has suggested that the linkages and feedbacks between ecological processes and hydrological processes may be fundamental (e.g. Rodriguez-Iturbe, 2000) to coupling between the event and the inter-event time scale (e.g. Rodriquez-Iturbe, 2000) and result in spatial patterns (e.g. Grayson and Blöschl, 2001). Also it has been shown that near-surface processes can be highly non-linear (e.g. Phillips, 2003), and that subsurface flow through the bedrock can be a significant contribution to streamflow (e.g. Anderson et al., 1997; Onda et al., 2001; Uchida et al., 2003).

This dissertation represents a fundamental re-examination of the standard hillslope hydrological model (Figure 1.1). This dissertation explores hillslope hydrological processes in light of these new ideas with the notion that hillslopes are a fundamental landscape unit for understanding runoff generation processes and a fundamental building block for many watershed models (Sivapalan, 2003). I hypothesize that spatial patterns across the hillslope may point to important hydrological controls on subsurface flow generation. Furthermore I suggest that it is more tractable to explore hydrological processes and patterns at the hillslope scale because it is possible to isolate first order processes without their being masked by other landscape units. If one would study the whole catchment, differences and patterns across the hillslope might become swamped by the larger differences (in soil depth, soil type, depth to water table, geochemistry and species distribution) between the hillslope and the riparian zone.

1.2 Thesis outline

Chapter 2 of this dissertation focuses on the non-linear relation between precipitation, soil moisture and subsurface flow using historic data from 147 storms between 1996 and 1998. This chapter is based on a 'black box approach', examining only the relation between precipitation and subsurface flow. Chapter 3 and Appendix 1 develop a process explanation for the observed threshold patterns. Appendix 1 describes the results of a numerical study (virtual experiment) that investigates the role of bedrock topography and variations in soil depth on subsurface flow response. The model results

show a lack of connectivity between the upslope and the downslope during medium size (< 50 mm) storms. Subsurface flow increases once connectivity between the lower hillslope and the upper hillslope is established. These model results were then tested through field measurements. The observed temporal and spatial patterns of transient subsurface saturation are described in Chapter 3. The field results show that bedrock micro-topographic depressions have to be filled with water before connectivity can be established and significant subsurface flow can occur. This results in the threshold-like relation between precipitation and subsurface flow described in chapter 2. While chapter 3 focuses on the role of bedrock topography on subsurface flow through the soil and over the bedrock topography, Chapter 6 focuses on subsurface flow through the bedrock and its influence on the hillslope scale and catchment scale water balance.

The feedbacks between the spatial and temporal patterns of soil moisture and the spatial and temporal patterns of transpiration and the relation of these feedback processes to soil depth are the focus of Chapter 4. Whereas most soil moisture measurements to date have focused on shallow soil moisture (< 0.30 m) (e.g. Nyberg, 1996; Western et al., 1999; Anctil et al., 2002; Meyles et al., 2003), soil moisture throughout the soil profile is discussed in this chapter. Chapter 4 focuses predominantly on soil moisture between events. Appendix 2 focuses on how pre-event soil moisture patterns influence subsurface stormflow generation at the event scale and shows that while soil moisture and subsurface flow are related, the pre-event soil moisture pattern does not determine the pattern of transient saturation, which is the main control on subsurface flow.

The soil moisture measurements described in Chapter 4 are point based and integrate over less than 50 mm^3. While point-scale soil moisture measurements are useful, the small sample volume inherently results in uncertainty and makes it difficult to scale up these point scale soil moisture measurements. In Chapter 5, a new electromagnetic induction device with a much larger measurement area (on the order of meters) is tested. The results show that this instrument can indeed be used to collect the spatial and

temporal soil moisture data that is needed for the assessment and calibration of spatially distributed models.

1.3 References

Anctil, F., R. Mathieu, L. Parent, A.A. Viau, M. Sbih, and M. Hessami, Geostatistics of near-surface moisture in bare cultivated organic soils, Journal of Hydrology 260: 30-37 2002.

Anderson, M.G., and T.P. Burt, The role of topography in controlling throughflow generation, Earth Surface Processes 3: 331-344. 1978.

Anderson, S.P., W.E. Dietrich, D.R. Montgomery, R. Torres, M.E. Conrad, and K. Loague, Subsurface flow paths in a steep, unchanneled catchment, Water Resources Research 33(12): 2637-2653, 1997.

Anderson, S.P., and W.E. Dietrich, Chemical weathering and runoff chemistry in a steep headwater catchment, Hydrological Processes 15: 1791-1815, 2001.

Atkinson, T. C. Techniques for measuring subsurface flow on hillslopes, in: Hillslope hydrology, edited by Kirkby, M. J., John Wiley and Sons Inc., New York: 73-120, 1978.

Buttle, J. M., and D.S. Turcotte, Runoff processes on a forested slope on the Canadian Shield, Nordic Hydrology 30: 1-20, 1999.

Bonell, M., Selected challenges in runoff generation research in forests from the hillslope to headwater drainage basin scale, Journal of the American Water Resources Association 34(4): 765-785, 1998.

Burns, D. A., R.P. Hooper, J.J. McDonnell, J.E. Freer, C. Kendall and K. Beven, Base cation concentrations in subsurface flow from a forested hillslope: The role of flushing frequency, Water Resources Research 34(12): 3535-3544, 1998.

Burt, T.P.; Park S.J., The distribution of solute processes on an acid hillslope and the delivery of solutes to a stream: I. Exchangeable bases, Earth Surface Processes and Landforms 24(9): 781-797, 1999.

Creed, I.F., L.E. Band, N.W. Foster, I.K. Morrison, J.A., Nicolson, R.S. Semkin, and D.S. Jeffries, Regulation of nitrate-N release from temperate forests: A test of the N flushing hypothesis, Water Resources Research 32(11): 3337-3354, 1996.

Dunne, T., and R.D. Black, An experimental investigation of runoff production in permeable soils, Water Resources Research 6: 478-490, 1970.

Grayson, R., and G. Blöschl, Spatial patterns in catchment hydrology: Observations and modeling, Cambridge University Press, Cambridge, 404 p. 2001.

Hill, A.R., W.A. Kemp, J.M. Buttle, and D. Goodyear, Nitrogen chemistry of subsurface storm runoff on forested Canadian Shield hillslopes, Water Resources Research 35(3): 811-821, 1999.

Hornberger, G.M., J.P. Raffensperger, P.L. Wiberg, and K.N. Eshleman, Elements of physical hydrology, The John Hopkins University Press Ltd., London, 303 p., 1998.

Iverson R.M., Landslide triggering by rain infiltration, Water Resources Research 36(7): 1897-1910, 2000.
McDonnell, J.J., A rationale for old water discharge through macropores in a steep, humid catchment, Water Resources Research 26(11): 2821-2832, 1990.
McGlynn, B., J.J. McDonnell, and D. Brammer, A review of the evolving perceptual model of hillslope flowpaths at the Maimai catchment, New Zealand. Journal of Hydrology 257: 1-26, 2002.
Meyles, E., A. Williams, L. Ternan, and J. Dowd, Runoff generation in relation to soil moisture patterns in a small Dartmoor catchment, Southwest England, Hydrological Processes 17: 251-264, 2003.
Montgomery D.R.; Dietrich W.E.; Heffner J.T., Piezometric response in shallow bedrock at CB1: Implications for runoff generation and landsliding, Water Resources Research 38(12): 101-1018, 2002.
Nyberg, L., Spatial variability of soil water content in the covered catchment at Gardsjon, Sweden, Hydrological Processes 10: 89-103, 1996.
Onda, Y., Y. Komatsu, M. Tsujimora, and J. Fujihara, The role of subsurface flow runoff through bedrock on storm flow generation, Hydrological Processes 15: 1693-1706, 2001.
Peters, D.L., J.M. Buttle, C.H. Taylor, and B.D. LaZerte, Runoff production in a forested, shallow soil, Canadian Shield basin, Water Resources Research 31(5): 1291-1304, 1995.
Phillips, J.D., Sources of nonlinearity and complexity in geomorphic systems, Progress in Physical Geography 27(1): 1–23, 2003.
Rodriguez-Iturbe, I., Eco-hydrology: A hydrologic perspective of climate-soil-vegetation dynamics, Water Resources Research 36(1): 3-9, 2000.
Sivapalan, M., Process complexity at hillslope scale, process simplicity at the watershed scale: is there a connection?, Hydrological Processes 17: 1037–1041, 2003.
Sklash, M.G., M.K. Stewart, and A.J. Pearce, Storm runoff generation in humid headwater catchments: A case study of hillslope and low-order stream response, Water Resources Research 22(8): 1273-1282, 1986.
Tani, M., Runoff generation processes estimated from hydrological observations on a steep forested hillslope with a thin soil layer, Journal of Hydrology 200: 84-109, 1997.
Uchida,T., Y. Asano, N. Ohte, and T. Mizuyama, Seepage area and rate of bedrock groundwater discharge at a granitic unchanneled hillslope, Water Resources Research 39(1): 1018, Doi:10.1029/2002wr001298, 2003.
Ward, R.C., and M. Robinson, Principles of hydrology, McGraw-Hill Publishing Company, 450 p., 2000.
Weyman, D.R., Measurements of the downslope flow of water in a soil, Journal of Hydrology 20(3): 267-288, 1973.
Welsch, D.L., C.N. Kroll, J.J. McDonnell, and D.A. Burns, Topographic controls on the chemistry of subsurface stormflow, Hydrological processes 15: 1925-1938, 2001.
Western, A. W., and R.B. Grayson, The Tarrawarra data set: Soil moisture patterns, soil characteristics, and hydrological flux measurements, Water Resources Research 34(10): 2765-2768. 1998.

Western, A. W., R.B. Grayson, G. Bloschl, G.R. Willgoose, and T.A. McMahon, Observed spatial organization of soil moisture and its relation to terrain indices, Water Resources Research 35(3): 797-810, 1999.

Western, A.W., S. Zhou, R.B. Grayson, T.A. McMahon, G. Blöschl, and D.J. Wilson, Spatial correlation of soil moisture in small catchments and its relation to dominant spatial hydrological processes, Journal of Hydrology 286:113-134, 2004.

Whipkey, R.Z., Subsurface stormflow from forested slopes, Bull. Int. Assoc. Sci. Hydrol. 2: 74-85, 1965.

Wigmosta, M.S., L. Vail, and D. P. Lettenmaier, A distributed hydrology-vegetation model for complex terrain, Water Resources Research 30: 1665-1679, 1994.

Figure 1.1 The classic conceptual model of subsurface flow generation on hillslopes with thin soils. The lines represent the expansion of the saturated wedge with increasing precipitation.

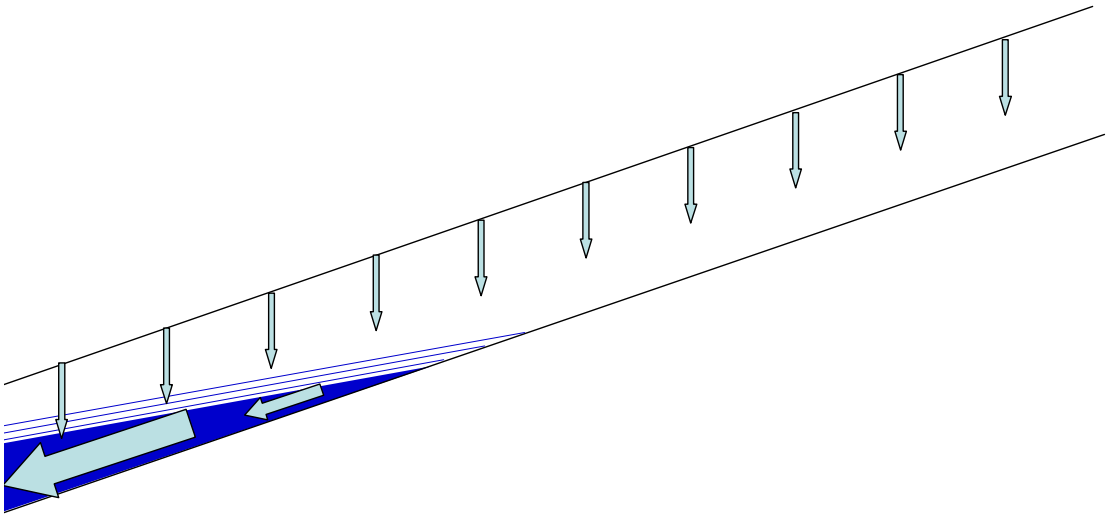

2 Threshold relations in subsurface flow: A 147 storm analysis of the Panola hillslope trench

2.1 Introduction

Hillslopes are fundamental landscape units for understanding runoff generation processes and fundamental building blocks for many watershed models. Recent studies have suggested, however, that complexities at the hillslope scale may prevent their appropriateness as a model building block (Sivapalan, 2003). Indeed, hillslopes are complex. Numerous studies in the past decades have revealed staggering complexity of hydraulic conductivity, vertical preferential flow, lateral soil pipes, impeding layers, etc. One might question, then, whether we should continue to focus on the dynamics of hillslope response since every hillslope appears unique (Beven, 2001).

So, what have been the methods used to characterize hillslope processes? Excavations at experimental hillslopes have been a common method for quantifying subsurface stormflow and water mixing in response to storm rainfall and snowmelt. Hillslope trench analyses of subsurface stormflow date back to the 1960's and 1970's (for reviews see Kirkby, 1978; Bonell, 1993 and 1998). Early studies focused mainly on the temporal dynamics of throughflow and often used small (<1 m wide) trenches (Atkinson, 1978). The importance of subsurface stormflow as a main runoff generation mechanism was noted. Important observations were made about (1) the influence of soil horizon contacts in generating lateral subsurface stormflow (Whipkey, 1965; Mosley, 1979), (2) saturated wedge development and growth from the trench face upslope (Dunne and Black, 1970; Weyman 1973), (3) the importance of lateral soil pipes in fast delivery of water and the rapid response of subsurface flow (Mosley, 1982), and more recently (4) pre-event water dominating subsurface stormflow even when pipe flow appeared to dominate total flow at the trench (Sklash et al., 1986; McDonnell, 1990; Anderson et al., 1997). In fact, lateral pipe flow of chemically dilute (Burns et al., 1998) pre-event water (Sklash et al., 1996; Peters, 1995; Uchida et al., 1999) emanating from study trench faces has been a common observation.

Notwithstanding these important observations, our ability to generalize hillslope findings has been minimal. Some progress has been made in recent studies that have

increased the width of experimental trenches, often extending many 10's of meters across the base of a hillslope, to analyze the spatial patterns of subsurface stormflow and transport in relation to the surface and subsurface topography. Using this whole-slope based excavation approach, Woods and Rowe (1996) showed the large effect of antecedent wetness (quantified using an antecedent precipitation index) and storm size on the lateral distribution of subsurface stormflow, the amount of subsurface stormflow, and the timing of subsurface stormflow at the Maimai hillslope, New Zealand. For the trenched experimental hillslope at the Panola Mountain Research Watershed (PMRW) in Georgia USA (the site of the investigation discussed in this paper), McDonnell et al. (1996 and 1998) and Freer et al. (1997 and 2002) showed for three rainstorms that flow at the trench face was highly correlated with the upslope contributing area defined by the bedrock topography (rather than the often-assumed surface topography derived contributing area). The spatial pattern of the bedrock topographic index as a control on lateral subsurface stormflow patterns was also observed by Peters et al. (1995) at the Plastic Lake hillslope in Ontario Canada, by Tani (1997) at the Minamitani hillslope on Honsyu Island, Japan, by McDonnell et al. (1998) at the Maimai hillslope, and by Hutchinson and Moore (2000) at a hillslope in British Colombia, Canada,.

So whilst the subsurface topography may be a way to seek commonality in understanding lateral subsurface stormflow distribution, we nevertheless do not understand how input maps to output even on these intensively studied slopes in New Zealand, the USA, Canada and Japan. Part of the problem is that subsurface stormflow amounts from all of these studies do not appear to be proportional to the inputs across the entire range of observations. More problematic still is that even at these intensively studied sites, we rarely have more than a handful of storms to work with, due to the extreme difficulty and cost of obtaining the data and maintaining the infrastructure. Thus, the stability of the observed spatial patterns across seasons, or with changes in precipitation and antecedent moisture conditions has rarely been assessed. This paper presents analyses of subsurface flow at the Panola trench face from 147 rainstorms from February 1996 to May 1998. This large number of rainstorms allows exploration of

questions regarding to the persistence of spatial patterns in time and the influence of storm size and antecedent soil moisture conditions on subsurface stormflow patterns. Here we address the following questions:

- How often does the hillslope deliver water laterally to the slope base and therefore to riparian zones and stream banks?
- What is the contribution of lateral pipe flow to total flow at the trench face?
- Does total trench flow and its subcomponents of matrix flow and lateral pipe flow increase linearly with storm size?
- How persistent are the spatial patterns of flow at the trench face across seasons, soil moisture conditions, and storm characteristics?

What follows is a summary of the 147 storms collected at the Panola Mountain Research Watershed trench. We explore the questions above and present evidence for nonlinear dynamics in subsurface stormflow. We define this nonlinearity in the context of threshold behavior for the initiation of lateral subsurface stormflow where subsurface stormflow amounts are not proportional to the inputs. We argue that this new recognition of a clear threshold behavior may be a way forward in collapsing the vast array of process complexities into a more clear integrated hillslope behavioral description.

2.2 Study Site and Methods

The Panola Mountain Research Watershed (PMRW) is located about 25 km southeast of Atlanta, Georgia USA, in the southern Piedmont. The forested watershed is dominated by hickory, oak, tulip poplar, and loblolly pine (Carter, 1978). The 10-ha western upper catchment at Panola (within which the trench is located) is underlain by the Panola Granite, which is a biotite-oligoclase-quartz-microcline granodiorite (Crawford et al., 1999). Soils on the study hillslope are light colored sandy loam soils with little textural differences. The upper 0.15 m of the soil profile is humus rich. There are no large differences in soil type across the study hillslope. Soil depths on the study hillslope range from 0 to 1.86 m and average 0.63 m.

The climate is humid and subtropical with a mean annual air temperature of 16.3° C and mean annual precipitation of 1240 mm, spread uniformly over the year (NOAA, 1991). Rainfall tends to be of long duration and low intensity in winter, when it is associated with the passage of fronts, and of short duration but high intensity in summer, when it is associated with thunderstorms. Streamflow at PMRW has a strong seasonal pattern; the highest baseflows occur during the dormant season (November through April), and the lowest occur during the growing season (May through October). Annual stream yield from the 41-ha catchment varied from 8% to 50% of precipitation during 1986-99 (Peters et al., 2000).

A 20-m long trench was excavated normal to the fall line of the slope down to bedrock at a midslope position in 1995. Early results were reported in McDonnell et al. (1996). Figure 2.1 shows the accumulated area distribution for the study slope calculated using the surface and the bedrock topography. Figure 2.1c shows a front view of the trench face including the location of the five individual plumbed soil pipes, which are developed from decayed tree roots. The trench was divided into ten 2-m sections and discharge from each 2-m trench section and from five individual soil pipes was measured by routing the flow through tipping-bucket gages. We define the total lateral flow from these five plumbed pipes as *pipe flow* and flow from the remaining sections as *matrix flow*. It should be noted that a portion of the matrix flow actually comes from several smaller preferential flow paths within the soil profile and at the soil-bedrock interface, which were not individually plumbed. *Total flow* at the trench face is defined as the sum of *pipe flow* and *matrix flow*. For this analysis, the trench sections were regrouped into 4-m sections based on similar topographic characteristics. When total flow for a 4-m section was calculated, flow from a pipe in that section was added to the measured matrix flow. When a pipe was located on the border of two sections (M8, see Figure 2.1c), flow from that pipe was partitioned between the two adjacent sections. Additional details of the trench and flow-collection system are described in McDonnell et al. (1996), Freer et al. (1997 and 2002) and Burns et al. (1998).

In this study, we examine two years of subsurface flow data: from February 19th 1996 to May 10th 1998. This period contained 147 rainstorms. The *start of a storm* was defined as a rainstorm that produced the following streamflow characteristics at the 41-ha gauging station that our hillslope ultimately drained into: a 0.4 l/s rise in discharge within 3 hours or a 30% rise in discharge within 3 hours. For calculation of *total storm precipitation*, the *end of the storm* was determined when streamflow reached either 10% of the difference between the streamflow maximum and pre-event streamflow or a baseflow level of 5 l/s. The *end of the storm for subsurface stormflow* at the study trench (total flow, matrix flow and pipe flow at each trench section) was defined as the start of the next storm using the criteria above.

We acknowledge that it is possible that there was a small "under catch" of subsurface flow or a change in timing of measured subsurface flow at the end of the analyzed two year period due to possible trench degradation. We assume that this did not have a large influence on the analysis of the number of subsurface flow producing rainstorms, the total volume of trench flow nor the distribution of subsurface flow across the trench. To test this assumption we examined data from each individual calendar year and found no systematic changes in the distribution of subsurface flow across the trench or differences in the volume or ratios of subsurface flow to storm rainfall.

2.3 Results

2.3.1 Total volume and number of storms producing subsurface stormflow

Analysis of rainfall and subsurface flow indicates that 22% of the rainstorms did not produce any measurable flow at the trench face. Most of the rainstorms (93%) did not produce significant flow at the trench face, defined as more than 1 mm total measured subsurface flow. For most rainstorms (89%), the runoff coefficient was less than 1%. Total subsurface flow produced by all of the 147 rainstorms was only 5% of total precipitation. The maximum runoff coefficient for an individual storm was 27%, although the runoff coefficient was more than 10% for only eight of the 147 rainstorms.

There was a strong seasonality in the runoff coefficient. The seasonal averages varied from 5.7% to 9.8% to 0.8% to 0.04% for fall, winter, spring and summer, respectively. Seasonality in streamflow runoff coefficients at Panola was reported by Peters et al. (2003).

The second 4-m section from the left side (looking upslope) of the trench (section D, 12-16 m), which had the largest contributing drainage area using the bedrock surface (see Figure 2.1), produced more subsurface flow and more frequent subsurface flow than the other sections of the trench (Figure 2.2). These multi-storm results are consistent with the individual storm results of McDonnell et al. (1996) and Freer et al. (1997 and 2002) and support, indirectly, the flushing frequency hypothesis of Burns et al. (1998). Subsurface flow was highest at the single 4-m section with the largest bedrock contributing area (section D) for 61% of the rainstorms that produced any subsurface flow.

2.3.2 Role of pipe flow

Pipe flow contributed significantly to total flow at the trench during the study period. Of the total measured trench flow during the 147 rainstorms, 42% came from the five individually plumbed soil pipes. One large pipe (M14), located 14 m from the right side (when looking upslope) of the trench, in the section with the high bedrock contributing area (section D) and 0.70 m below the soil surface (see Figure 2.1c), delivered 25% of all measured subsurface flow. For the 147 rainstorms, there was a very strong linear relation ($r^2 = 0.96$) between storm-based total subsurface flow and storm total pipe flow (Figure 2.3), suggesting a similar mechanism for the initiation of both matrix flow and pipe flow (see Uchida et al., 2003).

Pipe flow was a large contributor to total subsurface flow at the trench during winter periods and during a large (153 mm) rainfall event in the fall of 1997. Pipe flow was not important during the rainstorms in summer and spring except for a few very small subsurface flow producing rainstorms. Pipe flow accounted for 50% of total

subsurface flow during fall, 41% during winter, 0% during spring and 2% during summer. During individual rainstorms pipe flow ranged from 0 to 100% of the total measured flow and represented a high percentage of total flow only during wet conditions and very dry conditions (as defined by measured TDR readings on a nearby hillslope at 0.70 m depth (Figure2.4a)). This relation was less clear for soil moisture measured at 0.15 m depth (Figure 2.4b). It should be noted that during very dry conditions, when the percentage of pipe flow to total flow was large, the total flow was very small. The percentage of pipe flow to total subsurface flow did not correlate with total rainfall, the maximum 5-minute rainfall intensity or the maximum 1-hour rainfall intensity.

The relative importance of the five individually plumbed soil pipes to total pipe flow (as we defined earlier in this paper) varied seasonally (Figure 2.5). Pipe M14 was the most important soil pipe in terms of total pipe flow production during winter and spring. Pipe M2, located in section A, 2 m from the right side (looking upslope) of the trench at 0.59 m depth below the soil surface (see Figure 2.1c), was the only soil pipe that flowed during very dry conditions.

2.3.3 Threshold response of subsurface flow

Our analyses suggest that there is a clear threshold for significant subsurface flow to occur; significant subsurface flow occurred only during rainstorms larger than 55 mm (Figure 2.6). For storms larger than this threshold, there was an almost two orders of magnitude increase in subsurface flow compared to subsurface flow from storms smaller than this threshold (see inserts in Figure 2.6). This precipitation threshold was similar for total flow, matrix flow and pipe flow, but was higher for all of these components under drier conditions. From the available data, we infer that if there is a threshold under dry conditions, this threshold is somewhere between 90 and 140 mm depending on the pre-storm soil moisture conditions. Even within our large data set of measured storms, there were not enough “very large” rainstorms under dry conditions to determine if the subsurface flow response continued to be linear with increasing total rainfall or if there is yet-unobserved behavior for exceptionally large events. Figure 2.7 shows that both

antecedent moisture conditions at depth and total precipitation amount determine whether or not significant flow (>1 mm) occurs. This figure shows that soil moisture content at the start of the storm and total storm precipitation form three "zones" with respect to the depth of total subsurface stormflow (no flow, < 1 mm, and > 1 mm total subsurface flow). However, we acknowledge that the boundary between "no flow" and "less than 1 mm total flow" is not very sharp.

To test how well defined the precipitation threshold is, we calculated the sum of the deviations from the average of subsurface flow above and below each precipitation depth. If there is a well defined precipitation threshold (or step in the function), this should lead to a clear minimum in the sum of the deviations at the threshold. We found that for the 147 storms the threshold was very well defined. We randomly selected subsets from the dataset and determined the threshold for that subset of data. This was done 1000 times for each subset size. The cumulative probability distributions of the thresholds were then calculated (Figure 2.8). The threshold was well defined as long as the dataset was relatively large (90% of the total dataset) but became less well defined for smaller subsets. However, even for the smaller subsets there would be a high probability that the precipitation threshold would be between 40 and 60 mm.

Total subsurface flow, matrix flow and pipe flow were also a function of antecedent soil-moisture content at depth, i.e., as measured by TDR at 70 cm depth. Except for the very large (153 mm) storm in October 1997 and an 88 mm storm in April 1997 significant subsurface flow (> 1mm) did not occur when the soil-moisture content at depth at the start of the storm was less than 40%. During both the October 1997 storm and the April 1997 storm, flow at the trench was not observed before the soil-moisture content at 0.70 m was greater than 40%. Total subsurface flow, total matrix flow, and total pipe flow did not correlate with the 5-minute or 1-hour maximum rainfall intensity.

2.3.4 Distribution of flow across the trench face

McDonnell et al. (1996) and Freer et al. (1997 and 2002) have shown that the topography of the bedrock surface is an important control on trench flow for three rainstorms in 1996. Analysis of the 147 rainstorms in this study generally confirms this but shows that the distribution of total flow across the trench face is highly dependent on storm total rainfall and antecedent moisture conditions. Subsurface flow became more uniform across the trench as total subsurface stormflow increased, i.e., with increasing storm size, wetter antecedent conditions and during winter months (Figure 2.9). During small, low runoff producing rainstorms, subsurface flow was concentrated in sections D and E, the section with high bedrock contributing area and the section underlain by shallow soils, respectively (see Figure 2.1). With increasing precipitation, antecedent soil-moisture content, and total subsurface stormflow, the relative contribution of section E (shallow soils) decreased and the contribution of the other sections (A, B and C) increased. In the extreme during very large rainstorms, most of the flow did not occur in the section D (the highest bedrock contributing area section) but occurred in section A, which is a section with a slightly higher bedrock contributing area compared to the trench average. During the summer months almost all flow (90%) came from section E (the section with the thinnest soils, where the bedrock is very close to the surface).

2.4 Discussion

The Panola hillslope, like many research hillslopes around the world, shows a highly complex set of behaviors in terms of its response to rainfall events. Previous studies at the site have shown how bedrock topography controls the movement of mobile subsurface stormflow laterally down the hillslope (Freer et al., 2002), how base cation concentrations in subsurface stormflow are lower at the slope base where seepage is concentrated (Burns et al., 1998) and how water movement vertically through the soil (McIntosh et al., 1999) and laterally downslope (McDonnell et al., 1996) is dominated by preferential flowpaths. However, all of these previous studies have belied the fact that response from event-to-event was always somewhat different. This different behavior, even at one well studied hillslope, was always a limitation to using the Panola hillslope

observations to say anything generalizable about hillslope behavior, let alone, use it to explain the response of adjacent ungauged hillslopes.

2.4.1 Threshold effects elsewhere

Our analysis of the 147 storms in this study (including those few storms used as the basis for the papers cited above) showed a clear and unequivocal threshold in the hillslope rainfall-runoff relation. We show how these thresholds influence the initiation of subsurface flow and how matrix flow and lateral pipe flow show similar threshold behavior. Re-examining earlier hillslope literature, and examining figures and tables from these studies and plotting these rainfall data versus hillslope flow data suggests that thresholds for subsurface flow generation have been observed in the past. For example Whipkey (1965), showed a relation between total flow and precipitation for dry and wet conditions in his early trench flow studies in the Northeast United States. A rainfall threshold of about 35 mm during dry conditions can be inferred from his data (Figure 2, page 79 in Whipkey, 1965), but a threshold is not evident during wet conditions. A plot of quickflow volumes against total precipitation from Mosley (1979) for the Maimai catchment suggests a rainfall threshold of about 23 mm is necessary to initiate subsurface stormflow. We base this on his data in Table 1 (page 798, Mosley 1979)—however, we should acknowledge that there is insufficient data to fully demonstrate this threshold and the data could suggest an exponential relation as well.

More recently, Peters et al. (1995) show a rainfall threshold of 8 and 17 mm to produce a hillslope and stream response at their Plastic Lake catchment in Canada. Tani (1997) showed a clear threshold response from a 6-m wide trench at the base of a slope in Japan. He found a precipitation threshold dependent on antecedent soil-moisture conditions. The data from Tani (1997; Figure 5, page 91) indicates that trench flow occurs for rainstorms greater than about 20 mm. After the threshold was reached there was an almost 1:1 relation between precipitation above the threshold and flow from the trench. This was not observed in the data for Panola where for rainstorms larger than 55 mm, the trench flow runoff coefficient after the precipitation threshold ranged from 30%

to 80% of precipitation after the threshold, with the largest runoff coefficients occurring for the storms with the highest 5-minute maximum precipitation intensities. A threshold response for pipe flow to precipitation was also apparent in data from other studies; however, these studies often do not mention this threshold response. Guebert and Gardner (2001) show a threshold between 10 and 20 mm of precipitation for pipe flow initiation at their upper pit. While Noguchi et al. (2001) do show a threshold based response function of total storm precipitation for some pipes, they do mention that for wet conditions only small precipitation inputs are needed to initiate hydrologic response. Our work at Panola shows that the threshold for matrix and pipe flow is large even under wet conditions. Consideration of this body of work suggests that the precipitation thresholds for subsurface flow and pipe flow generation may be a wide spread phenomena, even if not explicitly acknowledged in previous work.

2.4.2 Implications for how we view the role of hillslopes in the hydrology of the Panola watershed

The trench flow runoff coefficient of individual rainstorms reported in this paper show that the runoff coefficient was greater than 10% for only eight of the 147 rainstorms. This confirms the limited role of hillslopes in direct streamflow generation, inferred from the hydrochemical and hydrometric analysis by Peters and Ratcliffe (1998), and geochemical analysis by Hooper et al. (1998) and Burns et al. (2001). Our analysis revealed that the relation between subsurface flow and total storm precipitation and antecedent soil-moisture content was threshold-like. The observed threshold behavior can explain the low overall runoff coefficient and why the hillslopes are disconnected from the stream or the riparian zone most of the time (as suggested by Burns et al. (2001) and Hooper et al. (1998)). Analysis of meteorological data of a 12-year period (1987-98) reveals that there were 51 rainstorms larger than 55 mm (using the same classification parameters to define the 147 rainstorms in this study). This represents an average of 4.3 rainstorms per year where hillslopes might be able to contribute water and solutes to the channel. Significant flow at the trench did not occur during the summer. During the 1987-98 period, 38 rainstorms larger than 55 mm occurred during fall, winter and spring,

which averages 3.2 rainstorms per year. Only 17 of these rainstorms occurred in the winter when the watershed is generally wettest and trench-flow runoff coefficients are the highest. This corresponds to an average of 1.4 rainstorms per year. This analysis shows that subsurface flow from the hillslope does not contribute to streamflow during most of the year because only a few rainstorms per year are large enough (larger than the threshold) to produce significant subsurface flow on the hillslopes.

Matrix flow and pipe flow had very similar precipitation thresholds for initiating significant flow at the trench (Figure 2.6). This, combined with the good linear relation between total flow and total pipe flow (Figure 2.3), could suggest that a similar mechanism is responsible for initiation of lateral matrix flow and lateral pipe flow. We hypothesize that this mechanism relates to the (storm event) transient water table development at the soil-bedrock interface (as described by McDonnell (1990)). The threshold then relates functionally to the depth of water necessary to exceed the soil moisture deficit at depth for producing positive pore pressures at this interface. Lateral pipe flow occurred only when soil moisture conditions at depth were either very dry or wet. Only one pipe delivered flow during rainstorms with dry antecedent conditions. We hypothesize that during dry conditions, a watertable does not develop, and thus total subsurface flow is minimal (less than 0.01 mm). Nevertheless cracking of the soils combined with possibly seasonal hydrophobic soil surfaces allows for rapid delivery to depth and, it would appear, to pipe M2. This pipe delivered all of the trench-scale pipe flow during the summer rainstorms.

The differences in the relative contributions of different parts of the trench face to total flow with changes in total precipitation, antecedent wetness and seasons suggests that the bedrock topography might not be the dominant control on subsurface flow during all rainstorms (as was suggested by the analysis of only a few rainstorms by McDonnell et al. (1996, 1997) and Freer et al. (1997 and 2002)). Our multi-storm analysis suggests that soil depth controls subsurface flow during small rainstorms and during storms with dry antecedent soil-moisture conditions. The bedrock topography appears to be the

primary control during medium to large rainstorms. The 147-storm dataset shows another control for very large rainstorms: the production of increased flow from section A (Figure 2.9), an area with higher-than-average bedrock contributing area but not the highest bedrock contributing area. The reasons for this shift to dominance of section A are subject for further research. The shift in dominant areas of flow with increasing antecedent soil-moisture content, storm size and total flow corresponds well with the temporal changes in the relative importance of different trench sections as found by Freer et al. (2002) for one storm in 1996 during which section A started to produce flow later than the other sections.

2.5 Conclusions

Analysis of 147 rainstorms at the Panola trench shows a clear threshold based response of hillslope runoff initiation with total storm precipitation and, secondarily, with antecedent conditions. We detected changes in the relative importance of different parts of the hillslope with changes in total flow, modulated by changes in precipitation and antecedent moisture conditions. We demonstrated the importance of pipe flow for determining the volume of subsurface flow measured at the trench. We found a linear relation between lateral pipe flow and matrix flow but with pronounced seasonal changes in the relative importance of different soil pipes at the trench face. These data, showing more flow and more often flow from the high bedrock contributing area sections support the flushing frequency theory proposed by Burns et al. (1998). This analysis also supports the limited role of hillslopes in streamflow production (Hooper et al., 1998 and Burns et al., 2001). Most importantly perhaps, these analyses demonstrate both the importance of record length and the need for analyzing different storm size, antecedent conditions and seasons for interpreting hillslope dynamics. The ‘over-arching conclusion’ of this work though is that the high degree of complexity often observed for single rainstorms on experimental hillslopes, when viewed over a long record, may become much simpler in terms of thresholds that define gross system behavior.

2.6 Acknowledgements

This work was support by NSF grant EAR 0196381. We thank Brent Aulenbach for his help with the data assembly and Jim Freer and Doug Burns for the initial trench construction efforts. Taro Uchida is thanked for his useful input during a visit to our lab. We also thank Markus Weiler for his help along the way.

2.7 References

Anderson, S.P., W.E. Dietrich, D.R. Montgomery, R. Torres, M.E. Conrad, and K. Loague, Subsurface flow paths in a steep, unchanneled catchment, Water Resources Research 33(12): 2637-2653, 1997.

Atkinson, T. C. Techniques for measuring subsurface flow on hillslopes, in: Hillslope hydrology, edited by Kirkby, M. J., John Wiley and Sons Inc., New York: 73-120, 1978.

Beven, K.J., Uniqueness of place and process representations in hydrological modeling, Hydrology and Earth System Science 5: 1-12, 2001.

Bonell, M., Progress in the understanding of runoff generation dynamics in forests, Journal of Hydrology 150: 217-275, 1993.

Bonell, M., Selected challenges in runoff generation research in forests from the hillslope to headwater drainage basin scale, Journal of the American Water Resources Association 34(4): 765-785, 1998.

Burns, D.A., R.P. Hooper, J.J. McDonnell, J.E. Freer, C. Kendall, and K. Beven, Base cation concentrations in subsurface flow from a forested hillslope: The role of flushing frequency, Water Resources Research 34(12): 3535-3544, 1998.

Burns, D.A., J. J. McDonnell, R.P. Hooper, N.E. Peters, J.E. Freer, C. Kendall, and K. Beven, Quantifying contributions to storm runoff through end-member mixing analysis and hydrologic measurements at the Panola Mountain Research Watershed (Georgia, USA), Hydrological Processes 15: 1903-1924, 2001.

Carter, M.E.B., A community analysis of the Piedmont deciduous forest of Panola Mountain State Conservation Park: Atlanta, Georgia, M. S. thesis, 126 pp., Emory Univ., Atlanta, Ga., 1978.

Crawford T.J., M.W. Higgins, R.F. Crawford, R.L. Atkins, J.H. Medlin, and T.W. Stern, Revision of stratigraphic nomenclature in the Atlanta, Athens, and Cartersville 30 ð 60 quadrangles, Georgia. Georgia Geologic Survey Bulletin B-130: Atlanta, Georgia; 48, 1999.

Dunne, T., and R.D. Black, An experimental investigation of runoff production in permeable soils, Water Resources Research 6: 478-490, 1970.

Freer, J.E., J.J. McDonnell, K.J. Beven, D. Brammer, D.A. Burns, R.P. Hooper, and C. Kendal, Topographic controls on subsurface stormflow at the hillslope scale for two hydrologically distinct small catchments, Hydrological Processes 11(9): 1347-1352, 1997.

Freer, J.E., J.J. McDonnell, K.J. Beven, N.E. Peters, D.A. Burns, R.P. Hooper, B.T. Aulenbach, and C. Kendall, The role of bedrock topography on subsurface stormflow, Water Resources Research, 10.1029/2001WR000872, 2002.

Guebert, M.D., and T.W. Gardner, Macropore flow on a reclaimed surface mine: infiltration and hillslope hydrology, Geomorphology 39: 151-169, 2001.
Hooper, R.P., B.T. Aulenbach, D.A. Burns, J.J. McDonnell, J.E. Freer, C. Kendall, and K.J. Beven, Riparian control of stream-water chemistry: implications for hydrochemical basin models, in Hydrology, Water resources and Ecology in Headwaters, Proceedings of the HeadWater '98 conference held at Meran/Merano, Italy 1998, IAHS publication 248: 451-458, 1998.
Huntington, T.G., R.P. Hooper, N.E. Peters, T.D. Bullen, and C. Kendall, Water, energy, and biogeochemical budgets investigation at Panola Mountain Research Watershed, Stockbridge, Georgia—A research plan, U.S. Geological Survey Open File Report, 93–55, 39 pp., 1993.
Hutchinson, D.G., and R.D. Moore, Throughflow variability on a forested hillslope underlain by compacted glacial till, Hydrological Processes 14(10): 1751-1766, 2000.
Kirkby, M.J., Hillslope hydrology, John Wiley and Sons Inc., New York, 389 p. 1978.
McDonnell, J.J., A rationale for old water discharge through macropores in a steep, humid catchment, Water Resources Research 26(11): 2821-2832, 1990.
McDonnell, J.J., Comment on "the changing spatial variability of subsurface flow across a hillside" by Ross Woods and Lindsay Rowe, Journal of Hydrology, New Zealand 36(1): 97-100, 1997.
McDonnell, J.J., J.E. Freer, R.P. Hooper, C. Kendall, D.A. Burns, K.J. Beven, and N.E. Peters, New method developed for studying flow in hillslopes, EOS, Transactions of the American Geophysical Union 77(47): 465, 1996
McDonnell, J.J., D. Brammer, C. Kendall, N. Hjerdt, L. Rowe, M. Stewart, and R. Woods, Flow pathways on steep forested hillslopes: The tracer, tensiometer and trough approach, in Environmental Forest Science, M. Tani, editor, Kluwer Academic Publishers, 463-474, 1998.
McIntosh, J., J.J. McDonnell, and N.E. Peters, Tracer and hydrometric study of preferential flow in large undisturbed soil cores from the Georgia Piedmont, USA, Hydrological Processes 13: 139-155, 1999.
Mosley, M.P., Streamflow generation in a forested watershed, Water Resources Research 15: 795-806, 1979.
Mosley, M.P., Subsurface flow velocities through selected forest soils, South Island, New Zealand, Journal of Hydrology 55: 65-92, 1982.
National Oceanic and Atmospheric Administration, Local climatological data, annual summary with comparative data, 1990, Atlanta, Georgia, 6 pp., Asheville, N. C., 1991.
Noguchi, S., Y. Tsuboyama, R.C. Sidle, and I. Hosoda, Subsurface runoff characteristics from a forest hillslope soil profile including macropores, Hitachi Ohta, Japan, Hydrological Processes 15: 2131-2149, 2001.
Peters, D.L., J.M. Buttle, C.H. Taylor, and B.D. LaZerte, Runoff production in a forested, shallow soil, Canadian Shield basin, Water Resources Research 31(5): 1291-1304, 1995.

Peters, N.E., and E.B. Ratcliffe, Tracing hydrologic pathways using chloride at the Panola Mountain Research Watershed, Georgia, USA. Water, Air and Soil Pollution 105(1/2): 263-275, 1998.

Peters, N.E., R.P. Hooper, T.G. Huntington, and B.T. Aulenbach, Panola Mountain, Georgia—a water, energy, and biogeochemical budgets program site, U.S. Geological Survey Fact Sheet 162-99(4), 2000.

Peters, N.E., J.E. Freer, and B.T. Aulenbach, Hydrologic dynamics of the Panola Mountain Research Watershed, Georgia, Groundwater 41(7): 973-988, 2003.

Sivapalan, M., Process complexity at hillslope scale, process simplicity at the watershed scale: is there a connection?, Hydrological Processes 17: 1037–1041, 2003.

Sklash, M.G., M.K. Stewart, and A.J. Pearce, Storm runoff generation in humid headwater catchments: A case study of hillslope and low-order stream response, Water Resources Research 22(8): 1273-1282, 1986.

Sklash, M.G., K.J. Beven, and K. Gilman, Isotope studies of pipe flow at Plynlimon, Wales, UK, Hydrological Processes 10(7): 921-944, 1996.

Tani, M., Runoff generation processes estimated from hydrological observations on a steep forested hillslope with a thin soil layer, Journal of Hydrology 200: 84-109, 1997.

Uchida, T., K. Kosugi, and T. Mizuyama, Runoff characteristics of pipe flow and effects of pipe flow on rainfall-runoff phenomena in a mountainous watershed, Journal of Hydrology 222(1): 18-36, 1999.

Uchida,T., Y. Asano, N. Ohte, and T. Mizuyama, Seepage area and rate of bedrock groundwater discharge at a granitic unchanneled hillslope, Water Resources Research 39(1): 1018, Doi:10.1029/2002wr001298, 2003.

Weyman, D.R., Measurements of the downslope flow of water in a soil, Journal of Hydrology 20(3): 267-288, 1973.

Whipkey, R.Z., Subsurface stormflow from forested slopes, Bull. Int. Assoc. Sci. Hydrol. 2: 74-85, 1965.

Woods, R., and L. Rowe, The changing spatial variability of subsurface flow across a hillside, Journal of Hydrology (NZ) 35(1): 51-86, 1996.

Figure 2.1 Map of the Panola hillslope: accumulated area based on surface topography (a) and bedrock topography (b) and a front view of the trench face with the location of the plumbed soil pipes (black diamonds) (c).

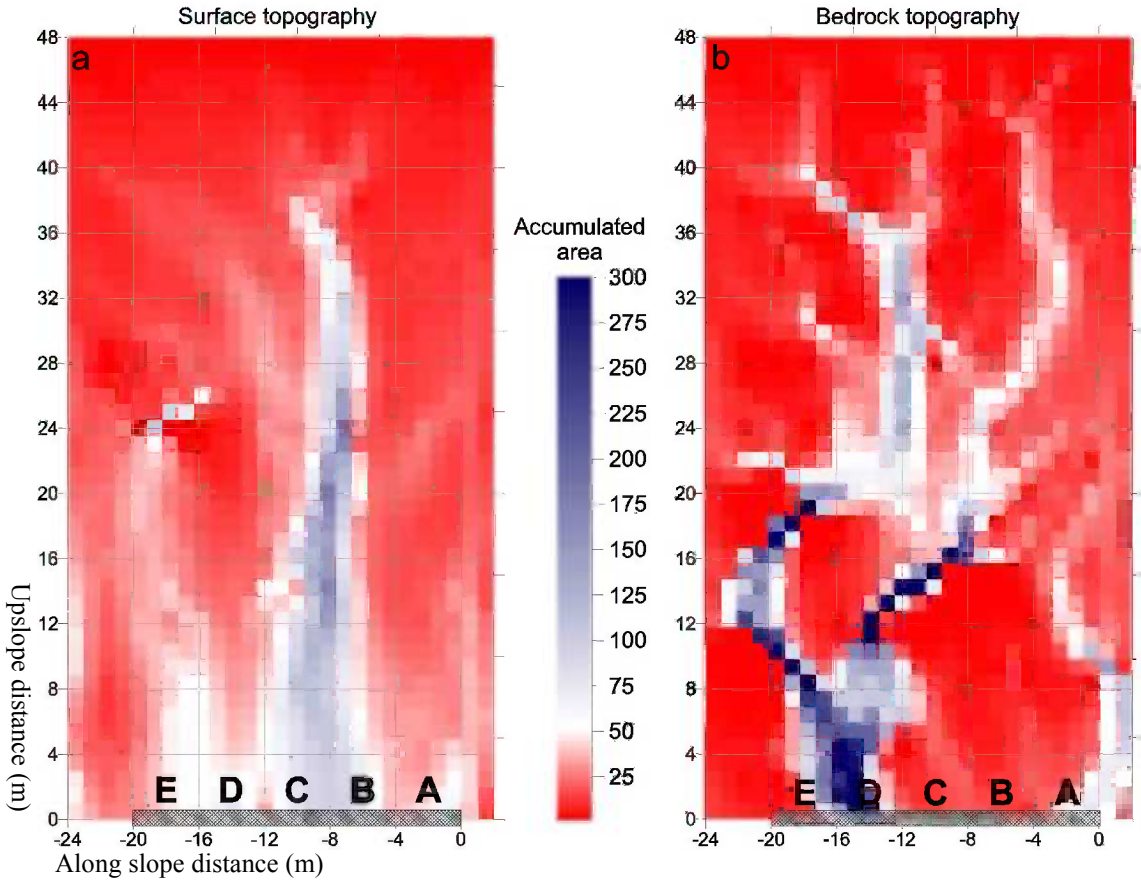

Figure 2.2 Total flow (a) and the number of storms producing measurable subsurface flow for each 4-m section of the trench (b). For the location of the trench sections see Figure 2.1c.

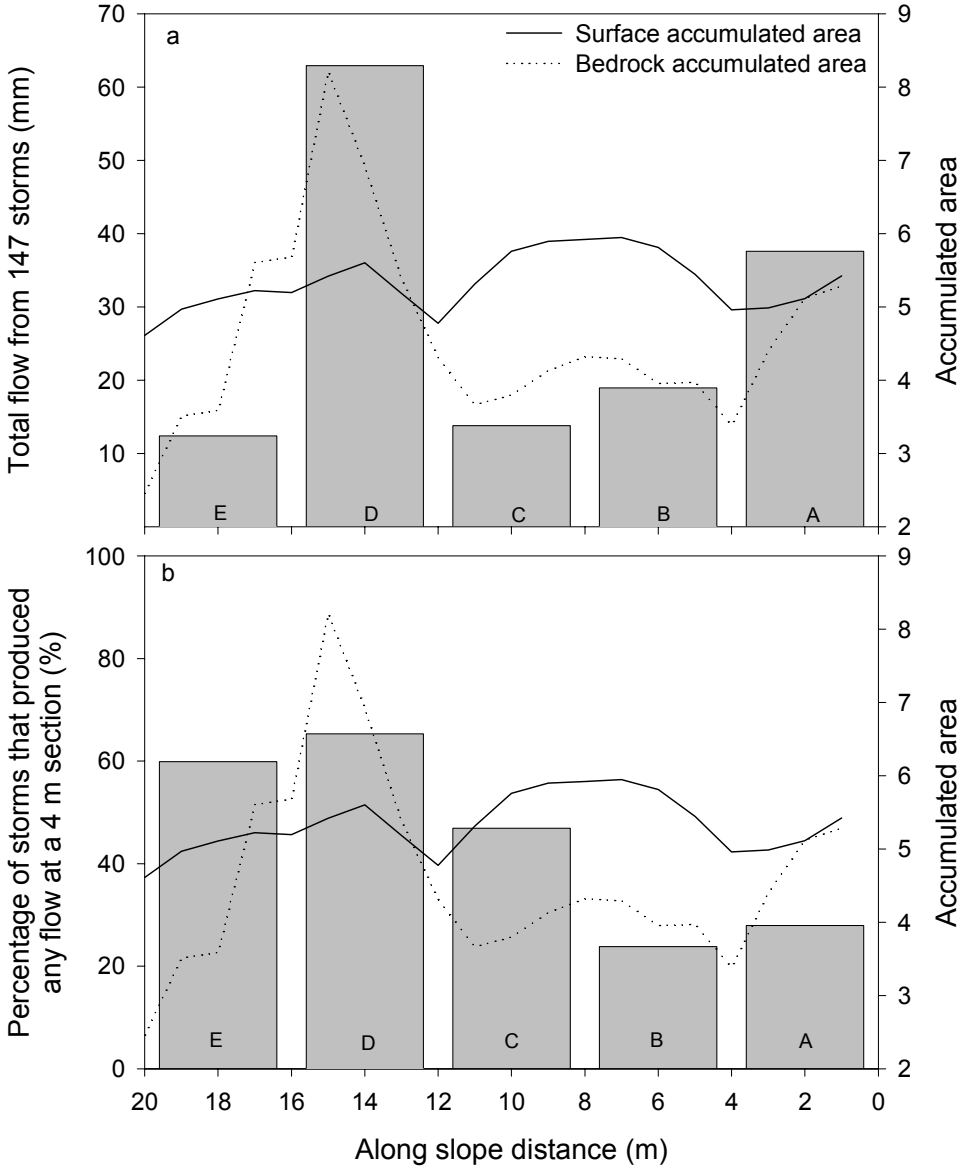

Figure 2.3 The relationship between storm total pipe flow and total subsurface flow at the trench face. The insert shows the relation on a log – log scale to show the smaller volumes. The solid line represents the regression line and the dotted line represents the 1 to 1 line.

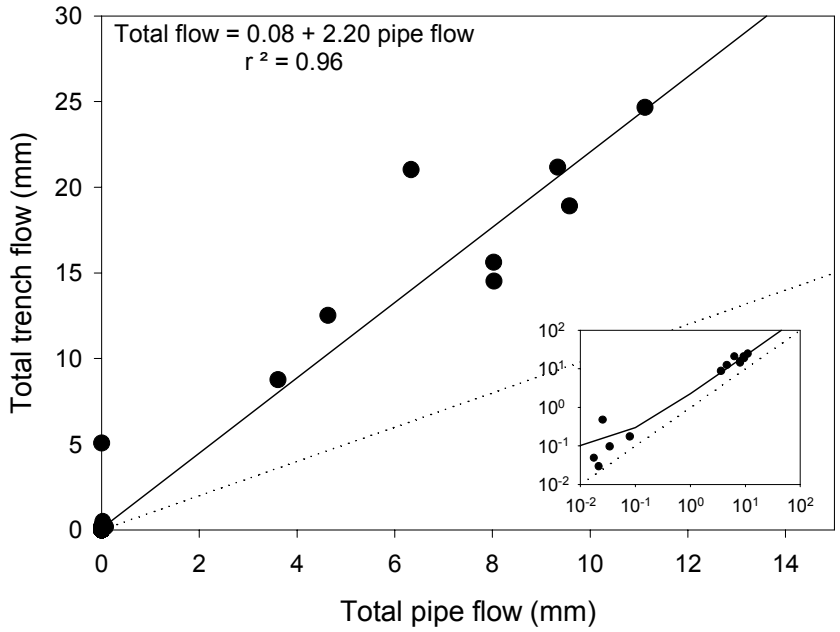

Figure 2.4 The relationship between the contribution of pipe flow to total flow and the soil moisture readings at 0.70 m (a) and at 0.15 m below the soil surface at the start of a storm (b).

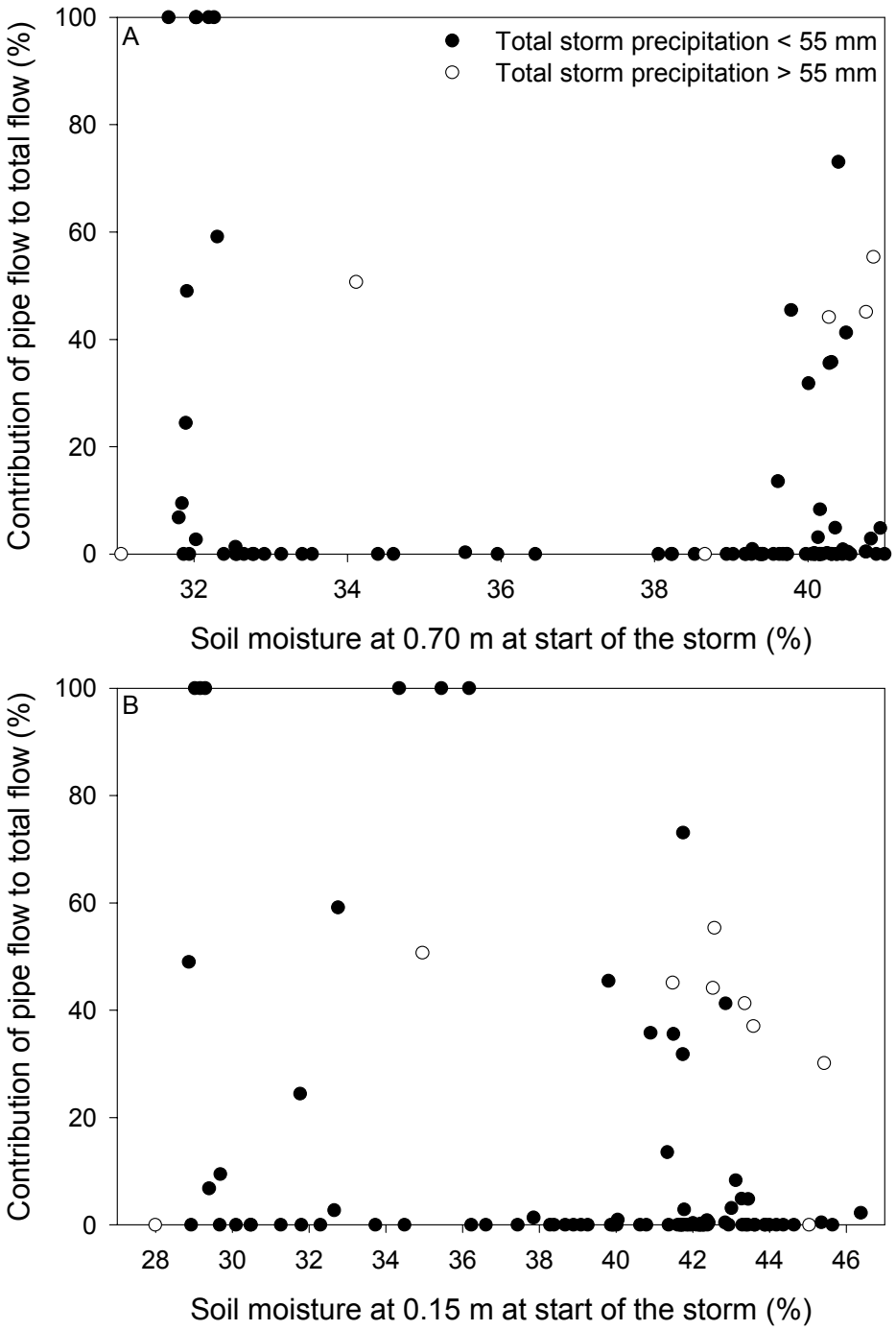

Figure 2.5 Seasonality in the relative importance of the individual soil pipes to total pipe flow. For the location of the soil pipes see Figure 2.1c.

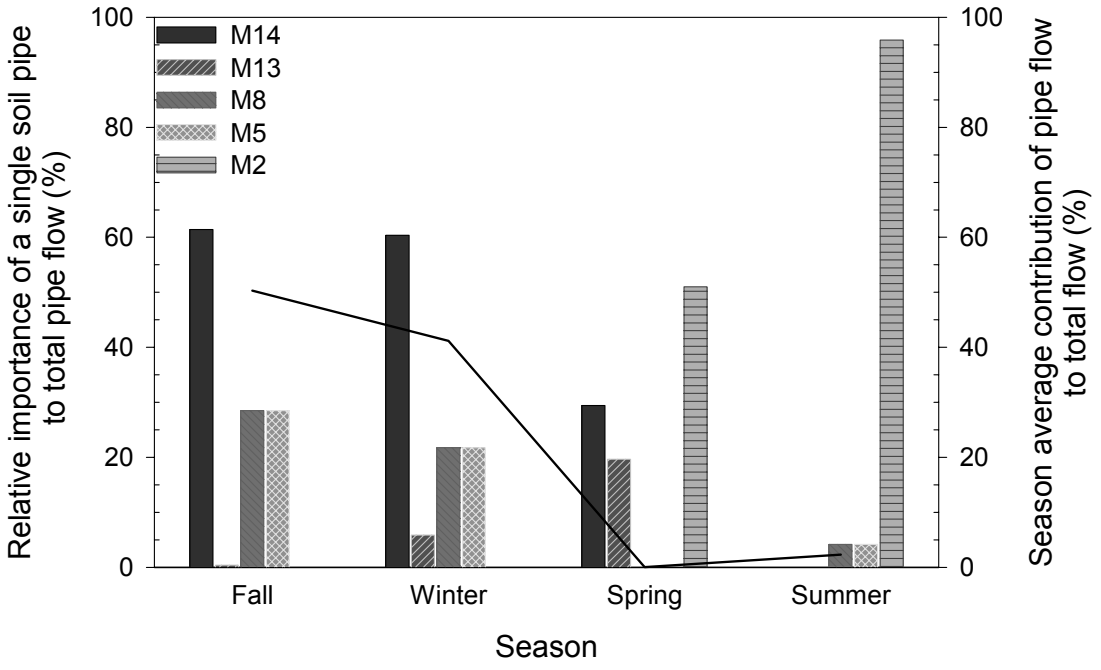

Figure 2.6 The threshold relationship between total storm precipitation and total flow (a), total matrix flow (b), and total pipe flow (c). The inserts show the same plots on a log–linear scale to show the smaller flow volumes and the two orders of magnitude increase in flow for storms larger than the threshold compared to storms smaller than the threshold.

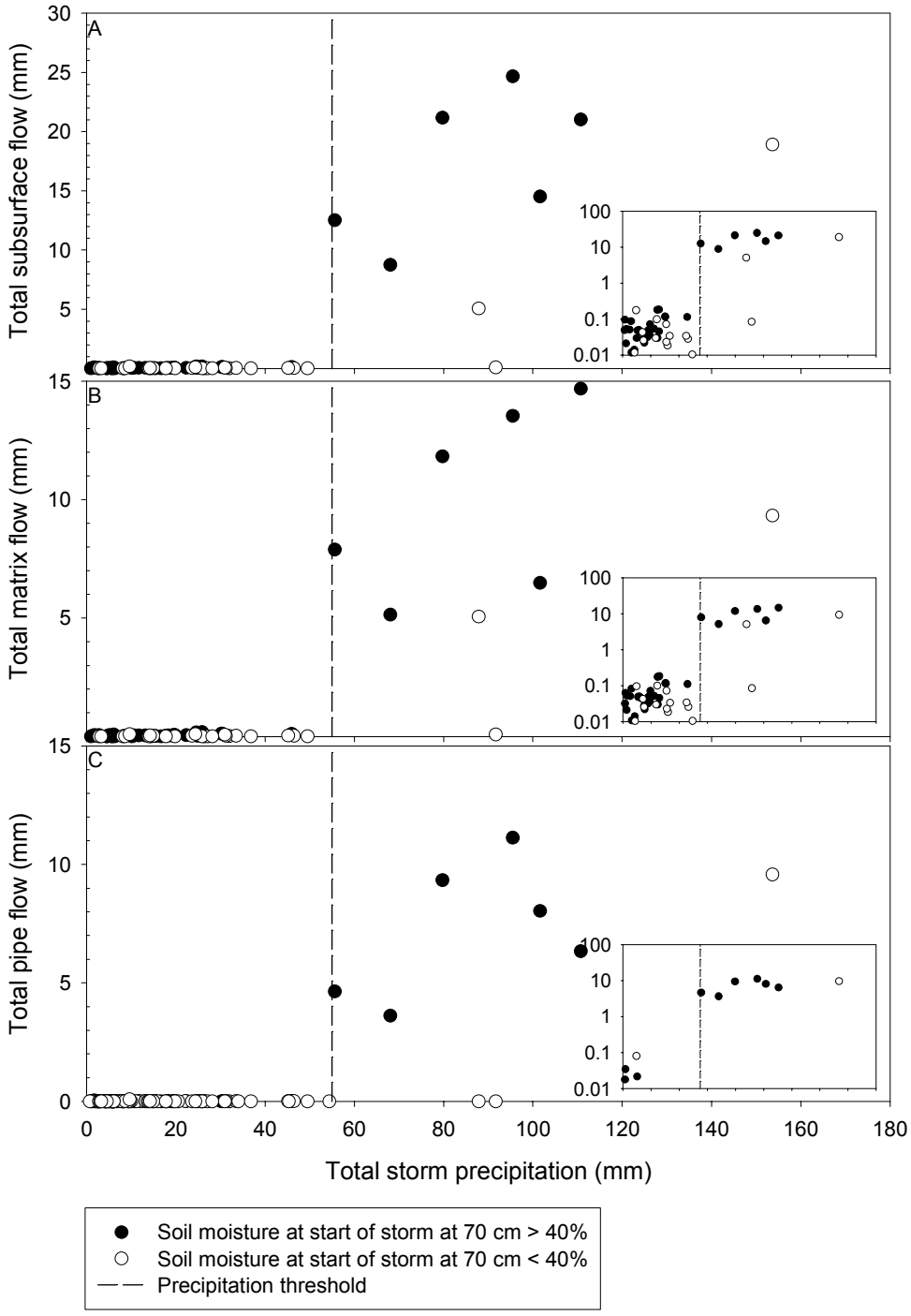

Figure 2.7 The relationship between total storm precipitation, volumetric soil moisture content at 0.70 m depth at the start of a storm and storm total subsurface flow.

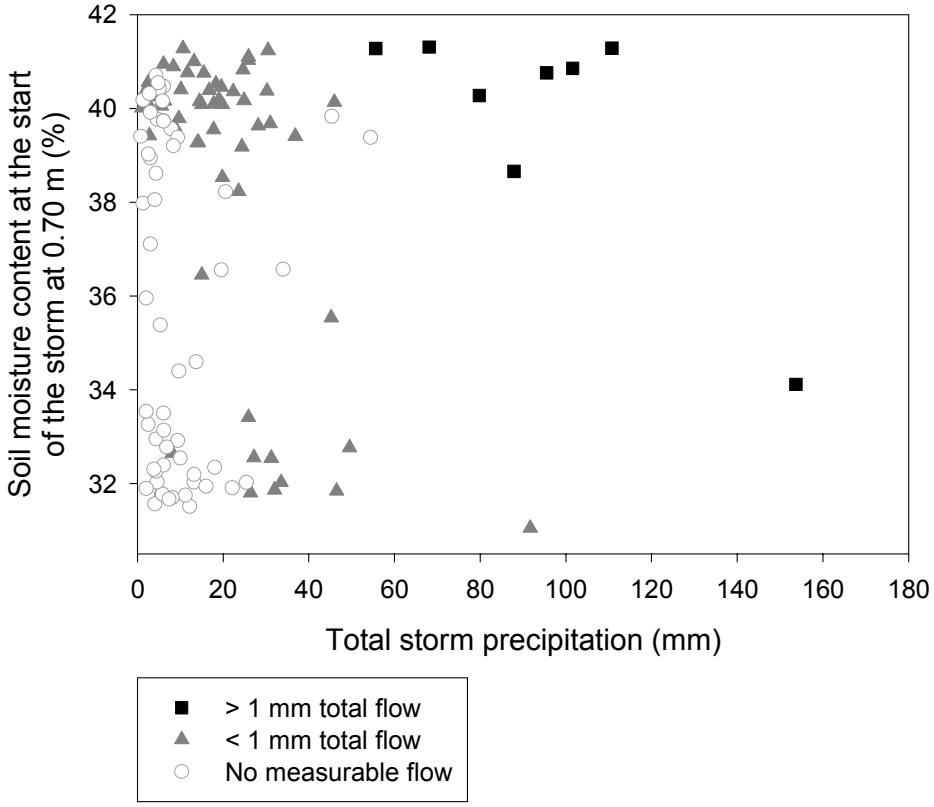

Figure 2.8 Cumulative frequency distribution of the calculated threshold for different subsets of the 147 storm dataset.

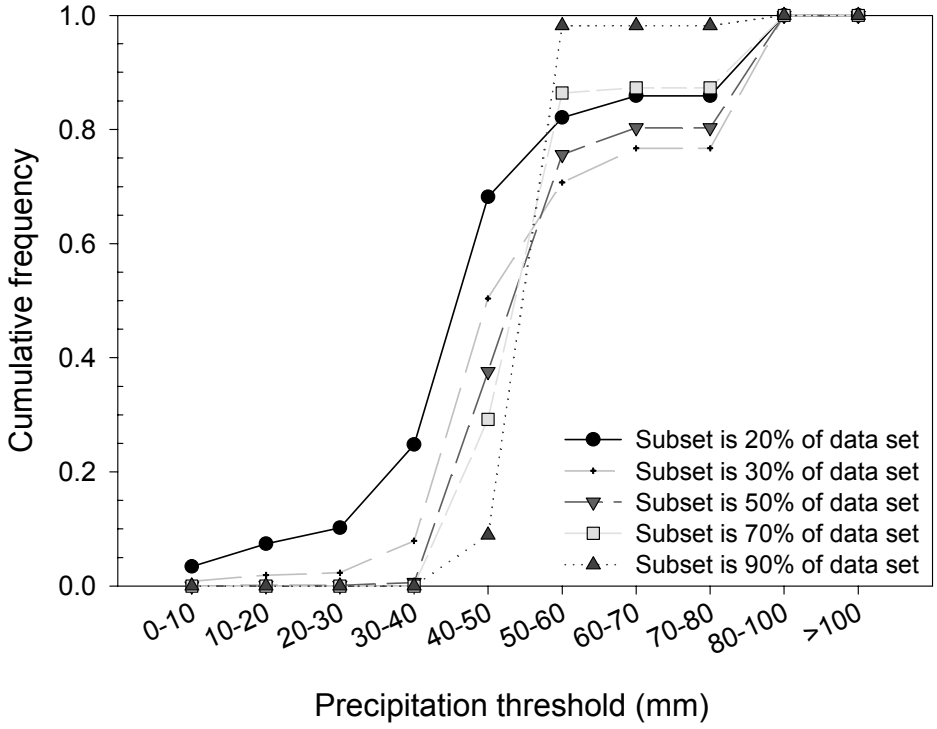

Figure 2.9 The distribution of flow across the trench face with increasing total flow (a), increasing total storm precipitation (b), antecedent moisture conditions (c) and for the different seasons (d). The dotted lines represents the average of the variance of the relative importance of trench sections to subsurface flow for all storms in a group.

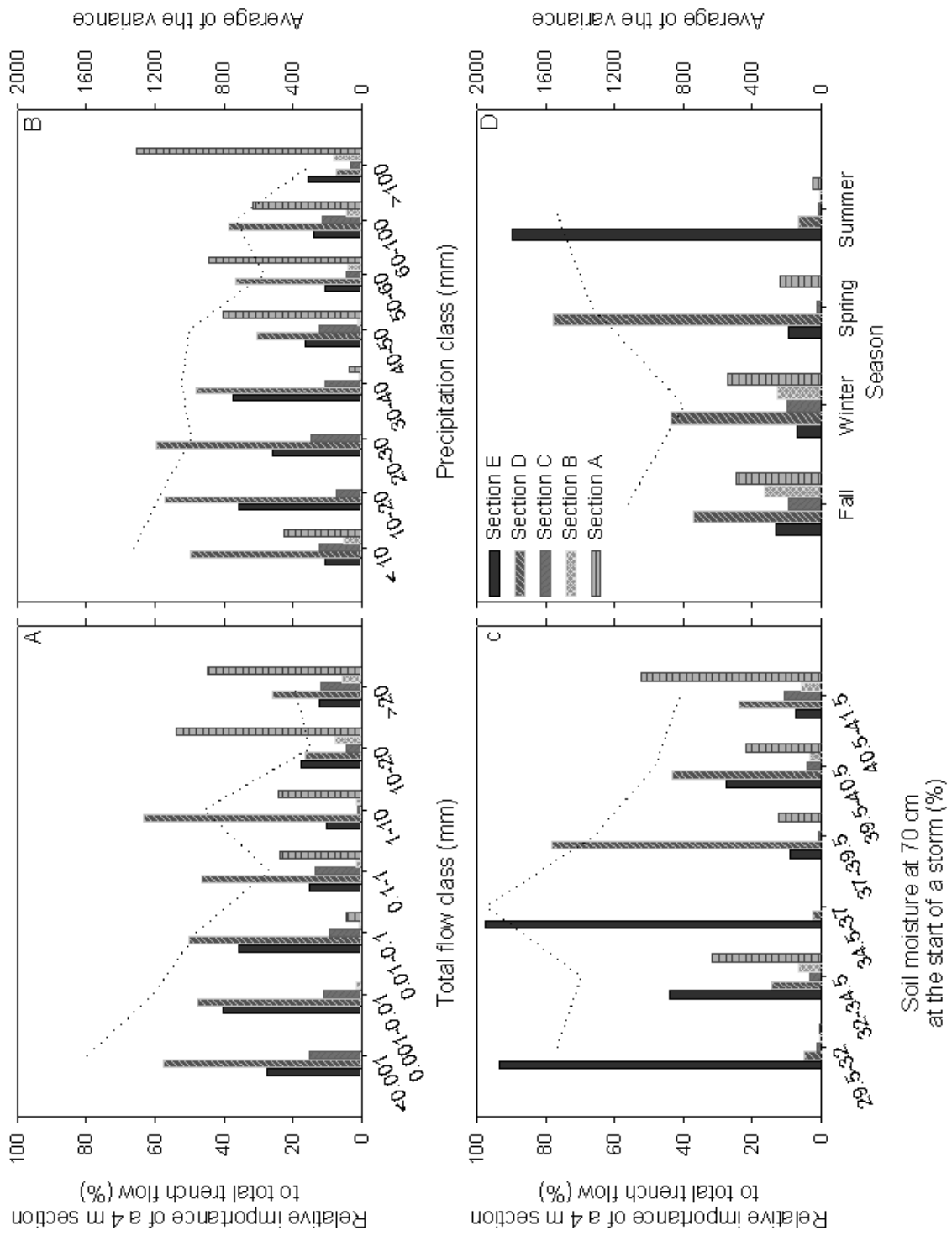

3 The fill and spill hypothesis: an explanation for observed threshold behavior in subsurface stormflow

3.1 Introduction

Subsurface stormflow is a dominant runoff producing mechanism in many upland environments around the world (Bonell, 1998). One of the most common prerequisites for subsurface stormflow initiation and generation is the development of saturation at the soil-bedrock interface during events (McGlynn et al., 2002). Few studies have quantified the development of subsurface saturation spatially and its relation to hillslope characteristics. The most common observation from transect studies to date on impermeable bedrock is that there is a saturated wedge that expands upslope from a streambank, riparian zone or trench with increasing precipitation (e.g. Whipkey, 1965; Weyman, 1973; Atkinson, 1978; Wilson et al., 1990; Buttle and Turcotte, 1999). For soils underlain by highly permeable bedrock Anderson et al. (1997) showed that the areas of subsurface saturation correspond to the areas of bedrock exfiltration.

While subsurface stormflow has been studied in detail for decades, only recently has the non-linearity of the process been realized. Threshold-like subsurface storm has been reported for the Panola trenched hillslope (the site of the present study). An analysis of 147 storms (Chapter 2) showed a 55 mm precipitation threshold for significant (>1 mm) subsurface flow to occur. For storms with more than 55 mm of precipitation, storm total subsurface flow was almost two orders of magnitude larger than storm total subsurface flow from storms smaller than 55 mm.

Precipitation thresholds for subsurface stormflow generation may be a wide spread phenomena. Re-examining earlier hillslope literature suggests that, while not always explicitly acknowledged, thresholds for subsurface stormflow generation have been observed in the past (Figure 3.1). For example, Whipkey (1965) showed a precipitation threshold of about 35 mm for subsurface flow initiation during dry conditions (Figure 2, page 79 in Whipkey, 1965), but a threshold is not evident during wet conditions. Data in Mosley (1979) (Table 1, page 798) suggests a precipitation threshold for flow initiation of about 23 mm for the Maimai catchment in New-Zealand. Peters et al. (1995) showed a precipitation threshold of 8-17 mm to produce hillslope and

stream response at their Plastic Lake catchment in Canada. Tani (1997) showed a 20 mm precipitation threshold response for subsurface flow from a hillslope trench on Honsyu Island in Japan.

Notwithstanding the observation of threshold-like subsurface stormflow, a clear process understanding for what is responsible for the threshold behavior at the hillslope scale is lacking. It was hypothesized that the development of subsurface saturation at the soil-bedrock interface was the first order control on lateral subsurface flow and the precipitation threshold (Chapter 2). Results from a 2-dimensional finite element model (HYDRUS-2D, Šimůnek et al., 1999) for a transect with actual surface and bedrock topography data from the study hillslope showed that subsurface saturation at the soil-bedrock interface occurred for storms smaller than 55 mm. Micro-topographic relief of the bedrock inhibited the extension and connection of subsurface saturated areas down to the trench face during small to medium size storms (Appendix 1). The 2-D transect model results indicated that subsurface saturation began in upslope areas, where the soil was shallowest and then expanded in a downslope direction. At local shallow depressions in the bedrock micro-topography, transient saturation filled up these depressions before water spilled laterally over the bedrock ridge on the edge of the depression. This appeared to be the first order control on how the subsurface saturated area expanded further downslope (Appendix 1). It was not only transient saturation development but bedrock micro-topographic relief that inhibited the connection of subsurface saturated area to the trench face, which was responsible for the observed non-linear relation between precipitation and subsurface flow.

While transect studies and 2-dimensional models are useful, they can not show the 3-dimensional spatial connectivity of subsurface saturation across the hillslope. We instrumented the Panola hillslope with a dense grid of maximum rise and recording wells to examine if the area of subsurface saturation expands in a downslope direction as shown by the model results or expands upslope in a saturated wedge like fashion.

The general aim of the paper is to develop an explanation for threshold behavior in subsurface stormflow at Panola and elsewhere. Specific questions we address using these new data are:

- What is the spatial pattern of subsurface saturation on the hillslope and how does this change with increasing precipitation?
- Is there a minimum water level necessary for significant (> 1mm) subsurface flow to occur at the trench face?
- Does the development of subsurface saturation across the hillslope explain the observed precipitation threshold for significant subsurface flow at the trench face?

3.2 Study site

The Panola Mountain Research Watershed (PMRW) is located in the Panola Mountain State Conservation Park about 25 km southeast of Atlanta, Georgia, USA. The forested watershed is dominated by hickory, oak, tulip poplar, and loblolly pine (Carter, 1978). The climate is humid and subtropical with a mean annual air temperature of 16.3^{o}C and mean annual precipitation of 1240 mm, spread relative uniformly over the year (NOAA, 1991). Rainfall tends to be of long duration and low intensity in winter, when it is associated with the passage of fronts, and of short duration but high intensity in summer, when it is associated with thunderstorms. On average there is one storm (defined as an event larger than 1 mm and separated by 24 hours of no precipitation) every 6.1 days. The dryness index (annual potential evaporation/annual precipitation) of the study site is 1.3, when potential evaporation is calculated using the Hargreaves equation (Hargreaves, 1975). Stream runoff at PMRW has a strong seasonal pattern. The highest baseflows occur during the dormant season (November through April), and the lowest during the growing season (May through October). Subsurface stormflow measured at the trenched hillslope is also highly seasonal. Average runoff ratios from the hillslope for the 1996-1998 are period 6, 10, 1 and less than 1% for the fall, winter, spring and summer respectively (Chapter 2).

The study hillslope is located 30 m upslope from an ephemeral stream. The lower boundary of the study hillslope is formed by a 20 m wide trench to bedrock while a small bedrock outcrop forms the upper boundary of the hillslope. The site and infrastructure have been described in detail in McDonnell et al. (1996), Freer et al. (2002) and only the features relevant to the present study are discussed below.

The surface topography of the study hillslope is relatively planar but has a small depression near the middle of the hillslope (Figure 3.2a). The bedrock topography is highly irregular and characterized by a dendritic shaped hollow (Figure 3.2b). Soil depth on the study hillslope was measured on a 2 by 2 m grid. The average soil depth of the study hillslope is 0.63 m and ranges from 0 to 1.86 m (Figure 3.2c). The correlation length of soil depth is 13 m. There is an area of deep soils across the hillslopes between 15-22 m upslope from the trench. This is caused by a large depression in the bedrock. This area of deep soils will be called the *bedrock depression* in the remainder of this paper. Upslope from the bedrock depression, soils are generally shallow. The average soil depth of the area more than 25 m upslope from the trench is 0.51 m. Directly downslope of the bedrock depression is an area of shallower soils which will be called the *bedrock ridge* in the remainder of this paper (Figure 3.3). This bedrock ridge results in an area of high bedrock downslope index approximately 16 m upslope from the trench (directly upslope from the bedrock ridge) (Figure 3.2d). The downslope index is a topography-based index and is considered a measure of impedance to local drainage by the downslope topography (Hjerdt et al., in review). A high downslope index indicates a large impedance to local drainage. Soil depth on the lower 15 m of the hillslope is highly variable. The deepest soils are located in the area with high bedrock accumulated area (the *bedrock hollow*). Figure 3.3 shows a representative profile of the surface and bedrock topography on an upslope transect.

The soil type across the study hillslope is relatively uniform and best described as a light colored sandy loam soil with little textural differences, except for the 0.15 m upper humus rich layer. We found a coarser more saprolitic layer under this soil profile only in

the area of very deep soils (located 18-22 m upslope from the trench). The thickness of the saprolitic layer was 0.15-0.35 m.

3.3 Methods

We installed 135 crest stage gauges filled with cork dust on an approximately 2 by 2 m grid across the lower hillslope and an irregular but close to 4 by 4 m grid across the remainder of the hillslope (Figure 3.2a). These 19 mm diameter PVC wells were augered to refusal, screened over the lower 200 mm and installed on the soil-bedrock contact. The maximum water level rise was measured after each storm during the January-August 2002 period. During two storms the maximum and actual water level were also measured during the storm. Subsurface saturation at the hillslope was short-lived, lasting less than 1 day after the end of a storm.

In addition to the grid of crest stage gauges, 29 recording wells were installed. These recording wells were located on two transects and in a region of high bedrock contributing area on the lower 15 m of the hillslope (Figure 3.2b). These 51 mm diameter PVC wells were augered to refusal and screened over the entire length. The water level was measured every 5 minutes from January-June 2002 using capacitance rods (Trutrack, New Zealand). The capacitance rods could not measure water levels within 75 mm of the soil-bedrock interface. Subsurface saturation was high and wide spread enough to be measured by the capacitance rods during two storms in the January-June 2002 period. These storms are the February 6 2002 storm, a low intensity long duration storm (59 mm) and the March 30 2002 storm, a small low intensity storm in the morning (12 mm) and in the afternoon (12 mm) followed by a very intense thunderstorm in the evening of that day (37 mm).

We also installed one piezometer pair in an area of deep soils and high bedrock downslope index (Figure 3.2d). The deep piezometer was augered to refusal and installed in the coarser more saprolitic layer below the soil. The shallow piezometer of the piezometer pair was located 0.38 m higher in the profile, immediately above the

saprolitic layer. Both piezometers were screened over the lower 0.15 m. The head in these piezometers was measured every 5 minutes between January and June 2002 with capacitance rods.

Lateral subsurface flow was measured at a 20-m long trench, excavated normal to the fall line of the slope down to bedrock in 1995. The trench was divided into ten 2-m sections and discharge from each 2-m trench section and from five individual soil pipes was measured by routing the flow through tipping-bucket gages. The number of tips was recorded every minute. Additional details of the trench and the flow-collection system are described in McDonnell et al. (1996), Freer et al. (1997 and 2002) and Burns et al. (1998).

3.4 Results

3.4.1 Spatial extent of subsurface saturation

The maximum extent of the area of subsurface saturation increased with increasing storm size (Figure 3.4 and 3.5a). The spatial pattern of subsurface saturation was persistent from one storm to another. During small storms (< 10 mm total rainfall) subsurface saturation at the soil-bedrock interface occurred only in a small area on the midslope near well 9.20 (see Figure 3.2c for the location of this well). During medium size storms (10-55 mm), the area of subsurface saturation increased in the across-slope and upslope direction compared to the area of subsurface saturation during smaller storms. In addition there were a few isolated spots of subsurface saturation closer to the trench face. For these events, the large and connected area of subsurface saturation however was located more than 18 m upslope from the trench and disconnected from the trench face. During the largest storms (>55 mm), subsurface saturation became more widespread across the hillslope and better connected to the trench face. There was a large increase in the area of subsurface saturation that was connected to the trench between the 52 mm rainstorm on January 22 and the 59 mm rainstorm on February 6. The antecedent conditions for these low intensity storms were similar. The 7-day antecedent precipitation index was 0.9 and 0.7 mm/day for the January 22 and February 6 storm respectively.

We found similar patterns of increasing subsurface saturated area with increasing precipitation during storms when measurements of the maximum (and current) water level were made during a storm.

The relation between storm total precipitation and the maximum area of subsurface saturation was nearly linear for the winter months (Figure 3.5a). The relation between the maximum area of subsurface saturation and total subsurface stormflow for this period was highly non-linear (Figure 3.5b).

3.4.2 Relation between maximum water level and total subsurface flow

The relation between storm total subsurface flow at the 20-m long trench and the maximum water level above bedrock in well 9.20 (near the location where subsurface saturation occurs during small storms (see Figure 3.4)) was highly threshold-like (Figure 3.6a). When the maximum groundwater level above bedrock in well 9.20 was less than 200 mm, storm total subsurface flow was small (less than 0.1 mm). When the maximum water level above bedrock in well 9.20 was higher than 225 mm, subsurface flow was more than 75 times larger than when the maximum water level above bedrock was less than 200 mm.

The relation between the maximum water level above bedrock in well 9.20 and the maximum subsurface flow rate was also very non-linear (Figure 3.6b). When the maximum water level in well 9.20 was less than 200 mm above bedrock, the maximum subsurface flow rate at the trench was less than 0.02 mm/hr. When the maximum water level was higher than 225 mm above bedrock, the maximum subsurface flow rate was more than 20 times higher than when the maximum water level was less than 200 mm. Although the February 6 and the March 30 storm had very different maximum rainfall intensities, the maximum subsurface flow rate was relatively similar. The 30-minute maximum rainfall intensity was 5.6 mm/hr during the February 6 storm and 62.4 mm/hr during the March 30 storm. The maximum subsurface flow rate was 0.29 and 0.36 mm/hr for the February 6 and March 30 storm respectively.

3.4.3 Temporal response of subsurface saturation

Figure 3.7 shows the temporal water level response in selected recording wells and the combined subsurface flow rate from a 4-m wide section of the trench below these wells. The wells shown in Figure 3.7 are located on a transect that follows the topographic lows in the bedrock topography, down from well 9.20 (Figure 3.2b). The 4-m wide trench section located downslope from this transect is the trench section with the highest bedrock contributing area and the section that delivers, on average, 43 % of storm total subsurface flow (Chapter 2).

During the February 6 storm there was an immediate (within 1 hour) eight fold increase in subsurface flow rate at 20:30 hr (Figure 3.7a). This large increase in subsurface flow rate was not related to an increase in rainfall intensity. Well 9.20, located in the area where subsurface saturation developed during the small storms (see Figure 3.4), was the first well to respond. After this well responded, all other wells located in the bedrock hollow downslope from this well (i.e. the area with high bedrock accumulated area, see Figure 3.2b) responded. The wells located closest to well 9.20 responded first and the wells located furthest downslope responded last. These wells located furthest downslope from well 9.20 responded before the large increase in subsurface flow rate. Wells located downslope from well 9.20, but outside the bedrock hollow, did not respond at all.

During the high intensity thunderstorm on March 30, flow at the trench started during the peak of the thunderstorm. The subsurface flow rate declined 15 minutes after the peak rainfall intensity; having a second peak on March 31 at 0:15 hr, almost 3 hours after the end of the thunderstorm (Figure 3.7b). Well 9.20 was the first well to respond to the small rainfall events during the morning and afternoon. The water level in well 9.20 increased rapidly in response to the thunderstorm. Similar to the February 6 storm, all wells downslope from well 9.20 responded later than well 9.20. Again, the upslope wells (closest to well 9.20) responded before the downslope wells (furthest from well 9.20) responded, and the wells furthest downslope responded before the second increase in

subsurface flow rate. Water levels in the upslope wells already started to recede before the wells furthest downslope had started to respond (Figure 3.7b).

The timing of subsurface saturation development was complex for wells located upslope from well 9.20. These wells responded after well 9.20 had started to respond. For the high intensity March 30 storm this lag was very small (on the order of minutes). During the March 30 storm, the time of first response was related to soil depth (the first response in the shallowest soil areas). This relation was not as clear for the February 6 storm.

We observed a similar response in wells located 2 to 4 m upslope from the riparian zone during the March 30 storm (Figure 3.8). Water levels in these wells showed either a double peak (e.g. well 6.8), a period of slower recession (e.g. well 6.10), or a first response (e.g. well 6.2) concurrent with or within 1.5 hours of the second peak in subsurface flow rate at the trench. Other wells showed only a single peak directly after the thunderstorm (e.g. well 6.12).

The relation between the time of the start of measurable subsurface saturation and the distance upslope from the trench face was linear (Figure 3.9). The time of response that was used for the trench (distance 0), was the time of the increase in subsurface flow rate (Figure 3.7). The time of response that was used for well 9.20 for the March 30 storm was the time of the rapid increase in water level (March 30 2002 21:20 hr). A similar linear relation also existed between the time of the maximum water level and the upslope distance. From this linear relation, the flux of the water that moved downslope over the bedrock could be calculated. The calculated flux was 4 m/hr during the February 5 event and 8 m/hr during the March 30 event. The vertical matrix saturated conductivity measured in a large soil core from an adjacent hillslope was 0.64 m/hr (McIntosh et al., 1999). However the lateral saturated conductivity of the hillslope could be larger than the vertical saturated conductivity of the soil core because of the presence of soil pipes and anisotropy. Soil pipes, particularly at the soil-bedrock interface, delivered water to the

trench face (minutes to two hours) before water seeped out of the trench face matrix during both storms.

For the March 30 storm, there was a third, but much smaller, increase in subsurface flow rate at 4:00 hr on March 31 (Figure 3.7b). This increase in subsurface flow rate was due mainly to an increase in pipeflow from one soil pipe. None of the recording wells showed an increase in water level before or during this third increase in subsurface flow rate but some wells on the upper hillslope showed a slower recession between 0:00 and 4:00 hr. We speculate that this third increase in subsurface flow rate might have been caused by the arrival of water from the outcrop that forms the upper boundary of the hillslope. If this increase in subsurface flow rate was indeed due to the arrival of the flux from the outcrop, this would imply a flux of approximately 8 m/hr, which is comparable to the flux calculated from Figure 3.9b.

Subsurface saturation was short-lived, lasting less than 1 day after the end of the storm. The wells located 20 m upslope from the trench were an exception to this. These wells were located in the deep soil section upslope from the high bedrock downslope index section (see Figure 3.2d). Subsurface saturation in these locations was longer lived, up to 5-7 days after the end of the storm. The water level in these locations dropped on average 55 mm/day. The lower 0.15-0.35 m of these wells was located in coarser more saprolitic layers.

We calculated the direction of flow from the interpolated water levels in the high bedrock contributing area with the dense grid of wells. Flow was in a pure downslope direction. Subsurface saturation started in the deepest soil section (i.e. lowest parts of the bedrock) and filled more of the bedrock hollow from there (Figure 3.10). The bedrock topography confined the area of subsurface saturation to the main bedrock low. The bedrock low located 14 m from the right side of the hillslope (when looking upslope) was connected to the location of well 9.20 by other lows in the bedrock and filled with water.

The bedrock low 4 m from the right side of the hillslope (when looking upslope) was not connected upslope to other bedrock depressions and did not fill with water.

3.5 Discussion

3.5.1 Fill and spill behavior

Many of the common textbook images of how hillslopes 'work' include a description of a saturated wedge that expands in an upslope direction with increasing precipitation and contracts as a result of drainage (e.g. Weyman, 1973; Atkinson, 1978). While field studies have reported the development of a saturated wedge (e.g. Whipkey, 1965; Weyman, 1973 Wilson et al., 1990; Buttle and Turcotte, 1999), many of these have been based on transect information or a limited number of wells across a hillslope.

Subsurface saturation at the Panola study hillslope does not occur in the form of a saturated wedge that expands upslope. On the contrary, it expands downward from the upslope part of the hillslope towards the trench face, similar to the results visualized by the model runs with HYDRUS-2D (Appendix 1). Transient saturation at the Panola hillslope was accomplished via a combination of subsurface saturation in shallow soil areas (located on the upslope part of the hillslope) and subsurface saturation in the bedrock depressions (located on the midslope). Subsurface saturation always starts near the same location and expands outward from there (Figure 3.4). There needs to be a build up of water in the main bedrock depression before the subsurface saturated area can become connected to the trench face (schematically shown Figure 3.11). When the water level rises high enough for water to flow over a ridge on the edge of the main bedrock depression, water spills downslope and flows through (and mixes with soil water in) the depressions in the bedrock topography towards the trench face (Figure 3.11). When this water reaches the trench face, the subsurface saturated area becomes connected to the trench face and there is an immediate increase or a second peak in subsurface flow rate (Figure 3.7). Because the peak in subsurface flow rate is the result of the spilling of water over the bedrock topography, the peak subsurface flow rate is less dependent on the peak

rainfall intensity than one might have expected. This is similar to the more muted subsurface flow response for the transect with rough bedrock than for the transect with smooth bedrock topography shown by the numerical model (Appendix 1). Lateral flow appears to be restricted to the bedrock lows and thus only takes place on part of the hillslope, even during relatively large storms.

We believe that the small volume of subsurface flow before the large increase in subsurface flow rate is generated from localized areas of subsurface saturation that are not connected to upslope areas. These subsurface saturated areas are so localized and thin that they were not observed by measurements on the 2 by 2 m grid of crest stage gauges during smaller events or in the early stages of larger events, when measurements were made throughout the storm.

Soil depth and the bedrock topography appear to be the first order controls on subsurface saturation. Only minor variations in soil moisture with depth or across the hillslope occur during the winter months (Chapter 4; Appendix 2). Thus pre-event soil moisture variations are not the main control on the distribution of subsurface saturation during winter storms (Appendix 2).

We view the relation between the increased subsurface flow rate and the connection of the area of subsurface saturation to the trench face as the subsurface analogue of studies that have shown the relation between the connection of upslope and downslope saturated areas and an increase or second peak in streamflow (e.g. Burt and Butcher, 1985). We view the filling of depressions at the soil-bedrock interface with water, and the spilling of water over micro-topographic bedrock ridges also as the subsurface analogue of depression storage in overland flow processes (Dunne et al., 1991 and 1995; Darboux et al., 2001 and 2002). There surface irregularities have to be filled before saturated areas can become connected and overland flow can start. Here depressions in the bedrock micro-topography have to be filled before the subsurface

saturated area can become connected to the trench face and significant subsurface flow can be measured at the trench.

We view the start of subsurface saturation in the bedrock depression, the spilling of water downslope over the bedrock ridge after the water level increased to a certain level and the confinement of that water to the main bedrock low also as the subsurface analogue of the wetting up and streamflow generation process at the Tarrawara catchment in Australia (Grayson et al., 1997). There local terrain features determine the initial location of surface saturation. These sites do not correspond to the sites that would saturate first if steady state flow assumptions were applied. At some point runoff is generated and water moves down the depression, rapidly saturating the drainage lines from above (Grayson et al., 1997). Similarly here, once water levels in the bedrock depression rise high enough and flow over the bedrock ridge starts, water moves down the bedrock hollow (i.e. the subsurface drainage lines) and the bedrock hollow is rapidly saturated from above.

A saturated wedge upslope from a trench face can be an artifact of the trench itself (Atkinson, 1978). Although this possibility is often acknowledged, it is also often believed that the observed saturated wedge is real and would have occurred even if the trench was not there (e.g. Buttle and Turcotte, 1999). However, data from some other studies also suggest that upslope areas respond faster than downslope areas. For example data from McDonnell (1990; Figure 7, page 2826) shows that in the Maimai catchment in New Zealand tensiometers upslope on the hillslope respond before tensiometers located further downslope respond and that flow increases after the downslope tensiometers have started to respond. Sidle (1984) reports for steep forested hillslopes in Alaska that piezometers upslope and downslope respond simultaneously and that the shallow piezometric response did not resemble a wedge building from the slope base. Wilson et al. (1990) note that a perched watertable develops most quickly on their ridge and upper convex positions. Thus, the fill and spill process and the lack of a saturated wedge

expanding in an upslope direction shown here for the Panola hillslope may be a more wide spread phenomenon.

Hutchinson and Moore (2000) show that the watertable configuration follows the topography of the compacted till layer at their study site in Canada, but that with increasing flow, hydraulic gradients become more uniform in magnitude and direction across the hillslope. Here we show that at Panola only the main bedrock depression fills up with water once the spilling over the bedrock ridge occurs. Subsurface saturation is confined to this main bedrock depression (Figure 3.10) and flow is in a pure downslope direction.

The water level never rose high enough to overflow the main bedrock low during the storms of the 2002 study period. However, the filling of the bedrock depression (Figure 3.10) and the pure downslope direction of flow does seem to suggest that if water levels would rise considerably higher than observed in this study, water could spread over a larger width of the hillslope. While the bedrock topography is more complex at Panola, the pattern of filling of the bedrock hollow (vertically and laterally) is similar to that shown by Torres et al. (1998) for a site in Western Oregon.

3.5.2 Relation to the observed precipitation threshold for subsurface flow

Storm total subsurface flow at Panola is a threshold function of precipitation (Chapter 2). For a long term data set of 147 storms, we observed that significant subsurface stormflow (> 1 mm) did not occur for storms smaller than 55 mm of rainfall. For storms larger than 55 mm total rainfall depth, there was an almost two orders of magnitude increase in subsurface flow compared to storms smaller than 55 mm. In Chapter 2 we speculated that this precipitation threshold is related to the precipitation depth necessary for subsurface saturation at the soil-bedrock interface to occur (i.e. to overcome the soil moisture deficit and convert from tension to pressure). In the present study, we show that subsurface saturation occurs during storms smaller than 55 mm and that the area of subsurface saturated area increases with increasing precipitation (Figure

3.5a). But the relation between the maximum area of subsurface saturation and storm total subsurface flow is non-linear (Figure 3.5b). In addition, there is a threshold-like relation between the maximum water level at an upslope location (well 9.20) and storm total subsurface flow or the maximum subsurface flow rate (Figure 3.6).

The observed development of subsurface saturation indicates that the precipitation threshold for subsurface flow is related to the extension of subsurface saturation to the trench face. When the subsurface saturated area becomes connected to the trench face, the subsurface flow rate increases more than seven fold. Results from this study show that this occurs when total storm precipitation is larger than 55 mm and the water level in the bedrock depression rises high enough that water spills downslope over the bedrock ridge. These results are similar to the HYDRUS-2D model results for this hillslope (Appendix 1). The precipitation threshold for significant flow to occur at the trench is thus dependent on the connection of the area of subsurface saturation to the trench face. This study thus shows that the small scale bedrock topography and the filling and spilling of water in depressions and over the bedrock micro-topography is responsible for the observed precipitation threshold for significant (>1 mm) subsurface flow.

One could speculate that if the trench would have been constructed 20 m upslope from the current location, so that it would be located upslope from the bedrock ridge, there might not be a precipitation threshold for significant subsurface flow because the subsurface saturated area that is connected to that trench face would increase more linearly with increasing precipitation. In that case, the fill and spill behavior observed in this study would not necessarily occur. Alternatively, if the trench would have been constructed further downslope, subsurface flow could be even more threshold-like if there would be more and deeper depressions in the bedrock between this point and the current trench. Comparison of the timing of water level response in wells located 2 to 4 m upslope from the riparian zone with the timing of subsurface stormflow at the trench however suggests that this difference might be small (Figure 3.8).

3.5.3 Why is well 9.20 the first to respond?

Subsurface saturation does not start at the trench but at locations upslope from the trench. These locations are characterized by shallow soils and a location of deep soils approximately 20 m upslope from the trench. We hypothesize that subsurface saturation occurs during medium size storms in the shallow soil areas because of the smaller soil moisture deficits in these areas compared to the deeper soil areas downslope. Prior to storms, soil moisture variations across the hillslope and with depth are small (Chapter 4; Appendix 2). Soil depth thus determines total soil moisture deficit. Well 9.20 is located in an area of high bedrock accumulated area (Figure 3.2b) and in an area of high bedrock downslope index (i.e. high impedance to drainage) (Figure 3.2d). We hypothesize that measurable subsurface saturation starts near the location of well 9.20 and occurs during small storms only in the area near well 9.20 because water is concentrated and then retained because of downslope damming. Only when the water level rises high enough, higher than the bedrock ridge downslope of the main depression in the bedrock, which is 200 mm at the location of well 9.20, does water spill downslope and does the subsurface saturated area become connected to the trench.

Alternatively, the area of subsurface saturation might be an area of exfiltration of water from the bedrock, as was shown in Anderson et al. (1997) for a permeable sandstone bedrock site in Western Oregon. We do not have piezometric data for the bedrock, but the head difference in the piezometer pair in the soil and saprolitic layer indicates that gradients were downward during the February 6 and March 30 storm.

3.6 Conclusion

We propose the fill and spill hypothesis as an explanation for observed threshold behavior in subsurface stormflow. This fill and spill hypothesis states that during small to medium size storms subsurface saturation occurs only (1) in areas with shallow soils, (2) in areas with a combination of high bedrock contributing area and high bedrock downslope index because water is concentrated and subsequently dammed by the bedrock topography downslope from it. Significant subsurface stormflow (> 1 mm)

occurs only when the subsurface saturated area becomes connected to the trench face. This occurs only when the bedrock depressions are filled and the water level in these depressions rises high enough for water to start spilling over the bedrock micro-topography (Figure 3.11). Then, water flows over the bedrock, through (and mixes with soil water in) the connected lows in the bedrock topography towards the trench face. When the flux of water reaches the trench face, the subsurface saturated area becomes connected to the trench face and there is an immediate seven fold increase in the subsurface flow rate. If the storm is large enough for the water level to rise high enough that spilling can occur (i.e. larger than the precipitation threshold), total subsurface flow is more than 75 times larger than when the spilling does not occur.

These results show that filling and spilling of water in the bedrock depression and over the bedrock ridge (Figure 3.11), thus the bedrock micro bedrock topography is responsible for the observed precipitation threshold for significant subsurface flow to occur (Figure 3.1).

The fill and spill hypothesis has significant implications for how we model subsurface stormflow behavior and the transport of nutrients associated with this flux. On sites with variable soil depth where explicit soil depth data is not available and an average soil depth across the hillslope is assumed, the filling and spilling of water in and over bedrock depressions is ignored and an important control on lateral flow, the distribution of subsurface saturated areas and the threshold behavior of subsurface flow generation are not represented.

3.7 References

Anderson, S. P., W.E. Dietrich, D.R. Montgomery, R. Torres, M.E. Conrad and K. Logue, Subsurface flow paths in a steep, unchanneled catchment, Water Resources Research 33(12): 2637-2653, 1997.

Atkinson, T. C. Techniques for measuring subsurface flow on hillslopes, in: Hillslope hydrology, edited by Kirkby, M. J., John Wiley and Sons Inc., New York: 73-120, 1978.

Bonell, M., Selected challenges in runoff generation research in forests from the hillslope to headwater drainage basin scale, Journal of the American Water Resources Association 34(4): 765-785, 1998.

Burns, D. A., R.P. Hooper, J.J. McDonnell, J.E. Freer, C. Kendall and K. Beven, Base cation concentrations in subsurface flow from a forested hillslope: The role of flushing frequency, Water Resources Research 34(12): 3535-3544, 1998.

Burt, T. P., and D.P. Butcher, Topographic controls of soil moisture distributions, Journal of Soil Science 36: 469-486, 1985.

Buttle, J. M., and D.S. Turcotte, Runoff processes on a forested slope on the Canadian Shield, Nordic Hydrology 30: 1-20, 1999.

Carter, M.E.B., A community analysis of the Piedmont deciduous forest of Panola Mountain State Conservation Park: Atlanta, Georgia, M. S. thesis, 126 pp., Emory Univ., Atlanta, Ga., 1978.

Darboux, F., Ph. Davy, C. Gascuel-Odoux and C. Huang, Evolution of soil surface roughness and flowpath connectivity in overland flow experiments, Catena 46: 125-139, 2001.

Darboux, F., Ph. Davy and C. Gascuel-Odoux, Effect of depression storage capacity on overland low generation for rough horizontal surfaces: water transfer distance and scaling, Earth Surface Processes and Landforms 27: 177-191, 2002.

Dunne, T., W. Zhang, and B. F. Aubry, Effects of rainfall intensity, vegetation, and microtopography on infiltration and runoff; Water Resources Research 27 (9): 2271-2285, 1991.

Dunne, T., K.X Whipple, and B.F. Aubry, Microtopography of hillslopes and the initiation of channels by Horton overland flow, In: Evolving Concepts in Fluvial Geomorphology, edited by: Costa J.E., A.J. Miller, K.W. Potter, P.R. Wilcock, American Geophysical Union, Geophysical Monograph, 27-44, 1995.

Freer, J., J. McDonnell, K.J. Beven, D. Brammer, D. Burns, R.P. Hooper and C. Kendal, Topographic controls on subsurface stormflow at the hillslope scale for two hydrologically distinct small catchments, Hydrological Processes 11: 1347-1352, 1997.

Freer, J.E., J.J. McDonnell, K.J. Beven, N.E. Peters, D.A. Burns, R.P. Hooper, B.T. Aulenbach and C. Kendall, The role of bedrock topography on subsurface stormflow, 10.1029/2001WR000872, 2002.

Grayson, R., A.W. Western, and F.H.S. Chiew, Preferred states in spatial soil moisture patterns: Local and nonlocal controls, Water Resources Research 33(12): 2897-2908, 1997.

Hargreaves, G.H., Moisture availability and crop production, Trans. Am. Soc. Agric. Eng. 18(5): 980-984, 1975.

Hjerdt, K.N., J. J. McDonnell, J. Seibert, and A. Rodhe, A new topographic index to quantify downslope controls on local drainage. Water Resources Research, in review.

Hutchinson, D. G., and R.D. Moore, Throughflow variability on a forested hillslope underlain by compacted glacial till, Hydrological Processes 14: 1751-1766, 2000.

McDonnell, J.J., A rationale for old water discharge through macropores in a steep humid catchment, Water Resources Research 26(11): 2821-2832, 1990.

McDonnell, J.J., J.E. Freer, R.P. Hooper, C. Kendall, D.A. Burns, K.J. Beven and N.E. Peters, New method developed for studying flow in hillslopes, EOS, Transactions of the American Geophysical Union 77(47): 465, 1996.

McGlynn, B., J.J. McDonnell, and D. Brammer, A review of the evolving perceptual model of hillslope flowpaths at the Maimai catchment, New Zealand. Journal of Hydrology 257: 1-26, 2002.

McIntosh, J., J.J. McDonnell and N.E. Peters, Tracer and hydrometric study of preferential flow in large undisturbed soil cores from the Georgia Piedmont, USA, Hydrological Processes 13: 139-155, 1999.

Mosley, M.P., Streamflow generation in a forested watershed, Water Resources Research 15: 795-806, 1979.

National Oceanic and Atmospheric Administration, Local climatological data, annual summary with comparative data, 1990, Atlanta, Georgia, 6 pp., Asheville, N. C., 1991.

Peters, D.L., J.M. Buttle, C.H. Taylor, and B.D. LaZerte, Runoff production in a forested, shallow soil, Canadian Shield basin, Water Resources Research 31(5): 1291-1304, 1995.

Sidle, R. Shallow groundwater fluctuations in unstable hillslopes of coastal Alaska, Zeitschrift fur Gletscherkunde und Glazialgeologie 20: 79-95, 1984.

Šimůnek, J., M. Sejna and M.Th. van Genuchten, The Hydrus-2d software package for simulating two-dimensional movement of water, heat and multiple solutes in variably saturated media. Version 2.0, IGWMC – TPS-53, International Groundwater Modeling Center, Colorado School of Mines, Golden, Colerado, 1999.

Tani, M., Runoff generation processes estimated from hydrological observations on a steep forested hillslope with a thin soil layer, Journal of Hydrology 200: 84-109, 1997.

Torres, R., W.E. Dietrich, D.R. Montgomery, S.P. Anderson and K. Logue, Unsaturated zone processes and the hydrologic response of a steep, unchanneled catchment, Water Resources Research 34(8): 1865-1879, 1998.

Weyman, D.R., Measurement of the downslope flow in a soil, Journal of Hydrology 20: 267-288, 1973.

Whipkey, R.Z., Subsurface stormflow from forested slopes, Int. Ass. Sci. Hydrol. Bull. 10(2): 74-85, 1965.

Wilson, G. V., P.M. Jardine, R.J. Luxmoore and J.R. Jones, Hydrology of a forested hillslope during storm events, Geoderma 46: 119-138, 1990.

Figure 3.1 Schematic representation of the threshold-like relationship between total storm precipitation and storm total flow under wet antecedent conditions. The lines represent the lines through the maximum observed storm total subsurface flow for a given storm total precipitation.

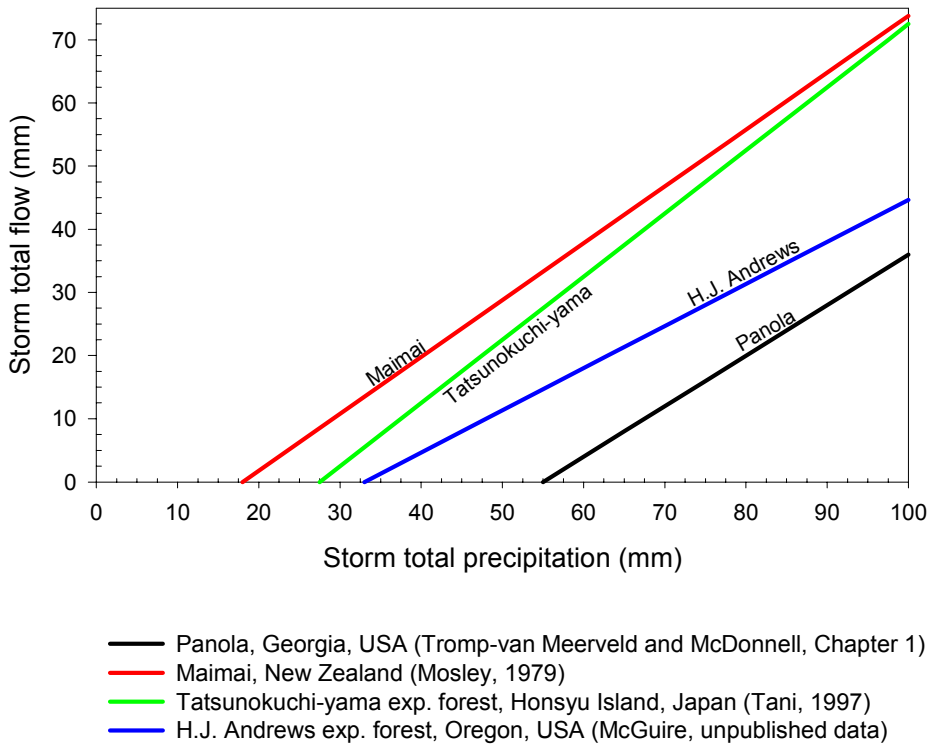

Figure 3.2 A map of the accumulated area based on the surface topography with the location of the crest stage gauges (a), the accumulated area based on bedrock topography with the location of the recording wells (b), soil depth with the location of well 9.20 (c), and the downslope index based on the bedrock topography with the location of the piezometer pair and the transect shown in Figure 3.10 (d). The filled squares shown in Figure 3.2b represent the recording wells shown in Figure 3.7.

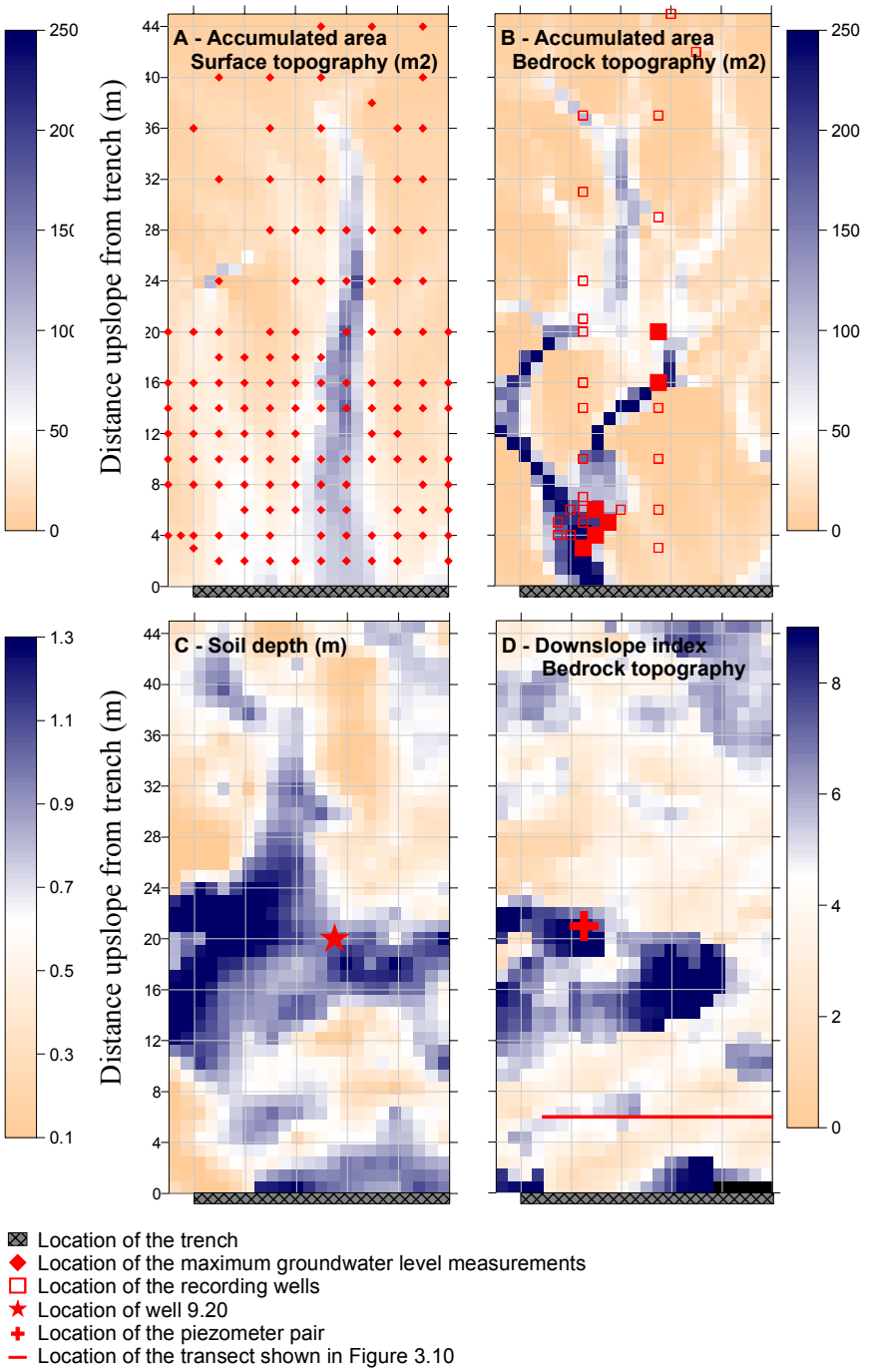

Figure 3.3 Surface and bedrock topography on an upslope transect across the hillslope.

Figure 3.4 The spatial distribution of subsurface saturation across the hillslope with increasing precipitation. The dark area indicates the area where subsurface saturation was observed; the white area indicates the area where no subsurface saturation was observed. The diamonds represent the measurement locations. Linear triangulation was used to interpolate between the measurement points.

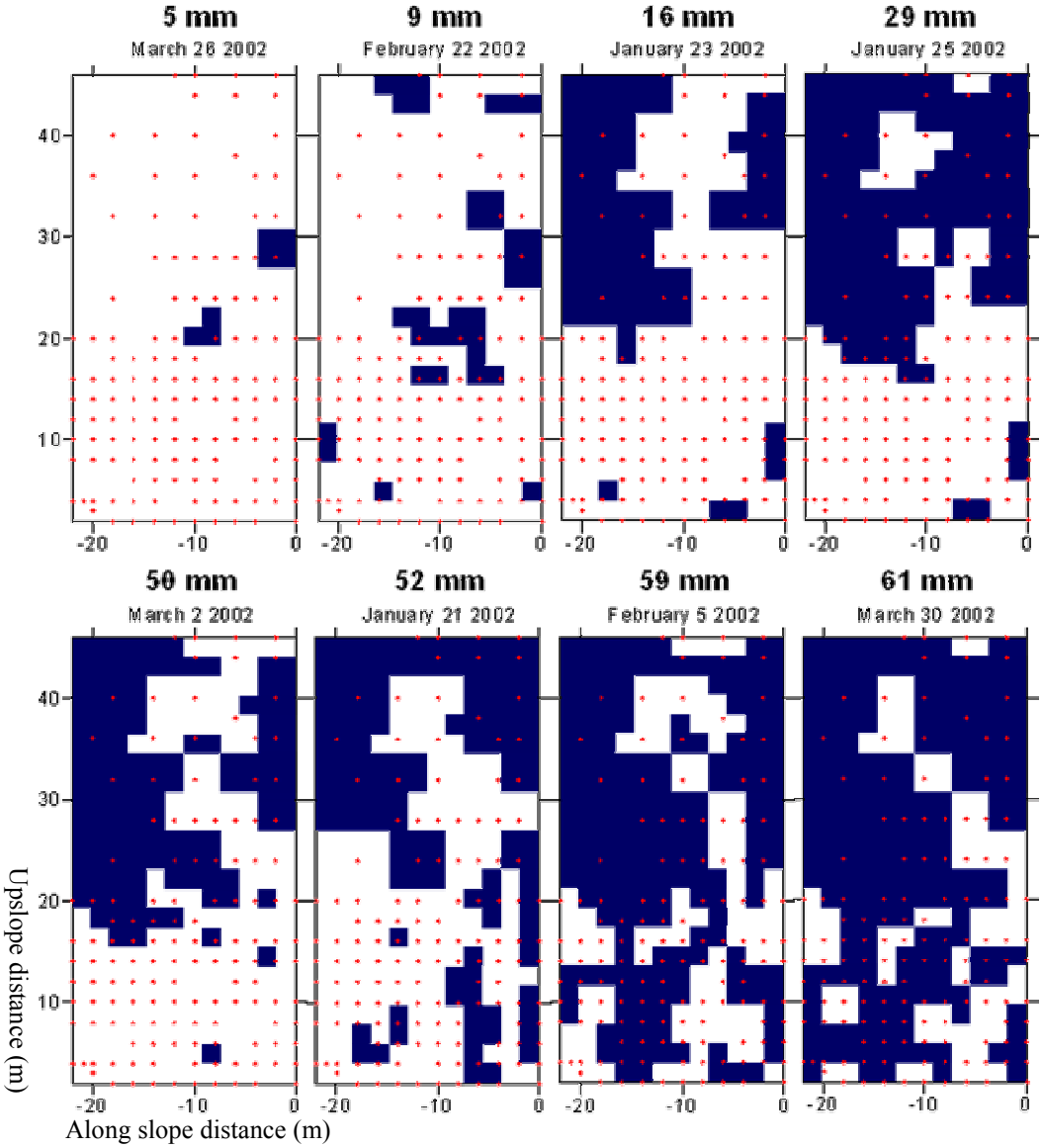

Figure 3.5 The relation between storm total precipitation and the maximum area of subsurface saturation (a) and the relation between the maximum area of subsurface saturation and storm total subsurface flow (b).

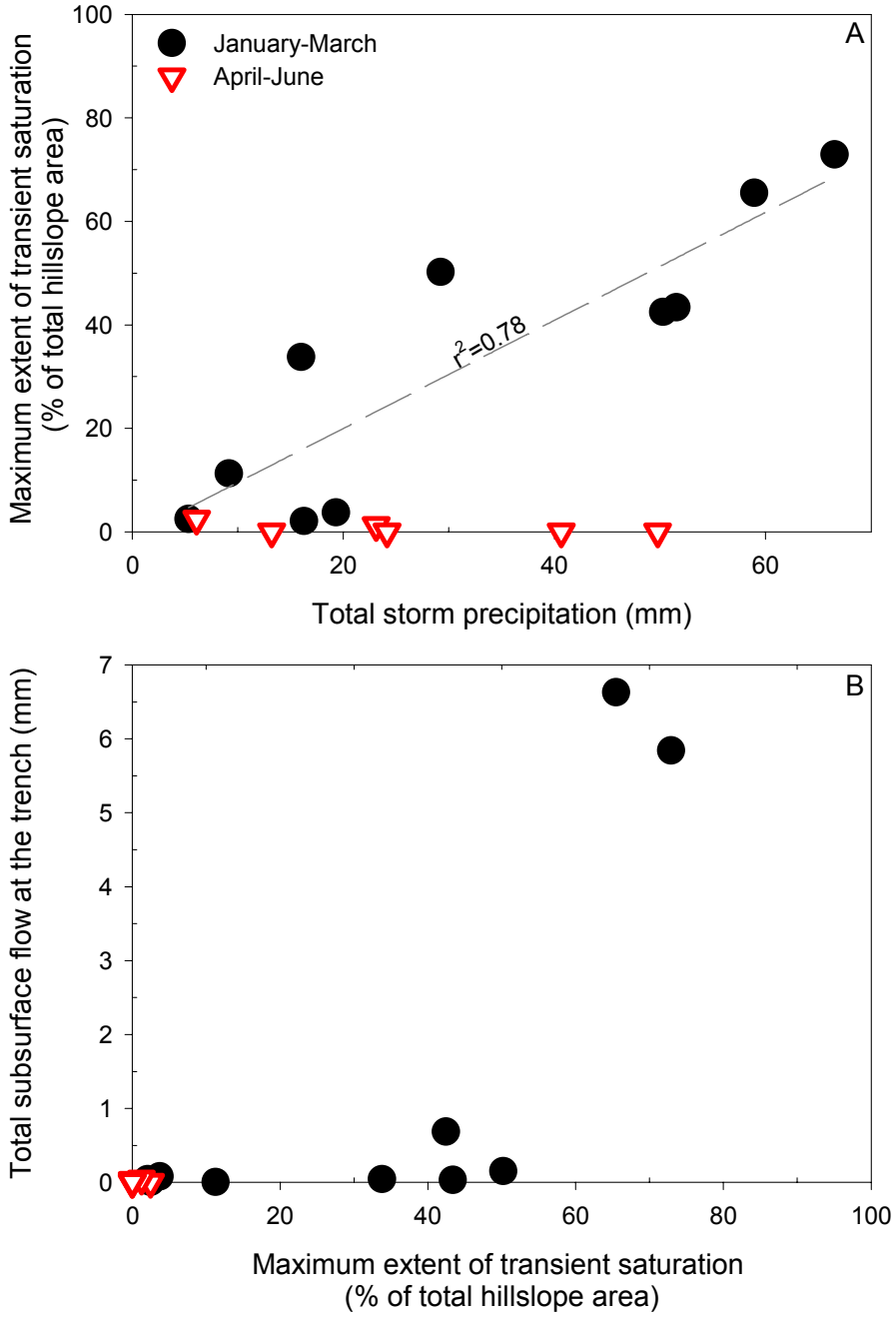

Figure 3.6 The relation between the maximum recorded water level in well 9.20 and total subsurface flow at the trench face (a) and the maximum subsurface flow rate (b).

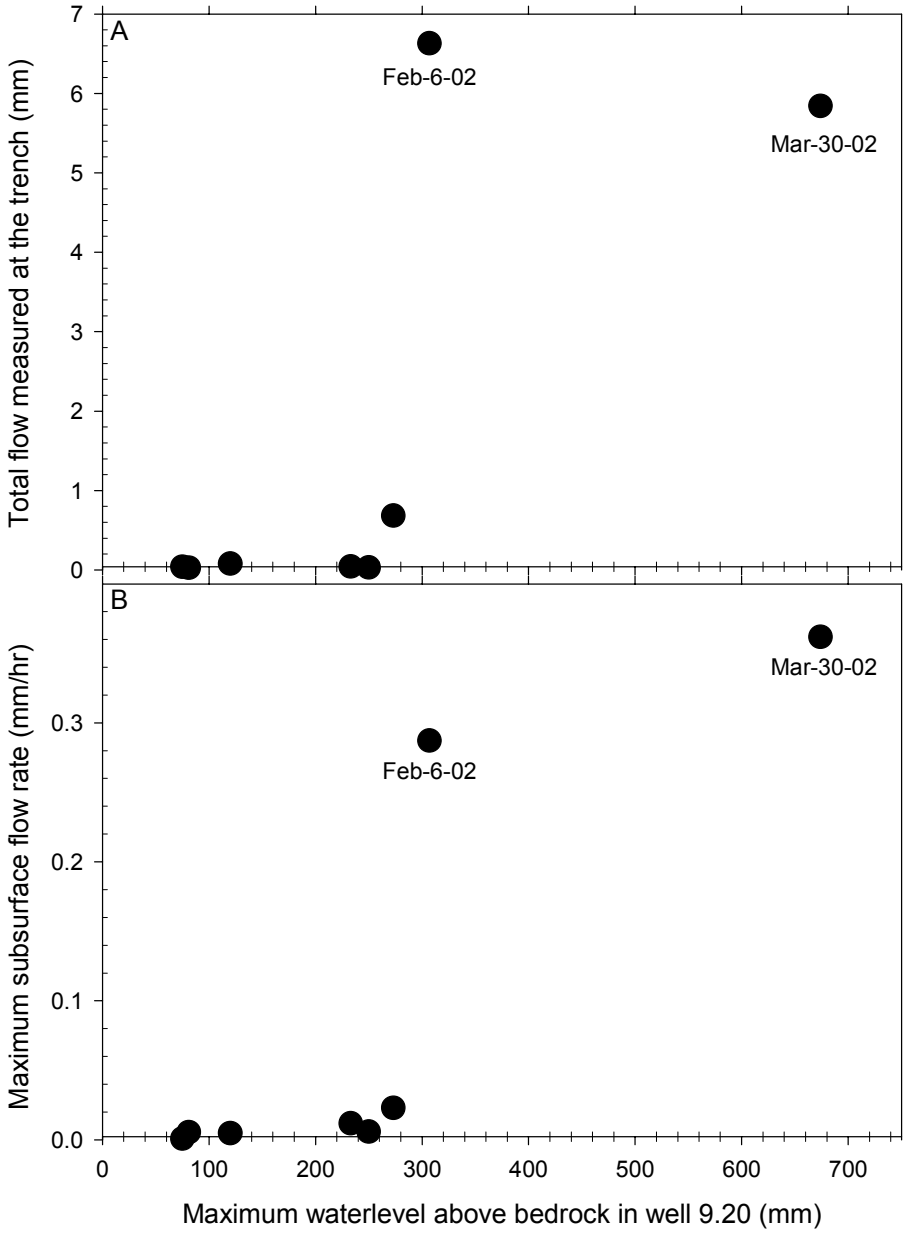

Figure 3.7 Precipitation intensity, well response and subsurface flow rate from the 4-m wide trench section directly downslope from the wells during the February 6 2002 storm (a) and the March 30 2002 storm (b). The locations of the wells shown in this figure are represented by filled squares in Figure 3.2b. The capacitance rods could not measure the water level within the first 75 mm from the bedrock.

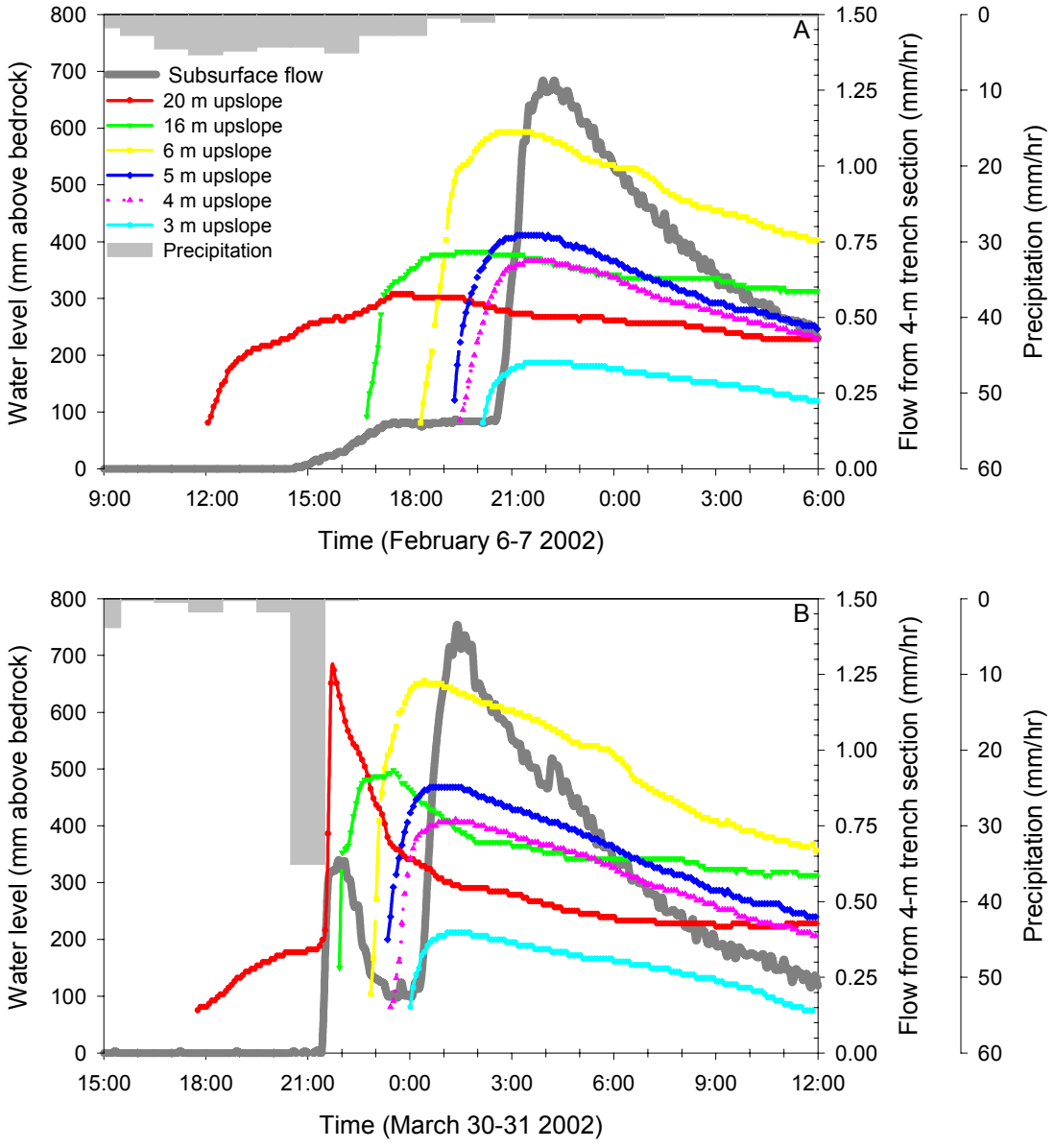

Figure 3.8 Total subsurface flow measured at the trench and water level response in wells 2-4 m upslope from the riparian zone during the March 30 2002 storm.

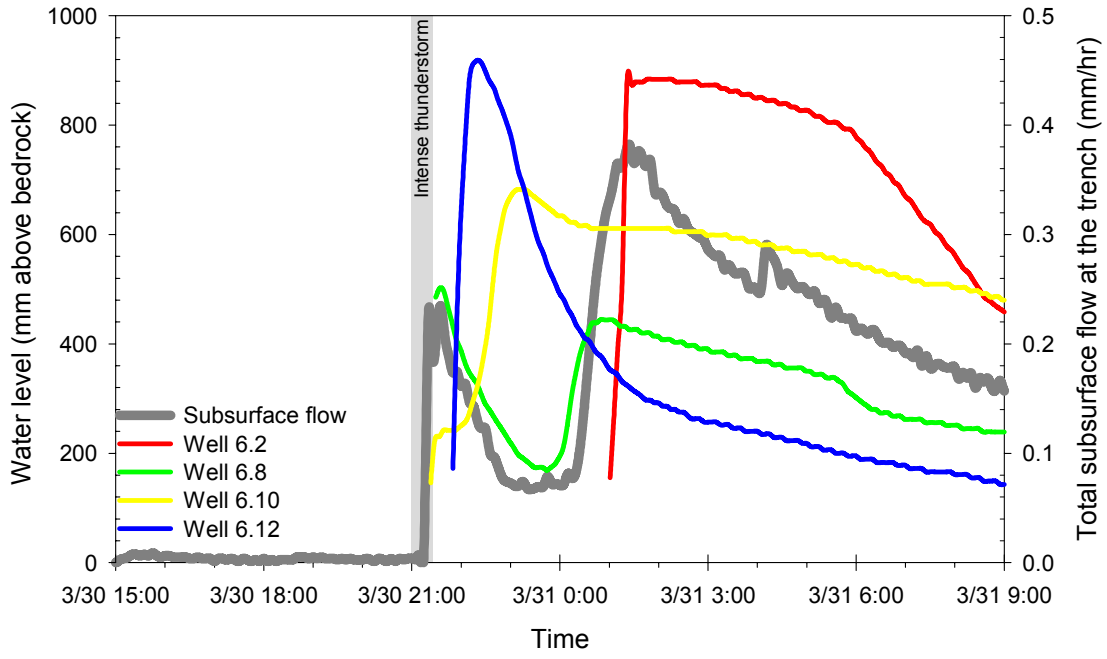

Figure 3.9 The difference between the time of the first response (closed circles) or time of the maximum water level for a recording well (open triangles) and the time of response in well 9.20 as a function of the distance of the well upslope from the trench for the February 6 2002 (a) and March 30 2002 storm (b). All wells located downslope from well 9.20 in the area with high (>150 m^2) bedrock accumulated area (i.e. bedrock low) are shown in this figure. See Figure 3.2b for the location of these wells.

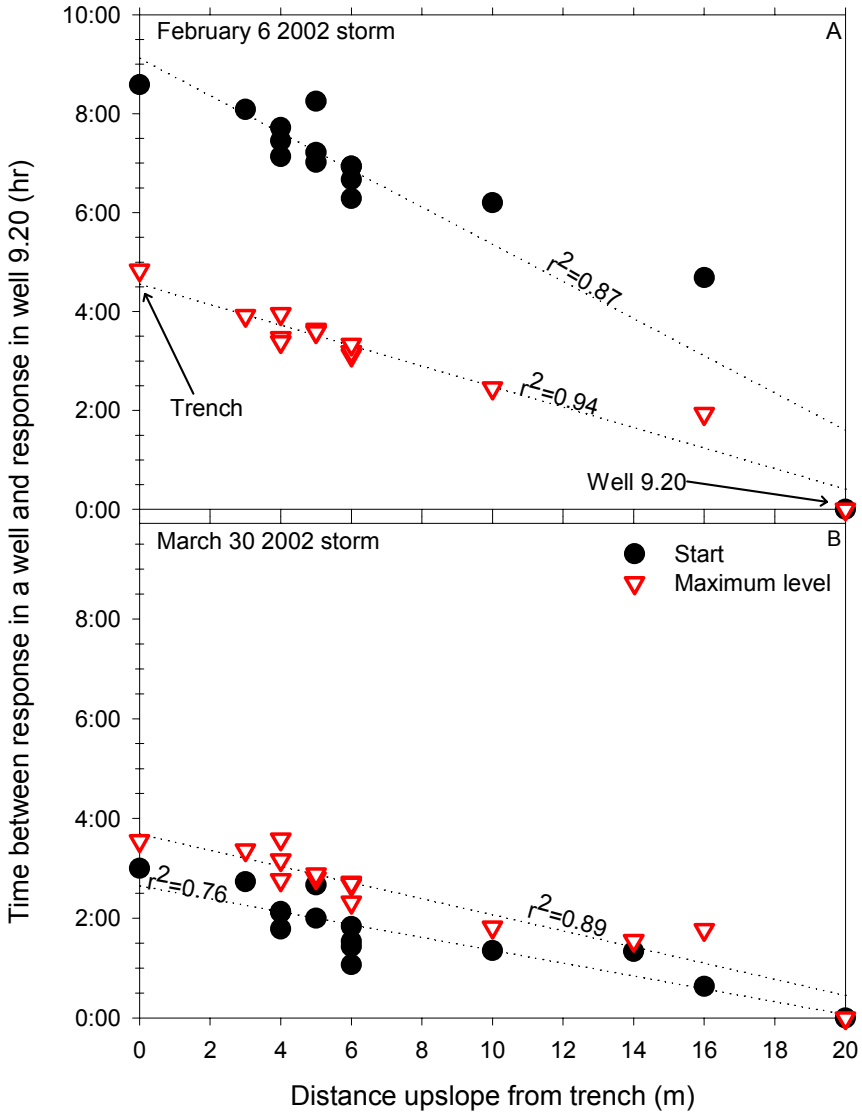

Figure 3.10 Water level rise on an across-slope transect located 6 m upslope from the trench during the February 6 (a) and March 30 2002 storm (b). The thick solid lines represent the surface topography and the bedrock topography, the black line represents the maximum groundwater level. The grey lines represent the pattern of water level rise at 10 minute intervals between 2/6/02 18:24 and 19:54 (a) and between 3/30/02 21:51 and 3/30/02 23:21 (b). The times next to the lines of water rise are in minutes after the start of the storm. The location of the transect is shown in Figure 3.2d.

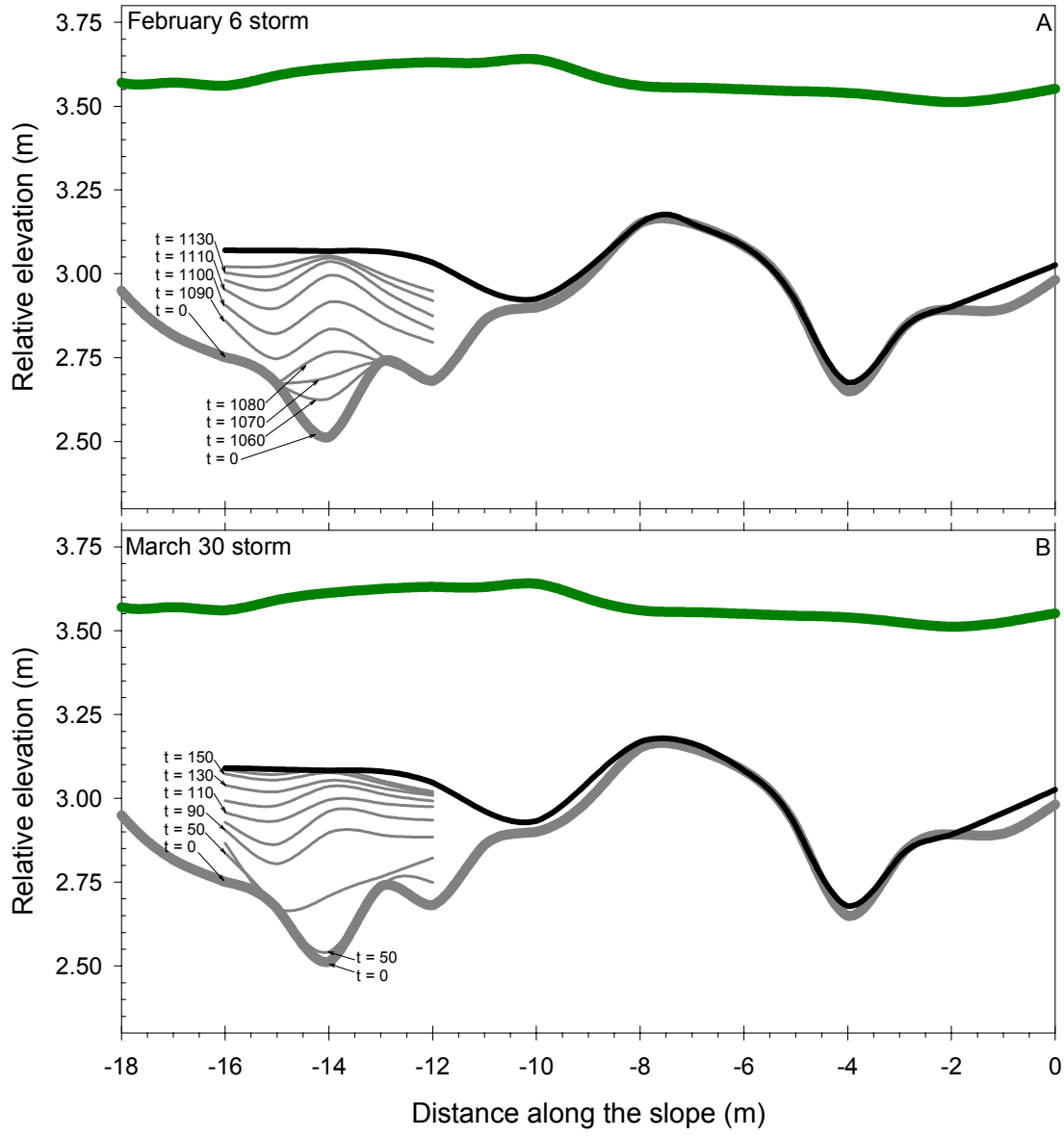

Figure 3.11 Schematic representation of the fill and spill process. Vertical exaggeration is 2x.

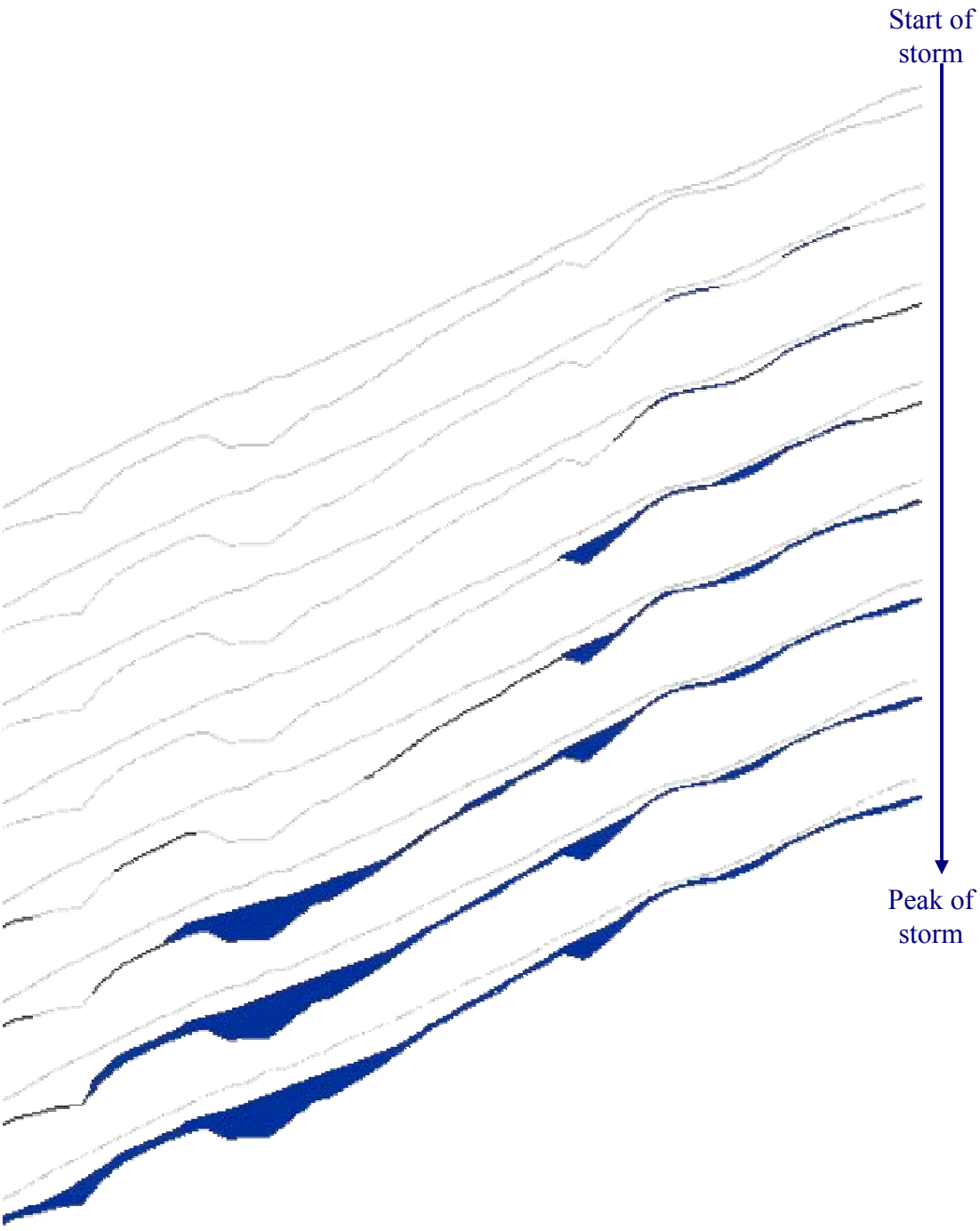

4 On the interrelations between topography, soil depth, soil moisture, transpiration rates and species distribution at the hillslope scale

4.1 Introduction

Soil moisture, plants and their coupling are at the heart of ecohydrology and the soil water balance. On the one hand, climate and soil moisture control vegetation dynamics; on the other hand vegetation exerts important controls on the entire water balance and is responsible for many feedbacks to the atmosphere (Porporato and Rodriguez-Itrube, 2002). The spatial structure of soil moisture and its evolution in time is both cause and consequence of vegetation (Rodriguez-Iturbe, 2000). Despite recent calls for focused ecohydrological study (Rodriguez-Iturbe, 2000; Kundzewicz, 2002; Nuttle, 2002), few investigations have examined systemically the interactions between physical, topographical and ecological form.

The hillslope scale is the basic building block for landscapes and the basic building block for catchment models (Sivapalan, 2003). Hillslope hydrologists have focused mostly on rainfall events and the conversion from vertical to lateral water transfers under event driven conditions (Bond, 2003). The studies that have examined the relations between topography and soil moisture have often been oriented at the small catchment scale (e.g. Nyberg, 1996; Western et al., 1999) or on transects (e.g. Famiglietti et al., 1998; Yeakley et al., 1998; Meyles et al., 2003). These studies have shown associations between shallow soil moisture and topography during wet periods, i.e. when potential evaporation is smaller than precipitation (e.g. Western et al., 1999). Notwithstanding, these associations are weak or absent during dry periods when potential evaporation is larger than precipitation. Plant transpiration has been hinted at as a cause for the reduced importance of subsurface water redistribution and the elimination of topographic control on soil moisture patterns (e.g. Western et al., 1999). However, this has not been examined in detail. To date, studies that have examined relations between soil moisture and topography have been restricted to examination of shallow soil moisture within the upper 0.3 m or less of the soil profile (e.g. Nyberg, 1996; Western et al., 1999; Anctil et al., 2002; Meyles et al., 2003). Tree water use is well beyond this exclusive shallow zone but studies have not examined how well these shallow soil moisture patterns represent soil moisture in the entire soil profile.

While the influence of transpiration on soil moisture depletion and the influence of soil moisture on transpiration rates are well known, few studies have examined systematically how spatial patterns of soil moisture influence transpiration patterns and vice versa at the hillslope or plot scale. A notable exception is the work of Hupet and Vanclooster (2002). They showed that spatially variable vegetation growth within a flat 6300 m^2 corn field induced variable evapotranspiration rates and consequently variable root water uptake rates. This resulted in spatially variable shallow soil moisture. Schume et al. (2003) showed that during a long drying cycle in spring, species specific transpiration and rooting depth were the main source of variation in volumetric soil moisture content in a mixed Norway spruce (*Picea abies*) and European Beech (*Fagus sylvatica*) stand. While these studies have shown the influence of vegetation on soil moisture patterns, they have not shown how the spatial patterns in soil moisture, caused by the vegetation, in turn influenced transpiration or vegetation growth. Thus despite this recent work, the feedbacks between spatial and temporal soil moisture patterns and transpiration patterns at the hillslope or plot scale remain poorly understood.

In this paper, we address the following questions on the interrelations between topography, soil moisture, transpiration rates and species distribution at the hillslope scale:

- How does soil moisture vary spatially and temporally at the hillslope scale?
- How does soil moisture vary with depth?
- How do terrain properties influence soil moisture patterns?
- How do vegetation and transpiration patterns affect soil moisture patterns in time and space at the hillslope scale?
- How do soil moisture patterns affect transpiration patterns in time and space at the hillslope scale?

We address these questions for a well instrumented 20 by 48 m study hillslope where we measured soil moisture in a 3-dimensional array from the soil surface to the soil-bedrock interface for a nine month period. We start with the hillslope scale because

of the uniformity of atmospheric forcing factors and the uniform soil type. Because of the relatively small area, planar topography and uniform azimuth of the study hillslope we do not expect differences in incoming solar radiation, relative humidity, temperature, wind speed or other climatic variables across the hillslope. This allows us to reduce competing processes and isolate the feedbacks between soil depth, soil moisture and transpiration patterns at this scale. If one would look for these interactions at the catchment scale the differences in soil type, soil depth, biogeochemistry and average soil moisture content between the hillslopes (without permanent groundwater) and the riparian zone (with permanent groundwater) could overwhelm the variations we might see at the hillslope scale and thus mask important patterns and relations at the hillslope scale.

4.2 Site description

The Panola Mountain Research Watershed (PMRW) is located within the Panola Mountain State Conservation Park in the southern Piedmont province southeast of Atlanta, Georgia (84˚10'W, 33˚37'N). Currently the watershed is 93% forested, consisting of hickory (*Carya* sp.), oak (*Quercus* sp.), tulip poplar (*Liriodendron tulipifera*), and loblolly pine (*Pinus teada*) (Carter, 1978). The remaining 7% of the watershed is comprised of bedrock outcrops with small vegetation islands, including a 3 ha outcrop in the southwestern corner of the watershed. The forest consists of predominantly even-aged deciduous or mixed deciduous and conifer stands and a smaller portion of predominantly coniferous stands. The forest composition and age structure at PMRW reflect historic land use and periods of agricultural abandonment typical for the Piedmont region in Georgia (Huntington et al., 2000). Historical records of regional land use and tree ring analysis at PMRW suggest that most of the timber was cut originally in ca 1820 and that the land was farmed (cotton cultivation and pasture) until the early 1900s and has remained relatively undisturbed since (Huntington et al., 2000). Hickory (*Carya* sp.) is the dominant species on the study hillslope (54% of the total basal area of 24.8 m^2/ha). Oak (*Quercus* sp.) is the next dominant species on the hillslope (25% of total basal area). Even though there are only two loblolly pine (*Pinus taeda*) trees on the study

hillslope, they are the species with the third largest basal area on the study hillslope (13.5%). Mixed species stands dominated by oak (*Quercus* spp.) and hickory (*Carya* sp.) overstories are common throughout the southeastern US in areas which have been permitted to reach late successional stages of development.

The climate at PMRW is classified as humid, subtropical. The mean annual temperature is 16.3 ˚C and mean annual precipitation is 1240 mm (NOAA, 1991). Rainfall tends to be of longer duration and lower intensity associated with the passage of fronts in the winter, and of shorter duration but higher intensity in the summer associated with thunderstorms. Streamflow at PMRW has a strong seasonal pattern, with the highest flow occurring in the November through March dormant season. Annual stream yield from the 41-ha catchment varies from 16 to 50 % of precipitation (1989-2001). The dryness index (annual potential evaporation/annual precipitation) of the study site is 1.3, where potential evaporation is calculated using the Hargreaves equation (Hargreaves, 1975). The 2002 study period was drier than average (Figure 4.1) mainly as a result of smaller storms (an average and median storm size of 16 mm and 11 mm respectively for the water year 2002 compared to an average and median storm size of 22 and 14 mm during the 1989-2001 period). For the water year 2002 there was on average one storm (defined as an event larger than 1 mm of precipitation separated by 24 hours of no precipitation) every 6.3 days while the 1989-2001 average was one storm every 6.1 days.

The study hillslope is located 30 m upslope from an ephemeral stream. The lower boundary of the study hillslope is formed by a 20 m wide trench to bedrock while the upper boundary is formed by a small bedrock outcrop.

The 10-ha western upper catchment at Panola (within which the study hillslope is located) is underlain by the Panola Granite, which is a biotite-oligoclase-quartz-microcline granodiorite (Crawford et al., 1999). The soil on the study hillslope is a light colored sandy loam without clear structuring or layering, except for a 0.15 m deep organic soil horizon. During augering for the installation of the soil moisture access tubes

and wells no differences in soil type or soil texture were observed across the study hillslope. The average soil depth across the study hillslope is 0.63 m and ranges from 0 to 1.86 m.

4.3 Methods

4.3.1 Soil moisture measurements

Soil moisture was measured at 64 locations on 85 occasions between January 26 and August 26 2002. Soil moisture was measured using the Aqua-pro sensor (Aqua-pro Sensors, Reno, NV) in polycarbonate access tubes that were installed to the soil-bedrock interface. The access tubes were located on a 4 by 4 m grid across the hillslope and on a 4 by 2 m grid on the lower 6 m of the hillslope. The Aqua-pro sensor is a capacitance (radio-frequency) sensor that measures soil moisture on a percent scale between 0 (in air or air dried soil) and 100 (in water or saturated soil). The relation between the Aqua-pro soil moisture values and gravimetrically determined volumetric soil moisture content is linear with a slope of approximately 1/240 and an intercept that depends on soil type [J. Selker, Oregon State University, Personal Communication] (Equation 4.1).

$$\theta_{vol} = \frac{Aqua - pro}{240} + b \qquad \text{(Equation 4.1)}$$

where θ_{vol} is the gravimetrically determined volumetric soil moisture content (%), *Aqua-pro* is the Aqua-pro measurement value (Aqua-pro %) and b is a constant that depends on the soil type. Unless explicitly mentioned in the text, all values reported are in Aqua-pro values (thus ranging between 0 and 100).

Soil moisture was measured at 0.05 m increments to 0.3 m below the soil surface and at 0.10 m increments between 0.3 m and the soil-bedrock interface. The profile average soil moisture at a measurement location was calculated by multiplying the soil moisture values at the different measurement depths by the distance between the

subsequent measurement depths and dividing this by the total soil depth at that measurement location. Hillslope average soil moisture was calculated by averaging the profile average soil moisture values for all measurement locations.

To obtain a measure of the '*total depth of water'* in the soil profile we multiplied the Aqua-pro soil moisture values at the different depths by the distance between the subsequent measurement depths and the 1/240 factor. Because we do not know the intercept of the relation between volumetric soil moisture and the Aqua-pro value and we omit the intercept from the calculation of the total depth of water in the soil profile, the calculated total depth of water is only a relative value.

Artificial water applications as part of a related study (Chapter 6) influenced soil moisture measurements at the lower 14-m of the hillslope during June 18-August 26 2002. For these dates, soil moisture measurements on the lower 15 m of the hillslope were excluded from the analyses. We observed no changes due to the artificial water applications in the soil moisture measurements at locations 16 m and further upslope from the trench.

4.3.2 Sapflow measurements

Transpiration was estimated from constant heat sapflow measurements using the thermal dissipation technique developed by Granier (1985 and 1987), generally following the procedures described by Phillips et al. (2002). Sapflow was measured at 15-minute intervals in 14 trees using 28 sensors. All trees had two sensors inserted 0-20 mm in the sapwood on the east and west side of the tree trunk. Sapflow was averaged to hourly intervals using the average of the two sapflow sensors in each tree. Constant heat sapflow sensors were installed in Hickory trees (*Carya* sp.) in one of two Diameter-at-Breast-Height (DBH) classes: 0.11-0.125 m (5 trees) or 0.175-0.215 m (9 trees). Hickory trees (*Carya* sp.) of these size classes were the dominant trees on the study hillslope. Eight of the trees with constant heat sapflow sensors were located on an upslope transect across

the middle of the study hillslope while the other trees with sapflow sensors were distributed across the hillslope.

All trees on or within approximately 5 m of the study hillslope were measured for DBH. We used the relations between DBH and sapwood area from Pataki and Oren (2003, Table 2 p. 1273) at the Duke Forest in North Carolina to estimate our hillslope sapwood area. We used the relation between DBH and sapwood area for the hickory trees for the species not listed by Pataki and Oren (2003). The estimated hillslope sapwood area was multiplied by the average sapflow flux from the 14 monitored trees, to obtain the estimated hillslope average transpiration rate. The Duke Forest is comparable to the forest in PMRW, not only in species composition but also in basal area and climate. The basal area in the Duke forest is 23.0 m^2/ha (Oren and Pataki, 2001), while the average basal area of the Panola study hillslope is 24.8 m^2/ha. The climate in the Duke forest is slightly drier and colder than PMRW (15.5 °C and 1140 mm for the Duke Forest (Oren and Pataki, 2001) vs. 16.5 °C and 1240 mm for PMRW). We acknowledge that even though the forests are similar, using the sapwood area DBH relationship from the Duke forest rather than a relationship between sapwood area and DBH from PMRW (which is not available) will inhibit us from being able to calculate an absolute transpiration value with certainty. However, it will allow us to look at temporal and spatial patterns in transpiration and to estimate the hillslope average transpiration rate.

4.3.3 Air temperature, relative humidity and precipitation measurements

Air temperature and relative humidity were measured at 3 m above the ground surface on a tripod in a clearing approximately 200 m from the study hillslope using a Campbell Scientific Model CS500 probe. Precipitation was recorded each minute at three locations using tipping bucket rain gauges, continuously using a weighing bucket gauge, and each week using several Tenite gauges. The tipping bucket rainfall data series were combined to yield one rainfall time series for the watershed. Throughfall was estimated from the rainfall measurements using a linear fit (r^2=0.99) to the measured throughfall

and precipitation data for the deciduous forest for 16 storms during the growing season at PMRW given by Cappellato et al. (1993; Table 1, p. 1118):

$$Throughfall = 0.97\,precipitation - 1.66 \qquad \text{(Equation 4.2)}$$

where throughfall is the estimated total throughfall for the storm (in mm) and precipitation is the measured total storm precipitation (mm)

4.3.4 Subsurface flow measurements

A 20-m long trench excavated down to bedrock normal to the fall line of the slope formed the lower boundary of the study hillslope. Total subsurface flow was measured by routing flow through tipping-bucket gages. The number of tips was recorded every minute. Additional details of the trench and the flow-collection system are described in McDonnell et al. (1996), Freer et al. (1997 and 2002) and Burns et al. (1998).

4.3.5 Soil depth measurements

The hillslope was surveyed on a 2 m grid. Depth to bedrock was measured on the same survey grid network using a 25.4 mm soil corer forced down to refusal. A small hand auger was used when soil depth was greater than 1.25 m. The multidirectional flow algorithm of Quinn et al. (1991) was used to calculate the drainage area for both the soil-bedrock interface and the soil surface. The topographic index (Kirkby, 1975) was calculated for both the surface topography and bedrock topography (Freer et al., 1997).

4.4 Results

4.4.1 Soil moisture patterns

The hillslope remained relatively wet throughout the winter and early spring period (until mid April) and dried quickly after (Figure 4.2b). The standard deviation of the soil moisture readings was smaller during the winter than during the summer months

(Figure 4.2b). Soil moisture responses to precipitation were distinct. From February to early April the hillslope drained to the same moisture level (~field capacity, ~70 %) while further soil moisture depletion occurred after mid April, the beginning of leaf out. The spatial soil moisture patterns at different depths below the soil surface at approximately 2-week intervals throughout the study period are shown in Figure 4.3. During the winter and spring the hillslope was in a wet state (i.e. hillslope average soil moisture > 70%), and changed into a dry state (i.e. hillslope average soil moisture < 45%) rather abruptly in May. The correlation length of soil moisture at every depth below the soil surface was shorter than 8m. While soil moisture at some locations on the hillslope was persistently lower or higher than the hillslope average, there was only very little spatial structure in soil moisture when the hillslope was in the wet state (Figure 4.3). Only during the drying down period (hillslope average soil moisture 45-70%, i.e. May 30-June 4 and June 10-24), was there some spatial structure. During the drying down period, soil moisture at 0.05 m below the soil surface was higher in the left (when looking upslope) upper corner of the hillslope and soil moisture at 0.30 m was higher in the midslope compared to other locations on the hillslope (Figure 4.4). The spatial drying down pattern was persistent in time. The soil moisture pattern on June 4 (before the 50 mm June 4-6 storm) was repeated after the storm (Figure 4.4). The grid resolution of soil moisture measurements did not allow for an accurate determination of the correlation length scale. Nevertheless, these data suggest that the correlation lengths of soil moisture were very small (varying between less than 4 m to 10 m for both the omni-directional variogram and the directional variogram, with the largest correlation lengths during the drying down and dry period).

There was not only very little spatial structure in soil moisture across the hillslope but also little variation in the temporal pattern of soil moisture at different depths below the soil surface (Figure 4.2c, 4.3 and 4.4). Soil moisture at the different depths was highly correlated to each other (Table 4.1). However, there was some stratification in soil moisture during and directly after storms during the drying down and dry period. Small storms rewetted the upper soil layers but did not penetrate to the soil-bedrock interface,

leading to stratification of soil moisture with depth during this short period. The June 4-6 2002 storm, for example, did not wet up all locations at 0.30 m depth on June 5 2002 10:00. By June 6 2002 11:30, storm induced increases in soil moisture were observed at 0.30 m below the soil surface at all measurement locations but soil moisture at 0.50 m depth remained unchanged at many locations.

Total water extraction between May 1 2002 and August 26 2002 was almost twice as much from 0.05 m depth below the soil surface than from 0.5 m depth because of soil moisture replenishment during frequent storms that did not penetrate to depth, (Figure 4.5). For many measurement locations total soil moisture extraction during the May 1st and August 26th was also higher near the soil-bedrock interface than at other deep soil layers (e.g. locations 7.16 and 11.24 in Figure 4.5). The actual soil moisture extraction values are higher than the calculated values because of soil moisture extraction between the time of a thunderstorm and the time of the actual soil moisture measurements. This affects the calculation for the upper soil layers especially because most storms did not penetrate to great depth.

4.4.2 Relation of soil moisture to topographic variables

Soil moisture was not well correlated to any of the computed topographic variables for the hillslope (Table 4.2). The exceptions were the relation between soil moisture at 0.30 m depth below the soil surface and soil depth and the relation between upslope distance and soil moisture at 0.30 m during the drying down and dry state. Not surprisingly, soil depth and distance upslope from the trench were correlated at the Panola hillslope. In general soils on the upslope part of the study hillslope were shallower than the soils on the midslope and lower slope. When the hillslope was in the wet state, soil moisture at 0.30 m below the soil surface was high and not correlated to soil depth (e.g. May 10 in Figure 4.6c). During the drying down period (e.g. June 10 in Figure 4.6c) soil moisture at 0.30 m below the soil surface decreased more rapidly at sites with relatively shallow soils, resulting in a relationship between soil depth and soil moisture at 0.30 m in the drying (e.g. June 10 in Figure 4.6c) and dry state (e.g. July 10 and August 9

in Figure 4.6c). This more rapid decrease in soil moisture at sites with relatively shallow soils was also observed (but was less clear) for soil moisture at greater depth (e.g. Figure 4.6d).

4.4.3 Transpiration patterns

Average calculated transpiration was 2.6 mm/day for the May 1-August 24 2002 period (Figure 4.7). Solar radiation alone explained 55% of the observed variation in estimated hillslope average transpiration. Solar radiation, average relative humidity, average air temperature and soil moisture combined explained only 58% of the observed variation in estimated hillslope average daily transpiration rate.

Even though the calculated hillslope average transpiration rate is uncertain (because we used the relationship between DBH and sapwood area from the Duke Forest in North Carolina rather than from PMRW), the difference between estimated throughfall (Equation 4.2), subsurface flow and hillslope average transpiration matched the observed hillslope soil moisture depletion during the early summer (May – mid July) well (Figure 4.8b). We did not include understory or soil evaporation in the water balance calculations because of the sparse understory at the study hillslope and because understory evaporation is generally less than 10% of the total canopy fluxes during the growing season (e.g. Wilson et al., 2000).

4.4.4 Influence of soil depth: Comparison of upslope and midslope

The average soil depth of the midslope (14-25 m upslope from the trench) is 0.93 m while the average soil depth of the upslope (more than 25 m upslope from the trench face) is 0.51 m (Table 4.3). During the wet state the average soil moisture on the upslope was similar to the average soil moisture on the midslope (Figure 4.9a). During the drying down and dry state the average soil moisture of the upslope was less than that of the midslope. The difference in the average soil depth of the two sections had a large effect on the calculated measure of total depth of water in the soil profile at the end of the

wet/dormant season (May 1 2002) (Figure 4.9b). During the drying down and dry state more water was removed from the midslope than from the upslope (Figure 4.9c). Thus the shallower upslope contained less water than the midslope at the end of the dormant season due to differences in soil depth (Figure 4.9b), dried down to a lower soil moisture level during the summer (Figure 4.9a) but lost less total water during the growing season than the midslope (Figure 4.9c). This is mainly due to the leveling off of soil moisture depletion on the upslope after early July while soil moisture depletion on the midslope continued throughout the summer (Figure 4.8c). One could argue that soil moisture depletion in the midslope leveled off in late August as well. But this is highly influenced by the soil moisture measurements on August 26 2002 and thus uncertain. There was 25 mm of precipitation in between the measurements on August 9 and 26, which could also be responsible for the apparent reduced soil moisture depletion. Unfortunately we have no soil moisture measurements after August 26 2002 to check if soil moisture depletion in the midslope continued with increasing drought conditions.

During the early summer (until July) we observed no differences in sapflow across the hillslope. During the late summer however, maximum daily sapflow in trees on the upslope was reduced with time after the last rainfall event while maximum daily sapflow in trees on the midslope did not decrease (Figure 4.10). Trees on the upslope showed a large increase in sapflow after a rainstorm while trees on the midslope and lower slope did not show such a large increase in sapflow after the storm (Figure 4.10). Profile average soil moisture measured on August 9, explained 57% of the observed variation in daily sapflow per unit sapwood area on August 15 (before the storm) and only 1 % on August 18 (after the storm) respectively. Thus, sapflow was related to soil moisture before the storm, when differences in average and shallow soil moisture were large. After the storm, when soil moisture in the upper soils was replenished, sapflow was no longer related to soil moisture before the storm. Soil moisture measurements were not made directly after the storm, thus we can not determine if sapflow after the storm was related to the shallow soil moisture pattern after the storm.

The soil depth and upslope effect on soil moisture and sapflow could be responsible for the distribution of species and basal area across the hillslope (Table 4.3). The average basal area for the upslope is only 67% of the average basal area of the midslope (Table 4.3). The upslope is characterized by a larger number of chinkapin (*Castanea*), sparkleberry (*Vaccinium arboretum*) and other small trees with a more shrubby appearance beside Hickory trees (*Carya* sp.) while the midslope is characterized by a larger number and larger size hickory (*Carya* sp.) and oak (Q*uercus* sp.) trees (Figure 4.11 and Table 4.3).

A weighted basal area was calculated for each location on the hillslope by summing the multiplication of the basal area of every tree on and next to the hillslope by an exponential distance function between that point and the tree:

$$\textit{Weighted basal area} = \sum_{alltrees} \{\textit{basal area}_{tree} \exp(\alpha \, \textit{distance})\} \qquad \textit{(Equation 4.3)}$$

where *Weighted basal area* is the calculated weighted basal area for a location on the hillslope*, basal area*$_{tree}$ is the basal area of a tree, *distance* is the distance between the tree and the location for which the weighted basal area is calculated, and α is a constant determining how rapidly the weighting of a tree declines with the distance from the tree. Thus the basal area of a tree located close to a certain point counted heavily while the basal area of a tree located further away counted less. The value of α used in Figure 4.11a is 0.2. This value was chosen so that the weight of a tree to areas outside the crown of the tree was less than 0.15 for the dominant trees on the hillslope. Soil depth and upslope distance together explained 63% of the observed variation in weighted basal area (Figure 4.11)

4.5 Discussion

4.5.1 Preferred states of soil moisture

Like Grayson et al. (1997), we observed two preferred states for soil moisture: wet (February-April) and dry (mid June-August), separated by a drying period (May-mid June). The transition from the wet state into the dry state lasted less than a month and occurred soon after full leaf out. The 50 mm rain event on June 4-6 2002 temporarily moved the hillslope from the drying period back into the wet state, but after this storm the transition from the wet state on June 6 2002 to the dry state occurred within 2 weeks.

Unlike Western et al. (1999), who found a high degree of organization of soil moisture during wet state, we found little spatial structure in our data. Western et al. (1999) attributed the spatial structure in soil moisture during the wet period to (surface and subsurface) lateral redistribution of water and the lack of spatial organization during dry periods to a lack of lateral redistribution of water. Here we show that there was more (but still not a lot of) spatial organization in soil moisture across the hillslope during the drying and dry state than during the wet state. Even during the dry state the correlation length of soil moisture was never larger than 10 m and most of the time less than 8 m. The lack of spatial structure during the wet period may be caused by the scale of this study, uniformity of soil type and texture across the study hillslope and the absence of clear surface drainage lines on the hillslope. However, there is a clear subsurface drainage line in the bedrock topography at this hillslope (Freer et al., 2002). Even though we anticipated that lateral re-distribution of soil moisture at depth (near the soil-bedrock interface) would result in soil moisture patterns at depth that would reflect the bedrock topography, soil moisture in between storms (pre-event soil moisture) in the wet state, was not correlated to the bedrock topography, i.e. soil moisture at depth was not highest in areas of high bedrock accumulated area or high bedrock topographic index values (Table 4.2, Appendix A2).

An alternative explanation for the lack of a spatial pattern in soil moisture during the wet state is that leakage to the bedrock (Chapter 6) results in predominantly vertical

fluxes. This results in a lack of topographic expression in soil moisture. Western et al. (2004) show a lack of a soil moisture pattern for the Point Nepean study site in Australia, which has very well drained deep sandy soils. There variations in soil moisture in the 13 ha site are mainly due to variations in soil texture.

In addition to the lack of a soil moisture pattern across the hillslope, soil moisture was also very uniform with depth. The exception was during and directly after storms during the drying down and dry state when soil moisture close to the surface was higher than soil moisture at depth (e.g. June 4-6 2002 in Figure 4.2c). Stratification in soil moisture during and directly after storms was also shown by Wilson et al. (2003).

Aqua-pro soil moisture values for the deeper soil layers were in general lower than the Aqua-pro soil moisture values for shallower soil layers, even when the soil drained to the constant soil moisture value (~ field capacity) between storms in the wet state (Figure 4.2c). We believe that this is not due to lower soil moisture at depth but rather due to a difference in the dielectric of the soil at depth compared to the dielectric of the soil closer to the soil surface, thus a different constant (b) in the relation between the Aqua-pro reading and actual volumetric soil moisture (Equation 4.1). Yu et al. (1999) show that the dielectric of the soil is mainly influenced by the surface area of the soil particles and only a little by soil solids, porosity or temperature. For the same soil composite dielectric constant, actual soil moisture is higher than calculated with the standard equation (Topp et al., 1980) when the porosity is lower, the dielectric of the solid is lower or the specific surface area of the soil particles is higher (Yu et al., 1999).

4.5.2 Transpiration patterns

Total water removal was higher from the upper 0.3 m of the soil profile and directly above the soil-bedrock interface than from the other depths (Figure 4.5). This corresponded well with the observed root density pattern. Even though roots were observed throughout the soil profile, there was a higher root density in the upper 0.3 m of the soil profile than at greater depth and a slightly higher root density near the soil-

bedrock interface. Frequent thunderstorms replenished soil moisture in the upper soil layer, but this water was transpired in a few days after the storm, such that there was no stratification in soil moisture with depth for the majority of the time during the drying and dry state.

Hillslope average daily transpiration at the study hillslope was correlated to net radiation. This is comparable to the results from Oren and Pataki (2001) for the Duke Forest in North Carolina, where daily stand transpiration increased linearly with the daily sum of photosynthetic radiation above the canopy. There, photosynthetic radiation above the canopy explained 59% of the variation in daily stand transpiration, while daytime mean vapor pressure deficit explained 22% and soil moisture deficit did not explain variations in measured daily stand transpiration when it was included in a multivariate regression with radiation and vapor pressure deficit.

Here we show that daily maximum sapflow in trees on the dry shallow upslope decreased with decreasing soil moisture and increased in response to precipitation. We also show that during the late summer the spatial pattern of daily sapflow per unit sapwood area was related to the soil moisture pattern before the storm. The increase in sapflow after a storm during dry conditions was also shown by Oren and Pataki (2001) for white oak (*Quercus alba*) in the Duke forest in North Carolina.

Pataki and Oren (2003) show for a hardwood forest that despite a severe drought during their study period only tulip poplar (*L. tulipifera*) (not Mockernut Hickory (*Carya tomentosa*), red oak (*Quercus rubra*), white oak (*Quercus alba*), or sweetgum (*L. styraciflua*)) showed a decline in canopy stomatal conductance with decreasing soil moisture and that the primary effect of the drought for the species (except for the tulip poplar) appeared to be early autumn leaf senescence and abscission beginning in mid to late September. We observed that by late August some trees on the upslope shed their leafs while trees on the midslope and lower slope did not do this.

4.5.3 Feedbacks between terrain, soil moisture and plant transpiration

The depth of water stored in the soil profile at the end of the dormant season (together with summer rainfall) determined the total volume of water that was available for transpiration during the growing season. Because soil moisture at the end of the dormant season (wet state) was relatively similar across the hillslope, variations in the depth of total water available for plant use were determined by variations in soil depth. Even if there would have been some variation in soil moisture at the end of the dormant season, the variations in soil depth would be larger than variations in soil moisture such that variations in soil depth would still be the dominant factor in determining the variations in the total depth of water in the soil profile.

Measured sapflow was spatially uniform across the hillslope during the early summer. Thus, the same depth of water was transpired from the soil profile across the hillslope during the early summer. Because the total depth of water stored in deeper soils was larger than the total depth of water stored in areas with shallower soils, the same depth of water could be removed from areas with deeper soils with less impact on soil moisture than from shallower soils. This resulted in a faster depletion of soil moisture in areas with shallower soils. This in turn increased the correlation between soil moisture and soil depth (Figure 4.6 c-d) and resulted in a spatial pattern in soil moisture during the drying down and dry state (Figure 4.3 and 4.4). Frequent small storms that replenished soil moisture in the upper soil layers erased the relation between soil depth and soil moisture content for the top soil (Figure 4.6a-b).

Because more water was stored in the deeper midslope soils, more water could be taken out of the soil profile without lowering soil moisture to such low levels that transpiration became severely limited, as was the case for the shallower upslope (Figure 4.10). The soil depth effect on soil moisture could also be responsible for the distribution of species and basal area across the hillslope (Figure 4.11 and Table 4.3). During the dry summer periods, soil moisture limited transpiration rates in areas with shallow soils (on the upslope). This limits growth and resulted in a smaller basal area compared to areas

with deeper soils (on the midslope and lower slope) where transpiration was not limited by soil moisture. In addition the lack of soil moisture could favor different species on the shallow soil sections (upslope) compared to the deeper soil sections (midslope or lower slope).

Part of the observed influence of soil depth and transpiration on the soil moisture patterns could be larger than during an average year because the measurements were made during a drier than average year. Total rainfall between May 1 and August 31 2002 was 250 mm while the 12-year (1989-2001) average rainfall for the same period is 430 mm (Figure 4.1).

It is often assumed that the spatially variable radiation influx is the main factor controlling the spatial variability of evapotranspiration (Western et al., 1999). We do not believe that climatic differences are responsible for the observed differences in soil moisture or sapflow at this hillslope because of the small scale of this hillslope and uniformity of incident radiation and atmospheric forcing variables across the hillslope. In addition, we do not believe that the observed variations in soil moisture and sapflow were primarily due to drainage of water from the upslope to the midslope because of the low soil moisture and thus very low hydraulic conductivity of the soil during the drying and dry state. Thus we attribute the differences in soil moisture and sapflow between the midslope and upslope during the summer (dry state) not to their topographic position but to the differences in the total depth of water stored in the soil profile at the beginning of the drying down period, which is determined by differences in soil depth.

Unlike Western et al. (1999), here we show that vegetation has a larger influence on soil moisture patterns than local surface or subsurface topography. Hupet and Vanclooster (2002) showed for a flat corn field in Belgium that spatially variable vegetation growth within the field induced spatially variable evapotranspiration rates and consequently variable root water uptake rates, resulting in spatially variable shallow soil moisture. Here we show the effect of transpiration on soil moisture for almost all but the

shallowest depths. We believe that this is due to the deeper rooting depth of the trees compared to corn and the frequent thunderstorms that replenish shallow soil moisture at this site. Here we show a feedback mechanism between soil moisture and transpiration. Spatial variability in soil depth results in spatial variability in the total depth of water stored in the soil at the beginning of the growing season. Uniform transpiration rates in the early season result in spatial patterns of soil moisture, which in turn result in spatial patterns of transpiration during the late season (Figure 4.12), which in turn is responsible for growth and species distribution. Thus soil moisture is both a cause and consequence of vegetation (Rodriguez-Iturbe, 2000).

4.6 Conclusion

We show the importance of soil depth measurements to understand the relations between soil moisture, transpiration and vegetation patterns during the growing season and the feedback between soil moisture and transpiration patterns at the hillslope scale. We show that there are no spatial patterns in soil moisture with depth or across the hillslope during the dormant season (wet state). During the early summer, transpiration is uniform across the hillslope. Because more water is stored in the deeper soils, removing the same amount of water from a deep soil section and a shallow soil section, results in a faster depletion of soil moisture in the shallower soil section. This in turn results in a relation between soil moisture and soil depth after leaf out. Because soil moisture during the mid to late summer is lower on the shallow soil sections, transpiration on the shallower soil sections is reduced. This in turn determines growth, which determines the basal area and its competitive ability, which affects species distribution.

4.7 Acknowledgements

We would like to thank Georgianne Moore for her help and advice with the sapflow measurements. We also would like to thank John Selker for sharing the Aqua-pro calibration data with us and Jake Peters for his help with the dataloggers. This work was supported by NSF grant EAR-0196381.

4.8 References

Anctil, F., R. Mathieu, L. Parent, A.A. Viau, M. Sbih, and M. Hessami, Geostatistics of near-surface moisture in bare cultivated organic soils, Journal of Hydrology 260: 30-37 2002.

Bond, B., Hydrology and ecology meet - and the meeting is good, Hydrological Processes 17: 2087–2089, 2003.

Burns, D. A., R.P. Hooper, J.J. McDonnell, J.E. Freer, C. Kendall and K. Beven, Base cation concentrations in subsurface flow from a forested hillslope: The role of flushing frequency, Water Resources Research 34(12): 3535-3544, 1998.

Cappellato, R., N.E. Peters, and H.L. Ragsdale, Acidic atmospheric deposition and canopy interactions of adjacent deciduous and coniferous forests in the Georgia Piedmont, Canadian Journal of Forest Research 23: 1114-1124, 1993.

Carter, M.E.B., A community analysis of the Piedmont deciduous forest of Panola Mountain State Conservation Park: Atlanta, Georgia, M. S. thesis, 126 pp., Emory Univ., Atlanta, Ga., 1978.

Crawford T.J., M.W. Higgins, R.F. Crawford, R.L. Atkins, J.H. Medlin, and T.W. Stern, Revision of stratigraphic nomenclature in the Atlanta, Athens, and Cartersville 30 ð 60 quadrangles, Georgia. Georgia Geologic Survey Bulletin B-130: Atlanta, Georgia; 48, 1999.

Famiglietti, J.S., J.W. Rudnicki, and M. Rodell, Variability in surface moisture content along a hillslope transect: Rattlesnake Hill, Texas, Journal of Hydrology 210 (1-4): 259-281, 1998.

Freer, J., J. McDonnell, K.J. Beven, D. Brammer, D. Burns, R.P. Hooper, and C. Kendal, Topographic controls on subsurface stormflow at the hillslope scale for two hydrologically distinct small catchments, Hydrological Processes 11: 1347-1352, 1997.

Freer, J.E., J.J. McDonnell, K.J. Beven, N.E. Peters, D.A. Burns, R.P. Hooper, B.T. Aulenbach, and C. Kendall, The role of bedrock topography on subsurface stormflow, Water Resources Research, 10.1029/2001WR000872, 2002.

Grayson, R., A.W. Western, and F.H.S. Chiew, Preferred states in spatial soil moisture patterns: Local and nonlocal controls, Water Resources Research 33(12): 2897-2908, 1997.

Granier A., Une nouvelle methode pour la mesure de flux de seve brute dans le tronc des arbres, Annales des Sciences Forestieres 42: 193–200, 1985.

Granier A., Evaluation of transpiration in a Douglas-fir stand by means of sapflow measurements, Tree Physiology 3: 309–320, 1987.

Hargreaves, G.H., Moisture availability and crop production, Trans. Am. Soc. Agric. Eng. 18(5):980-984, 1975.

Hupet, F., and M. Vanclooster, Interseasonal dynamics of soil moisture variability within a small agricultural maize cropped field, Journal of Hydrology 261: 86-101, 2002.

Huntington, T.G., R.P. Hooper, N.E. Peters, T.D. Bullen, and C. Kendall, Water, energy, and biogeochemical budgets investigation at Panola Mountain Research Watershed, Stockbridge, Georgia—A research plan, U.S. Geological Survey Open File Report, 93–55, 39 pp., 1993.

Huntington, T. G., R. P. Hooper, C. E. Johnson, B. T. Aulenbach, R. Cappellato, and A. E. Blum, Calcium Depletion in a Southeastern United States Forest Ecosystem, Soil Science Society of America Journal 64:1845–1858, (2000).

Kirkby, M. J., Hydrograph modelling strategies, in: Process in Physical and Human Geography, edited by R. Peel, M. Chisholm, and P. Haggett, Heinemann, Oxford, England: 69–90, 1975.

Kundzewicz, Z.W., Ecohydrology-seeking consensus on interpretation of the notion, Hydrological Sciences Journal 47(5): 799-807, 2002.

McDonnell, J.J., J.E. Freer, R.P. Hooper, C. Kendall, D.A. Burns, K.J. Beven, and N.E. Peters, New method developed for studying flow in hillslopes, EOS, Transactions of the American Geophysical Union 77(47): 465, 1996.

Meyles, E., A. Williams, L. Ternan, and J. Dowd, Runoff generation in relation to soil moisture patterns in a small Dartmoor catchment, Southwest England, Hydrological Processes 17: 251-264, 2003.

Nuttle, W.K., Eco-hydrology's past and future in focus, EOS 83(19): 205,211-212, 2002.

Oren, R., and D.E. Pataki, Transpiration in response to variation in microclimate and soil moisture in southeastern deciduous forests, Oecologia 127: 549-559, 2001.

Nyberg, L., Spatial variability of soil water content in the covered catchment at Gardsjon, Sweden, Hydrological Processes 10: 89-103, 1996.

Pataki D.E., and R. Oren, Species differences in stomatal control of water loss at the canopy scale in a mature bottomland deciduous forest, Advances in Water Resources 26 (12): 1267-1278, 2003.

Porporato, A., and I. Rodriquez-Iturbe, Ecohydrology-a challenging multidisciplinary research perspective, Hydrological Sciences Journal 47(5): 811-821, 2002.

Phillips N., B.J. Bond, N.G. McDowell, and M.G. Ryan, Canopy and hydraulic conductance in young, mature, and old Douglas-fir trees, Tree Physiology 22: 205–212, 2002.

Quinn, P.F., K. Beven, P. Chevallier, and O. Planchon, The prediction of hillslope flow paths for distributed modelling using digital terrain models, Hydrological Processes 5: 59–79, 1991.

Rodriguez-Iturbe, I., Eco-hydrology: A hydrologic perspective of climate-soil-vegetation dynamics, Water Resources Research 36(1): 3-9, 2000.

Schume, H., G. Jost, and K. Katzensteiner, Spatio-temporal analysis of the soil water content in a mixed Norway spruce (*Picea abies* (L.) Karst.)-European beech (*Fagus sylvatica* L.) stand, Geoderma 112(3-4): 273-287, 2003.

Sivapalan, M., Process complexity at hillslope scale, process simplicity at the watershed scale: is there a connection?, Hydrological Processes 17: 1037–1041, 2003.

Topp, G.C., J.L. Davis, and A.P. Annan, Electromagnetic determination of soil water content: Measurements in coaxial transmission lines, Water Resources Research 16: 574-582, 1980.

Western, A. W., R.B. Grayson, G. Bloschl, G.R. Willgoose, and T.A. McMahon, Observed spatial organization of soil moisture and its relation to terrain indices, Water Resources Research 35(3): 797-810, 1999.

Western, A.W., S. Zhou, R.B. Grayson, T.A. McMahon, G. Blöschl, and D.J. Wilson, Spatial correlation of soil moisture in small catchments and its relation to dominant spatial hydrological processes, Journal of Hydrology 286:113-134, 2004.

Wilson, K.B., P. J. Hanson, and D.D. Baldocchi, Factors controlling evaporation and energy partitioning beneath a deciduous forest over an annual cycle, Agricultural and Forest Meteorology 102 (2-3): 83-103, 2000.

Wilson, D.J., A.W. Western, R.B. Grayson, A.A. Berg, M.S. Lear, M. Rodell, J.S. Famiglietti, R.A. Woods, and T.A. McMahon, Spatial distribution of soil moisture over 6 and 30 cm depth, Mahurangi river catchment, New Zealand, Journal of Hydrology 276: 254-274, 2003.

Yeakley, J. A., W.T. Swank, L.W. Swift, G.M. Hornberger, and H.H. Shugart, Soil moisture gradients and controls on a southern Appalachian hillslope from drought through recharge, Hydrology and Earth System Sciences 2(1): 41-49, 1998.

Yu, C., W. Warrick, and M.H. Conklin, Derived functions of time domain reflectometry for soil moisture measurement, Water Resources Research 35(6): 1789-1796, 1999.

Figure 4.1 Comparison of daily average temperature (a) and cumulative precipitation during 2002 study period with the 12-year average (1989-2001) (b).

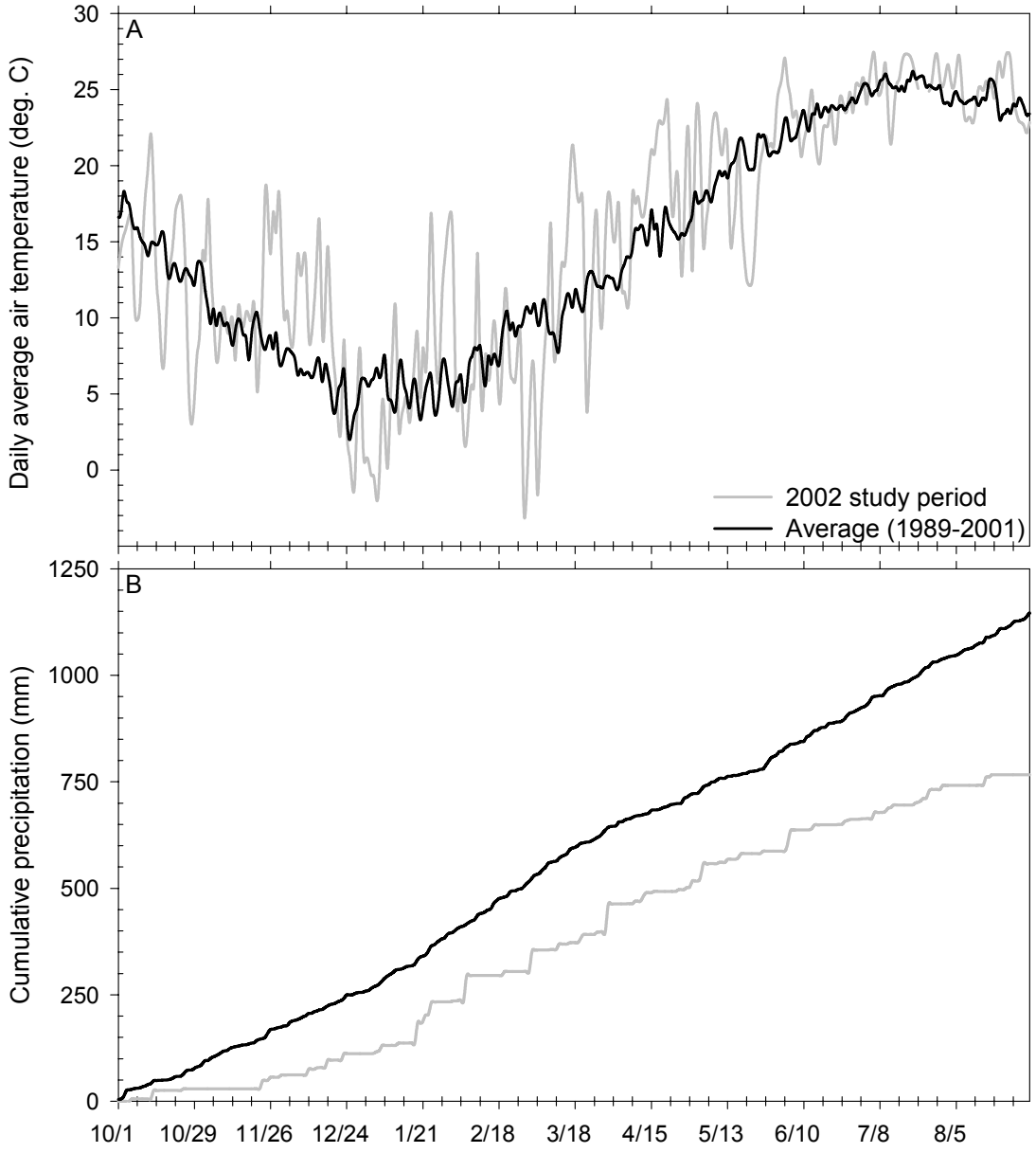

Figure 4.2 Graphs of the daily precipitation (a), the hillslope average soil moisture during the study period and standard deviation of the profile average soil moisture on the hillslope (b), and the hillslope average soil moisture at different depths throughout the study period (c).

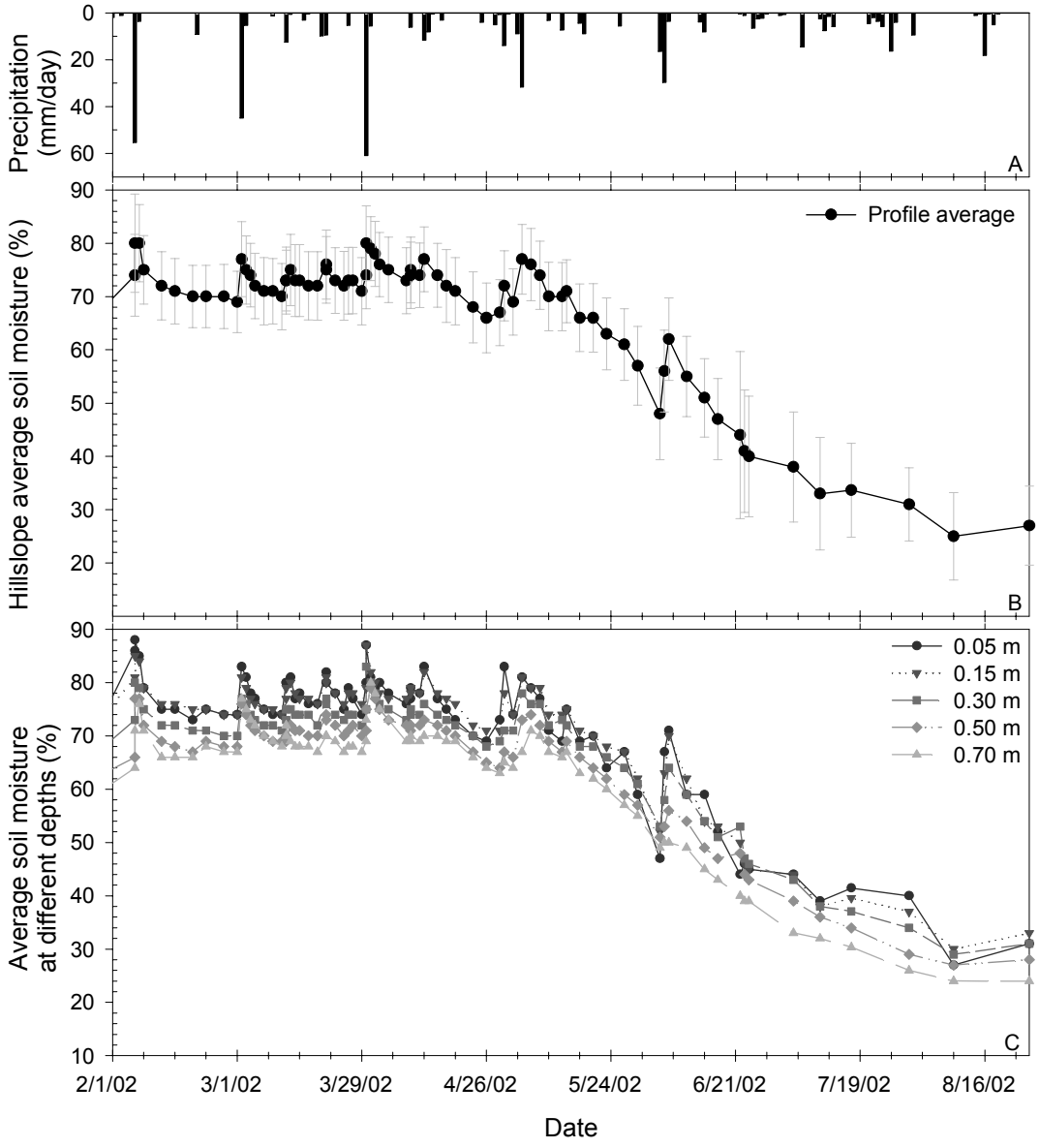

Figure 4.3 Maps of soil moisture at different depths (0.05, 0.15, 0.20 and 0.50 m) below the soil surface on selected dates throughout the study periods. The diamonds represent the measurement locations. We used linear triangulation to interpolate between the measurement locations. Soil moisture at the lower 15 m of the hillslope during June 18-August 26 is influenced by sprinkling experiments (Chapter 6) and not included in further analyses. The shaded grey area represents bedrock.

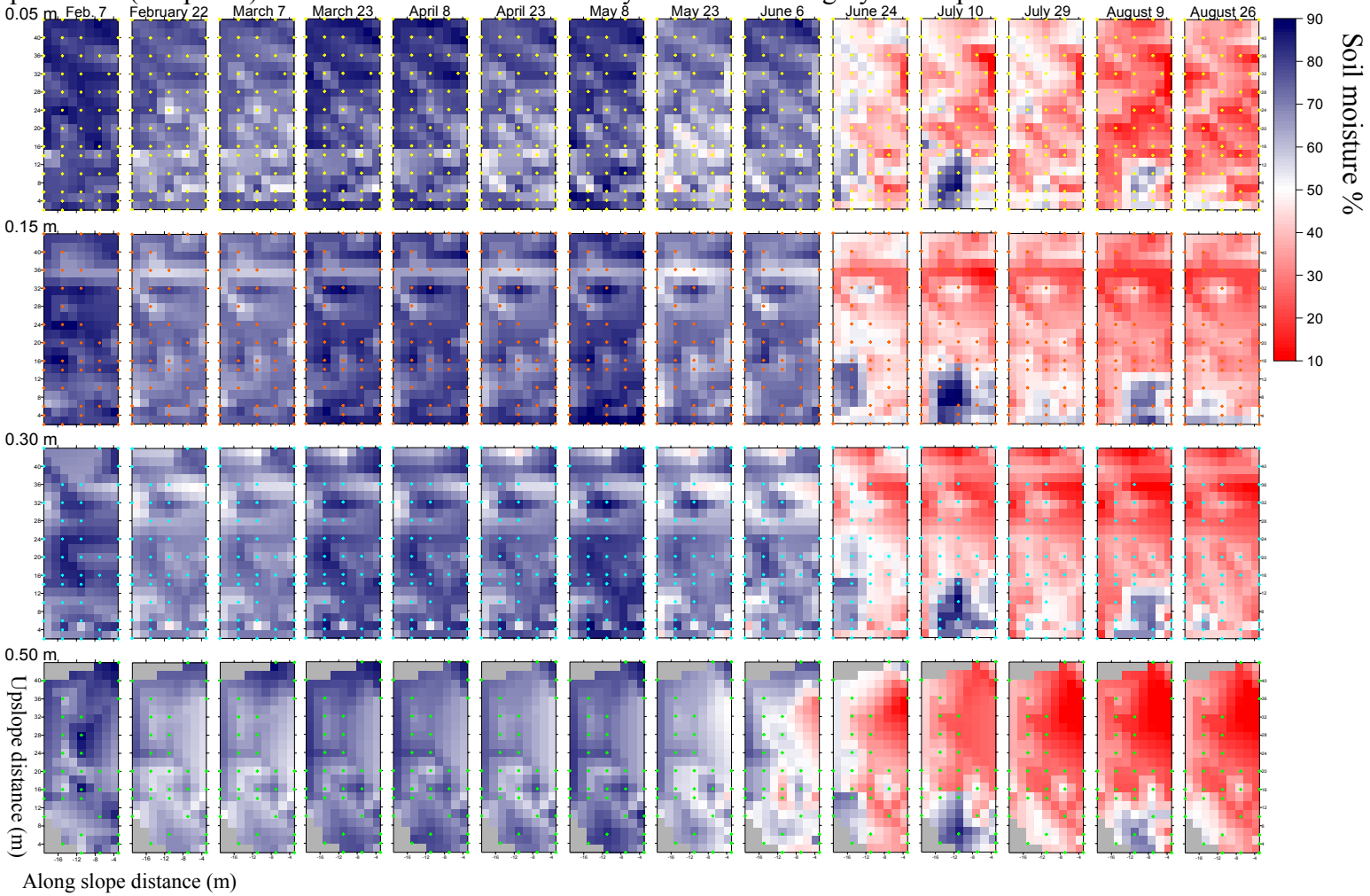

Figure 4.4 Maps of soil moisture at different depths (0.05, 0.15, 0.20 and 0.50 m) below the soil surface on selected dates throughout the drying down period. The diamonds represent the measurement locations. Soil moisture at the lower 15 m of the hillslope during June 18-August 26 is influenced by sprinkling experiments (Chapter 6) and not included in further analyses. The shaded grey area represents bedrock.

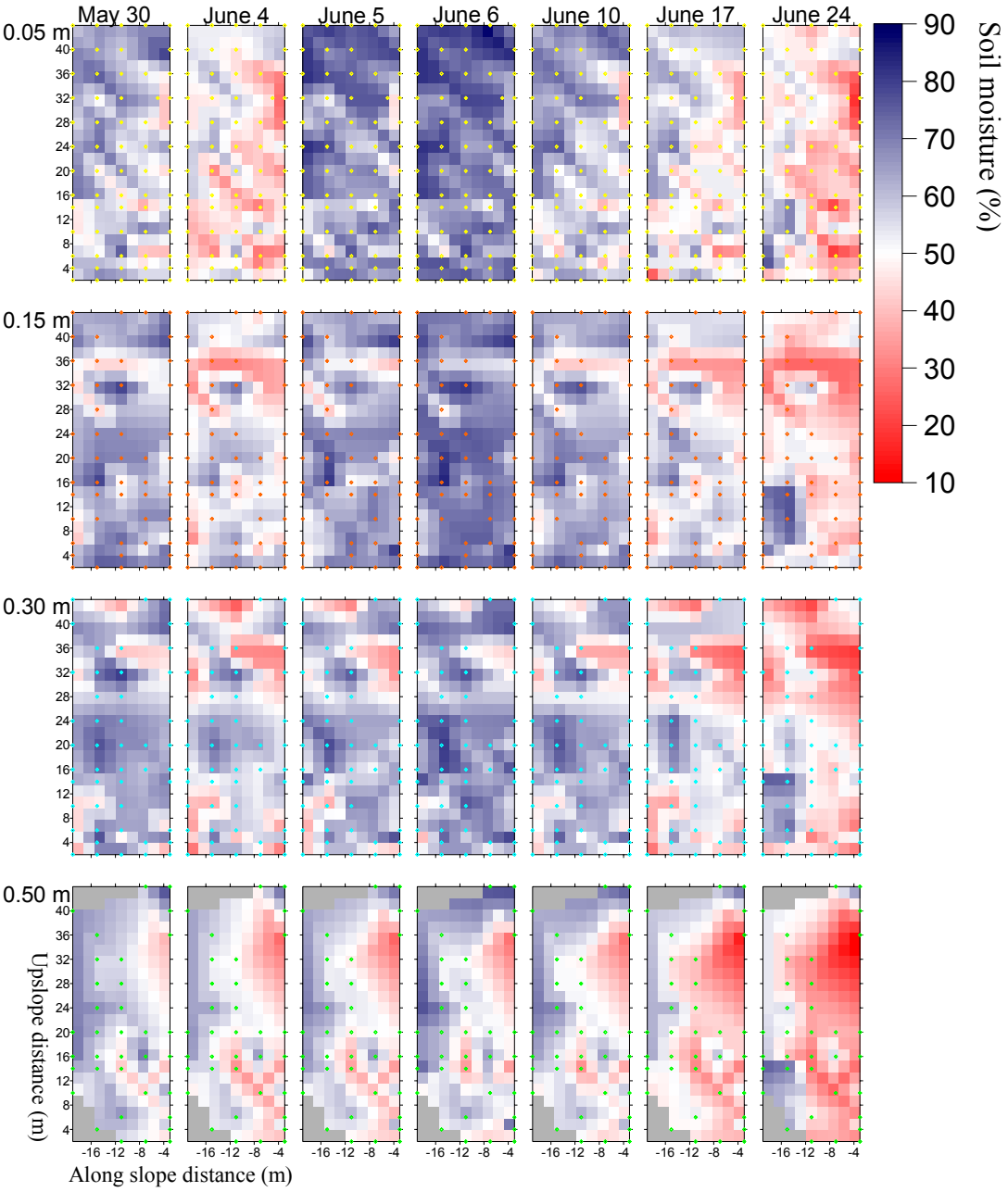

Figure 4.5 Total water extraction between May 1 and August 26 2002 as a function of depth below the soil surface.

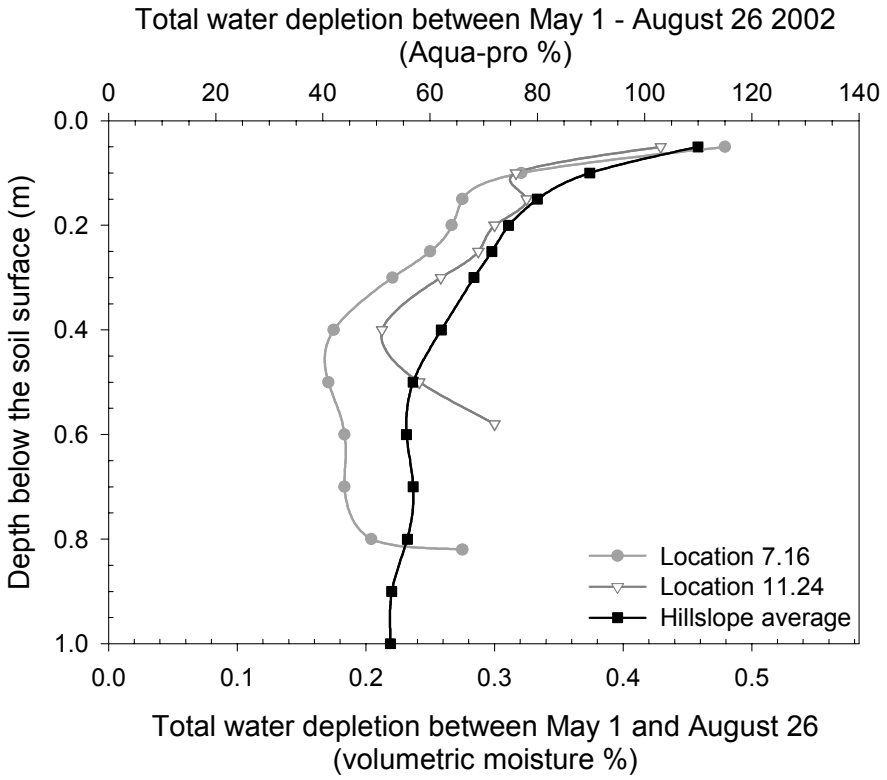

Figure 4.6 Relationship between soil depth and soil moisture at different depths.

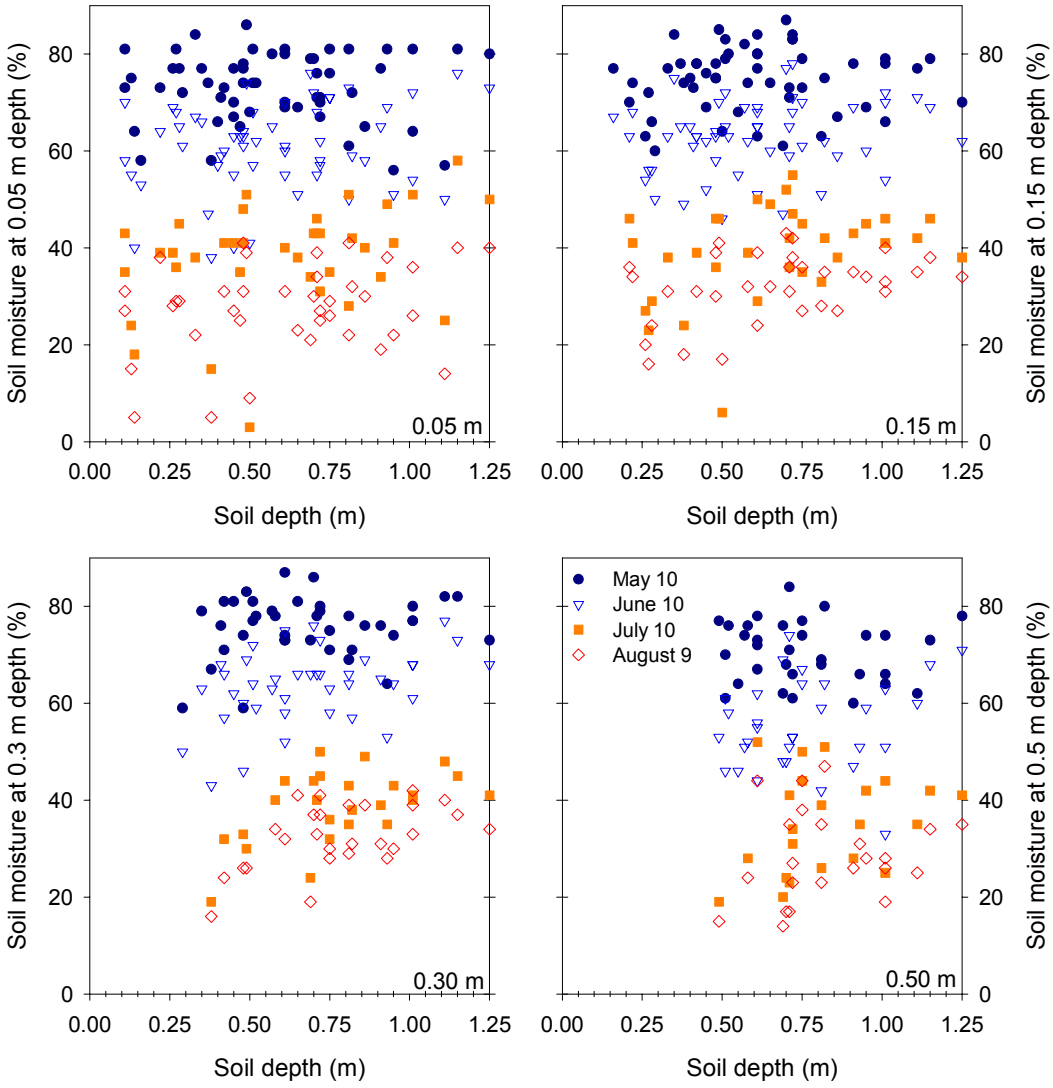

Figure 4.7 Time series of precipitation (a), hillslope average soil moisture (b), the 12-hr (6:00-18:00) and 24-hr average air temperature (c), the 12-hr and 24-hr average relative humidity (d), daily solar radiation (e) and hillslope average transpiration estimated from the sapflow measurements (f).

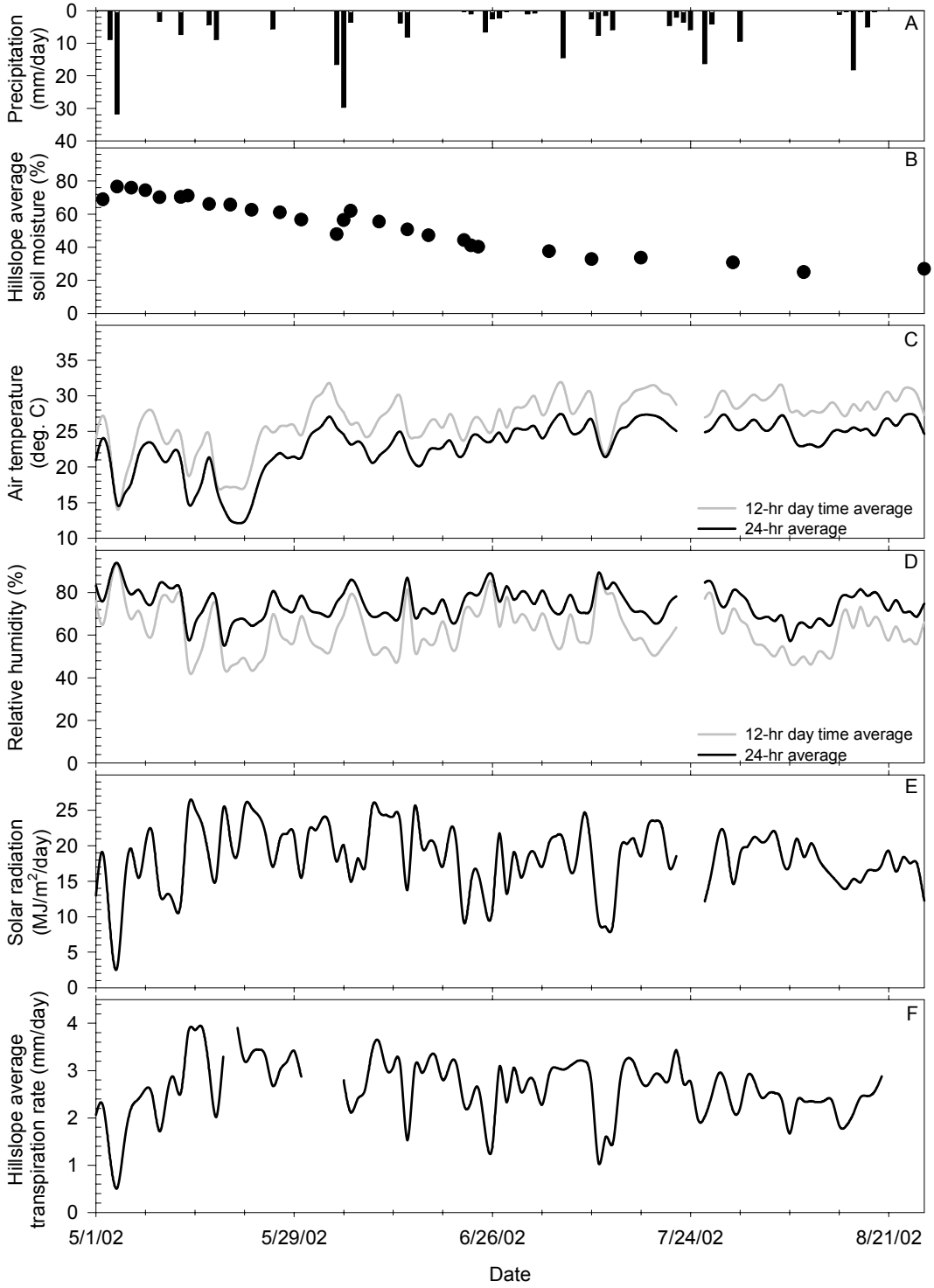

Figure 4.8 Time series of cumulative throughfall, subsurface flow and transpiration throughout the growing season. The error bars represent the cumulative standard error of hillslope average transpiration.

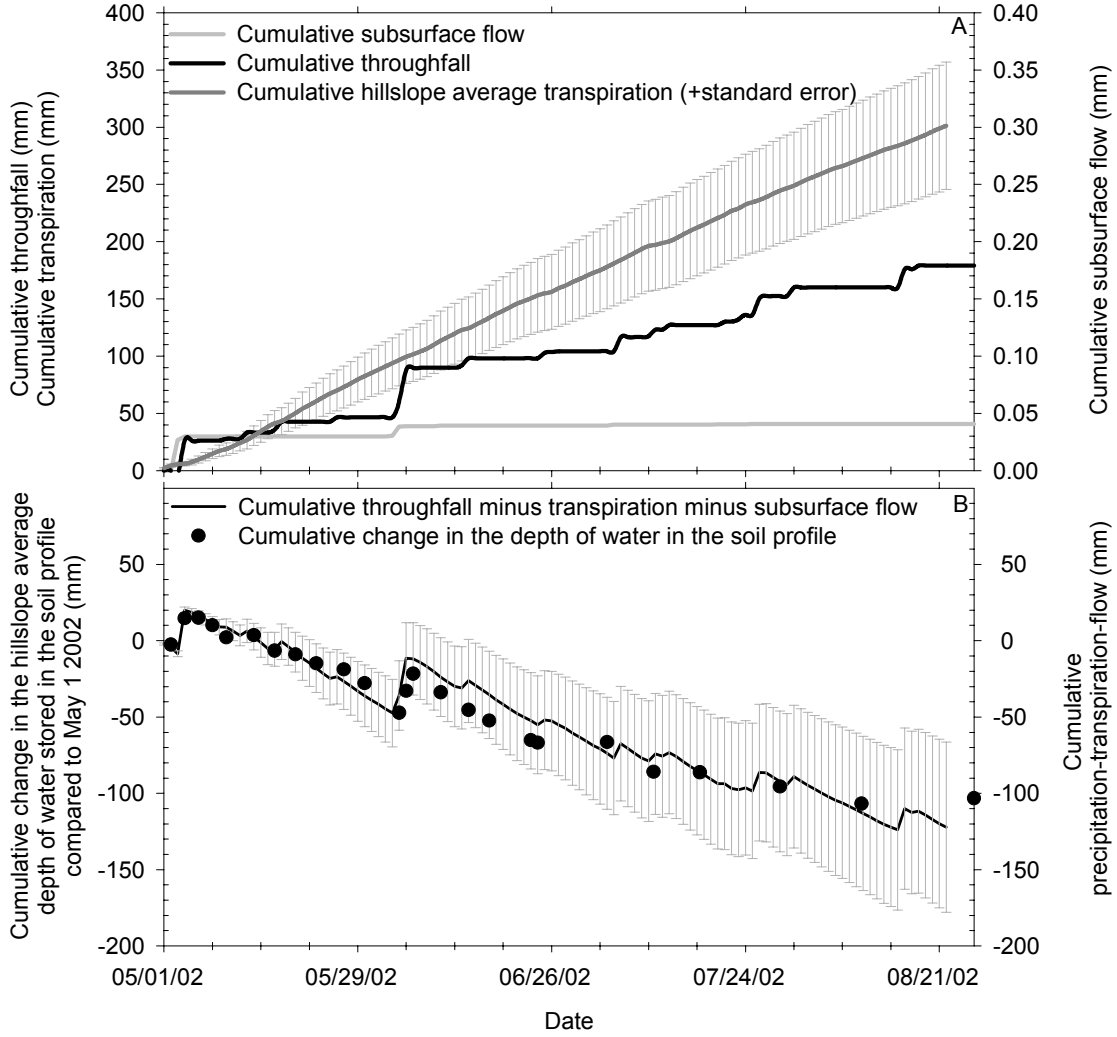

Figure 4.9 Daily precipitation (a) and a comparison of the profile average soil moisture of the upslope and the profile average soil moisture of the midslope (b), of the depth of water stored in the soil profile (c), and the change in the total depth of water stored in the soil profile during the study period (d). The bars in Figure 4.9b represent the standard deviation of the profile average soil moisture.

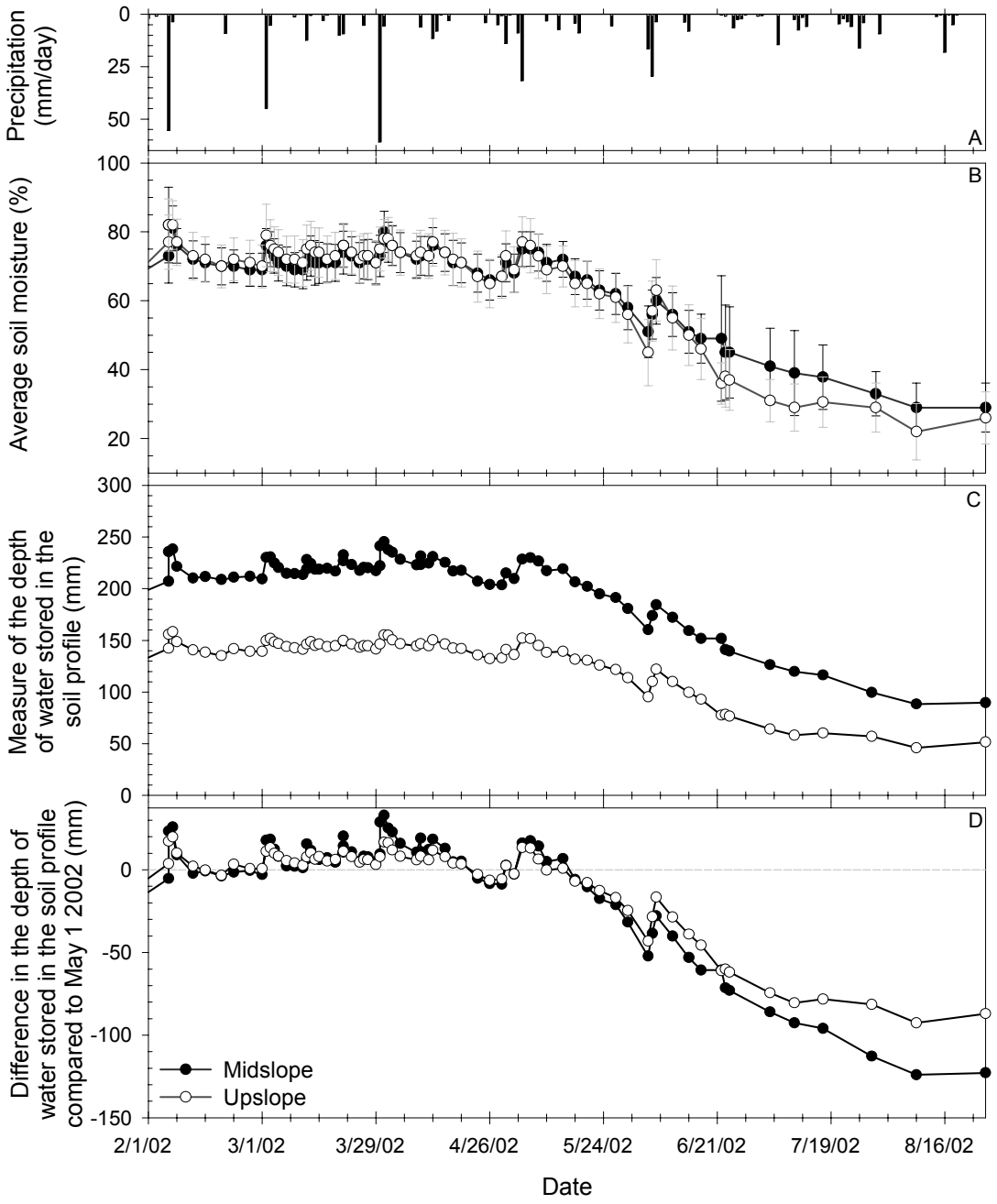

Figure 4.10 Precipitation (a), sapflow response in trees on the lower part of the midslope (b), the midslope (c), and upslope during the late summer (d). The two lines in Figures 4.10b-d represent sapflow measured in two different trees.

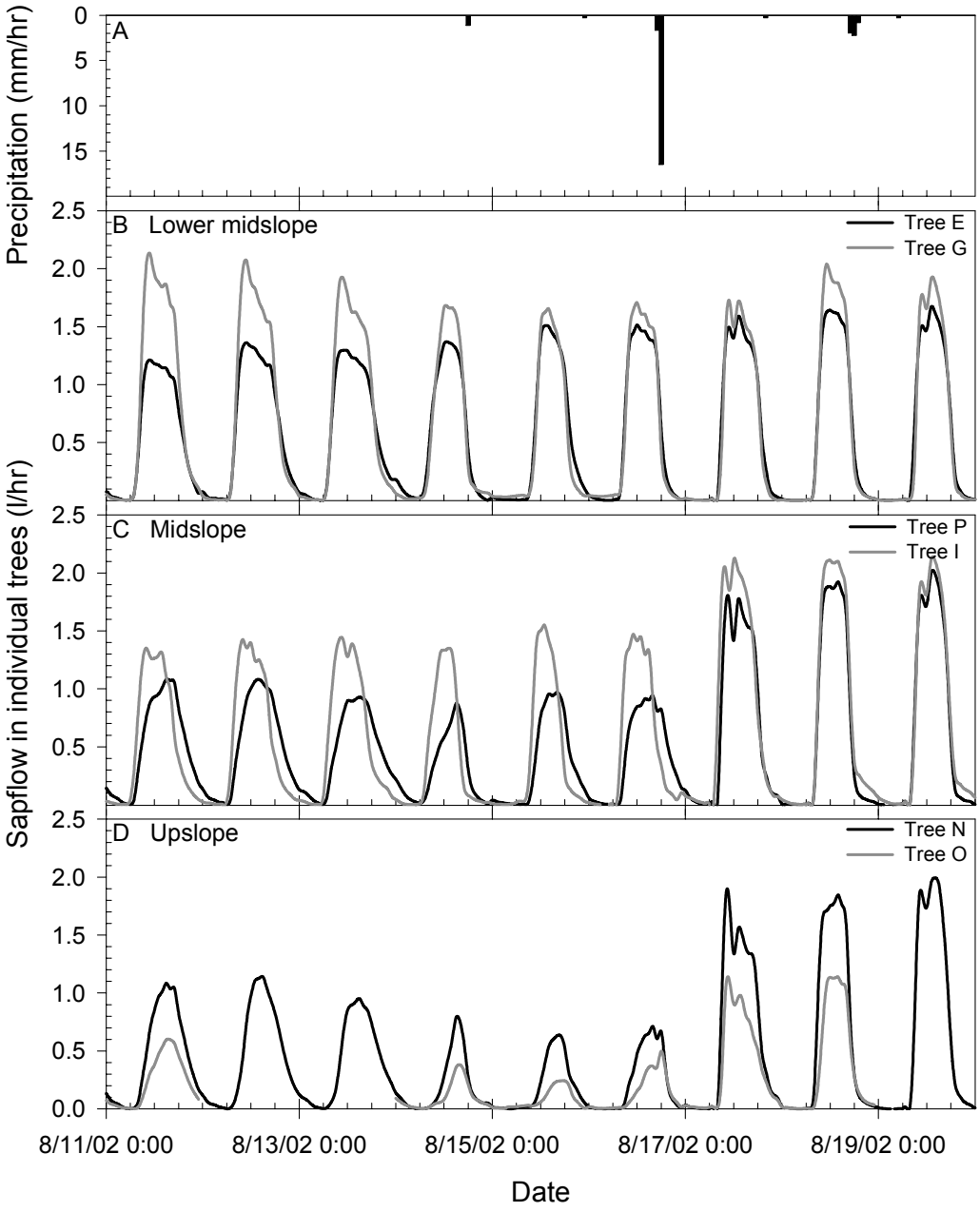

Figure 4.11 Weighted basal area, species distribution and soil depth across the hillslope. The letters in the circles refer to the trees where sapflow was measured. The diameter of the circles represents the DBH of the trees.

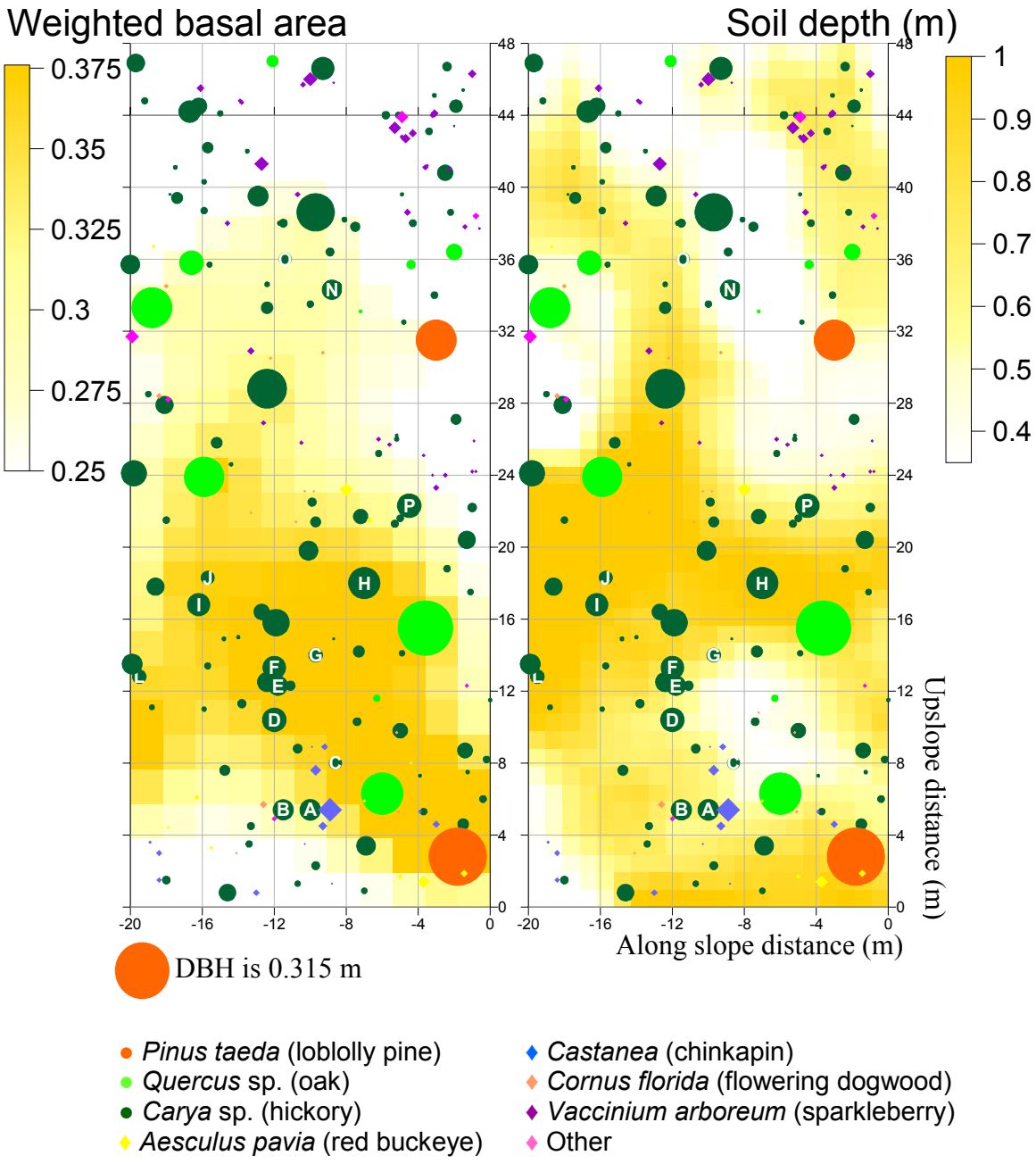

Figure 4.12 Schematic representation of the feedback processes between soil moisture and transpiration and the role of soil depth.

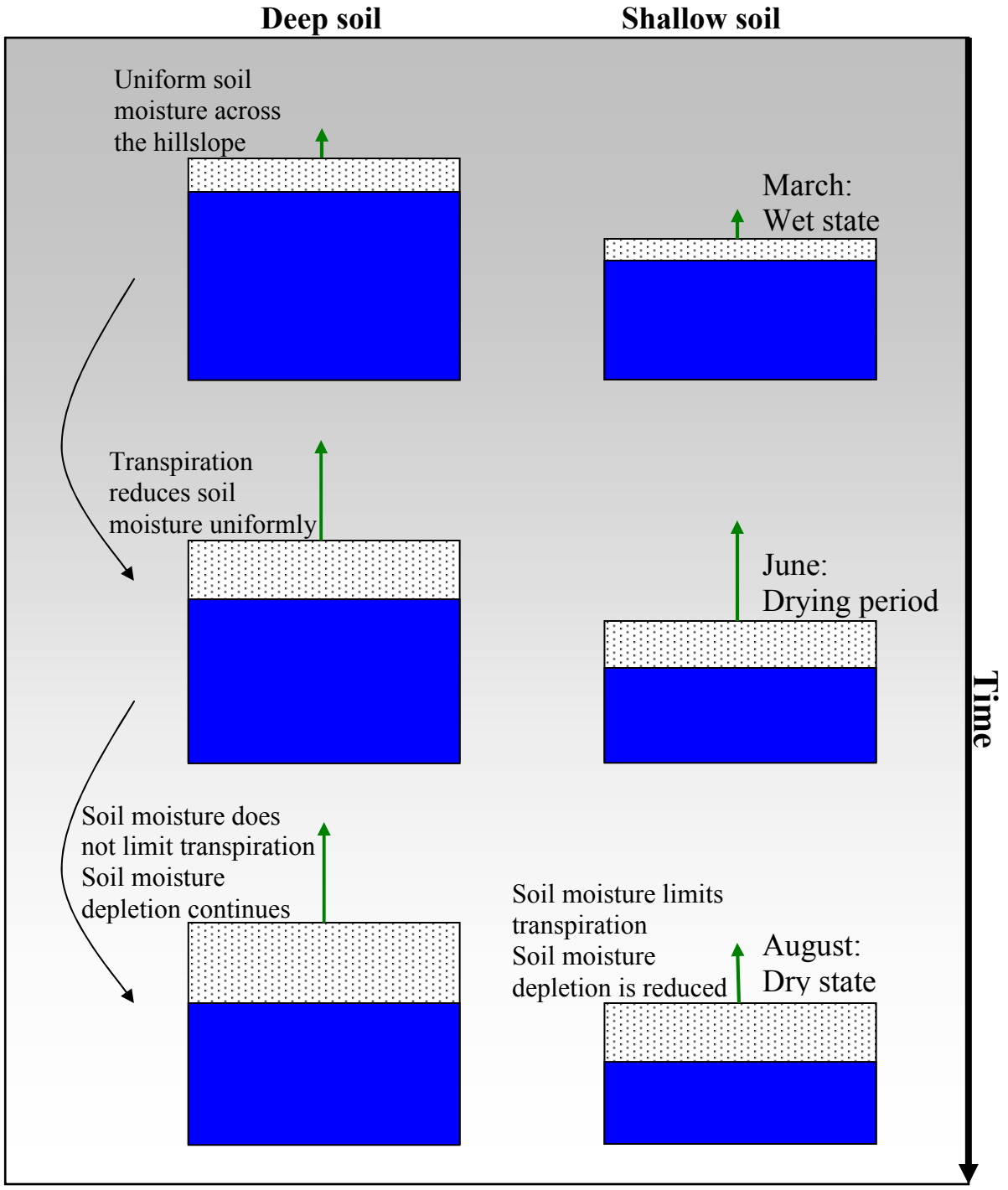

Table 4.1 The r^2 of the relationships between the average soil moisture at different depths in the upper half of the matrix and the slope of the relationships between the average soil moisture at different depths in the lower part of the matrix (in *italic*).

	0.05 m	0.15 m	0.30 m	0.50 m	0.70 m	Bedrock interface	Profile average
0.05 m	-	0.98	0.95	0.92	0.90	0.85	0.97
0.15 m	*1.03*	-	0.99	0.97	0.94	0.91	0.99
0.30 m	*1.11*	*1.08*	-	0.99	0.96	0.93	0.99
0.50 m	*1.07*	*1.05*	*0.97*	-	0.98	0.93	0.98
0.70 m	*0.98*	*0.96*	*0.88*	*0.91*	-	0.92	0.97
At bedrock interface	*0.77*	*0.76*	*0.70*	*0.72*	*0.77*	-	0.93
Profile average	*1.00*	*0.97*	*0.89*	*0.90*	*0.97*	*1.18*	-

Table 4.2 The period average of the Pearson correlation coefficients for the relation between soil moisture at specific depths and topographic variables.

Pearson correlation coefficients	Upslope distance	Topographic index – surface	Topographic index – bedrock	Soil depth	Weighted basal area
Wet state (February-April)					
0.05 m	0.30	-0.26	0.01	-0.06	-0.12
0.15 m	-0.22	0.13	0.03	0.14	-0.13
0.30 m	-0.05	0.04	0.09	0.37	0.09
0.50 m	0.25	0.03	-0.04	0.00	-0.13
0.70 m	0.11	0.14	0.03	-0.07	0.31
Profile average	0.06	-0.15	-0.14	-0.08	0.02
Transition period (May-June)					
0.05 m	0.24	-0.19	-0.05	0.02	-0.06
0.15 m	-0.23	0.13	0.00	0.19	-0.14
0.30 m	-0.10	0.08	0.05	0.42	0.04
0.50 m	0.17	0.01	-0.01	0.25	-0.11
0.70 m	0.04	0.07	-0.05	0.09	0.26
Profile average	-0.06	-0.09	-0.13	0.11	0.00
Dry state (July – August)					
0.05 m	0.13	-0.20	-0.01	0.18	0.21
0.15 m	-0.28	0.16	0.06	0.30	0.13
0.30 m	**-0.52**	0.26	0.13	**0.50**	0.20
0.50 m	-0.35	0.26	0.12	0.43	0.19
0.70 m	-0.40	0.13	0.05	0.22	0.47
Profile average	-0.37	-0.08	-0.02	0.28	0.29

Table 4.3 Comparison of the lower slope, midslope and upslope. Because of artificial water applications on the lower slope, the change in total water storage was not calculated for the lower slope.

	Lower slope	Midslope	Upslope
Upslope distance (m from trench)	0-14	14-25	25-48
Average soil depth (m)	0.67	0.93	0.51
Median DBH (mm)	59	61	54
Average DBH (mm)	88	101	78
Average basal area (m^2/ha)	25.4	31.7	21.3
Contribution to total sapwood area (%)	33	27	40
Contribution to basal area by oak, hickory and loblolly pine (%)	96	95	85
Change in total water storage between May 1 and August 26 (mm)		123	87

5 On the use of multi-frequency electromagnetic induction for the determination of temporal and spatial patterns of hillslope soil moisture

5.1 Introduction

Progress in process hydrology is limited by our ability to make measurements at space and time scales that are relevant to our models. Although soil moisture measurements have become much easier with the advent of Time Domain Reflectometry (TDR) (Topp, 1980; Jones et al., 2002), much of the measurement technology is still at the point scale. Although recent studies have begun to develop distributed data sets of soil moisture using mobile TDR, most notably the Tarawarra study of Western et al. (1999), these measurements are often restricted to shallow soil moisture, i.e. a depth specified by the TDR rod length that is inserted vertically into the soil. Despite a widespread reliance on topography as a surrogate for soil moisture distribution (throughout the soil profile), the Tarawarra work and other data by Western et al. (2004) have shown that terrain may explain little of the variance of observed soil moisture patterns, especially during very wet and very dry conditions.

With soil moisture measurements to date, there is a disconnect from the soil-instrument interface scale to the hydrological process scale of interest (Topp, 2003). Since the introduction of the neutron probe in the 1950's (Holmes, 1956), soil moisture measurement methods have focused on accuracy and precision at the point scale. They have remained highly invasive and often focused on particular depths. In addition, the traditional measurements have integrated only over a very small area or volume, which has been problematic for scaling up soil moisture measurements. Remote sensing on the other hand offers measurement potential at scales of 100s to 1000s of square meters but this scale is too large for hillslope or small catchment scale studies (Lakshmi, 2004). In addition, passive and active microwave measurements are often limited to skin moisture. These satellite and airborne measurements are also problematic in forested terrain.

Electromagnetic induction (EM) has been cited as a potential quick and non-invasive method to map soil moisture patterns at the hillslope to the catchment scale. Previous benchmark EM studies by Kachanoski et al. (1988 and 1990) and Sheets and

Hendrickx (1995) have shown that electromagnetic measurements can potentially be used for soil moisture mapping. Notwithstanding, EM work to date has focused largely on soil salinity assessments (e.g. Rhoades, 1984;Hendrickx et al., 1992; Doolittle et al., 2001), detection of buried objects (e.g. Bevan, 1983), soil type mapping (e.g. Doolittle et al., 2002), soil depth assessment (e.g. Bork et al., 1998), permafrost mapping (e.g. Hauck et al., 2001), detection of polluted plumes (e.g. Sweeney, 1984) and watertable mapping (e.g. Sherlock and McDonnell, 2003). Even though not focusing on soil moisture per se, many of these studies have commented on soil moisture in the course of their work. For instance, electromagnetic studies for salinity appraisals have pointed to the need to correct for the effect of soil moisture on the apparent conductivity measurements (e.g. Rhoades, 1984) but others found that the effect of soil moisture is small and negligible compared to the salinity effects (e.g. Hendrickx et al., 1992). Sherlock and McDonnell (2003) found a different slope for the relation between watertable level and apparent conductivity for each measurement date and suggested that this may be due to soil moisture changes, instrument drift or temperature changes.

Kachanoski et al. (1988) studied the relationships among the spatial variations of soil moisture content, soil texture and the electrical conductivity of the soil solution using the EM38. They showed that apparent conductivity could explain 96 % of the variation in soil moisture. The locations of their sampling sites were selected to obtain the maximum variation in soil moisture content and texture across the site. They found a curvilinear relationship between volumetric soil moisture content and apparent conductivity and significant correlation among all other variables. Kachanoski et al. (1990) found that approximately 50-60% of the variation in soil moisture content was explained by variation in apparent conductivity. Sheet and Hendrickx (1995) found that the temperature corrected apparent conductivity measured with the EM31 could explain between 58 and 64 % of the temporal soil moisture variation in the upper 1.5 m of the soil profile along a transect. Hanson and Kaita (1997) found during the drying of an irrigated field in California that the EM38 could explain between 76 and 95 % of the observed soil moisture variations in the upper 1.2 m of the soil profile, depending on the

salinity level of the field. Sherlock and McDonnell (2003) found for a hillslope in New-York that the EM38 could explain over 70% of the gravimetrically determined soil moisture variance in the upper 0.20 m on one measurement date. They could not check the robustness of the method and found a poor relationship between raw apparent conductivity data and volumetric soil moisture content at 0.10, 0.50 and 1.30 m depth estimated from a moisture release curve and tensiometer data.

EM measures the depth weighted average of the electric conductivity of a column of material to a specific depth, termed the apparent conductivity and is expressed in milliSiemens per meter (mS/m). A transmitter coil produces an electromagnetic field that induces current to flow through the subsurface. This current sets up a secondary electromagnetic field in the soil. By comparing differences in the magnitude and phase of these electromagnetic fields, an EM device measures the apparent conductivity. The profile weighted apparent electrical conductivity of the soil is influenced by the types and concentration of ions in solution, the amount and types of clay minerals, the volumetric water content, temperature and the phase of soil water (McNeill, 1980). Ambient conditions such as air temperature, humidity and atmospheric electricity (spherics) can also influence apparent conductivity measurements. The depth of penetration of the electromagnetic current is influenced by the instrument's coil orientation, the coil separation, the measurement frequency and the conductivity of the soil. Lower frequencies penetrate to greater depth. To date, only single frequencies have been used.

Several issues in relation to EM measurements and soil moisture and the applicability of EM measurements for hillslope hydrological investigations remain. Can EM represent the spatial patterns of soil moisture throughout the year? Can EM be used for soil moisture measurements in areas with shallow soils? And can multiple frequencies be used to extract additional information content from the EM approach and explain the depth profile of moisture? This study makes use of the new multi-frequency GEM-300 (Geophysical Survey Systems Inc., North Salem, NH) to test if certain frequencies are better suited for soil moisture measurements than other frequencies and to determine if it

is possible to obtain information about the depth distribution of soil moisture. Specific questions that we address are:

- Can the GEM-300 be used for soil moisture measurements on a hillslope with shallow soils?
- What frequency is better suited for soil moisture measurements?
- Can the different frequencies be used to derive a soil moisture profile with depth?
- How much of the temporal variance can be explained for individual measurement locations?
- How much of the spatial variance can be explained for individual measurement dates?
- Can a single calibration for one point on the slope be used as a 'master calibration' to obtain distributed soil moisture data?

5.2 Site description

The Panola Mountain Research Watershed (PMRW) is located within the Panola Mountain State Conservation Park southeast of Atlanta, Georgia (84˚10'W, 33˚37'N). The climate at PMRW is classified as humid subtropical. The mean annual temperature is 16.3 ˚C. Mean annual precipitation is 1240 mm and is distributed relatively uniform throughout the year. Rainfall tends to be of longer duration and lower intensity associated with the passage of fronts in the winter, and of shorter duration but higher intensity, associated with thunderstorms, in the summer. Streamflow at PMRW has a seasonal pattern with the highest flow occurring during the November through March dormant season. Bedrock at PMRW is dominated by the Panola Granite (granodiorite composition) of Carboniferous age, described as a biotite-oligioclase-quartz-microcline granite (Crawford et al., 1995).

The experimental hillslope is located approximately 30 m upslope from an ephemeral stream. A 20 m wide trench to bedrock forms the lower boundary of the hillslope and a small bedrock outcrop forms the upper boundary of the hillslope. Soils on

the experimental hillslope are best described as a light colored sandy loam with little textural differences and a 0.15 m humus rich horizon. No large differences in soil texture or soil type are observed across the hillslope. The average soil depth of the experimental hillslope is 0.63 m and ranges from 0-1.8 m. In general soils on the lower slope (<25 m upslope from the trench) are deeper than soils on the upslope (> 25 m upslope from the trench). The average soil depth of the lower slope and upper slope is 0.80 and 0.51 m respectively. The surface topography is relatively planar while the bedrock topography is more irregular, as mapped by McDonnell et al. (1996). The average slope is 13 degrees.

5.3 Methods

5.3.1 Electromagnetic measurements

Hillslope surveys were made with the GEM-300 over the course of a 10 month period (81 separate surveys between November 2001 and August 2002). This period represented the late wetting-up, wet, drying and dry part of the hydrological year. Measurements were made on average two to three times per week during the winter and early spring and once every two weeks during the late spring and summer. Measurements were made at 65 locations on an approximately 4 by 4 m grid across the hillslope and a 4 by 2 m grid on the lower 6 m of the hillslope. A complete hillslope survey took 45 minutes to complete. The vertical dipole at hip height (~0.85 m above the soil surface) configuration was used because this configuration was the most practical and the fastest configuration for EM data acquisition. Sheets and Hendrickx (1995) showed that there were negligible differences between different dipole configurations for the EM31. We assumed that this would apply to the GEM-300 measurements as well. Special care was given to assure the same position, height and direction of the instrument during each measurement. Four frequencies were recorded simultaneously: 7290, 9090, 11250 and 14010 Hz. The frequencies of the widely reported EM31 and EM38 are 9800 and 14600 Hz respectively. In theory, the depth of penetration for all four frequencies was deeper than the soil depth at the hillslope. However, previous studies have shown that the actual depth of observation (= the depth that contributes the largest part to the total EM

response) is much shallower than the theoretical depth of penetration (Roy and Apparao, 1971). Also, surface and shallow soil layers contribute more to the overall response than deeper layers. Thus we assumed that even though the theoretical depth of penetration was deeper than the soil depth, the conductivity response contained enough information from the shallow soil layers that these frequencies can be used to measure soil moisture on the hillslope. The lateral resolution of the measurement is approximately equal to the inter-coil spacing, which is 1.3 m for the GEM-300. Apparent conductivity values from measurements with the GEM-300 were relative to the calibration standard. Hillslope average apparent conductivity was calculated by averaging the apparent conductivity of all measurement locations.

On six measurement dates in this study, the measured apparent conductivity values were outside the range of the other measured apparent conductivity values. These measurements have been omitted from the analyses.

5.3.2 Soil moisture measurements

Soil moisture measurements were made during February-August 2002. Soil moisture was measured using the Aqua-pro (Aqua-pro Sensors, Reno NV) (radio frequency) capacitance sensor. Sixty-four polycarbonate access tubes were installed on a 4 by 4 m grid across the hillslope and a 4 by 2 m grid on the lower 6 m of the hillslope. The fixed tube locations ensured repeatability for EM calibration. Aqua-pro measurement values range from 0 (in air dried soil or air) to 100 % (in fully saturated soil). Soil moisture was measured at 0.050 m depth intervals between the soil surface and 0.30 m, and at 0.10 m depth intervals between 0.30 m below the soil surface and the depth of the soil-bedrock interface. Profile average soil moisture was calculated by multiplying the soil moisture values at the different measurement depths by the distance between the subsequent measurement depths and dividing this by the total soil depth. Hillslope average soil moisture was calculated by averaging profile average soil moisture from all measurement locations. Hillslope average soil moisture at a certain depth was calculated

by averaging all soil moisture measurements at a certain depth. More information about the soil moisture measurements and the observed spatio-temporal soil moisture patterns can be found in Chapter 4. We determined the relation between apparent conductivity from the EM measurements and soil moisture using only measurements made on the same day (55 occasions).

5.3.3 Soil depth measurements

The hillslope was surveyed on a 2 m grid. Depth to bedrock was measured on the same survey grid network using a 25.4 mm soil corer forced down to refusal. A small hand auger was used when soil depth was greater than 1.25 m. The multidirectional flow algorithm of Quinn et al. (1991) was used to calculate the drainage area for both the soil-bedrock interface and the soil surface. The topographic index (Kirkby, 1975) was calculated for both the surface topography and bedrock topography (Freer et al., 1997).

5.4 Results

5.4.1 Temporal patterns

The temporal response of the hillslope average apparent conductivity was very similar for the four measured frequencies (Figure 5.1b). There was a strong linear relation between the apparent conductivities measured with the four frequencies (Table 5.1). In general, apparent conductivity was high (positive) during the winter months and low during the summer months. Measured soil moisture showed no changes or stratification with depth during most of the study period (Figure 5.1c). Soil moisture at the different depths was highly correlated to each other (Table 5.2). Soil moisture stratification with depth occurred only directly after storms during the late spring and summer when rainfall did not penetrate to depth but rather increased only soil moisture near the surface (e.g. the 41 mm May 5-6 storm and the 50 mm June 4-6 storm, Figure 5.1c).

The relationship between hillslope average soil moisture at a certain depth and hillslope average apparent conductivity was linear (Figure 5.2). Nevertheless, there was a non-linear trend at high soil moisture. The relation between apparent conductivity and soil moisture did not depend on either the depth of the soil moisture measurement or the frequency. The relation between soil moisture and apparent conductivity was good for all depths and frequencies. Apparent conductivity at discrete measurement locations and measured soil moisture at the same sites were also linearly related (Table 5.3).

On the few measurement dates when there was a difference between soil moisture at the different depths below the soil surface, the ratio of apparent conductivity measured by the different frequencies was related to the ratio of soil moisture at the different depths (Figure 5.3).

The relationship between soil moisture and measured apparent conductivity was strong for most measurement locations (r^2 larger than 0.75 for 55 % of all locations) (Figure 5.4a). The relation between soil moisture and apparent conductivity was not as strong for some locations on the lower 14 m of the hillslope (Figure 5.5). The low r^2 for these locations was caused by several outliers. These outliers occurred during artificial water applications on the lower 14 m of the hillslope between June 18 and August 20 2002, associated with another experiment (which is described in Chapter 6). Soil moisture was increased artificially but the measured apparent conductivity remained close to constant or decreased. When the soil moisture measurements that were influenced by the artificial water applications were excluded from the analysis, the r^2 increased to larger than 0.75 for 85 % of the measurement locations (Figure 5.4b). There was no relation between the r^2 of the linear relation between soil moisture at depth and the apparent conductivity with any of the computed topographic variables (up-slope distance, along-slope distance, surface elevation, bedrock elevation, topographic index based for the surface and bedrock topography, soil depth).

The relation between soil moisture and apparent conductivity had a different slope and intercept for each measurement location (Table 5.4). The slope and intercept of the linear relation between soil moisture and apparent conductivity were linearly related to each other (r^2=0.70-0.83 depending on the depth of the soil moisture measurements). The slope and intercept were also related to the soil depth at that measurement location (r^2=0.11-0.50). For sites with deeper soils, the intercept was smaller (more negative) and the slope was larger than for sites with shallower soils. There was no relation between the slope or intercept and any of the other topographic variables.

We used the linear relation between soil moisture and apparent conductivity and the measured apparent conductivity values to convert the apparent conductivity values to calculated soil moisture values. We did this by (1) using the linear relation between soil moisture and apparent conductivity for each individual measurement location and (2) by using the same linear relation between soil moisture and apparent conductivity for all measurement locations. The temporal patterns of calculated soil moisture (from the apparent conductivity measurements) represented the temporal patterns of hillslope average soil moisture at the different depths well (Figure 5.6). Calculated soil moisture was larger than observed soil moisture during the winter months. The general dry down after late April was well represented. Although soil moisture was over predicted, the EM signal also showed the clearly wetting and drying of the soil in response to the measured rainfall events (inserts in Figure 5.6); but the calculated increase in soil moisture after the 50 mm storm on June 4-6 was less than observed. There were also some discrepancies between calculated and observed soil moisture, e.g. the increase in calculated soil moisture on April 23-26 2002. There was less than 10 mm precipitation between April 15 and April 26 2002; thus the lack of an increase in measured soil moisture was real.

5.4.2 Spatial patterns

The spatial patterns of measured and calculated profile average soil moisture are shown in Figure 5.7. Here, we focus on the relatively short drying down period (as

opposed to the wet and dry period) where spatial and temporal variations in soil moisture were most dynamic. The observed profile average soil moisture pattern was not correlated to any of the topographic variables. Similarly, soil moisture at the different depths was not related to any of the topographic variables. One exception was soil moisture at 0.30 m during summer, which was correlated to soil depth (Chapter 4). Calculated soil moisture from the apparent conductivity measurements represented the seasonal drying down and the rewetting during the 50 mm June 4-6 2002 storm well despite not showing any response for the artificial wetting of the soil on the lower 14 m of the hillslope during the June 18-August 20 2002 period. The rewetting during the 50 mm June 4-6 2002 storm described by the EM measurements was not as complete as observed, especially for the 7290 and 9090 Hz frequencies that theoretically penetrate deepest.

The spatial soil moisture pattern during the drying down period was well represented when the individual relations between soil moisture and apparent conductivity for each measurement location were used for conversion from apparent conductivity values to soil moisture values. Nevertheless the spatial soil moisture pattern was smoothed and more uniform when the same relationship between soil moisture and apparent conductivity was used for all measurement locations. Calculated soil moisture was consistently wetter or drier than measured for some measurement locations but there was no spatial pattern in the difference between observed and calculated soil moisture. The correlation length of observed and calculated soil moisture also agreed well (Figure 5.8). The correlation length of observed soil moisture and calculated soil moisture was short during the winter and increased (but was still short (<10 m)) during the summer.

The spatial pattern of calculated soil moisture represented up to 92% of the observed spatial soil moisture pattern on a measurement day, when the individual relationships between soil moisture and apparent conductivity for each individual measurement location were used. The measured apparent conductivity could represent more of the observed spatial pattern in soil moisture during the winter months when the

average soil moisture was high, than during the summer months, when soil moisture was low (Table 5.5). When only one master relationship was used to convert the measured apparent conductivity values to soil moisture values, the calculated soil moisture pattern did not represent the observed soil moisture pattern well (Table 5.5).

The range of soil moisture values calculated when using one master relationship to convert the apparent conductivity values into soil moisture values was much smaller than the range in observed soil moisture values during the wet period, the drying period and dry period (Figure 5.9).

5.5 Discussion

5.5.1 Four frequencies: same signal

All four frequencies could be used to predict soil moisture at the Panola hillslope. While the higher frequencies (11250 and 14010 Hz) represented the wetting up after the June 4-6 2002 storm better than the lower frequencies (7290 and 9090 Hz), all four frequencies were linearly related to each other (Table 5.1). This limited our ability to use the four different frequencies to obtain a soil moisture profile with depth. This situation could be due to the good correlation between soil moisture at the different depths at this site (Table 5.2). Data does suggest that when there is a difference between soil moisture at the different depths below the soil surface, the ratio of apparent conductivity measured by the different frequencies is related to the ratio of soil moisture at the different depths (Figure 5.3). There is thus still a need to test if it is possible to use the multiple frequencies of the GEM-300 to obtain a depth distribution of soil moisture on a site with larger variations in soil moisture with depth. Doolittle et al. (2001) found during a comparison of the GEM-300 and the EM-38 for a salinity appraisal study that although each instrument and frequency had a different theoretical penetration depth, the instruments had similar depths of observation (the depth that contributes the largest part to the total EM response). They concluded that the close similarity in the data collected at different frequencies indicated that the sensitivity of the GEM-300 to variations in

conductivity with increasing depth was diminished by the high conductivity of the upper part of the soil profile at their study site. At Panola, there were no high conductivity soils, but still, the multi-frequency EM was not usable to resolve a soil moisture profile with depth. The manufacturer of the EM31 and EM38 (Geonics Ltd.) notes that in principle, multi-frequency EM can not be used to obtain a depth distribution of apparent conductivity because of equivalence issues, i.e. many different layered models give the same measured response (McNeill, 1996).

5.5.2 External influences on EM response

On six measurement dates in this study, the measured apparent conductivity values were outside the range of the other measured apparent conductivity values. These occasions occurred after or during rain events and were omitted from the analyses. These measurements could have been influenced by external factors, e.g. lightening. Air temperature and relative humidity variations could also have been responsible for part of the differences between the temporal patterns of observed soil moisture and calculated soil moisture on some days (e.g. the increase in calculated soil moisture on April 23-26 2002, Figure 5.6).

Apparent conductivity measurements can vary due to changes in soil temperature (Slavich and Petterson, 1990). We standardized the field measured apparent conductivity values to an equivalent electrical conductivity at a reference temperature of 25 ºC using measured soil temperature at 0.4 m below the soil surface and a conversion function given by Sheets and Hendricks (1995). Standardizing the apparent conductivity measurements to a reference temperature changed the range but not the temporal pattern of the apparent conductivity measurements during the study period and did not affect the relationship between measured soil moisture and the apparent conductivity. Both the temperature standardized and the uncorrected apparent conductivity were a linear function of soil moisture. Hence we did not use the temperature standardized apparent conductivity values in the analyses.

EM measurements can be influenced by (thermal) drift (Robinson et al., 2004). The GEM-300 was usually left outside to thermally equilibrate for at least 30 minutes before the measurements were made on each recording session. Because of the short time to complete the measurements on the hillslope, we initially assumed that drift would be minimal. However, there was a linear relationship between station number and apparent conductivity on seven measurement dates (mostly during the winter). Because of the configuration of the measurements, this also corresponded to a relation between apparent conductivity and upslope distance. There was no relation between observed soil moisture and upslope distance on these days. The relation between apparent conductivity and station number could be due to insufficient time to thermally equilibrate the GEM-300. On one occasion we kept the GEM-300 stationary and took measurements at one location for five hours, during which the air temperature increased from 11ºC to 21ºC and the apparent conductivity changed by 7 mS/m. The relationship between air temperature and apparent conductivity was non-linear during this drift experiment. Drift effects can also be caused by sun flecks, which result in differential heating of the GEM-300. During the drift experiment described above, the instrument was continuously in the shade. During the real measurements on the hillslope, sun flecks could have influenced the measurements during the winter period when the canopy did not provide complete and uniform shade. Sudduth et al. (2000) found for the EM38 that drift in apparent conductivity may not be caused by temperature variations, but that drift may merely be a function of instrument instability integrated over time. In their tests drift per time was relatively constant within a test but varied from day to day. They concluded that the causative factors of drift in apparent conductivity appear to be complex, and not readily compensated for with additional readily obtained measurements, such as ambient air temperature.

5.5.3 Periods when EM was not sensitive to changes in soil moisture

During the winter months, calculated soil moisture was larger than observed soil moisture. This was due to the non-linearity in the relation between apparent conductivity

and soil moisture at high soil moisture. Using a more complex relation (or two relations; one for high soil moisture and one for lower soil moisture) to describe the relation between soil moisture and apparent conductivity eliminates this over-prediction.

During the artificial water applications a small area (approximately 12 by 5.5 m) was brought to near saturation while the neighboring soil was dry. The area of wet soil was larger than the theoretical lateral resolution of the GEM-300 (1.3 m). However, the GEM-300 was not able to detect the fact that, after the artificial water applications, this area of the hillslope was still wetter than the surrounding soil (e.g. June 24 in Figure 5.7). An increase in soil moisture was at least partially represented in the apparent conductivity measurements after the 50 mm storm on June 4-6 2002. This storm did not penetrate to more than 0.50 m at most soil moisture measurement locations. Part of the EM signal came from deeper than the shallow soil and the lower frequencies of the GEM-300 therefore did not capture the total extent of the rewetting of the shallow soil layers on the hillslope during the June 4-6 2002 storm.

The artificial water applications changed the soil temperature under the area of the artificial water applications. Artificial water applications on another site in the catchment changed soil temperature at 0.40 m depth by 4.5 °C. To check the influence of spatial variations in soil temperature on the apparent conductivity measurements, we standardized the field measured apparent conductivity values on June 24 2002 to an equivalent electrical conductivity at a reference temperature of 25 ºC by using a conversion function given by Sheets and Hendricks (1995). A change of soil temperature by 4.5 °C changed the temperature standardized apparent conductivity by a factor of 1.27. An increase in apparent conductivity by a factor of 1.27 corresponded to an increase in the calculated profile average soil moisture on June 24 2002 from 47 to 60 % at location 19.10 (located 19 m from the right side of the hillslope when looking up and 10 m upslope from the trench). Calculated profile average soil moisture at this location on June 17 2002 (prior to the artificial water applications) was 48 %. Observed profile average soil moisture at this location before and after the artificial water applications was 45 and

62 % respectively. Thus the spatial pattern of soil temperature due to the artificial water applications could have been responsible for the lack of the expression of the wetting up of the soil after the artificial water applications.

5.5.4 Representing spatial variability when one master relationship is used

The correlation length of observed soil moisture on this hillslope was small during most of the study period (Figures 5.8). The range of observed soil moisture values on this hillslope was also small during most of the study period (Figure 5.9). When a different relationship between soil moisture and apparent conductivity was used for each location, the calculated soil moisture pattern and frequency distribution resembled the observed soil moisture pattern and frequency distribution well. But when a single master relationship was used for all measurement locations, the soil moisture patterns were smoothed and did not resemble the observed soil moisture pattern well (Figure 5.7). In addition the range in soil moisture values was reduced compared to observed soil moisture (Figure 5.9). We believe that a large part of the smoothing was due to the much larger measurement area of the GEM-300 compared to the Aqua-pro measurements. The lateral resolution of an EM measurement is approximately equal to the inter-coil spacing (1.3 m for the instrument used in this study) while the measurement volume of the Aqua-pro sensor is approximately $5x10^{-5}$ m^3. In addition, some of the Aqua-pro measurements could be influenced by small roots, rocks or gaps/air pockets next to the access tubes. This would influence soil moisture measurements made with the Aqua-pro sensor but not the soil moisture measurements with the GEM-300. This would lead to a different calibration relationship between soil moisture and apparent conductivity at these measurement locations compared to other measurement locations because this effect was incorporated into the calculated soil moisture measurements, when the individual relationship between soil moisture and apparent conductivity was used for each measurement location. This leads to more variation and a calculated soil moisture pattern that could explain more of the observed soil moisture pattern. Notwithstanding, this

pattern might be largely influenced by small scale soil moisture variation and may not represent the real soil moisture pattern well.

There was no pattern in the calculated versus measured soil moisture residuals. This indicated that the differences between calculated and observed soil moisture patterns were not due to differences in texture, clay mineralogy or solute concentrations across the hillslope but rather, were due to small- and local scale features. Hence, calculated soil moisture at some locations was persistently higher or lower than observed soil moisture at some locations. The smoothing of soil moisture may therefore not be due the inability of the EM to detect differences in soil moisture, but rather the difference in the area-of-influence of the measurements.

5.6 Conclusion

The GEM-300 appears to be a useful tool for gathering distributed soil moisture information in shallow soils. The relationship between soil moisture at different depths below the soil surface and apparent conductivity was good for all four frequencies. It was not possible to obtain a depth distribution of soil moisture with the different frequencies of the GEM-300 because the four frequencies were themselves highly correlated. Nevertheless, at the Panola study hillslope, measured soil moisture at different depths was also correlated, except directly after storms in spring and summer. During these more dynamic moisture periods (e.g. the June 4-6 2002 storm) the higher EM frequencies represented the wetting up of the upper soil better than the lower EM frequencies.

When only one relationship between soil moisture and apparent conductivity was used (our so called master relation) to convert the apparent conductivity values at all locations to soil moisture values at individual measurement locations, the spatial patterns of soil moisture were not represented well. The calculated soil moisture pattern was smoothed compared to the observed soil moisture pattern. We believe that this is due mainly to the difference in measurement area between the soil moisture measurements

made with the EM and the Aqua-pro sensor. The correlation length of both observed and calculated soil moisture was short.

Although soil moisture data obtained with EM is not as precise and accurate as point measurements with TDR and while the EM is more susceptible to external influences, the possibility of obtaining a spatial soil moisture pattern and a measurement that integrates over a larger area (and is thus less susceptible to local disturbances around the probe) makes EM useful in catchment or hillslope studies. We believe that apparent conductivity data together with a few soil moisture measurements (to obtain the relationship between soil moisture and apparent conductivity) is a potential way forward for obtaining spatially distributed data for the calibration of spatially distributed models. We believe that EM measurements are especially useful in a spatial or temporal pattern approach, where the temporal changes in soil moisture or the spatial patterns of soil moisture are more important than the absolute volumetric soil moisture content values at a point.

5.7 Acknowledgements

We would like to thank Mr. L. Gordon (Geophysical Survey Systems Inc) for his advice and assistance with some technical issues we had with the GEM-300. This work was supported by NSF grant EAR-0196381.

5.8 References

Bevan, B., Electromagnetics for mapping buried earth features, Journal of Field Archeology 10: 47-54, 1983.

Bork, E.W., N.E. West, J.A. Doolittle, and J.L. Boettinger, Soil depth assessment of sagebrush grazing treatments using electromagnetic induction, Journal of Range Management 51(4): 469-474, 1998.

Crawford T.J., M.W. Higgins, R.F. Crawford, R.L. Atkins, J.H. Medlin, and T.W. Stern, Revision of stratigraphic nomenclature in the Atlanta, Athens, and Cartersville 30 ð 60 quadrangles, Georgia. Georgia Geologic Survey Bulletin B-130: Atlanta, Georgia; 48, 1999.

Doolittle, J.A., M. Petersen, and T. Wheeler, Comparison of two electromagnetic induction tools in salinity appraisals, Journal of Soil and Water Conservation 56: 257-262, 2001.

Doolittle, J.A., S.J. Indorante, D.K. Potter, S.G. Hefner, and W.M. McCauley, Comparing three geophysical tools for locating sand blows in alluvial soils of southeast Missouri, Journal of Soil and Water Conservation 57: 175-182, 2002.

Freer, J., J. McDonnell, K.J. Beven, D. Brammer, D. Burns, R.P. Hooper, and C. Kendal, Topographic controls on subsurface stormflow at the hillslope scale for two hydrologically distinct small catchments, Hydrological Processes 11: 1347-1352, 1997.

Hanson, B.R., and K. Kaita, Response of Electromagnetic Conductivity Meter to soil salinity and soil-water content, Journal of irrigation and Drainage Engineering 123(2): 141-143, 1997.

Hauck, C., M. Gugliemin, K. Isaksen, and D. Vonder Muhl, Application of frequency-domain and time-domain electromagnetic methods for mountain permafrost studies, Permafrost and Periglacial Processes 12: 39-52, 2001.

Hendrickx, J.N.H., B. Baerends, Z.I. Raza, M. Sadig, and M. Akram Chaudhry, Soil Salinity Assessment by Electromagnetic Induction of Irrigated Land, Soil Science Society of America Journal 56: 1933-1941, 1992.

Holmes, J.W., Calibration and field use of the neutron scattering method of measuring soil water content, Australian Journal of Applied Science 7: 45-58, 1956.

Jones, S.B., J.M. Wraith, and D. Or, Time domain reflectometry measurement principles and applications, Hydrological Processes 16: 141–153, 2002.

Kachanoski, R.G., E.G. Gregorich, and I.J. van Wesenbeeck, Estimating spatial variations of soil water content using nononcontacting electromagnetic inductive methods, Canadian Journal of Soil Science 68:715-722, 1988.

Kachanoski, R.G., E. de Jong, and J. van Wesenbeeck, Field scale patterns of soil water storage from non-contacting measurements of bulk electrical conductivity, Canadian Journal of Soil Science 70: 527-541, 1990.

Kirkby, M. J., Hydrograph modelling strategies, in: Process in Physical and Human Geography, edited by R. Peel, M. Chisholm, and P. Haggett, Heinemann, Oxford, England: 69–90, 1975.

Lakshmi, V., The role of satellite remote sensing in the Prediction of Ungauged Basins, Hydrological Processes 18: 1029-1034, 2004.

McDonnell, J.J., J.E. Freer, R.P. Hooper, C. Kendall, D.A. Burns, K.J. Beven, and N.E. Peters, New method developed for studying flow in hillslopes, EOS, Transactions of the American Geophysical Union 77(47): 465, 1996.

McNeill, J.D., Electrical conductivity of soils and rocks, Technical Note TN-5, Geonics Ltd. Mississauga, Ontario, 22p, 1980.

Quinn, P.F., K. Beven, P. Chevallier, and O. Planchon, The prediction of hillslope flow paths for distributed modelling using digital terrain models, Hydrological Processes 5: 59–79, 1991.

Robinson, D.A., I. Lebron, S.M. Lesch, and P. Shouse, Minimizing Drift in Electrical Conductivity Measurements in High Temperature Environments using the EM-38, Soil Science Society of America Journal 68: 339-345, 2004.

Roy, A., and A. Apparao, Depth of investigation in direct current methods, Geophysics 36: 943-959, 1971.

Sheets K.R., and J.M.H. Hendrickx, Noninvasive soil water content measurement using electromagnetic induction, Water Resources Research 31(10): 2401-2409, 1995.

Sherlock, M. D., and J. J. McDonnell, Spatially distributed groundwater level and soil water content measured using electromagnetic induction, Hydrological Processes 17(10): 1965-1978, 2003.

Slavich, P.G., and G.H. Petterson, Estimating average rootzone salinity from electromagnetic induction (EM-38) measurements, Australian Journal of Soil Research 16: 574-582, 1980.

Sudduth, K.A., S.T. Drummond, and N.R. Kitchen, Accuracy issues in electromagnetic induction sensing of soil electrical conductivity for precision agriculture, Computers and Electronics in Agriculture 31(3): 239-264, 2001.

Sweeney, J.J., Comparison of electrical resistivity methods for investigation of groundwater conditions at a landfill site, Groundwater Monitoring Review 4: 52-59, 1984.

Topp, G.C., J.L. Davis, and A.P. Annan, Electromagnetic determination of soil water content: Measurements in coaxial transmission lines, Water Resources Research 16: 574-582, 1980.

Topp, G.C., State of the art of measuring soil water content, Hydrological Processes 17: 2993-2996, 2003.

Western, A.W., R.B. Grayson, G. Blöschl, G.R. Willgoose, and T.A. McMahon, Observed spatial organization of soil moisture and its relation to terrain indices, Water Resources Research 35(3): 797-810, 1999.

Western, A.W., S.-L. Zhou, R.B. Grayson, T.A. McMahon, G. Blöschl, and D.J. Wilson, Spatial correlation of soil moisture in small catchments and its relationship to dominant spatial hydrological processes, Journal of Hydrology 286 (1-4): 113-134, 2004.

Figure 5.1 Time series of daily precipitation (a), hillslope average apparent conductivity measured by the four frequencies (b), and hillslope average soil moisture at different depths below the surface (c).

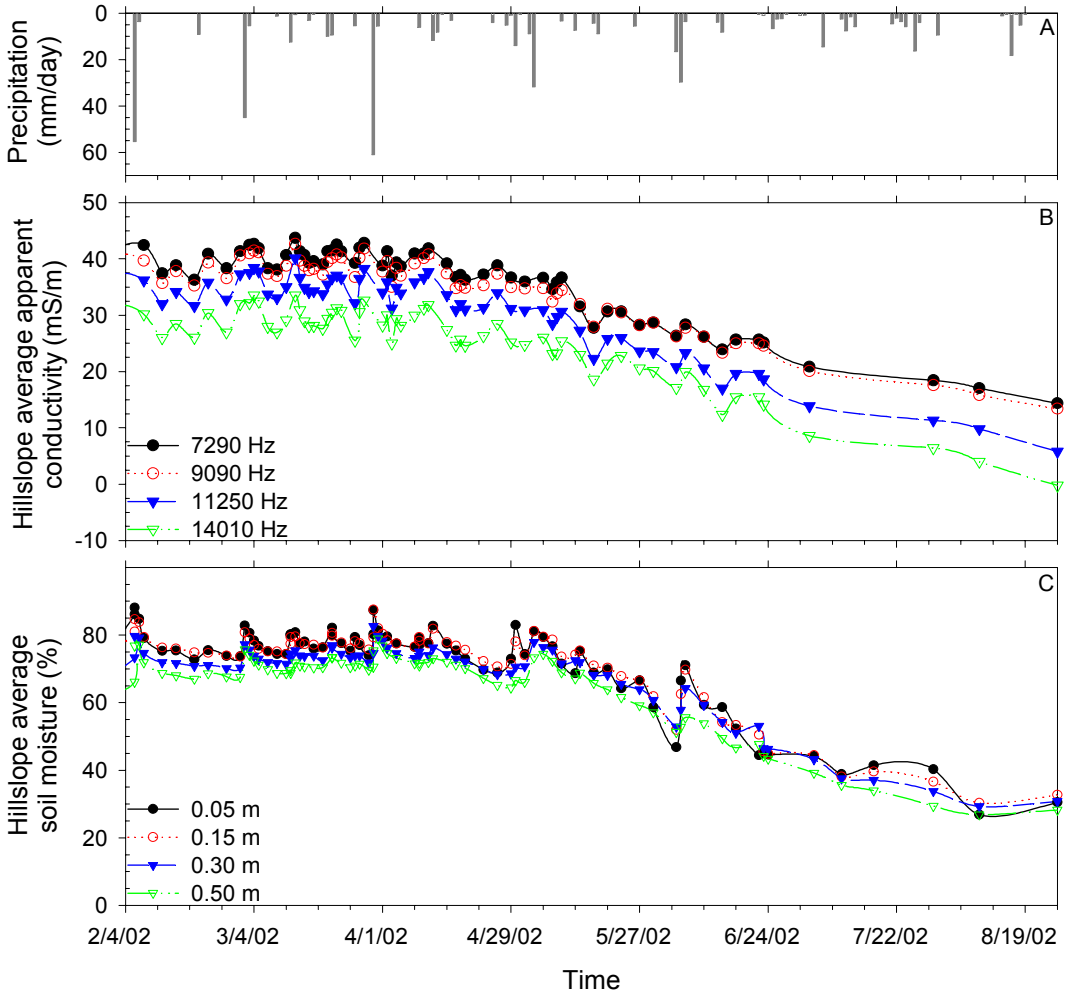

Figure 5.2 The linear relation between hillslope average apparent conductivity (9090 Hz) and hillslope average soil moisture at different depths below the surface. Relationships between the 7290, 11250, 14010 Hz frequencies and soil moisture are similar to the results shown for the 9090 Hz frequency.

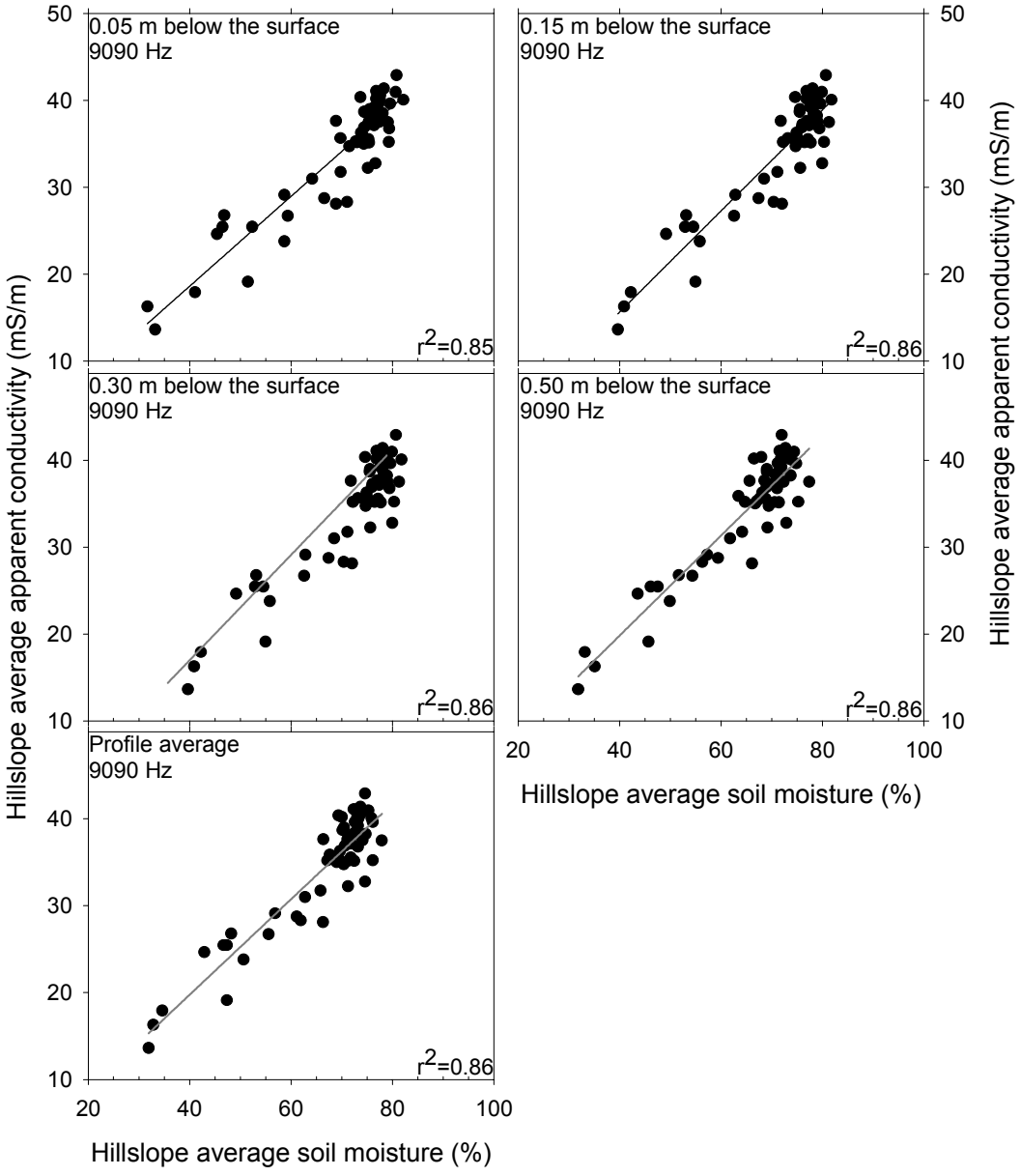

Figure 5.3 The relation between the ratio of measured hillslope average soil moisture at different depths and the ratio of hillslope average apparent conductivity measured with different frequencies.

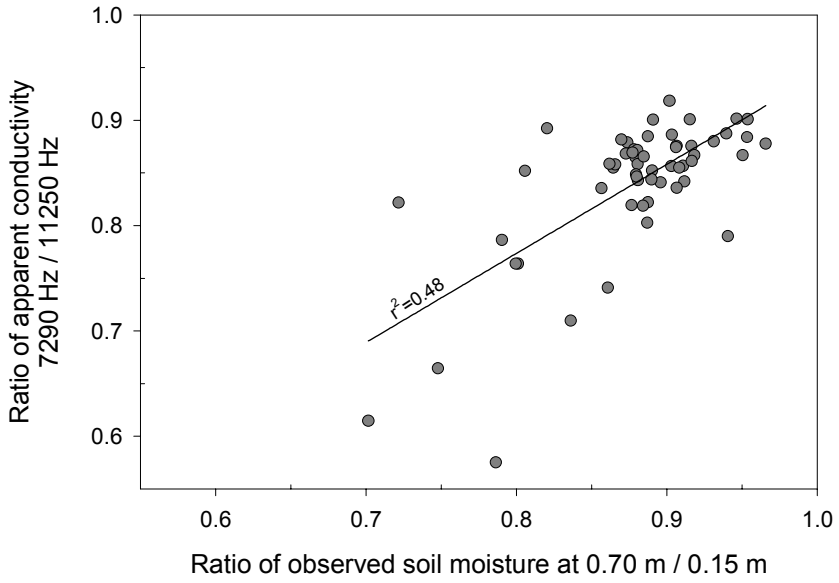

Figure 5.4 The distribution of the r^2 of the linear association between soil moisture and measured apparent conductivity (9090 Hz) for all measurement locations (a) and only the locations located more than 14 m upslope from the trench (b). The lines represent the 25th, 50th and 75th quartile, the whiskers represent the 10th and 90th percentile and the dots represent all outliers. Results for the 7290, 11250 and 14010 Hz frequency are similar to the results shown for the 9090 Hz frequency.

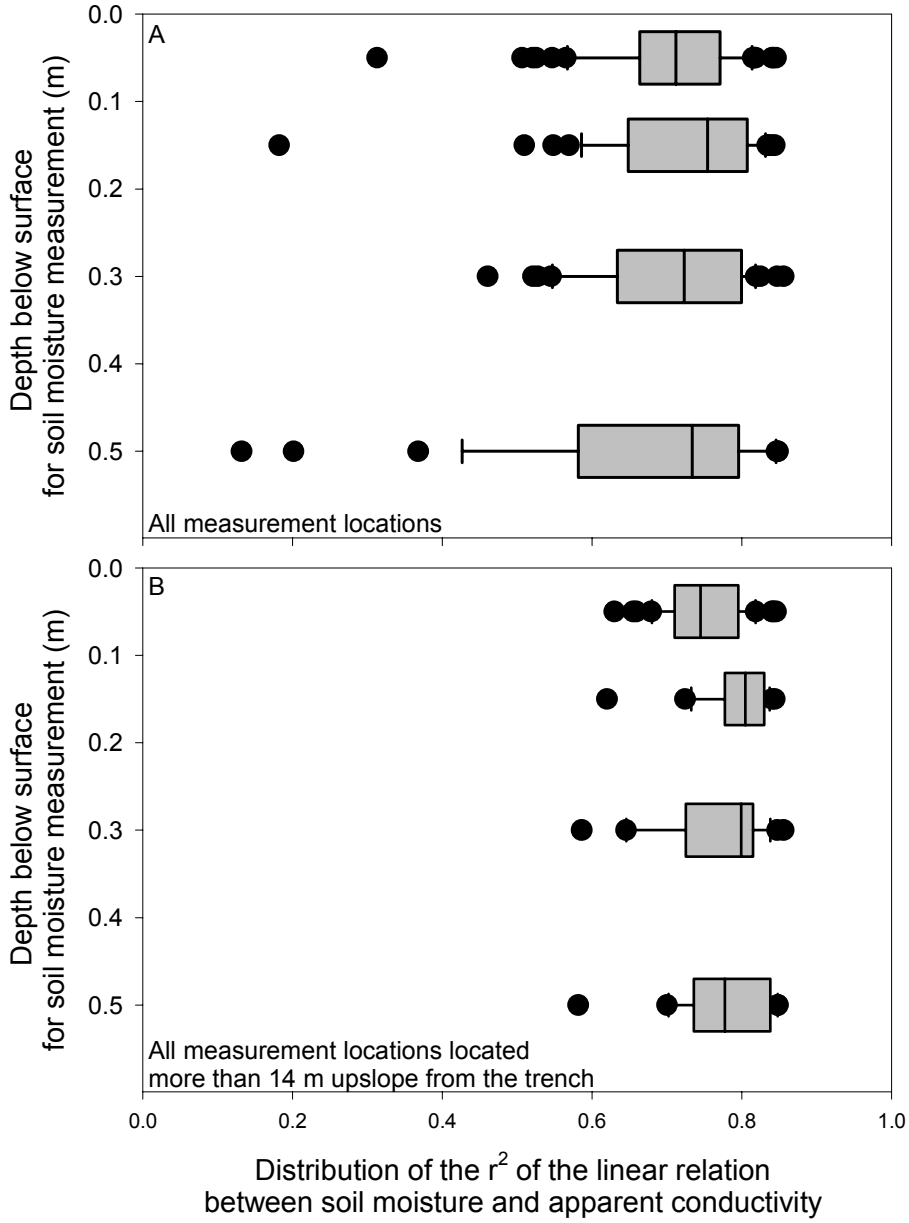

Figure 5.5 The spatial pattern of the square of the Pearson correlation coefficient (r^2) of the linear relation between measured profile average soil moisture and apparent conductivity (9090 Hz). The diamonds represent the locations of the collocated soil moisture and EM measurements. Results for the 7290, 11250 and 14010 Hz frequencies are similar to the results shown for the 9090 Hz frequency.

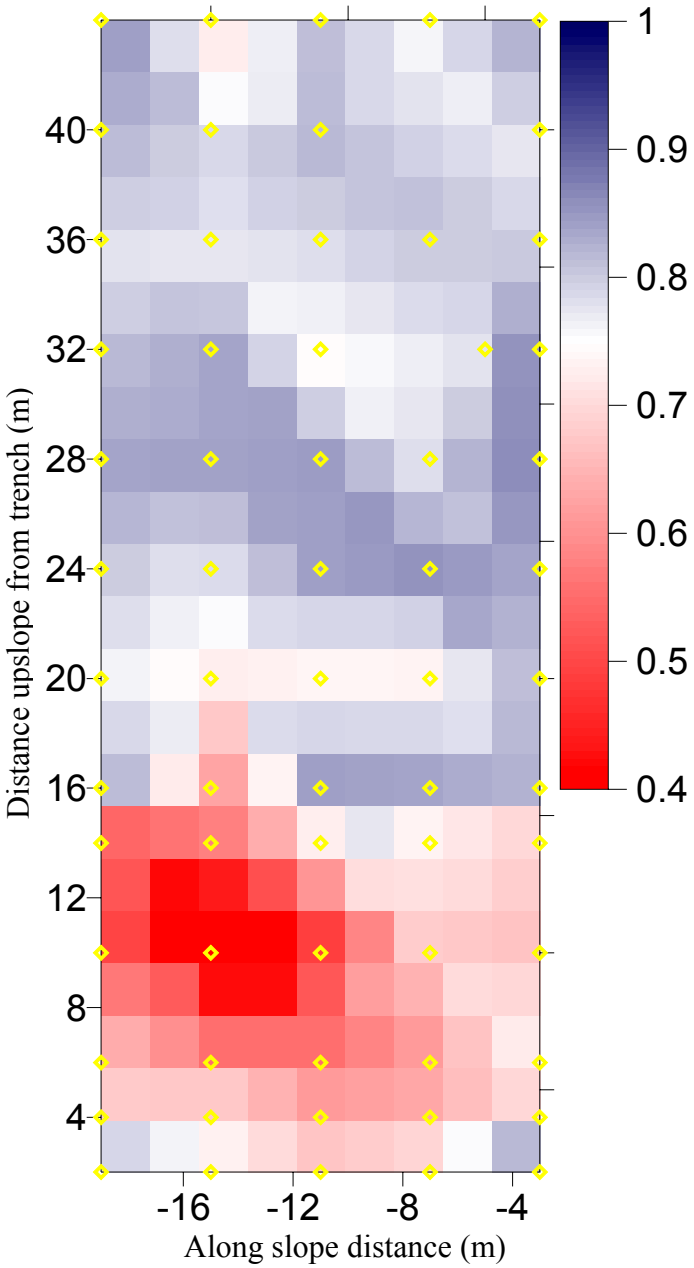

Figure 5.6 Time series of hillslope average measured soil moisture (closed circles), hillslope average calculated soil moisture using the individual relations between soil moisture and apparent conductivity for each measurement location (open diamonds), and hillslope average calculated soil moisture using the same relation between soil moisture and apparent conductivity for all measurement locations (open triangles). The inset graphs show the period between February 26 and March 21 in more detail. Time series of hillslope average calculated soil moisture using the apparent conductivity from the 7290, 11250 and 14010 Hz frequencies are similar to the results shown here for the 9090 Hz frequency.

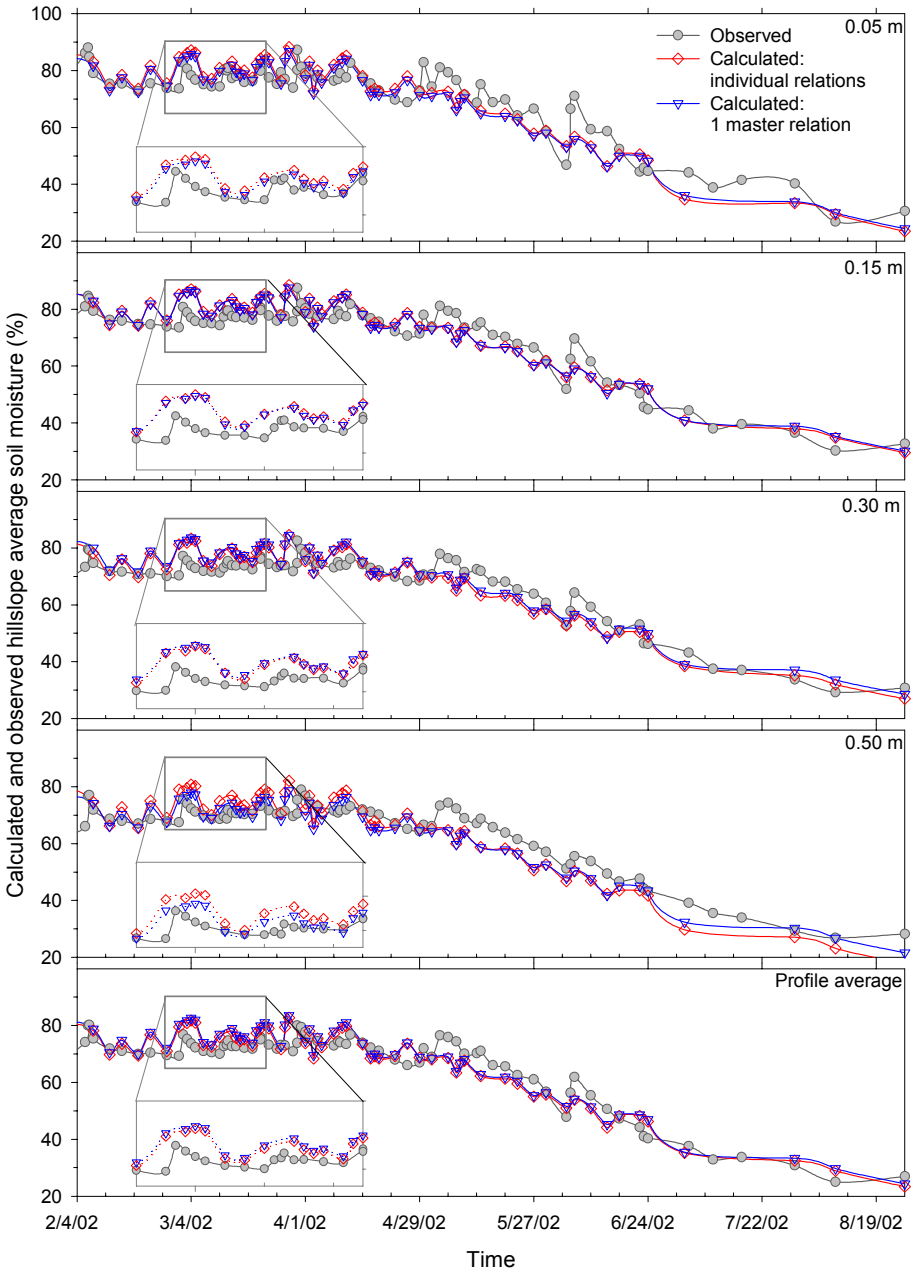

Figure 5.7 Maps of measured profile average soil moisture (a), calculated profile average soil moisture using the individual linear relations between soil moisture and the apparent conductivity (9090 Hz) for each measurement location (b), and the calculated profile average soil moisture using one single linear relation for all measurement locations (c). Soil moisture on the lower 14 m of the hillslope was influenced by artificial water applications between June 18 and August 26 2002. The diamonds represent the locations of the soil moisture measurements and the EM measurements. Results for the 7290, 11250 and 14010 Hz frequencies are similar but not shown.

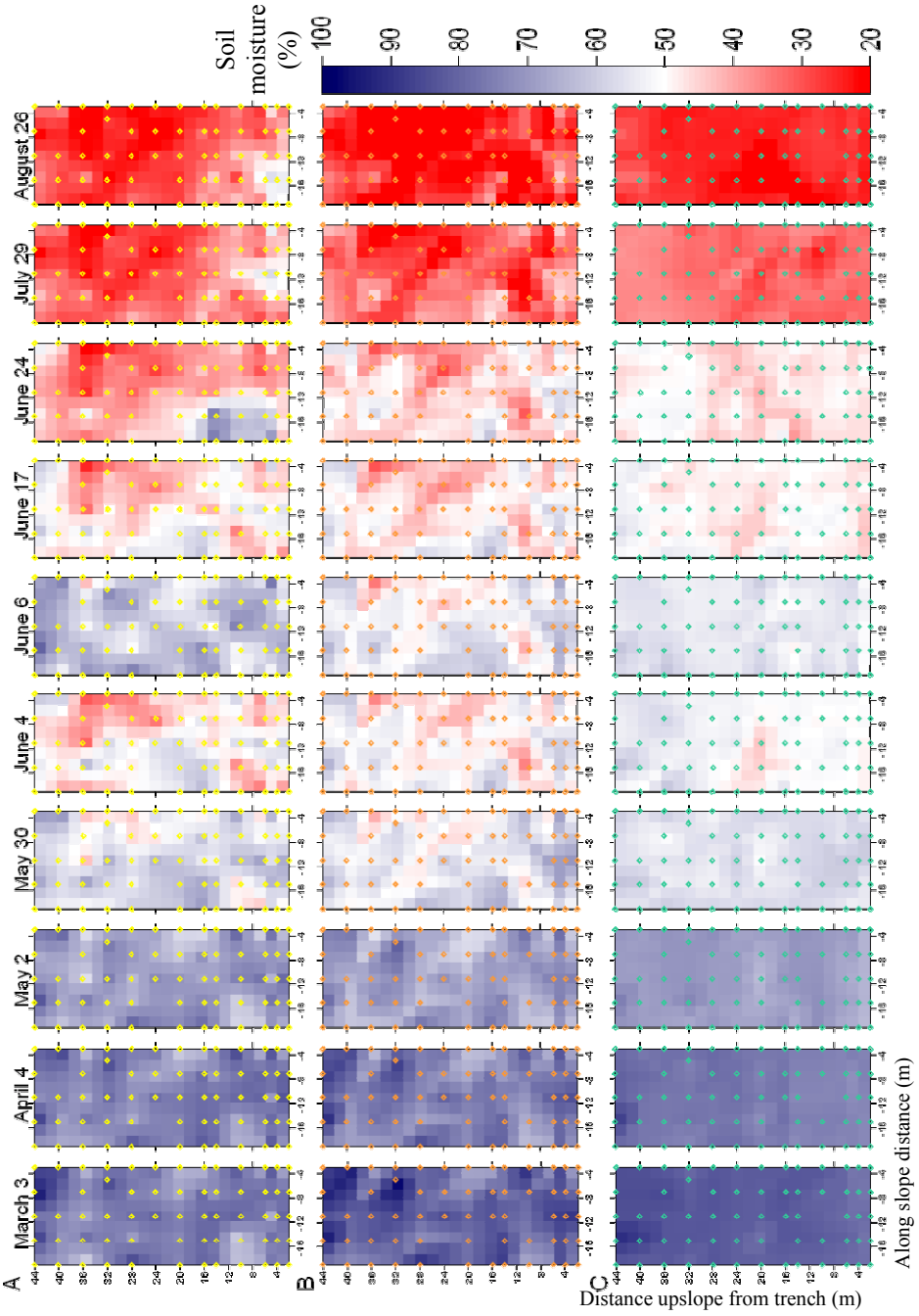

Figure 5.8 Standardized variograms (omni-directional) of observed profile average soil moisture (closed circles) and calculated profile average soil moisture from the apparent conductivity measurements using the linear relations between soil moisture and apparent conductivity for each location (open diamonds), and using the same relation between soil moisture and apparent conductivity for all locations (open triangles). Maps of the observed and calculated soil moisture patterns are shown in Figure 5.6.

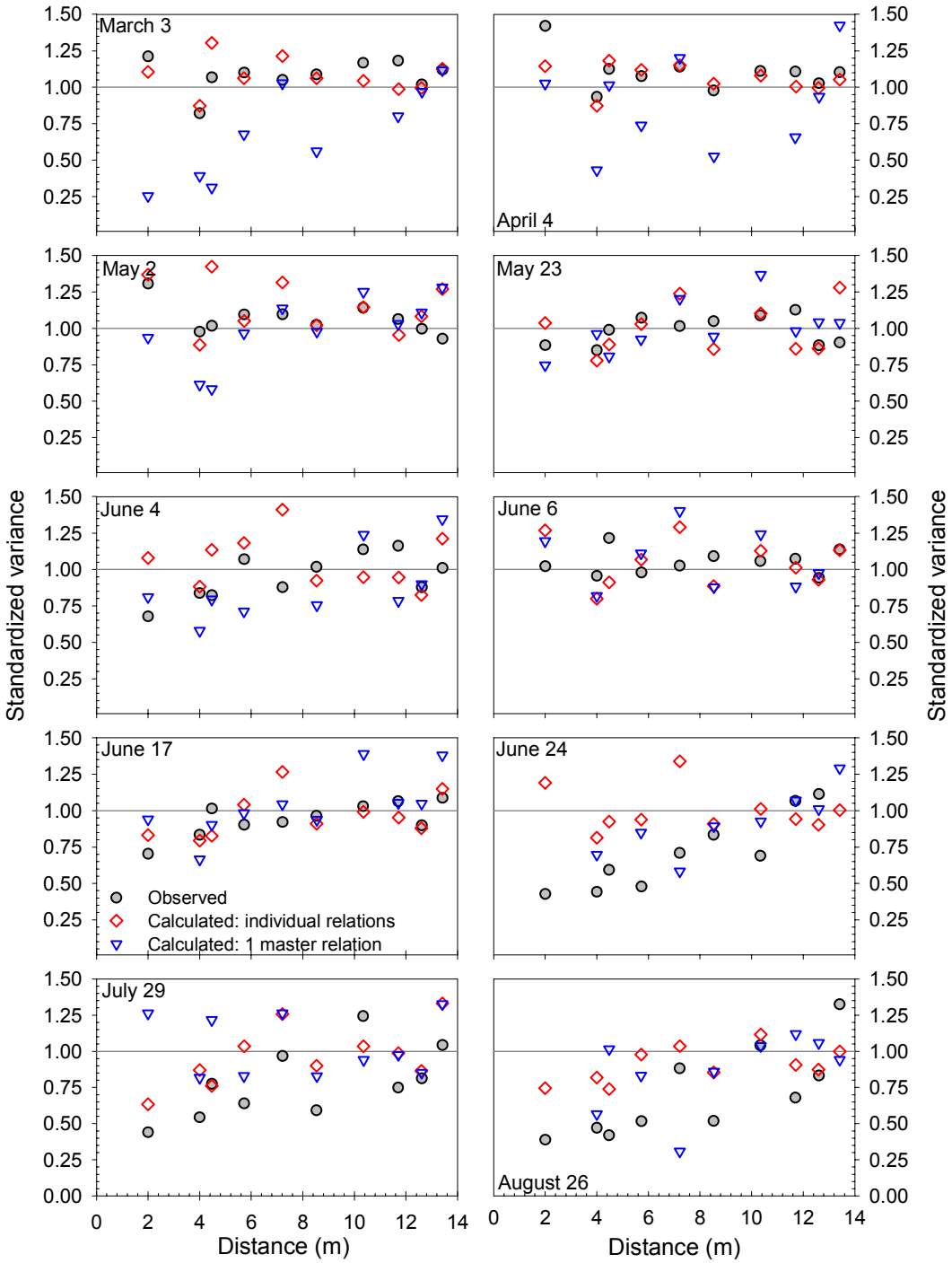

Figure 5.9 Frequency distributions of measured profile average soil moisture (closed circles), calculated profile average soil moisture using the individual linear relations between soil moisture and the apparent conductivity (9090 Hz) for each measurement location (open diamonds), and calculated profile average soil moisture based on one single linear relation for all measurement locations (open triangles). Maps of the spatial patterns of observed and calculated soil moisture are shown in Figure 5.6.

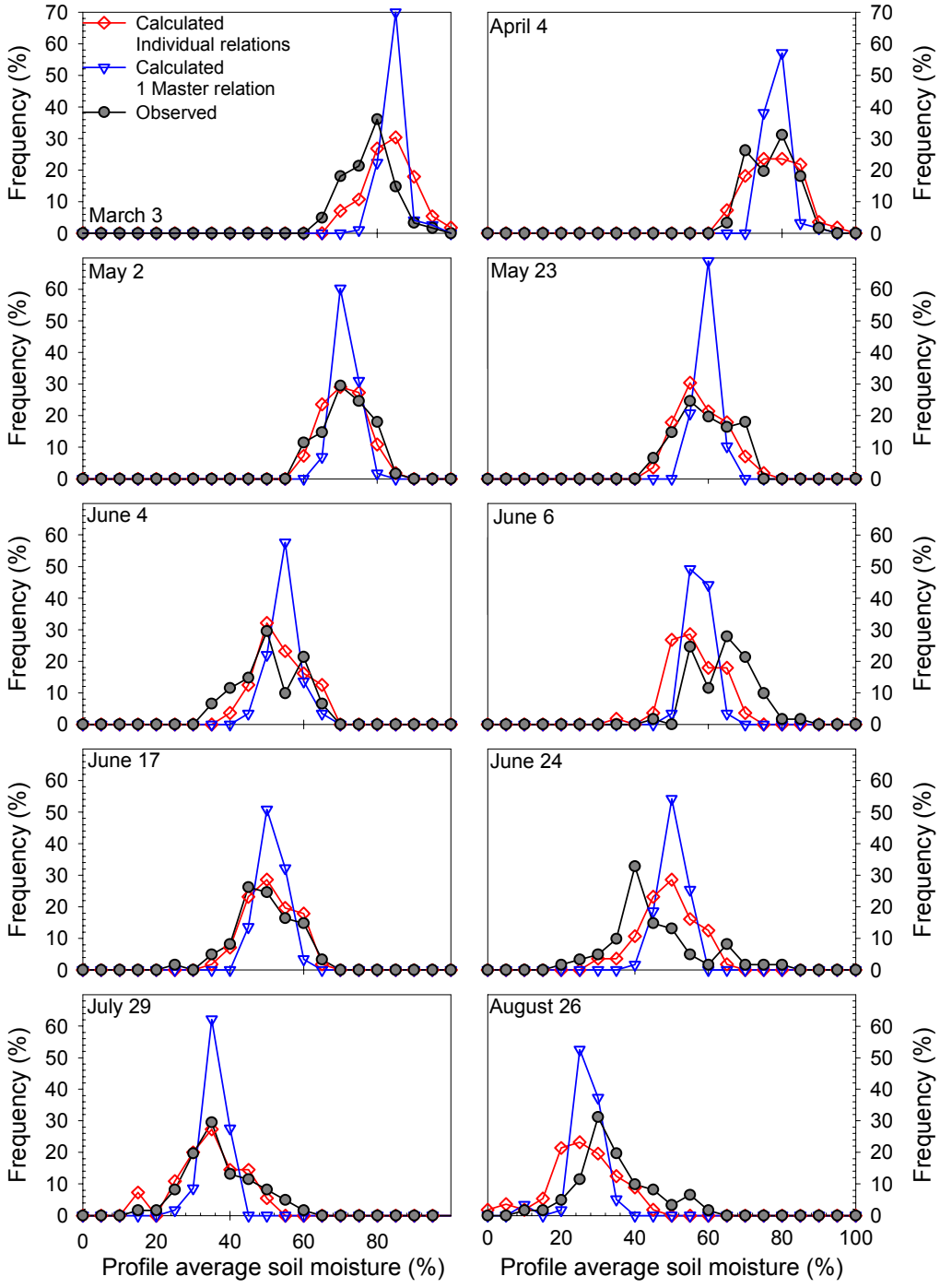

Table 5.1 The average (in the upper cells) and the range (*in the lower cells*) of the r^2 of the linear relations between the apparent conductivities measured by the four frequencies for each measurement location on the hillslope.

.

Frequency (Hz)	7290	9090	11250	14010
7290	-	0.87	0.87	0.86
9090	*0.81-0.99*	-	1.00	0.99
11250	*0.78-0.97*	*0.99-1.00*	-	1.00
14010	*0.73-0.94*	*0.95-1.00*	*0.98-1.00*	-

Table 5.2 The r^2 of the linear relation between hillslope average soil moisture measured at different depths (upper part of the matrix) and the slope of the linear relation between hillslope average soil moisture measured at different depths (*lower part of the matrix*).

	0.05 m	0.15 m	0.30 m	0.50 m	Profile average
0.05 m	-	0.98	0.95	0.92	0.97
0.15 m	*1.03*	-	0.99	0.97	0.99
0.30 m	*1.11*	*1.08*	-	0.99	0.99
0.50 m	*1.07*	*1.05*	*0.97*	-	0.98
Profile average	*1.00*	*0.97*	*0.89*	*0.90*	-

Table 5.3 The median and the range of the r^2 of the linear relation between soil moisture at different depths and the apparent conductivity.

		7290 Hz	9090 Hz	11250 Hz	14010 Hz
0.05 m	median	0.71	0.71	0.70	0.71
	range	0.31-0.85	0.31-0.85	0.31-0.84	0.27-0.84
0.15 m	median	0.74	0.75	0.73	0.71
	range	0.18-0.85	0.18-0.84	0.18-0.86	0.16-0.85
0.30 m	median	0.70	0.72	0.72	0.71
	range	0.48-0.86	0.42-0.86	0.46-0.86	0.41-0.86
0.50 m	median	0.73	0.72	0.73	0.73
	range	0.21-0.86	0.13-0.85	0.20-0.85	0.20-0.85
Profile average	median	0.76	0.77	0.76	0.75
	range	0.30-0.86	0.30-0.86	0.30-0.86	0.26-0.86

Table 5.4 Statistics of the slope and intercept of the linear relation between profile average soil moisture and the measured apparent conductivity for each measurement location on the study hillslope.

		Minimum	Maximum	Median	Standard deviation
7290 Hz	*slope*	0.34	0.71	0.51	0.08
	intercept	-12.36	14.25	1.33	6.03
9090 Hz	*slope*	0.32	0.67	0.48	0.08
	intercept	-11.73	14.00	1.64	5.86
11250 Hz	*slope*	0.37	0.75	0.57	0.09
	intercept	-21.09	6.49	-7.39	6.43
14010 Hz	*slope*	0.35	0.71	0.53	0.09
	intercept	-24.94	4.75	-10.14	6.28

Table 5.5 Median explanatory power of the calculated soil moisture pattern for the observed soil moisture patterns during two month periods.

Median explanatory power (%)	February - March	April-May	June-August
Using the individual relation between soil moisture and apparent conductivity for each measurement location			
0.05 m	77	78	43
0.15 m	72	77	39
0.30 m	85	84	53
0.50 m	83	83	46
Profile average	79	80	40
Using the same relation between soil moisture and apparent conductivity for all measurement locations			
0.05 m	2	0	1
0.15 m	2	1	2
0.30 m	1	3	2
0.50 m	6	1	1
Profile average	1	1	1

6 The importance of subsurface flow through bedrock at the Panola study hillslope

6.1 Introduction

Much of hillslope hydrology is based on the notion of transmissive soils over impermeable bedrock such that water ponds at the soil-bedrock interface, creating transient subsurface saturation which in turn results in lateral subsurface flow (e.g. Weyman, 1973; McDonnell, 1990; Peters et al., 1995; Tani, 1997; Buttle and Turcotte, 1999; McGlynn et al., 2002). In the past decade, some studies have shown that subsurface flow through bedrock can be significant and even constitute a major source of channel storm flow (e.g. Anderson et al., 1997; Onda et al., 2001, Uchida et al., 2002, Uchida et al., 2003). Anderson et al. (1997), for example, found for a site in the Oregon Coast Range that bromide injected into saturated hillslope materials rapidly flowed through the sandstone bedrock to the catchment outlet, and that water from bedrock pathways exfiltrated into the colluvium mantle and mixed with younger vadoze zone water, creating a subsurface saturated area near the stream channel head. Subsurface saturation occurred only at locations where bedrock water exfiltrated. Similarly Uchida et al. (2002) showed for sites in Japan with weathered granite bedrock that water emerged from the bedrock at the slope base and mixed with pre-event soil water in the subsurface saturated area after large storms with wet antecedent conditions. Asano et al. (2002) showed that water age increased in a vertical direction in areas with permeable bedrock, contrary to the now axiomatic assumption of water age increase in the downslope direction as defined in impermeable bedrock situations (Stewart and McDonnell, 1991).

Examination of the infiltration process of subsurface water into bedrock and its effects on hillslope response to storm rainfall is a pressing research need (McDonnell and Tanaka, 2001). Here we set out a series of sprinkling experiments with the objective to investigate the hydrologic connectivity between the soil mantle and the underlying bedrock at the Panola Mountain Research Watershed (PMRW), where so far studies have assumed that the bedrock is relatively impermeable. Previous studies have shown that the spatial distribution of subsurface flow at the study hillslope was highly correlated to the accumulated area based on the bedrock topography (McDonnell et al., 1996). Sections

with highest bedrock accumulated area delivered most of the water (Freer et al., 1997 and 2002; Chapter 2), suggesting that ponding of water at the soil-bedrock interface and lateral flow over the bedrock is the dominant subsurface flow delivery mechanism. Furthermore, transient saturation at the soil-bedrock interface is short lived and spatially discontinuous during winter storms and absent during the summer months (Chapter 3). Nevertheless, implicit in this understanding of how the Panola hillslope 'works' is the assumption that the bedrock is impermeable or nearly impermeable.

The Panola hillslope is a useful study site to examine the importance of flow through bedrock and its effect on subsurface flow because of the extensive measurement infrastructure at the site. The existing trench allowed us to measure lateral subsurface flow, and sapflow sensors in the dominant tree species across the hillslope allowed us to estimate hillslope scale transpiration. Thus, by making measurements of what comes in vertically (precipitation), what goes out laterally (subsurface stormflow) and what goes out vertically (transpiration), we could isolate and calculate the leakage to the bedrock.

We measured the bedrock moisture during spring storms, compared the breakthrough of a line source tracer in subsurface flow with the breakthrough in bedrock and set out a series of sprinkling experiments during which we measured all water balance components. The objective of this study was to determine the permeability of the bedrock underneath the Panola trenched hillslope and its effect on the hillslope scale and watershed scale water balance.

6.2 Study site

The Panola Mountain Research Watershed (PMRW) is located within the Panola Mountain State Conservation Park in the southern Piedmont province southeast of Atlanta, Georgia (84˚10'W, 33˚37'N). Historical land use included cotton cultivation, forest cutting and pasture land. Currently the watershed is 93% forested, consisting of hickory, oak, tulip poplar, and loblolly pine (Carter, 1978). The remaining 7% of the

watershed includes bedrock outcrops with small vegetation islands, including a 3.6 ha outcrop in the southwestern corner of the watershed. The catchment can be represented by three landscape units (Peters et al., 2003). Bedrock outcrops comprise a small landscape unit (~10%) that has little or no soil cover. Hillslopes comprise most of the catchment (>75%) and have shallow soils (<1 m). The riparian zone, which has the deepest soils (≤ 5 m) is relatively narrow (<50 m) and occupies less than 15% of the total catchment area.

Bedrock at PMRW is dominated by the Panola Granite (granodiorite composition) of Carboniferous age, described as a biotite-oligioclase-quartz-microcline granite (Crawford et al., 1999). Locally, the Panola Granite has intruded the Clairmont member of the Stonewall Gneiss, described as a tectonic mélange with a variety of clasts that float in a sheared and granitized matrix (Crawford et al., 1999). Chemical weathering studies near the ridge top at PMRW have shown that bedrock permeability is primarily intragranular and is created by internal weathering networks of interconnected plagioclase phenocrysts (White et al., 2001). On the ridge top at PMRW, 2-3 m thick porous saprolite (soft disintegrated granite) under the soil, retained the original granodiorite texture and graded from friable saprock to competent bedrock over an interval of several centimeters at a depth of 4.7 m (White et al., 2002). In general the thickest saprolite layers are found near broad gentle ridge tops. On steeper side slopes the weathered zones are thinnest (Daniels and Hammer, 1992). During the installation of wells and soil moisture access tubes across the study hillslope, saprolite was found only in the deepest soil section of the hillslope located 20-22 m upslope from the trench. Bedrock in the trench is competent. While cores have been taken from the bedrock and chemical weathering studies have been done at PMRW (White et al., 2001 and 2002), no studies have examined the permeability of the bedrock or the effect of subsurface flow through the bedrock on the hillslope- or catchment scale water balance.

The climate at PMRW is classified as humid, subtropical. The mean annual temperature is 16.3 ˚C and mean annual precipitation is 1240 mm, spread relatively

uniform throughout the year. Rainfall tends to be of longer duration and lower intensity associated with the passage of fronts in the winter and of shorter duration but higher intensity in the summer when it is associated with thunderstorms. Streamflow at PMRW has a strong seasonal pattern, with the highest flows occurring in the November through March dormant season. Data from PMRW for the 1985 –1999 period shows that annual stream yield varied from 15 % to 50 % of precipitation. Streamflow response to rainfall is strongly affected by the 3.6-ha bedrock outcrop in the headwater that provides runoff rapidly during rainstorms (Shanley and Peters 1988).

End Member Mixing Analysis (EMMA) (Hooper et al., 1990 and1998; Burns et al., 2001) and hydrochemical and hydrometric analysis (Peters and Ratcliffe, 1998) have shown a limited role of hillslopes in direct streamflow generation, suggesting that hillslopes, which are the largest landscape unit in the watershed, are disconnected from the stream most of the time. Burns et al. (2001) examined the relative role of the hillslope and riparian zone in contributing to streamflow at the upper 10 ha gauge for two winter rainstorms. They concluded that runoff from the bedrock outcrop was the dominant source of streamflow under the drier antecedent conditions of the two rainstorms (both occurred when the catchment was generally wet), followed by riparian groundwater, which dominated under slightly wetter conditions. Chlorofluorocarbon and tritium/helium-3 dating of riparian groundwater at PMRW showed that the age of the water mid-way down the valley in the 10 ha catchment was six to seven years (Burns et al., 2003).

The study hillslope is located approximately 30 m upslope from an ephemeral stream in the south-west corner of the watershed opposite from the 3.6 ha bedrock outcrop. The lower boundary of the study hillslope is formed by a 20 m long trench. The upper boundary is formed by a small bedrock outcrop. Soils on the study hillslope are best described as light colored sandy loam soils with a 0.15 m humus rich horizon. The average soil depth is 0.63 m and ranges from 0 to 1.8 m. Average runoff ratios from the study hillslope for the 1996-1998 period are 6, 10, 1 and less than 1% for the fall, winter,

spring and summer respectively (Chapter 2). The runoff coefficient from the study hillslope was greater than 10% for only eight of 147 rainstorms during the 1996-1998 period (Chapter 2). The maximum runoff ratio was 26.5 % for an 80 mm storm with a maximum 1-hour rainfall intensity of 21 mm/hr. This storm had very wet antecedent conditions.

6.3 Methods

6.3.1 Water applications

We used an oscillating sprinkler and nearby residential water supply to apply water to parts of the lower 14 m of the hillslope. The area to which water was applied varied from 69 to 79 m^2 (see Table 6.1). In general water was applied to an approximate 5.5 m wide and 12 m long area located 3 m upslope from the trench to minimize the possibility of sprinkling directly onto the trench during wind gusts. We conducted five sprinkling experiments on four areas of the hillslope, covering ultimately the entire width of the hillslope (Figure 6.1). Water was applied continuously for 8-9 days during each experiment, except for sprinkling experiment 1 when water was applied for only 4.5 days (Table 6.1). The water application rate was ~8 mm/hr for all sprinkling experiments, except for the later part of sprinkling experiment 5 (Table 6.2). The application rate was higher than the natural rainfall intensity during long duration low intensity winter storms but lower than the rainfall intensity during high intensity short duration thunderstorms at this site. Sprinkling experiment 5 was a repeat of sprinkling experiment 1 during the first six days of the experiment. After six days of sprinkling we reduced the area over which water was applied by half, by making the sprinkler oscillate only half of the arc, thus doubling the water application rate for this area. The sprinkler was also moved 1 m further downslope.

To estimate the spatial distribution and depth of water applied to the sprinkled area, we placed 20 precipitation gauges across the sprinkled area, which were read and emptied four to five times per day. Water was applied very uniformly across the

sprinkled area, except for a measured decrease in water application near the edges of the sprinkled area (~0.8 m around the edge)

Two rain events occurred during sprinkling experiment 3; a 14.5 mm storm on July 6 2002 20:00 hr (called storm 1) and a 7.4 mm storm on July 11 2002 13:00 hr (called storm 2). While there were some other small thunderstorms during the sprinkling experiments, only these storms were large enough to have a noticeable effect on measured groundwater levels and subsurface flow rate and are therefore analyzed in more detail.

6.3.2 Soil moisture measurements

Soil moisture was measured using the Aqua-pro sensor (Aqua-pro Sensors, Reno NV) in polycarbonate access tubes that were installed on the soil-bedrock interface (i.e. the point of refusal). The access tubes were distributed on a 4 by 4 m grid across the hillslope and on a 4 by 2 m grid on the lower 6 m of the hillslope (Figure 6.1a). The Aqua-pro sensor is a capacitance sensor (radio frequency) that measures soil moisture on a percent scale between 0 (in air or air dried soil) and 100 (in saturated soil or water). Soil moisture was measured approximately four times per day throughout the sprinkling experiments at 0.05 m increments to 0.3 m below the soil surface and at 0.1 m increments between 0.3 m and the soil-bedrock interface.

We also installed three access tubes in the bedrock on the downslope side of the water collection system in the trench (Figure 6.2). This allowed us to estimate temporal changes in bedrock wetness. These access tubes were inserted 40, 70 and 110 mm into the competent bedrock by drilling a tight fit hole into the bedrock. During the sprinkling experiments, bedrock moisture was measured four to five times per day using the Aqua-pro sensor. Bedrock moisture was also measured on a regular basis (approximately once per week) during the spring and several times per day during two relatively small storms with wet antecedent conditions in April 2002.

6.3.3 Measurements of transient saturation

We installed 135 crest stage gauges spatially distributed across the hillslope. These crest stage gauges were located on an approximately 2 by 2 m grid across the lower 16 m of hillslope and an irregular but close to 4 by 4 m grid across the remainder of the hillslope (Figure 6.1b). These 19 mm diameter PVC wells were augered to refusal, installed on the soil-bedrock contact and screened over the lower 200 mm. Water level rise was measured manually four to five times per day during the sprinkling experiments.

In addition, 29 recording wells were installed on two transects across the hillslope and in a region of deeper soils on the lower 15 m of the hillslope; the area of sprinkling experiment 3 (Figure 6.1c). These 51 mm diameter PVC wells were augered to refusal and screened over the entire length. The water level was measured every 5 minutes using capacitance rods (Trutrack, New Zealand). The capacitance rods could not measure water levels within 75 mm of the soil-bedrock interface.

6.3.4 Sapflow measurements

Transpiration was estimated from constant heat sapflow measurements using the thermal dissipation technique developed by Granier (1985 and 1987), generally following the procedures described by Phillips et al. (2002). Sapflow was measured at 15 minute intervals in 14 trees using 28 sensors. All trees had two probes inserted 0-20 mm in the sapwood. Sapflow was averaged to hourly intervals using the average of the two sapflow sensors in each tree. The 14 trees that were installed with constant heat sapflow sensors were all Hickory trees (*Carya* sp.) of one the following two diameter at breast height classes: 0.11-0.125 m (5 trees) or 0.175-0.215 m (9 trees) (Figure 6.1d). Hickory trees of these size classes were the dominant trees on the study hillslope. Tree A and B were located on the edge of sprinkling experiment 3 and 4 while tree K and L were located on the edge of sprinkling experiments 1 and 5 (Figure 6.1d). The other trees with sapflow sensors were located upslope from the sprinkling experiments and were used to determine

if there were increases in sapflow in response to the sprinkling experiments in trees close to the sprinkling areas.

6.3.5 Lateral subsurface flow measurements

Lateral subsurface flow was measured at a 20-m long trench, excavated normal to the fall line of the slope down to bedrock (Figure 6.2). The trench was divided into ten 2-m sections along the bedrock surface using PVC sheets that funneled flow through PVC-lined hose to tipping buckets. The number of tips was recorded every minute. For the sprinkling experiments we calculated the depth of subsurface flow by dividing the total measured subsurface flow volume by the area of the sprinkled region. Additional details of the trench and the flow-collection system are described in McDonnell et al. (1996), Freer et al. (1997 and 2002) and Burns et al. (1998).

Total water loss was calculated as the difference between the volume of water applied and observed subsurface flow during the late period of the sprinkling experiments. *Total water loss* was divided into *evaporative loss* and *non-evaporative loss*. The *evaporative loss* was calculated as the difference between an interpolated line connecting the maximum daily flows and the actual measured subsurface flow. Transpiration was negligible during the period of maximum flow (i.e. late night/early morning). We assumed that evaporation from the wet soil was also negligible during the late night because of the high relative humidity during the night and low wind speed under the canopy. *Non-evaporative loss* was calculated as the difference between calculated total water loss and the calculated evaporative loss. For the two storms during sprinkling experiment 3, we assumed that evaporative water loss was negligible and that non-evaporative water loss was thus equal to total water loss.

6.3.6 Line tracer test

As part of a related study, a 20 m wide line source of 512 g Lithium Bromide was applied 11 m upslope from the trench at 0.15 m below the soil surface on March 1 2002 20:00 (Figure 6.1d). Subsurface flow samples were collected for chemical analysis in 100-ml polyethylene bottles from the tipping buckets when they spilled. Bedrock water was collected after March 25 2002 from three suction lysimeters located downslope from the water collection system in the trench at 70-200 mm depths below the soil-bedrock interface (Figure 6.2). The suction lysimeters were pumped to ~0.7 bar prior to sample collection. The bromide concentration in each sample was determined using a Dionex Model DX500 ion chromatograph with an AS9-HC column. The samples were shelf-stored prior to analysis.

6.4 Results

6.4.1 Bedrock moisture response to natural precipitation events during the spring

Bedrock moisture responded quickly to natural precipitation during early spring rainstorms (Figure 6.3). During the 13 mm April 12 2002 storm with very wet antecedent conditions, bedrock moisture increased 6 $\%_{\text{Aqua-pro}}$ within a 4-hour period (see insert in Figure 6.3). Bedrock moisture did not respond to the 50 mm June 4-6 2002 storm. The wetting front during this storm did not penetrate more than 0.5 m vertically through the soil profile at most locations on he hillslope (Chapter 4).

6.4.2 Tracer breakthrough in response to natural precipitation events

While there was some tracer breakthrough in subsurface flow during the 50 mm storm on March 2-3 2002 directly after tracer application, the peak breakthrough occurred after peak subsurface flow during the 61 mm event on March 30 2002 (Figure 6.4). This storm consisted of a 24 mm storm in the morning and afternoon followed by a 37 mm high intensity thunderstorm during the evening. The 30-minute maximum rainfall intensity of the thunderstorm was 62 mm/hr. Breakthrough of tracer in the bedrock was 2

days delayed compared to the breakthrough in subsurface flow (but still quite fast) (Figure 6.4). Bromide in the bedrock was remobilized during the 20 mm precipitation event on April 12-13 2002. During this storm only 0.04 mm of subsurface flow was measured in the trench, of which 46 % was delivered by the trench sections with shallow soils on the left 4 m (when looking upslope) of the trench (Figure 6.2).

6.4.3 Sprinkling experiments

6.4.3.1 Sprinkling experiment 1

No subsurface flow was observed at the trench during sprinkling experiment 1. Subsurface saturation at the soil-bedrock interface started approximately 1 day after the start of the water application. Piezometers outside the sprinkled area and next to the trench remained dry, indicating that water did not flow around the edges of the trench face. Bedrock moisture downslope from the sprinkled area did not change during the experiment. Soil moisture 3 m downslope from the sprinkled area did not increase either.

6.4.3.2 Sprinkling experiment 2

Subsurface flow was only a minor fraction of the volume of water applied during sprinkling experiment 2 (Figure 6.6c and Table 6.2). Subsurface flow decreased with increasing time after the onset of subsurface flow. This coincided with a decrease in water level in the wells inside the sprinkled area (Figure 6.6c-d). Subsurface saturation at the soil-bedrock interface developed within one day of the start of the sprinkling experiment at most measurement locations in the sprinkled area (Figure 6.6d). Bedrock moisture measured downslope and 1 m to the left (when looking upslope) of the sprinkled area (see Figure 6.1b and 6.2) increased one day after the start of subsurface flow at the trench (Figure 6.6e). Soil moisture inside the sprinkling area reached steady state soon after the start of the water applications. Soil moisture measured 3 m or more outside (above or beside) the sprinkling area did not change (Figure 6.6f). Sapflow in trees (~6 m) outside the sprinkling area did not change considerably during the sprinkling experiments either.

Diurnal variations in subsurface flow, water level and soil moisture were clear. The lag between the diurnal signal in temperature or sapflow and the diurnal signal in subsurface flow was 3-4 hours (maximum subsurface flow occurred 3-4 hours after minimum temperature or sapflow). Calculated non-evaporative loss was much larger than the calculated evaporative loss and also much larger than measured subsurface flow (Table 6.2). Since the calculations were made over the latter part of the sprinkling experiment when soil moisture did not change, we assumed that non-evaporative loss was due mainly to loss of water to the bedrock and not due to changes in soil moisture storage. The bedrock area through which water could have infiltrated was larger than the sprinkled area because the sprinkled area was not located directly upslope from the trench. Since the volumes of calculated evaporative loss and non-evaporative loss were normalized by the sprinkled area, the actual infiltration rate through the bedrock is smaller than reported in Table 6.2. The sprinkled area plus the area between the sprinkled area and the trench was approximately 1.2 times larger than the sprinkled area.

The calculated evaporative loss for sprinkling experiment 2 was smaller than for the other sprinkling experiments and smaller than the average calculated transpiration rate during the sprinkling experiment based on sapflow data (2.6 mm/day). It is possible that part of the subsurface flow flowed around the trench because the sprinkled area was on the edge of the trench excavation (Figure 6.1b). If we assume that the trench captured only half of total subsurface flow, total subsurface flow would be 8.1 mm/day, non-evaporative loss would be 188 mm/day and evaporative loss would be 3.62 mm/day. This compares better with the calculated evaporative loss during the other sprinkling experiments and the calculated transpiration rate. We assume that the difference between the calculated evaporative loss from the diurnal signal in subsurface flow and calculated transpiration from the sapflow measurements is at least in part due to evaporation from the wet soil during the sprinkling experiments.

6.4.3.3 Sprinkling experiment 3

Similar to sprinkling experiment 2, subsurface flow during sprinkling experiment 3 was only a minor fraction of the total volume of water applied (Figure 6.7c and Table 6.2). Bedrock moisture increased approximately 16 hours after the onset of subsurface flow (Figure 6.7e). Transient saturation at the soil-bedrock interface developed soon (within one day) after the start of the sprinkling experiment at most measurement locations in the sprinkled area. After the onset of subsurface flow, water levels in the wells decreased. There was a good relation between the decrease in water level and the decrease of subsurface flow. But for the same water level above bedrock, the subsurface flow rate was lower early in the sprinkling experiment than later in the sprinkling experiment (Figure 6.8). The lag between the diurnal signal of maximum water level and maximum subsurface flow rate was 1 hour. The lag between maximum subsurface flow and minimum air temperature or sapflow was 3-4 hours, similar to sprinkling experiment 2.

The temporal pattern of soil moisture and sapflow was similar to those discussed for sprinkling experiment 2. Soil moisture measured 2 m downslope from the sprinkling area increased during the sprinkling experiments. Soil moisture at depth increased before the onset of subsurface flow. With increasing time, shallower soil layers wetted up as well (Figure 6.9).

Similar to sprinkling experiment 2, the calculated non-evaporative loss was much larger than the calculated evaporative loss and also much larger than measured subsurface flow (Table 6.2). During both the sprinkling experiment and the storms, the 3-hour average of subsurface flow and calculated non-evaporative loss were linearly related to the water level above bedrock (Table 6.3). This is in keeping with infiltration theory, if one views the water level above bedrock as the depth of ponding (h_0). The vertical infiltration in the soil matrix can be calculated using the Green-Ampt approach (Green and Ampt, 1911):

$$I = K\frac{\psi + h_0 + z_{wf}}{z_{wf}} \qquad \text{(Equation 6.1)}$$

where I is the infiltration rate, K the saturated conductivity, ψ the wetting front suction, h_0 the depth of the surface ponding, and z_{wf} is the depth of the wetting front. We assume that ψ is close to zero during the latter part of the sprinkling experiments because a very large amount of water had been applied to the sprinkled area. The thunderstorms during sprinkling experiment 3 temporarily increased the water level above bedrock, thus head (h_0), leading to increased infiltration into the bedrock and thus increased non-evaporative loss (Table 6.3). Thus only a fraction of the additional water applied by the thunderstorm resulted in additional subsurface flow (Table 6.2).

6.4.3.4 Sprinkling experiment 4

During sprinkling experiment 4, subsurface saturation was also observed to the left (when looking upslope) from the sprinkling area (the location of sprinkling experiment 3, see Figure 6.1 and 6.2). Subsurface flow was observed only directly downslope from the sprinkled area during the other sprinkling experiments. The bedrock topography under the sprinkled area of experiment 4 slopes towards the left (when looking upslope), thus towards the area of sprinkling experiment 3 and the trench sections where subsurface flow was observed. Bedrock moisture increased at the same time as the onset of subsurface flow (Figure 6.10e). Transient saturation at the soil-bedrock interface developed soon (within 12 hours) after the start of the sprinkling experiment (Figure 6.10d). Similar to sprinkling experiments 2 and 3, there was a decrease in water level in the wells on the hillslope coinciding with a decrease in measured subsurface flow. Similar to sprinkling experiments 2 and 3, total subsurface flow was only a small fraction of total water applied. Because water flowed over the bedrock to the area of sprinkling experiment 3, the actual area over which water could have infiltrated was larger than the sprinkled area. Thus the calculated non-evaporative loss was larger than the actual bedrock infiltration rate. Finally, the temporal pattern of soil moisture and sapflow during sprinkling experiment 4 were similar to those described for sprinkling experiment 2.

6.4.3.5 Sprinkling experiment 5

During the first six days of sprinkling experiment 5 with the same water application intensity as sprinkling experiment 1 (before doubling the water application intensity), we did not measure any subsurface flow (Figure 6.11c). Piezometers outside the sprinkled area and next to the trench remained dry, indicating that water did not flow around the edges of the trench face. Subsurface flow occurred only after the sprinkler was moved 1 m downslope and the sprinkling intensity was increased combined with the further addition of a 16.5 mm/hr thunderstorm. Both the storm and the increase in sprinkling intensity lead to a temporary increase or first occurrence of subsurface saturation in the sprinkled area (Figure 6.11d). Subsurface flow was very small, even when compared to subsurface flow measured during the other sprinkling experiments (Figure 6.11c). Subsurface flow was intermittent; subsurface flow occurred only during the night (when evaporative loss was negligible). In addition, part of the subsurface flow measured during the 18 mm thunderstorm on August 16 2002 18:00 was due to localized overland flow into the trench. Overland flow was not generated from the sprinkled area but from the area downslope of the sprinkled area directly upslope (< 1 m) from the trench. Overland flow appeared to be due to the seasonal hydrophobicity of the upper soil and litter layer.

6.5 Discussion

6.5.1 Importance of subsurface flow through the bedrock at PMRW

Despite the assumption in previous hillslope hydrological studies at Panola, bedrock underlying the trenched hillslope is not impermeable. Bedrock moisture increased rapidly in response to natural precipitation events during the early spring (Figure 6.3). Peak tracer breakthrough in the bedrock downslope from the trench was delayed only 2 days relative to peak tracer breakthrough in subsurface stormflow (Figure 6.4). Flow through bedrock was a very large component of the water balance during the sprinkling experiments (Table 6.2). If one assumes that during the late period of the sprinkling experiments the infiltration rate into the bedrock approached the saturated

conductivity of the bedrock, the conductivity of the bedrock is 5.8 mm/hr for the area of sprinkling experiment 3. This corresponds to a saturated conductivity of $1.6x10^{-6}$ m/s, which is in the range (10^{-4} – 10^{-9} m/s) of saturated conductivities for fractured crystalline rock given by Freeze and Cherry (1979). The measured saturated hydraulic conductivity of the saprolite at 2.35 m below the soil surface on the ridgetop at PMRW is $5x10^{-6}$ m/s (White et al., 2002). While the observed infiltration rates into the bedrock and the saturated hydraulic conductivity of the bedrock is high, these rates are small compared to the vertical saturated conductivity of 644 mm/hr (=$1.79x10^{-4}$ m/s) measured in a large soil core from this hillslope (McIntosh et al., 1999). Thus, while the bedrock has high infiltrability, the conductivity contrast between the soil and the bedrock at the Panola hillslope still allows for ponding of water at the soil-bedrock interface during storms, as is assumed in most conceptual models with impermeable bedrock. Thus there is both flow through bedrock and lateral flow of water over the bedrock surface during storms at the Panola hillslope.

There are many granite blocks (approximately 0.2-0.4 m thick), parallel to the surface, on both the bedrock outcrop across the study hillslope and the bedrock outcrop upslope from the study hillslope. These blocks appear to be caused by weathering of exfoliation fractures in the bedrock. The trench (McDonnell et al., 1996) was excavated to competent bedrock, but this could be a block with exfoliation fractures running more or less parallel to the land surface. In fact, the bedrock topography of the trench face has the shape of three blocks sloping towards the left (when looking upslope) with one block extending from 3-15 m in the along slope distance and one block to the left and the right (when looking upslope) from this main block (Figure 6.2). The bedrock on the left side of the trench with very shallow soils (downslope from sprinkling area 1 and 5) has the shape of a large block (along slope distance 16-20 m in Figure 6.2). Excavation in the trench showed that there was indeed some space under the bedrock (light line in Figure 6.2). If the trench at this location is located on top of a block, it is not surprising that subsurface flow was not measured during sprinkling experiment 1 and the early part of sprinkling experiment 5. Bedrock moisture downslope from this sprinkling area did not increase,

suggesting also that water did not flow through the bedrock (block) but could have flowed underneath the block. Only when the sprinkler was moved downslope, the application rate was doubled, and further addition through the thunderstorm, was there some minimal subsurface flow. While this trench section delivered a very large portion of total subsurface flow during small natural storms, its contributions during larger natural storms was minor (Chapter 2), suggesting that the contributing area of this trench section is very small.

Matrix flow in the bedrock and flow through exfoliation fractures parallel to the surface are an important component of the water balance at this site. Flow through the bedrock could be responsible for the very low runoff coefficients from the hillslope (Chapter 2), and very long mean residence times of riparian groundwater (Burns et al., 2003). The runoff ratios during the sprinkling experiments on the middle hillslope sections (i.e. sprinkling experiments 3 and 4) was 6-7%. For these sprinkling experiments, the calculated non-evaporative loss was approximately 90% of total water applied. These values compare well with the average runoff ratio of 10% for winter storms during 1996-1998 (Chapter 2).While the hillslope might be disconnected from the stream at the storm time scale, as was suggested by EMMA (Hooper et al., 1998), hydrochemical and hydrometric studies (Peters and Ratcliffe, 1998), and the low runoff ratios from the study hillslope (Chapter 2), it appears that the hillslopes are connected to the stream at time scales longer than the storm time scale via flow through the bedrock. Measured mean residence time of riparian groundwater downslope from the study hillslope is 6 to 7 years (Burns et al., 2003). This is an order of magnitude greater than what one would expect or compute based on soil water fate and transport alone.

The few other studies that have examined subsurface flow through bedrock, have focused mainly on the influence of exfiltrating bedrock water on subsurface flow or streamflow (e.g. Anderson et al., 1997; Onda et al., 2001; Uchida et al., 2003). At the Panola hillslope, measured head in a piezometer pair indicate there was always a negative gradient on this hillslope (Chapter 3), suggesting infiltration from the soil into the

bedrock. The absence of bedrock groundwater exfiltration at this hillslope suggests that lateral subsurface stormflow over the soil-bedrock interface 'loses' water to the bedrock along the way, much like an influent stream is losing water to its streambed along the way.

6.5.2 Re-examination of previous studies at Panola in light of bedrock infiltration

While other studies at PMRW have not looked at the influence of subsurface flow through bedrock, there is additional circumstantial evidence for subsurface flow through bedrock. The small subsurface flow runoff ratio in response to the widely published 96 mm March 6-7 1996 storm (McDonnell et al., 1996, Freer et al., 1997 and 2002, Burns et al., 1998 and 2001, Appendix 1) also suggests that there was leakage to bedrock during this winter storm. Less than 0.4 mm of subsurface flow was generated at the 20 m long trench in response to the 49 mm March 6 1996 storm while 24 mm of subsurface flow was generated in response to the 47 mm March 7 1996 storm. Thus the runoff ratio of the March 7 1996 storm was only 51%. Since the March 6 1996 storm replenished the soil moisture deficit, one would expect a much higher runoff ratio (closer to 100%) for the March 7 1996 event if the bedrock was impermeable.

A water balance calculation over the February 22 – April 20 2002 period also shows that subsurface flow is only a small fraction of total precipitation (Figure 6.12). We can assume that total transpiration during this 2-month period was negligible (especially compared to the large total precipitation flux) since leaf out did not occur until mid April 2002. While there were changes in soil moisture during this period, hillslope average soil moisture on February 22 2002 was similar to hillslope average soil moisture on April 20 2002 (Figure 6.12a), such that the net change in soil moisture was zero. Thus the difference between total precipitation (188 mm) and total subsurface flow (7.05 mm) during this period must have been due to infiltration into the bedrock, suggesting a very large role for subsurface flow through the bedrock.

Storm total subsurface flow from the study hillslope is a threshold function of storm total precipitation (Chapter 2). For the 147 storms examined in chapter 2, subsurface flow increased only 0.3-0.8 times the addition precipitation after the threshold is reached. This is contrary to the results by Tani (1997), who found a 1:1 relation between storm total subsurface flow and precipitation after a threshold. The slope of the relation between total subsurface flow and precipitation after a threshold is a function of infiltration into the bedrock (Appendix 1). Thus these results suggest that losses through the bedrock during large natural storms vary between 20-70% of total storm precipitation.

A critical evaluation of the water balance of the three landscape units at PMRW also suggests that there has to be some contribution of flow through the bedrock to streamflow. If one assumes a simple three component mixing model:

$$Y_{stream} = Y_{riparian}\, A_{riparian} + Y_{hillslope}\, A_{hillslope} + Y_{outcrop}\, A_{outcrop} \qquad \text{(Equation 6.2)}$$

where Y is water yield, A is the contribution of a landscape unit to the entire watershed area, Y_{stream} is the average stream yield, and the subscripts *riparian*, *hillslope* and *outcrop* refer to the three main landscape units. Average annual stream yield for the 41 ha gauging station at Panola is 30% (Huntington et al., 1993). The estimated yield of the bedrock outcrops, which cover 10% of the basin area, is 85% maximum. The average yield of the hillslopes, which cover more than 75% of the basin, is 5% (Chapter 2). If one assumes a simple three component mixing model the yield from the riparian zone (using Equation 6.2) is a very unrealistic 133%. If one assumes a four component mixing model:

$$Y_{stream} = Y_{riparian}\, A_{riparian} + Y_{hillslope}\, A_{hillslope} + Y_{outcrop}\, A_{outcrop} + BR \qquad \text{(Equation 6.3)}$$

where *BR* refers to the contribution of subsurface flow through bedrock to streamflow and all other symbols are similar to equation 6.2, and also assumes a water yield of 50% for the riparian zone, then the contribution of bedrock water to streamflow is at least 12 % (Equation 6.3)

6.5.3 Why do long duration low intensity storms produce subsurface flow?

Given the sprinkling observations and other circumstantial evidence for subsurface flow through bedrock presented in this paper, one could ask the question "how can subsurface flow be produced at the trench face during long low intensity storms?" During the 59 mm February 6 2002 storm for example, 6.6 mm of subsurface flow was measured at the trench even though the 30-minute maximum rainfall intensity of this storm was only 5.6 mm/hr (Chapter 3), which is smaller than the observed infiltration rates into the bedrock (~5.8 mm/hr for sprinkled area 3, if one assumes that the area of infiltration is 1.2 times the sprinkled area, see Table 6.2).

Unlike the sprinkling experiments, natural rainfall events include water delivery to the soil-bedrock interface from water infiltrating locally but also lateral flow from upslope positions. We would expect that the infiltrating water from local precipitation, together with lateral flow from the upslope, might be larger than the infiltration rate into the bedrock even during large low intensity storms.

We observe no transient saturation at the soil-bedrock interface on the lower 15 m of the hillslope during small to medium size (<55 mm) storms (Chapter 3). Transient saturation on the lower 15 m of the hillslope occurred only during large storms (> 55 mm) (Chapter 3). Well data on the study hillslope also suggest that this water comes from upslope and flows at the soil-bedrock interface over the lower slope towards the trench within a few hours (Chapter 3). We hypothesize that infiltration into the bedrock could take place during these few hours but is not fast/great enough for all water to infiltrate, such that subsurface flow does appear at the trench.

One hypothesis for why subsurface flow occurs during large but low intensity storms even though we show that infiltration into the bedrock during the sprinkling experiments is large is that subsurface saturation at the soil-bedrock interface started on the upslope because soil moisture deficits are smaller on these shallower upslope soils (Chapter 3). Bedrock on the upslope may also be less permeable than on the lower slope.

We hypothesize that once transient saturation develops on the upslope, there is lateral flow over the bedrock to the downslope. While there is infiltration into the bedrock, this flux is not as great as the lateral flow flux from the upslope augmented by locally infiltrating water, such that subsurface flow at the trench does indeed occur during large low intensity storms.

6.6 Conclusion

Although conceptual models of how the Panola hillslope 'works' assume that the bedrock is relatively impermeable, flow through bedrock is an important component of the water balance at PMRW and can not be ignored. Bedrock moisture increased rapidly in response to natural precipitation during the late winter/early spring (Figure 6.3). Peak tracer breakthrough in bedrock was only two days delayed compared to peak tracer breakthrough in subsurface flow (Figure 6.4). During 8-9 day long sprinkling experiments, when more than the yearly average precipitation was applied to a 69-79 m^2 area, measured subsurface flow was only a small fraction (<10%) of total water applied (Table 6.2). Even though the observed infiltration rates into the bedrock are high, there is a large permeability contrast between the saturated conductivity of the soil and the bedrock at this hillslope. Thus while there is leakage to the bedrock, lateral subsurface flow over the bedrock occurs as well.

These results suggest that the hillslopes, which are the largest landscape unit at PMRW, are not disconnected from the stream as was suggested by earlier studies (Peters and Ratcliffe, 1998; Hooper et al., 1998; Burns et al., 2001). Rather they are connected at a longer than the storm time scale. The relation between precipitation after a threshold and total subsurface flow (Chapter 2) suggests that at least 20% of precipitation during large storms results in subsurface flow through the bedrock. A water balance calculation for the February 22-April 20 2002 period, during which there were no net changes in soil moisture and transpiration was assumed to negligible, showed that subsurface flow was only 3.8% of total precipitation. A simple four component water balance calculation

shows that subsurface flow through the bedrock contributes at least 12 % of streamflow. Future research and modeling efforts at PMRW should thus acknowledge the importance of subsurface flow through the bedrock and attempt to better quantify its behavior at all time scales.

6.7 References

Anderson, S. P., W.E. Dietrich, D.R. Montgomery, R. Torres, M.E. Conrad and K. Logue, Subsurface flow paths in a steep, unchanneled catchment, Water Resources Research 33(12): 2637-2653, 1997.

Asano, Y., T. Uchida, and N. Ohte, Residence times and flow paths of water in steep unchanneld catchments, Tanakami, Japan, Journal of Hydrology 261: 173-192, 2002.

Burns, D.A., R.P. Hooper, J.J. McDonnell, J.E. Freer, C. Kendall, and K. Beven, Base cation concentrations in subsurface flow from a forested hillslope: The role of flushing frequency, Water Resources Research 34(12): 3535-3544, 1998.

Burns, D.A., J. J. McDonnell, R.P. Hooper, N.E. Peters, J.E. Freer, C. Kendall, and K. Beven, Quantifying contributions to storm runoff through end-member mixing analysis and hydrologic measurements at the Panola Mountain Research Watershed (Georgia, USA), Hydrological Processes 15: 1903-1924, 2001.

Burns, D.A., L.N. Plummer, J.J. McDonnell, E. Busenberg, G.C. Casile, C. Kendall, R.P. Hooper, J.E. Freer, N.E. Peters, K. Beven and P. Schlosser, The Geochemical evolution of riparian groundwater in a forested Piedmont catchment, Groundwater 41(7): 913-925, 2003.

Buttle, J. M., and D. S. Turcotte, Runoff processes on a forested slope on the Canadian Shield, Nordic Hydrology 30: 1-20, 1999.

Carter, M.E.B., A community analysis of the Piedmont deciduous forest of Panola Mountain State Conservation Park: Atlanta, Georgia, M. S. thesis, 126 pp., Emory Univ., Atlanta, Ga., 1978.

Crawford T.J., M.W. Higgins, R.F. Crawford, R.L. Atkins, J.H. Medlin and T.W. Stern, Revision of stratigraphic nomenclature in the Atlanta, Athens, and Cartersville 30 ð 60 quadrangles, Georgia. Georgia Geologic Survey Bulletin B-130: Atlanta, Georgia; 48, 1999.

Daniels, R.B., and R.D. Hammer, Soil Geomorphology, John Wiley and Sons Inc., New York, 236 p., 1992.

Freer, J.E., J.J. McDonnell, K.J. Beven, D. Brammer, D.A. Burns, R.P. Hooper, and C. Kendal, Topographic controls on subsurface stormflow at the hillslope scale for two hydrologically distinct small catchments, Hydrological Processes 11(9), 1347-1352, 1997.

Freer, J.E., J.J. McDonnell, K.J. Beven, N.E. Peters, D.A. Burns, R.P. Hooper, B.T. Aulenbach and C. Kendall, The role of bedrock topography on subsurface stormflow, Water Resources Research, 10.1029/2001WR000872, 2002.

Freeze, R.A., and J.A. Cherry, Groundwater, Prentice Hall, New-York, 604 p., 1979.

Granier, A., Une nouvelle methode pour la mesure de flux de seve brute dans le tronc des arbres, Annales des Sciences Forestieres 42: 193–200, 1985.

Granier, A., Evaluation of transpiration in a Douglas-fir stand by means of sapflow measurements, Tree Physiology 3: 309–320, 1987.

Green, W.H., and G.A. Ampt, Studies on soil physics: I Flow of air and water through soils, Journal of Agricultural Science 4:1-24, 1911.

Hooper R.P., N. Christopherson and N.E. Peters, Modelling streamwater chemistry as a mixture of soilwater end-members: an application to the Panola Mountain catchment, Georgia, U.S.A. Journal of Hydrology 116: 321-343, 1990.

Hooper, R.P., B.T. Aulenbach, D.A. Burns, J.J. McDonnell, J.E. Freer, C. Kendall and K.J. Beven, Riparian control of stream-water chemistry: implications for hydrochemical basin models, in Hydrology, Water resources and Ecology in Headwaters, Proceedings of the HeadWater '98 conference held at Meran/Merano, Italy 1998, IAHS publication 248: 451-458, 1998.

Huntington, T.G., R.P. Hooper, N.E. Peters, T.D. Bullen, and C. Kendall, Water, energy, and biogeochemical budgets investigation at Panola Mountain Research Watershed, Stockbridge, Georgia—A research plan, U.S. Geological Survey Open File Report, 93–55, 39 pp., 1993.

McIntosh, J., J.J. McDonnell, and N.E. Peters, Tracer and hydrometric study of preferential flow in large undisturbed soil cores from the Georgia Piedmont, USA, Hydrological Processes 13: 139-155, 1999.

McDonnell, J.J., A rationale for old water discharge through macropores in a steep, humid catchment, Water Resources Research 26(11): 2821-2832, 1990.

McDonnell, J.J., J.E. Freer, R.P. Hooper, C. Kendall, D.A. Burns, K.J. Beven and N.E. Peters, New method developed for studying flow in hillslopes, EOS, Transactions of the American Geophysical Union, 77(47), 465, 1996.

McDonnell, J.J., and T. Tanaka, On the future of forest hydrology and biogeochemistry, Hydrological Processes 15: 2053-2055, 2001.

McGlynn, B., J.J. McDonnell, and D. Brammer, A review of the evolving perceptual model of hillslope flowpathsat the Maimai catchment, New Zealand. Journal of Hydrology 257: 1-26, 2002.

Onda, Y., Y. Komatsu, M. Tsujimora, and J. Fujihara, The role of subsurface flow runoff through bedrock on storm flow generation, Hydrological Processes 15: 1693-1706, 2001.

Peters, D.L., J.M. Buttle, C.H. Taylor, and B.D. LaZerte, Runoff production in a forested, shallow soil, Canadian Shield basin, Water Resources Research 31(5): 1291-1304, 1995.

Peters, N.E., and E.B. Ratcliffe, Tracing hydrologic pathways using chloride at the Panola Mountain Research Watershed, Georgia, USA. Water, Air and Soil Pollution, 105(1/2): 263-275, 1998.

Peters, N.E., J.E. Freer, and B.T. Aulenbach, Hydrologic dynamics of the Panola Mountain Research Watershed, Georgia, Groundwater 41(7): 973-988, 2003.

Phillips N., B.J. Bond, N.G. McDowell, M.G. Ryan, Canopy and hydraulic conductance in young, mature, and old Douglas-fir trees, Tree Physiology 22: 205–212, 2002.

Shanley, J.B., and N.E. Peters, Preliminary observations of streamflow generation during storms in a forested Piedmont watershed using temperature as a tracer, Journal of Contaminant Hydrology 3: 349-365, 1988.

Stewart, M.K., and J.J. McDonnell, Modeling baseflow soil water residence times from deuterium concentrations, Water Resources Research 27(10): 2681-2694, 1991.

Tani, M., Runoff generation processes estimated from hydrological observations on a steep forested hillslope with a thin soil layer, Journal of Hydrology 200: 84-109, 1997.

Uchida, T., K. Kosugi, and T. Mizuyama, Effects of pipe flow and bedrock groundwater on runoff generation in a steep headwater catchment in Ashiu, central Japan, Water Resources Research, 10.1029/2001WR000361, 2002.

Uchida,T., Y. Asano, N. Ohte and T. Mizuyama, Seepage area and rate of bedrock groundwater discharge at a granitic unchanneled hillslope, Water Resources Research 39(1): 1018, Doi:10.1029/2002wr001298, 2003.

Weyman, D.R., Measurements of the downslope flow of water in a soil, Journal of Hydrology 20(3): 267-288, 1973.

White, A.F., T.D. Dullen, M.J. Schulz, A.E. Blum, T.G. Huntington and N.E. Peters, Differential rates of feldspar weathering in granitic regoliths, Geochimica et Cosmochimica Acta 65(6): 847-869, 2001.

White, A.F., A.E. Blum, M.S. Schulz, T.G. Huntington, N.E. Peters, and D.A. Stonestrom, Chemical weathering of the Panola Granite: Solute and regolith elemental fluxes and the weathering rate of biotite, in: Hellmann, R., and S.A. Wood (ed.), Water-Rock interactions, Ore deposits, and Environmental Chemistry: A tribute to David A. Crerar, The Geochemical Society, Special Publication 7: 37-59, 2002.

Figure 6.1 Location of the sprinkled areas during sprinkling experiments 1-5 (shaded areas) and the location of the soil moisture measurements (a), the crest stage gauges (b), the recording wells (c), the line source tracer application and the location of the trees with the sapflow sensors (d). During the later part of sprinkling experiment 5, the sprinkler was moved 1 m downslope and water was applied only to the lower part of the hillslope (see text). The shaded rectangle represents the location of the trench.

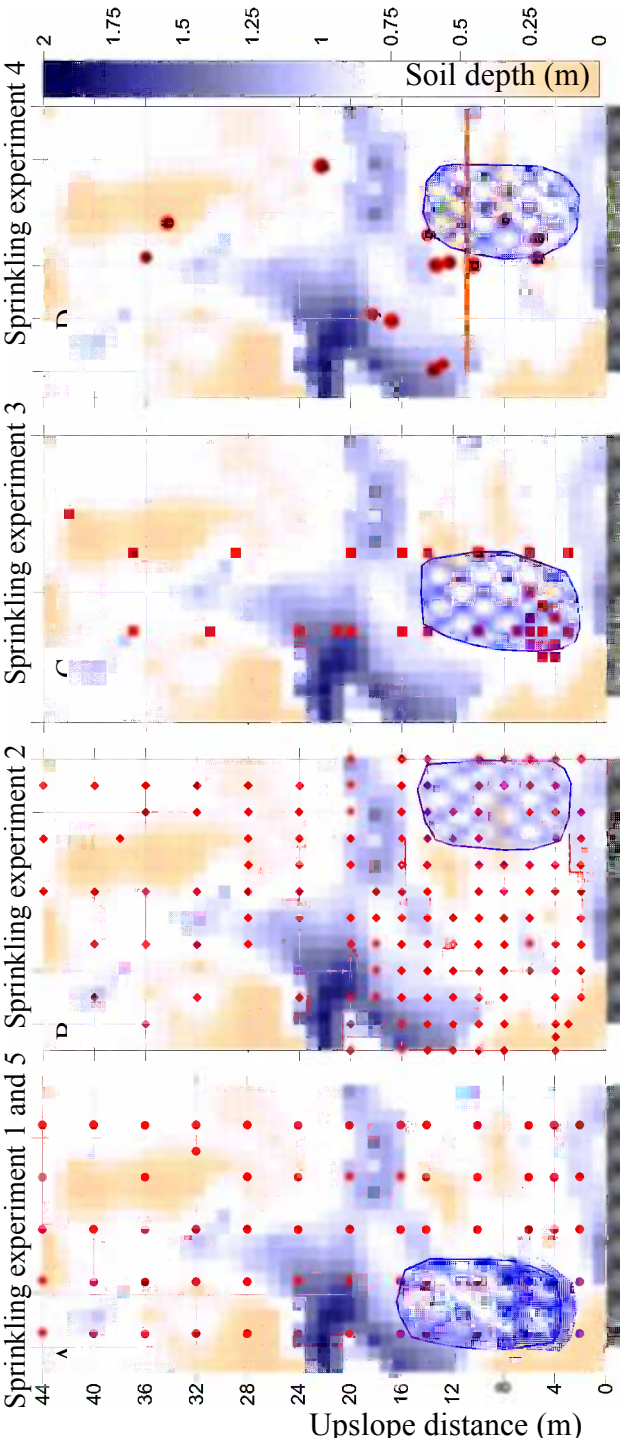

Figure 6.2 Schematic front view of the trench face and the along slope locations of the bedrock moisture measurements (closed circles) and the suction lysimeters in the bedrock (open squares) downslope from the trench. The horizontal lines represent the sections that produced subsurface flow during the sprinkling experiments.

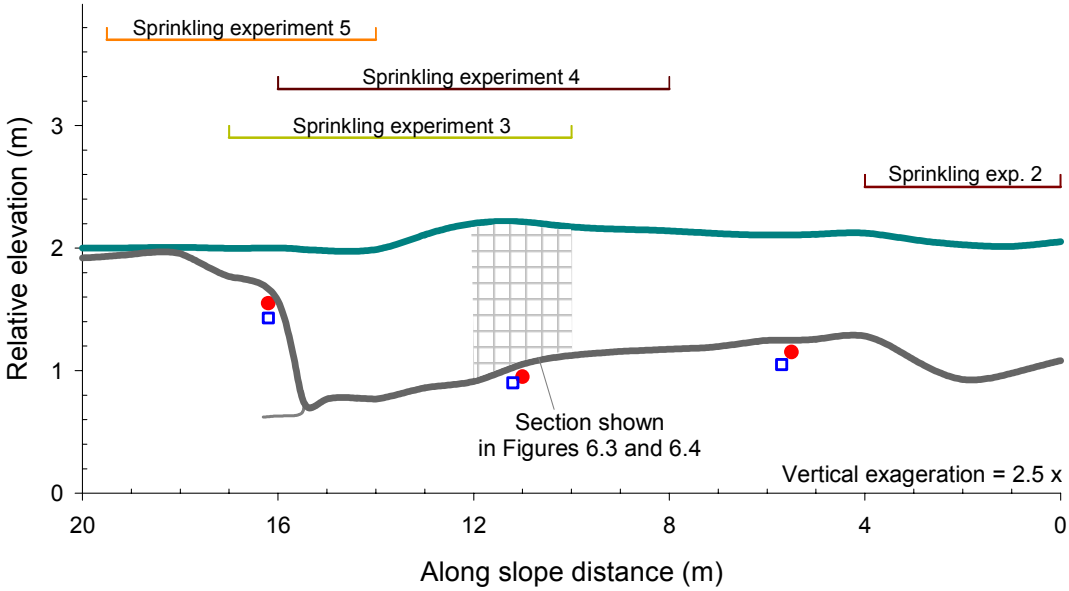

Figure 6.3 Measured bedrock moisture at 50 mm below the (competent) bedrock surface near the middle of the trench (see Figure 6.2) during the spring of 2002. The insert shows the April 9-14 2002 period, when measurements were made throughout two storms, in more detail.

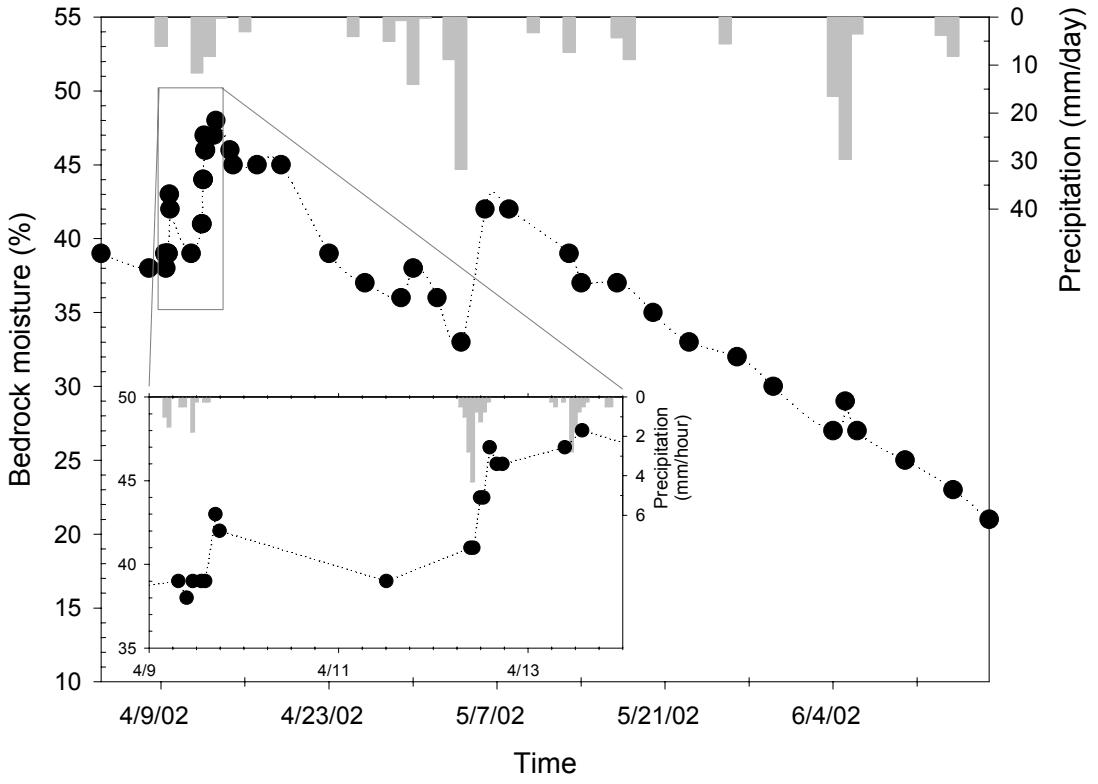

Figure 6.4 Breakthrough curves of bromide from a line source application in subsurface flow (circles) and the bedrock (triangles) and measured subsurface flow from the 2-m wide trench section in the middle of the trench (see Figure 6.2). Bromide was applied 11 m upslope from the trench on March 1 2002 20:00.

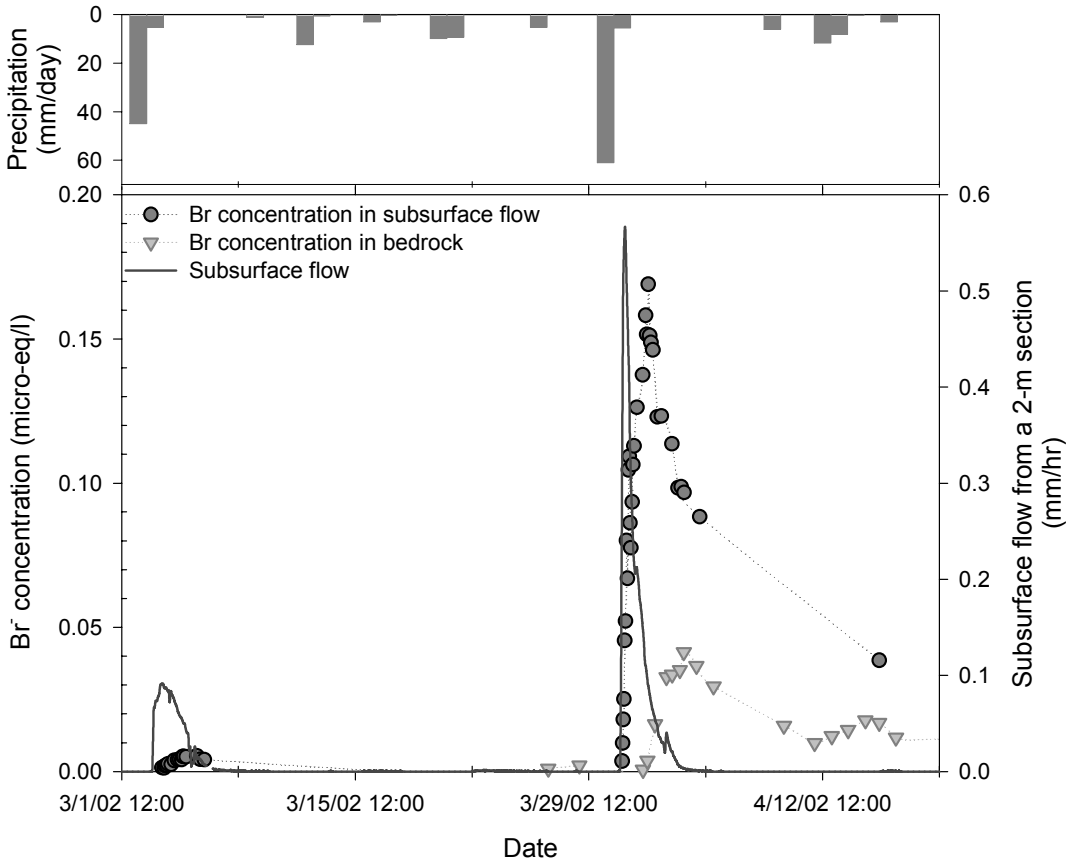

Figure 6.5 Precipitation (a), water applied (b), measured subsurface flow (c), water level in selected wells (d), bedrock moisture (e), soil moisture at a location inside the sprinkled area and just outside the sprinkled area (f), and sapflow measured in two trees close the sprinkling area during sprinkling experiment 1 (g). Note the different x-axis compared to Figures 6.6, 6.7, 6.10, and 6.11.

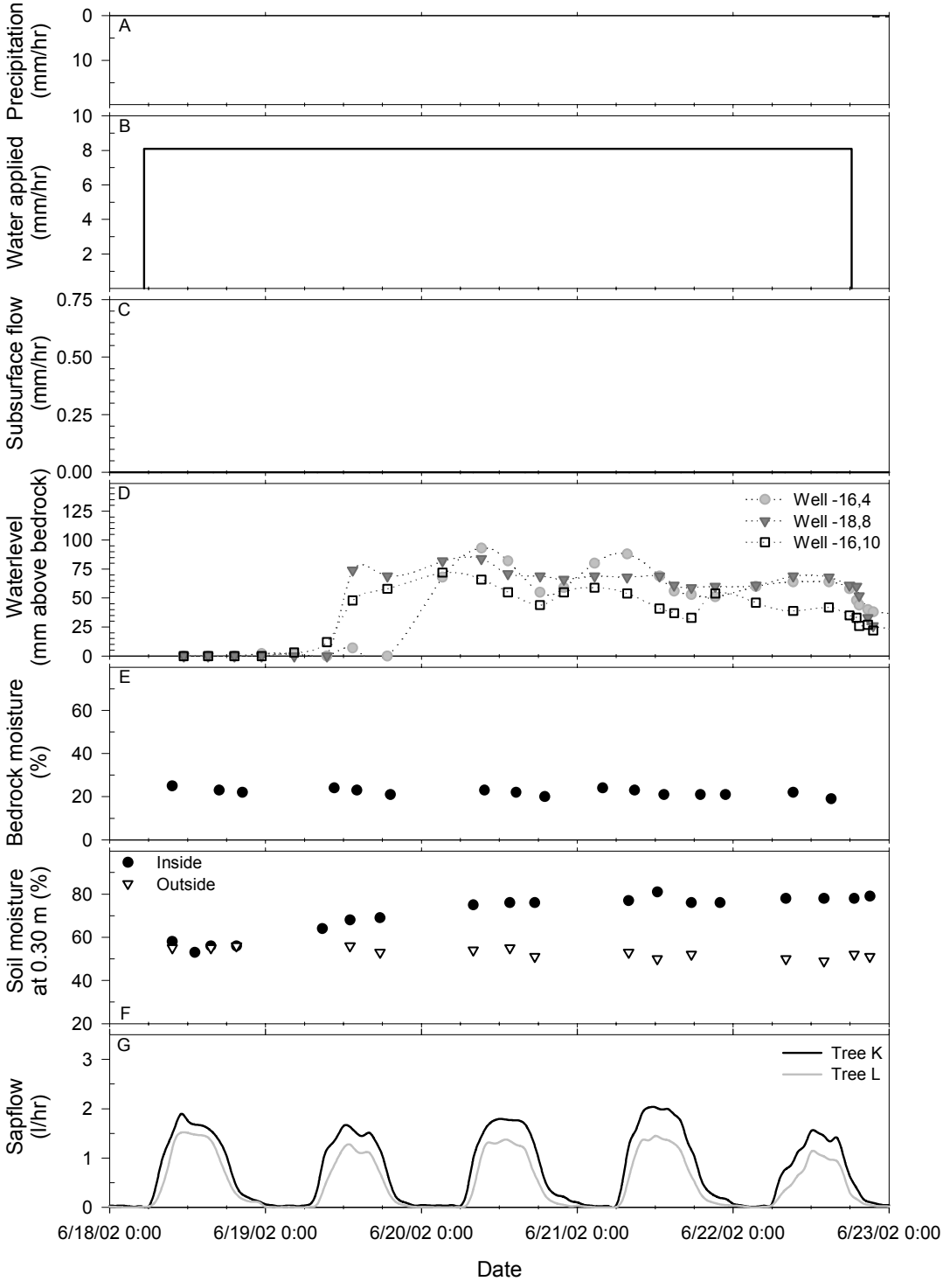

Figure 6.6 Precipitation (a), water applied (b), measured subsurface flow (c), water level in selected wells (d), bedrock moisture (e), soil moisture at a location inside the sprinkled area and just outside the sprinkled area (f), and sapflow measured in two trees close the sprinkling area during sprinkling experiment 2 (g). Note the different scale for water level compared to Figure 6.5d, 6.7d, 6.10d, and 6.11d.

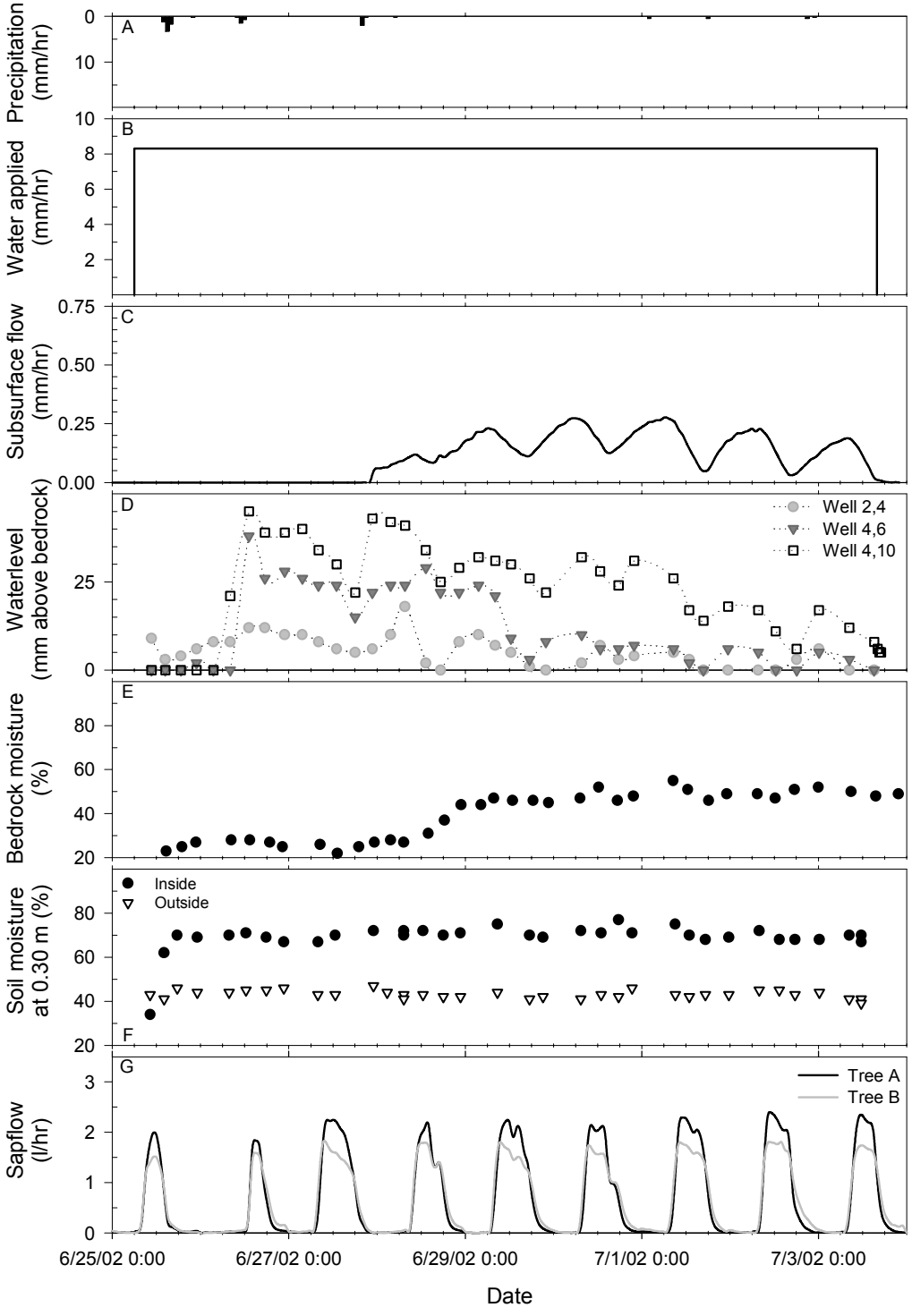

Figure 6.7 Precipitation (a), water applied (b), measured subsurface flow (c), water level in selected wells (d), bedrock moisture (e), soil moisture at a location inside the sprinkled area and just outside the sprinkled area (f), and sapflow measured in two trees close the sprinkling area during sprinkling experiment 3 (g). Note the different scale for subsurface flow and water level compared to Figures 6.5c, 6.6c and 6.10c.

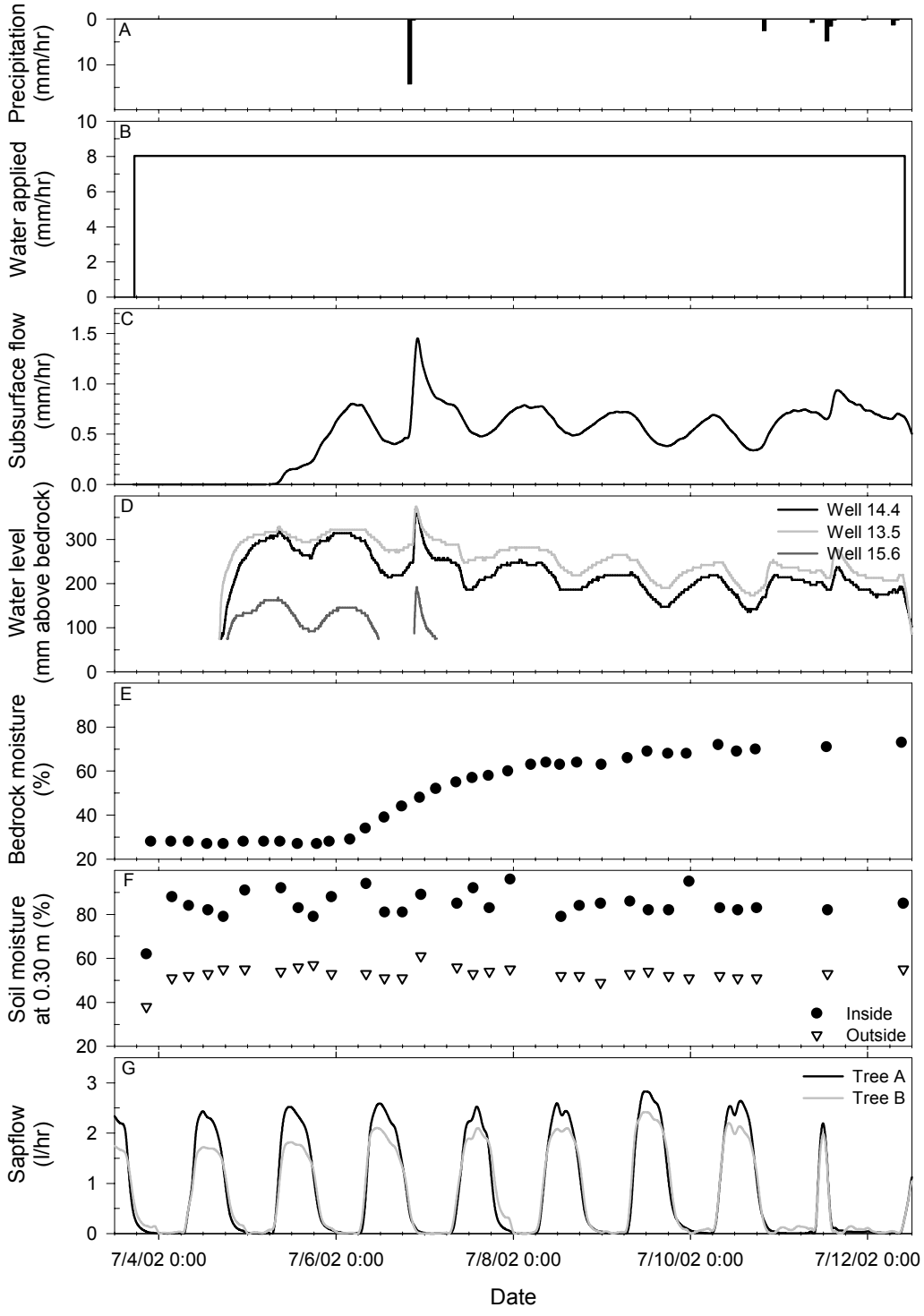

Figure 6.8 The relation between subsurface flow and water level above bedrock in two wells during sprinkling experiment 3.

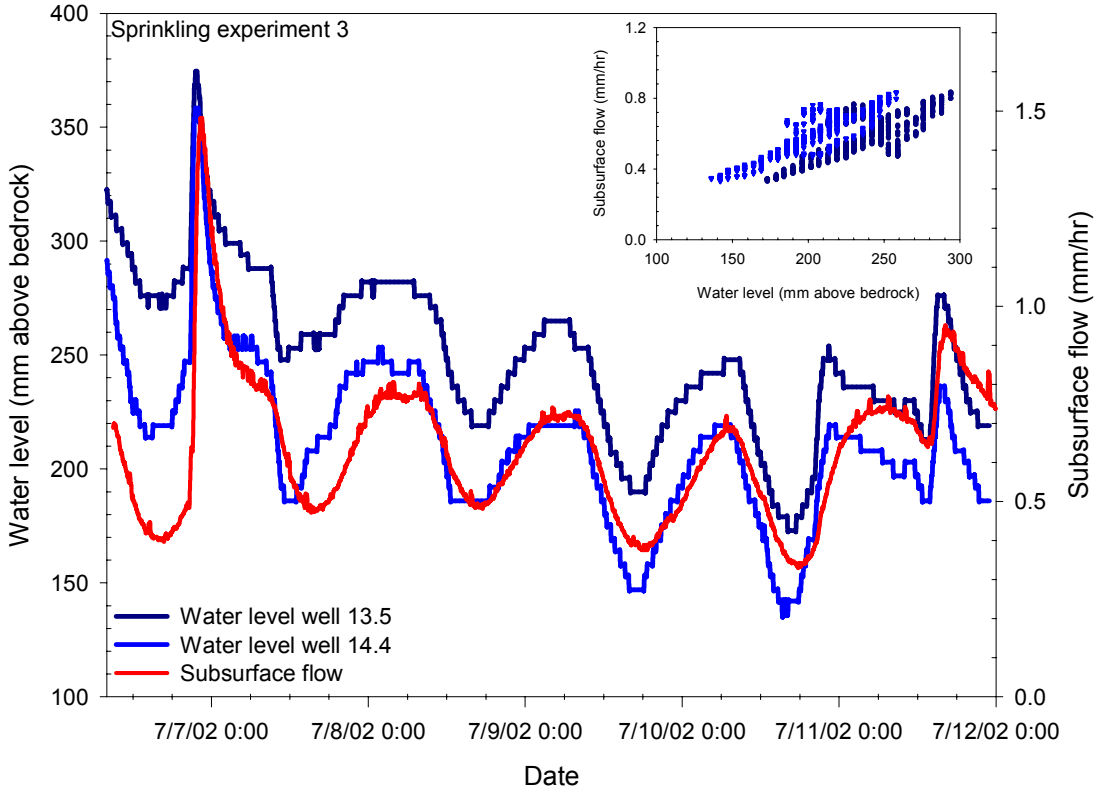

Figure 6.9 Soil moisture at different depths below the soil surface for measurement location 11.2, located downslope from the sprinkled area during experiment 3.

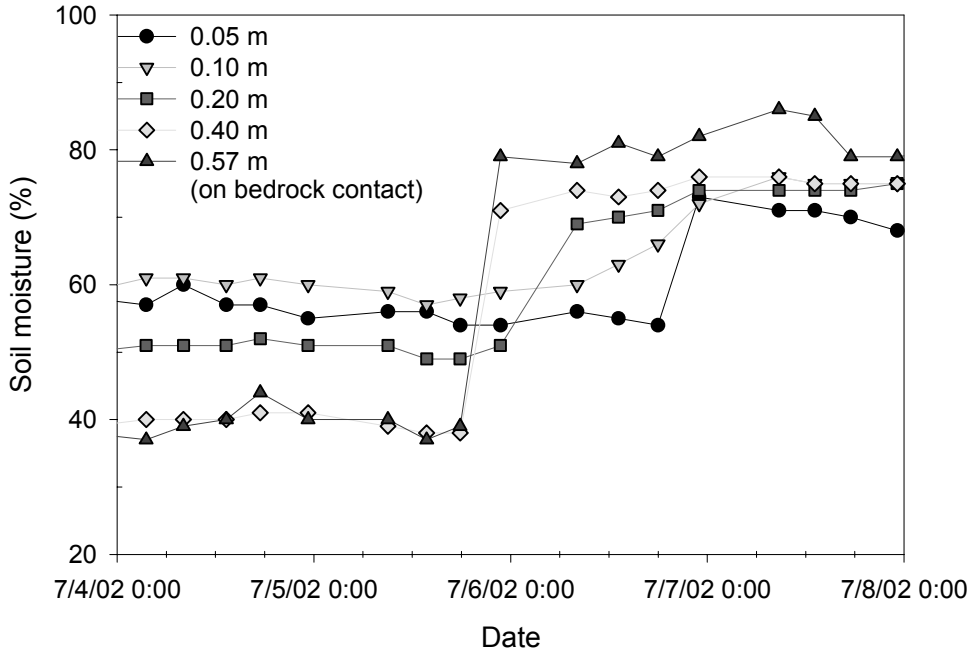

Figure 6.10 Precipitation (a), water applied (b), measured subsurface flow (c), water level in selected wells (d), bedrock moisture (e), soil moisture at a location inside the sprinkled area and just outside the sprinkled area (f), and sapflow measured in two trees close the sprinkling area during sprinkling experiment 4 (g).

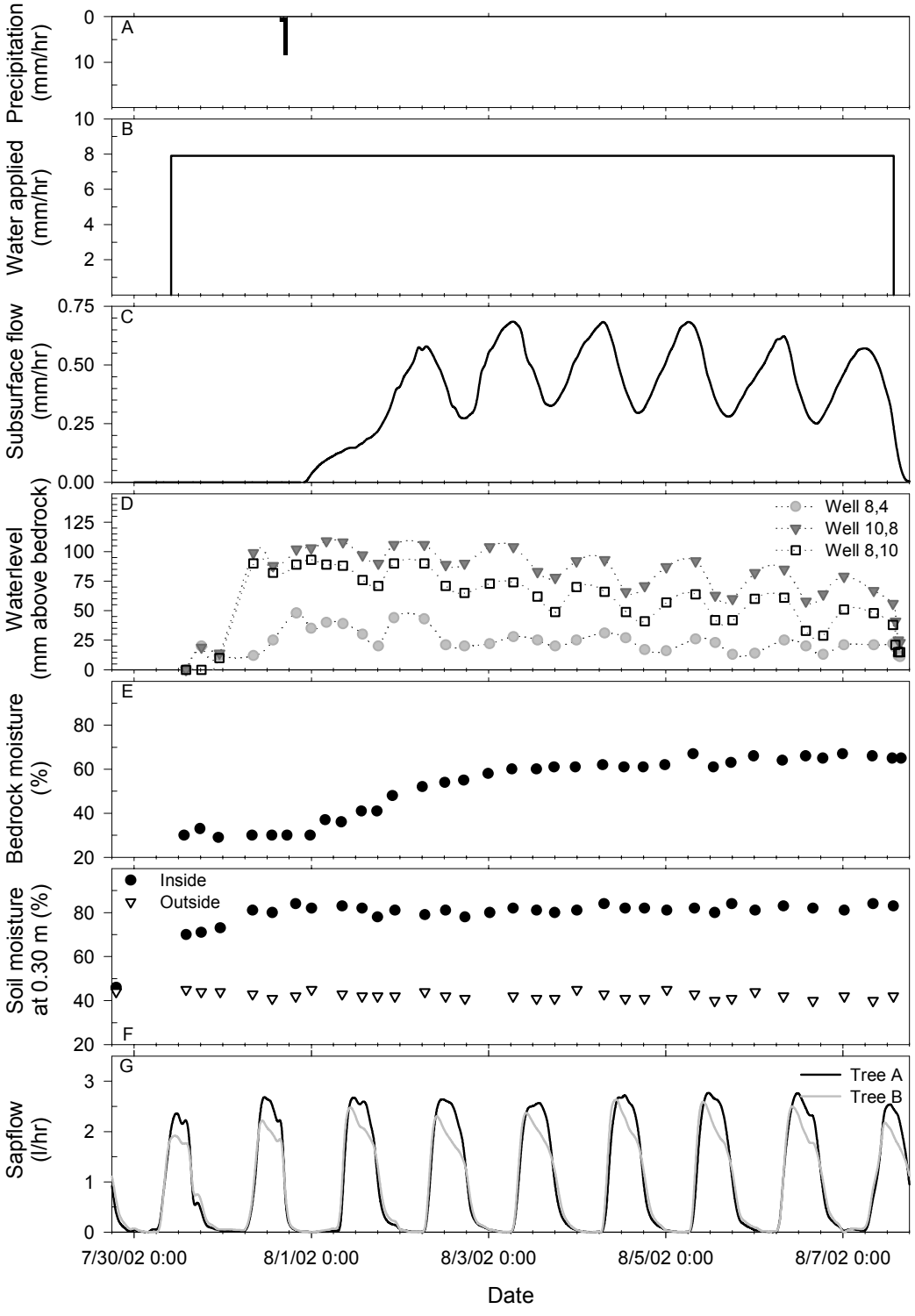

Figure 6.11 Precipitation (a), water applied (b), measured subsurface flow (c), water level in selected wells (d), bedrock moisture (e), soil moisture at a location inside the sprinkled area and just outside the sprinkled area (f), and sapflow measured in two trees close the sprinkling area during sprinkling experiment 5 (g). Note the different scale for water applied, subsurface flow, water level and bedrock moisture compared to Figures 6.5, 6.6, 6.7 and 6.10.

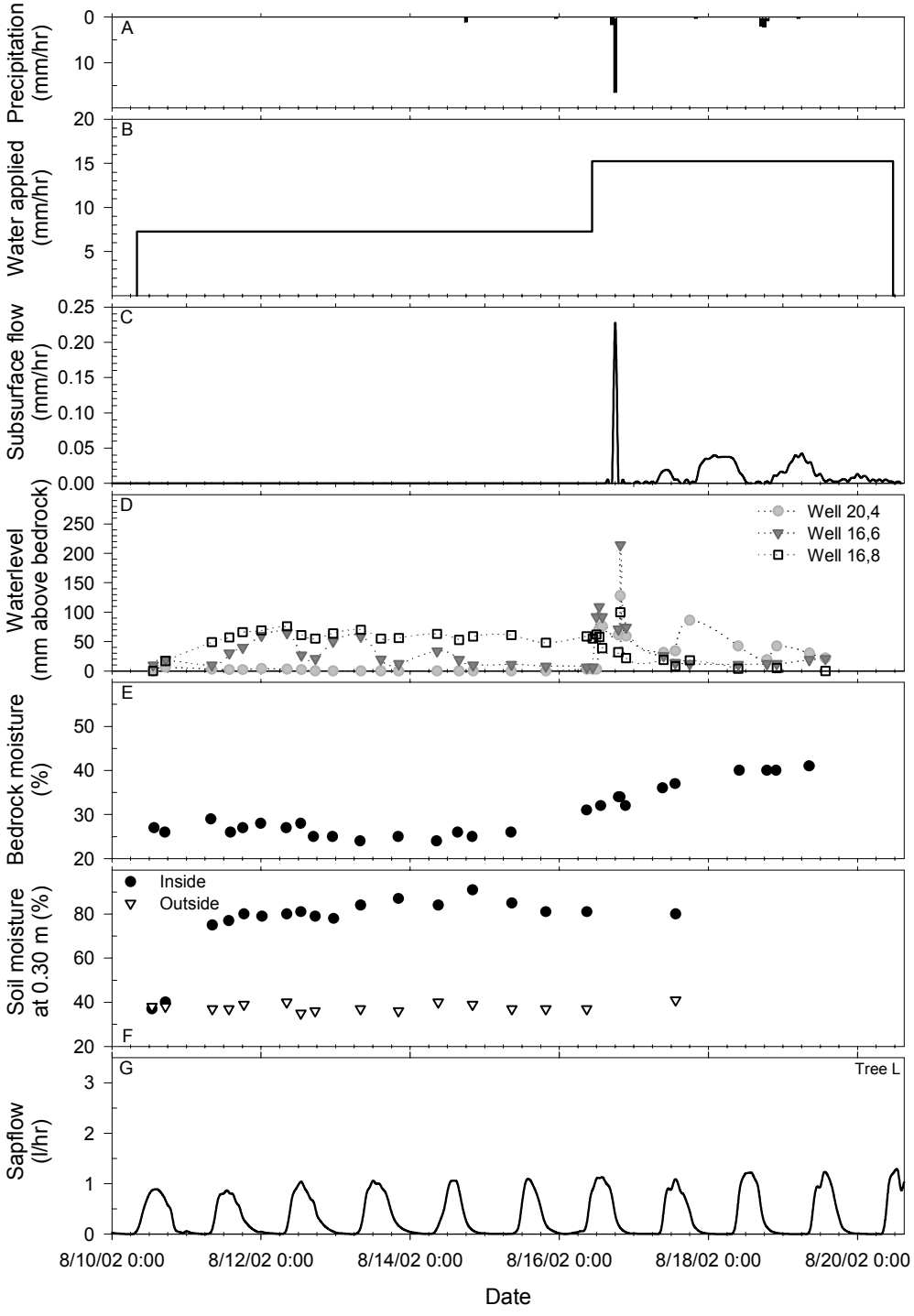

Figure 6.12 Hillslope average soil moisture (a), cumulative precipitation and cumulative subsurface flow during late winter and early spring 2002 (b). Hillslope average soil moisture was calculated by averaging the profile average soil moisture for all measurement locations. Profile average soil moisture was calculated for each measurement location by multiplying the measured Aqua-pro values at the different depths by the distance between the subsequent measurement depths and multiplying this by the soil depth at the measurement location.

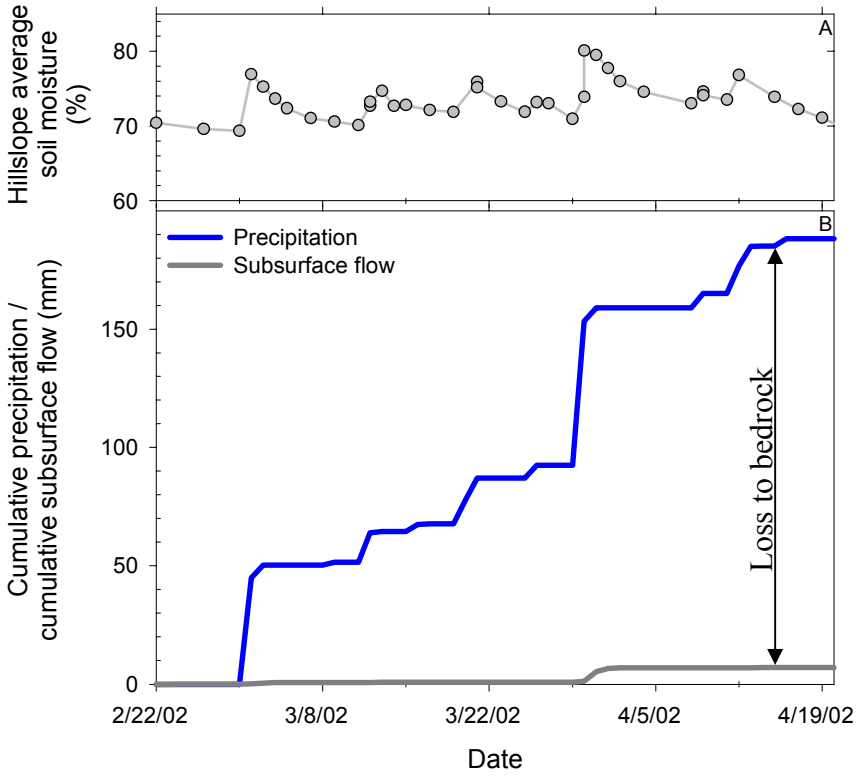

Table 6.1 Specifications of the sprinkling experiments. Average yearly precipitation for PMRW is 1240 mm. During sprinkling experiment 5, the sprinkling area was reduced and moved 1 m downslope after 6 days (see text).

#	Start time	End time	Sprinkling area (m^2)	Total water applied (mm)	Center of water application (x,y) (m)
1	6/18/02 5:18	6/22/02 18:16	71.2	882	17.5, 10
2	6/25/02 6:02	7/3/02 15:56	69.4	1675	7.5, 8.5
3	7/3/02 17:19	7/12/02 10:04	71.7	1676	12.5, 8.5
4	7/30/02 10:00	8/7/02 13:46	73.0	1545	7.5, 8.5
5	8/10/02 8:04	8/20/02 11:25	79.2	1770	17.5, 9

Table 6.2 Calculated components of the water budget during the late period of the sprinkling experiments. Total subsurface flow due to the storms was calculated as the difference between measured subsurface flow and an interpolated sinusoidal line that represented the estimated subsurface flow if the storm would not have occurred. All values are normalized by the area of the water application (see Table 6.1).

#	Total water applied (mm/day)	Total subsurface flow (mm/day)	Evaporative loss (mm/day)	Non-evaporative loss (mm/day)	Runoff ratio (%)
1	194	0	194		0
2	200	4.1	1.81	194	2.04
3	193	13.8	3.7	175	7.2
Storm 1	14.5	3.79	0	10.7	26.2
Storm 2	7.4	1.90	0	5.5	25.8
4	189	11.6	4.5	173	6.1
5 late period	369	0.4	368		0.1

Table 6.3 Three-hour average of the depth of water applied, measured subsurface flow, the runoff ratio, the calculated non-evaporative loss, and the water level in well 13.5 during sprinkling experiment 3. All values are normalized by the area of the water application. The difference between total water applied and subsurface flow plus non-evaporative loss is evaporative loss. Changes in storage during the 3-hour period are ignored.

#	Total water applied (mm/hr)	Total subsurface flow (mm/hr)	Runoff ratio (%)	Non-evaporative loss (mm/hr)	Water level (mm above bedrock)
Prior to storm 1	8.0	0.5	5.9	7.5	282
Storm 1	12.9	1.3	10.0	11.6	368
Prior to storm 2	8.0	0.7	8.6	7.3	230
Storm 2	10.2	0.9	8.9	9.3	276

7 Conclusion

7.1 Introduction

Most hillslope hydrological studies during the past decades have been flow centric and focused at the event time scale. An implicit assumption has been that subsurface flow responses are continuous. However, recent commentary in the broad hydrologic literature has called for examination of the linkages and feedbacks between ecological processes and hydrological processes (e.g. Rodriguez-Iturbe, 2000), examination of both the event and the inter-event time scale (e.g. Rodriquez-Iturbe, 2000; Bond, 2003), examination of spatial patterns (e.g. Grayson and Blöschl, 2001), and non-linear processes (e.g. Phillips, 2003). The dissertation chapters and the new refined conceptual model for hillslope scale subsurface storm flow generation and the hillslope scale water balance described below are a response to these recent challenges.

7.2 Conceptual model

7.2.1 Classic conceptual model

The classic conceptual model is described in Chapter 1.1. The main principle of the classic conceptualization of hillslope hydrology is that water ponds at the soil-bedrock interface or at a soil horizon contact due to the permeability contrast between the soil layers. This creates transient subsurface saturation (in the form of a saturated wedge), which in turn results in lateral subsurface flow. Total subsurface stormflow and the pattern of subsurface stormflow across the hillslope are determined by soil moisture content. Subsurface flow through the bedrock is negligible.

7.2.2 Refined conceptual model

A new refined conceptual model for the Panola hillslope is described below, and shown schematically in Figure 7.1. The refined conceptual model includes both vertical and lateral fluxes, processes at the event and inter-event time scale and a coupling between the geosphere and the biosphere. The refined conceptual model is divided into

three states (wet, transition and dry), with distinctly different responses to precipitation. The three states are separated by differences in average soil moisture conditions across the hillslope.

7.2.2.1 Wet state

During the wet state pre-event soil moisture is similar across the hillslope (Chapter 4 and Appendix 2). Because of the smaller total soil moisture deficit in the shallow soil areas, lateral flow at the soil-bedrock interface starts first in areas with shallow soils. While there is leakage into the bedrock, transient saturation at the soil-bedrock interface does occur during storms because of the large difference in saturated conductivity between the soil and bedrock (Chapter 6). Lateral flow over the bedrock fills up the depressions in the bedrock topography. Only during large storms (> 55 mm) when the bedrock depressions are filled, does water spill over the depression edges and flow over the soil-bedrock interface and through the bedrock lows to the trench. This is when the subsurface saturated area becomes connected to the trench face. Water infiltrates into the bedrock while it flows downslope through the bedrock lows. Connectivity between the subsurface saturated areas and the trench results in a large increase in subsurface flow (Chapter 3 and Appendix 1). The disconnection of subsurface saturated areas from the trench during medium size (30-55 mm) storms results in only limited subsurface flow from localized areas close to the trench during medium size storms (Chapter 3) and a threshold-like relation between subsurface storm flow and precipitation (Chapter 2).

In between events the hillslope drains to field capacity through both subsurface flow and especially leakage to the bedrock. This results in a uniform soil moisture pattern across the hillslope (Chapter 4 and Appendix 2). Drainage in between storms is rapid compared to the average time between consecutive events (6 days) such that the hillslope is essentially re-set for the next storm, i.e. pre-event soil moisture conditions for each storm are similar to the pre-event storm conditions of the previous storm (Appendix 2). Transpiration is limited during the wet state because the wet state corresponds with the dormant season (January-early April).

Fluxes during the wet state are predominantly vertical into to bedrock (Chapter 6), and lateral over the soil-bedrock interface during storms (Chapter 3). During the wet state there are numerous small and medium size storms but only a few large storms. Because lateral flow during medium size storms occurs only on the shallow soil sections, there is more lateral flow from the shallow soil areas during the wet state than lateral flow from the deeper soil areas (which is represented by the larger lateral flow arrow for the shallower upslope soils in Figure 7.1a). This water is held up in depressions in the bedrock on the midslope where it infiltrates into the bedrock.

7.2.2.2 Transition (drying) state

The shift from the wet state to the transition state coincides with the beginning of leaf out and significant transpiration, i.e. the shift in the hydrological state is induced by a shift in an ecological process. Transpiration results in lower soil moisture across the hillslope during the transition state than during the wet state (Chapter 4). Lower soil moisture results in much lower hydraulic conductivity and thus less lateral flow compared to the wet state. Fluxes during the transition state are predominantly vertical (transpiration and local infiltration). The onset of a vertical ecological process (transpiration) thus reduces the importance of the lateral hydrological processes. Because soil moisture is lower during the transition state than during the wet state, only very large storms result in transient saturation at the soil-bedrock interface and lateral flow. These very large storms move the hillslope temporarily (less than 1 week) back into the wet state (Chapter 4). During medium size storms, localized areas directly upslope from the trench face generate limited subsurface flow. Connectivity between the trench and the upper slope does not occur during the medium size storms during the transition state (Figure 7.1b). Very large storms that move the hillslope back temporarily into wet state do result in connectivity.

Transpiration is uniform across the hillslope, resulting in a uniform depletion of total water stored in the soil profile. Because less total water is stored in the shallower soil sections at the end of the wet state, soil moisture in the shallower soil sections

decreases faster, resulting in a positive correlation between soil moisture and soil depth (Chapter 4). Frequent storms during the transition state replenish soil moisture in the top soil layers but the wetting front does not penetrate to depth, resulting in a vertical gradient in soil moisture with depth during and directly after storms (Chapter 4). Transpiration after a storm reduces soil moisture in the upper soil layers, resulting in a uniform soil moisture distribution with depth within days after the storm (Chapter 4).

7.2.2.3 Dry state

Uniform transpiration across the hillslope during the transition state results in lower soil moisture in the shallow soil areas (Chapter 4). Low soil moisture in the shallow soil areas limits transpiration during the dry state. Transpiration on the deeper soil areas is not limited by soil moisture (Chapter 4). Storms during this period only rewet the surface soil layers. The wetting front does not penetrate to depth (less than 0.3 m). Transient saturation at the soil-bedrock interface does not occur during this period (Chapter 3 and 4). Fluxes during the dry state are thus predominantly vertical. Limited subsurface flow is generated only from localized areas directly upslope from the trench. There is no connectivity between the lower slope and the upper slope during the dry state. Transpiration on the shallow soil areas increases temporarily after precipitation, resulting in uniform transpiration across the hillslope (similar to the transpiration pattern during the transition state) in days following the storm (Chapter 4). This results in a rapid local exchange of water between the atmosphere and the soil for the shallow soil sections (which is represented by the larger circular arrow for the shallower soils in Figure 7.1c).

7.3 Way forward

The conceptual model described above shows a large influence of bedrock micro-topography and hillslope scale variations in soil depth on hydrological and ecological processes. During the wet state more lateral flow is generated from the shallow soil sections because of smaller pre-storm moisture deficits. During medium size storms lateral flow is produced on the shallow soil sections but not the deep soil sections. In

addition, the small scale variations in soil depth (bedrock micro-depressions) have a large influence on hillslope connectivity, resulting in threshold-like subsurface flow responses. Bedrock depressions (i.e. deep soil sections) have to be filled with water before the subsurface saturated area can become connected to the trench face. Once depressions in the bedrock are filled, water follows the lows in the bedrock, resulting in spatially variable subsurface flow. This is the fill and spill hypothesis set forth in Chapter 3. Burns et al. (1998) have shown that this spatially variable subsurface flow is also highly variable in base cation concentrations. Mobile water from sections that deliver most subsurface flow is dilute. During the drying and dry state soil moisture at depth becomes a function of soil depth. During the dry state, transpiration in the shallow soil areas is soil moisture limited because of the smaller total water storage at the end of the wet state in the shallow soil areas compared to deeper soil sections.

These results suggest that small scale variations in soil depth result in spatially variable fluxes at the hillslope scale. It is thus important to consider small scale variations in soil depth. However, it is currently not feasible or practical to obtain small scale spatially distributed soil depth data across a catchment. One way forward to include soil depth variations (and resulting spatially variable fluxes) into hydrological and ecological models is to generate random distributions of soil depth with the same mean, standard deviation and correlation length as the measured soil depth variations at an intensive research hillslope or small area of the catchment. This method has shown promise for modeling the spatial variability of subsurface flow regionalized to other areas of the catchment (van Verseveld et al., 2003; Tromp-van Meerveld et al., 2004).

7.4 References

Bond, B., Hydrology and ecology meet—and the meeting is good, Hydrological Processes 17: 2087–2089, 2003.

Burns, D. A., R.P. Hooper, J.J. McDonnell, J.E. Freer, C. Kendall and K. Beven, Base cation concentrations in subsurface flow from a forested hillslope: The role of flushing frequency, Water Resources Research 34(12): 3535-3544, 1998.

Grayson, R., and G. Blöschl, Spatial patterns in catchment hydrology: Observations and modeling, Cambridge University Press, Cambridge, 404 p. 2001.

Phillips, J.D., Sources of nonlinearity and complexity in geomorphic systems, Progress in Physical Geography 27(1): 1–23, 2003.

Rodriguez-Iturbe, I., Eco-hydrology: A hydrologic perspective of climate-soil-vegetation dynamics, Water Resources Research 36(1): 3-9, 2000.

Tromp-van Meerveld, H.J., M. Weiler and J.J. McDonnell, Modeling the influence of subsurface topography on the spatial and temporal variability of subsurface stormflow at the hillslope scale and streamflow at the catchment scale, European Geophysical Society, (Abstract EGU04-A-06473), 2004.

van Verseveld, W.J., H.J. Tromp-van Meerveld, M. Weiler and J.J. McDonnell, Modeling the influence of subsurface topography on spatial and temporal variability of subsurface stormflow. Eos Trans. AGU, 84(46), Fall Meet. Suppl., Abstract H42D-1112. 2003.

Figure 7.1 Schematic representation of lateral and vertical flow processes during the wet, transition and dry state. Precipitation vectors are not shown.

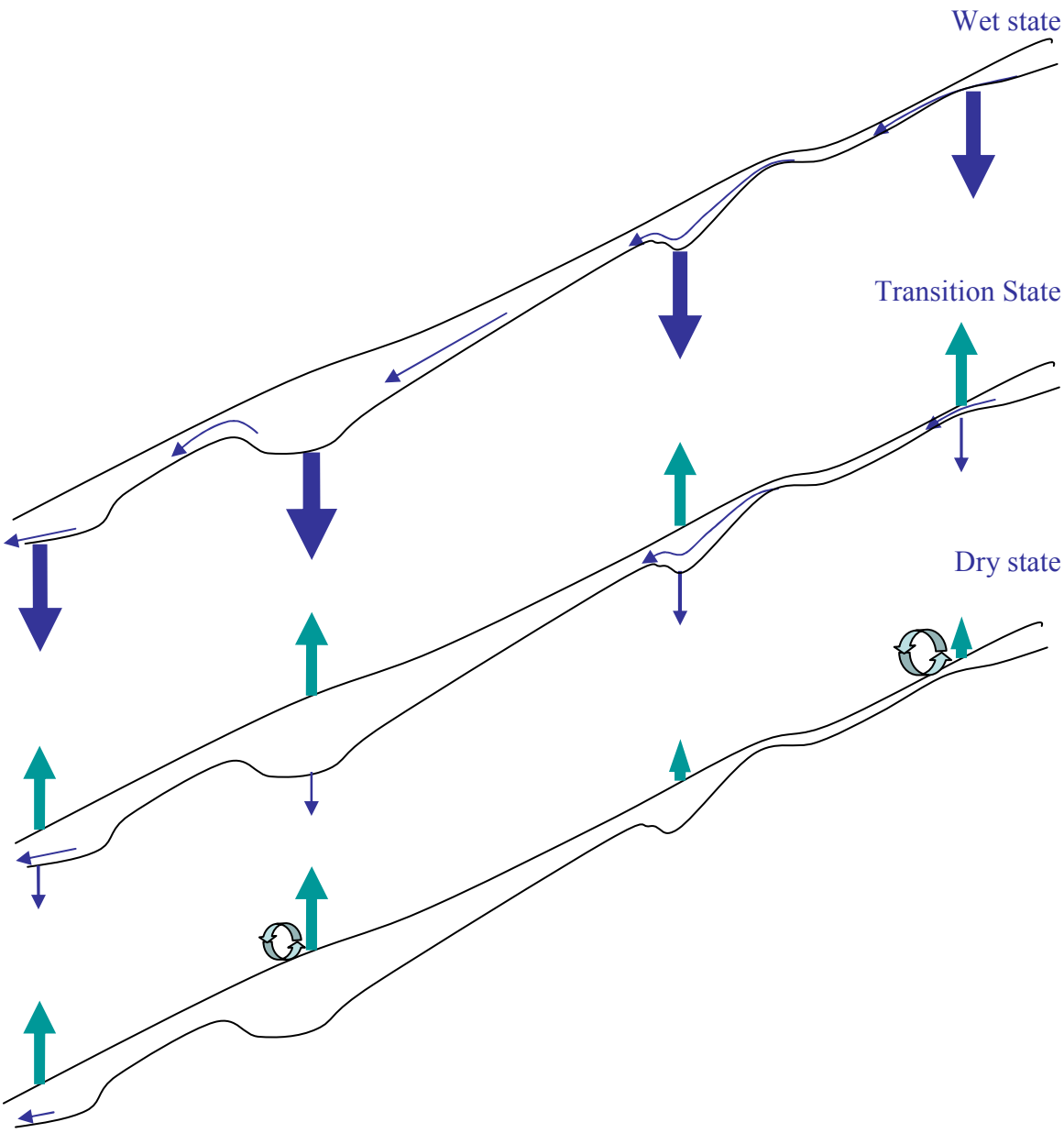

Bibliography

Anctil, F., R. Mathieu, L. Parent, A.A. Viau, M. Sbih, and M. Hessami, Geostatistics of near-surface moisture in bare cultivated organic soils, Journal of Hydrology 260: 30-37 2002.

Anderson, M. G., and T.P. Burt, The role of topography in controlling throughflow generation, Earth Surface Processes 3: 331-344, 1978.

Anderson, S.P., W.E. Dietrich, D.R. Montgomery, R. Torres, M.E. Conrad, and K. Loague, Subsurface flow paths in a steep, unchanneled catchment, Water Resources Research 33(12): 2637-2653, 1997.

Anderson, S.P., and W.E. Dietrich, Chemical weathering and runoff chemistry in a steep headwater catchment, Hydrological Processes 15: 1791-1815, 2001.

Asano, Y., T. Uchida, and N. Ohte, Residence times and flow paths of water in steep unchanneld catchments, Tanakami, Japan, Journal of Hydrology 261: 173-192, 2002.

Atkinson, T. C. Techniques for measuring subsurface flow on hillslopes, in: Hillslope hydrology, edited by Kirkby, M. J., John Wiley and Sons Inc., New York: 73-120, 1978.

Bevan, B., Electromagnetics for mapping buried earth features, Journal of Field Archeology 10: 47-54, 1983.

Beven, K.J., Uniqueness of place and process representations in hydrological modeling, Hydrology and Earth System Science 5: 1-12, 2001.

Bond, B., Hydrology and ecology meet—and the meeting is good, Hydrological Processes 17: 2087–2089, 2003.

Bonell, M., Progress in the understanding of runoff generation dynamics in forests, Journal of Hydrology 150: 217-275, 1993.

Bonell, M., Selected challenges in runoff generation research in forests from the hillslope to headwater drainage basin scale, Journal of the American Water Resources Association 34(4): 765-785, 1998.

Bork, E.W., N.E. West, J.A. Doolittle, and J.L. Boettinger, Soil depth assessment of sagebrush grazing treatments using electromagnetic induction, Journal of Range Management 51(4): 469-474, 1998.

Burns, D. A., R.P. Hooper, J.J. McDonnell, J.E. Freer, C. Kendall and K. Beven, Base cation concentrations in subsurface flow from a forested hillslope: The role of flushing frequency, Water Resources Research 34(12): 3535-3544, 1998.

Burns, D.A., J. J. McDonnell, R.P. Hooper, N.E. Peters, J.E. Freer, C. Kendall, and K. Beven, Quantifying contributions to storm runoff through end-member mixing analysis and hydrologic measurements at the Panola Mountain Research Watershed (Georgia, USA), Hydrological Processes 15: 1903-1924, 2001.

Burns, D.A., L.N. Plummer, J.J. McDonnell, E. Busenberg, G.C. Casile, C. Kendall, R.P. Hooper, J.E. Freer, N.E. Peters, K. Beven and P. Schlosser, The Geochemical evolution of riparian groundwater in a forested Piedmont catchment, Groundwater 41(7): 913-925, 2003.

Burt, T. P., and D.P. Butcher, Topographic controls of soil moisture distributions, Journal of Soil Science 36: 469-486, 1985.

Burt, T.P.; Park S.J., The distribution of solute processes on an acid hillslope and the delivery of solutes to a stream: I. Exchangeable bases, Earth Surface Processes and Landforms 24(9): 781-797, 1999.

Buttle, J. M., and D.S. Turcotte, Runoff processes on a forested slope on the Canadian Shield, Nordic Hydrology 30: 1-20, 1999.

Cappellato, R., N.E. Peters, and H.L. Ragsdale, Acidic atmospheric deposition and canopy interactions of adjacent deciduous and coniferous forests in the Georgia Piedmont, Canadian Journal of Forest Research 23: 1114-1124, 1993.

Carter, M.E.B., A community analysis of the Piedmont deciduous forest of Panola Mountain State Conservation Park: Atlanta, Georgia, M. S. thesis, 126 pp., Emory Univ., Atlanta, Ga., 1978.

Crawford T.J., M.W. Higgins, R.F. Crawford, R.L. Atkins, J.H. Medlin and T.W. Stern, Revision of stratigraphic nomenclature in the Atlanta, Athens, and Cartersville 30 ð 60 quadrangles, Georgia. Georgia Geologic Survey Bulletin B-130: Atlanta, Georgia; 48, 1999.

Creed, I.F., L.E. Band, N.W. Foster, I.K. Morrison, J.A., Nicolson, R.S. Semkin, and D.S. Jeffries, Regulation of nitrate-N release from temperate forests: A test of the N flushing hypothesis, Water Resources Research 32(11): 3337-3354, 1996.

Daniels, R.B., and R.D. Hammer, Soil Geomorphology, John Wiley and Sons Inc., New York, 236 p., 1992.

Darboux, F., Ph. Davy and C. Gascuel-Odoux, Effect of depression storage capacity on overland low generation for rough horizontal surfaces: water transfer distance and scaling, Earth Surface Processes and Landforms 27: 177-191, 2002.

Darboux, F., Ph. Davy, C. Gascuel-Odoux and C. Huang, Evolution of soil surface roughness and flowpath connectivity in overland flow experiments, Catena 46: 125-139, 2001.

Doolittle, J.A., M. Petersen, and T. Wheeler, Comparison of two electromagnetic induction tools in salinity appraisals, Journal of Soil and Water Conservation 56: 257-262, 2001.

Doolittle, J.A., S.J. Indorante, D.K. Potter, S.G. Hefner, and W.M. McCauley, Comparing three geophysical tools for locating sand blows in alluvial soils of southeast Missouri, Journal of Soil and Water Conservation 57: 175-182, 2002.

Dunne, T., and R.D. Black, An experimental investigation of runoff production in permeable soils, Water Resources Research 6: 478-490, 1970.

Dunne, T., W. Zhang, and B. F. Aubry, Effects of rainfall intensity, vegetation, and microtopography on infiltration and runoff; Water Resources Research 27 (9): 2271-2285, 1991.

Dunne, T., K.X Whipple, and B.F. Aubry, Microtopography of hillslopes and the initiation of channels by Horton overland flow, In: Evolving Concepts in Fluvial Geomorphology, edited by: Costa J.E., A.J. Miller, K.W. Potter, P.R. Wilcock, American Geophysical Union, Geophysical Monograph, 27-44, 1995.

Famiglietti, J.S., J.W. Rudnicki, and M. Rodell, Variability in surface moisture content along a hillslope transect: Rattlesnake Hill, Texas, Journal of Hydrology 210 (1-4): 259-281, 1998.

Freer, J., J. McDonnell, K.J. Beven, D. Brammer, D. Burns, R.P. Hooper, and C. Kendal, Topographic controls on subsurface stormflow at the hillslope scale for two hydrologically distinct small catchments, Hydrological Processes 11: 1347-1352, 1997.

Freer, J.E., J.J. McDonnell, K.J. Beven, D. Brammer, D.A. Burns, R.P. Hooper, and C. Kendal, Topographic controls on subsurface stormflow at the hillslope scale for two hydrologically distinct small catchments, Hydrological Processes 11(9): 1347-1352, 1997.

Freer, J.E., J.J. McDonnell, K.J. Beven, N.E. Peters, D.A. Burns, R.P. Hooper, B.T. Aulenbach, and C. Kendall, The role of bedrock topography on subsurface stormflow, Water Resources Research, 10.1029/2001WR000872, 2002.

Freeze, R.A., and J.A. Cherry, Groundwater, Prentice Hall, New-York, 604 p., 1979.

Granier A., Evaluation of transpiration in a Douglas-fir stand by means of sapflow measurements, Tree Physiology 3: 309–320, 1987.

Granier A., Une nouvelle methode pour la mesure de flux de seve brute dans le tronc des arbres, Annales des Sciences Forestieres 42: 193–200, 1985.

Grayson, R., A.W. Western, and F.H.S. Chiew, Preferred states in spatial soil moisture patterns: Local and nonlocal controls, Water Resources Research 33(12): 2897-2908, 1997.

Grayson, R., and G.Blöschl, Spatial patterns in catchment hydrology: Observations and modeling, Cambridge University Press, Cambridge, 404 p. 2001.

Green, W.H., and G.A. Ampt, Studies on soil physics: I Flow of air and water through soils, Journal of Agricultural Science 4:1-24, 1911.

Guebert, M.D., and T.W. Gardner, Macropore flow on a reclaimed surface mine: infiltration and hillslope hydrology, Geomorphology 39: 151-169, 2001.

Hanson, B.R., and K. Kaita, Response of Electromagnetic Conductivity Meter to soil salinity and soil-water content, Journal of irrigation and Drainage Engineering 123(2): 141-143, 1997.

Hargreaves, G.H., Moisture availability and crop production, Trans. Am. Soc. Agric. Eng. 18(5): 980-984, 1975.

Hauck, C., M. Gugliemin, K. Isaksen, and D. Vonder Muhl, Application of frequency-domain and time-domain electromagnetic methods for mountain permafrost studies, Permafrost and Periglacial Processes 12: 39-52, 2001.

Hendrickx, J.N.H., B. Baerends, Z.I. Raza, M. Sadig, and M. Akram Chaudhry, Soil Salinity Assessment by Electromagnetic Induction of Irrigated Land, Soil Science Society of America Journal 56: 1933-1941, 1992.

Hill, A.R., W.A. Kemp, J.M. Buttle, and D. Goodyear, Nitrogen chemistry of subsurface storm runoff on forested Canadian Shield hillslopes, Water Resources Research 35(3): 811-821, 1999.

Hjerdt, K.N., J. J. McDonnell, J. Seibert, and A. Rodhe, A new topographic index to quantifiy downslope controls on local drainage. Water Resources Research, in review.

Holmes, J.W., Calibration and field use of the neutron scattering method of measuring soil water content, Australian Journal of Applied Science 7: 45-58, 1956.

Hooper R.P., N. Christopherson and N.E. Peters, Modelling streamwater chemistry as a mixture of soilwater end-members: an application to the Panola Mountain catchment, Georgia, U.S.A. Journal of Hydrology 116: 321-343, 1990.

Hooper, R.P., B.T. Aulenbach, D.A. Burns, J.J. McDonnell, J.E. Freer, C. Kendall, and K.J. Beven, Riparian control of stream-water chemistry: implications for hydrochemical basin models, in Hydrology, Water resources and Ecology in Headwaters, Proceedings of the HeadWater '98 conference held at Meran/Merano, Italy 1998, IAHS publication 248: 451-458, 1998.

Hornberger, G.M., J.P. Raffensperger, P.L. Wiberg, and K.N. Eshleman, Elements of physical hydrology, The John Hopkins University Press Ltd., London, 303 p., 1998.

Huntington, T.G., R.P. Hooper, N.E. Peters, T.D. Bullen, and C. Kendall, Water, energy, and biogeochemical budgets investigation at Panola Mountain Research Watershed, Stockbridge, Georgia—A research plan, U.S. Geological Survey Open File Report, 93–55, 39 pp., 1993.

Huntington, T. G., R. P. Hooper, C. E. Johnson, B. T. Aulenbach, R. Cappellato, and A. E. Blum, Calcium Depletion in a Southeastern United States Forest Ecosystem, Soil Science Society of America Journal 64:1845–1858, (2000).

Hupet, F., and M. Vanclooster, Interseasonal dynamics of soil moisture variability within a small agricultural maize cropped field, Journal of Hydrology 261: 86-101, 2002.

Hutchinson, D.G., and R.D. Moore, Throughflow variability on a forested hillslope underlain by compacted glacial till, Hydrological Processes 14(10): 1751-1766, 2000.

Iverson R.M., Landslide triggering by rain infiltration, Water Resources Research 36(7): 1897-1910, 2000.

Jones, S.B., J.M. Wraith, and D. Or, Time domain reflectometry measurement principles and applications, Hydrological Processes 16: 141–153, 2002.

Kachanoski, R.G., E.G. Gregorich, and I.J. van Wesenbeeck, Estimating spatial variations of soil water content using nononcontacting electromagnetic inductive methods, Canadian Journal of Soil Science 68:715-722, 1988.

Kachanoski, R.G., E. de Jong, and J. van Wesenbeeck, Field scale patterns of soil water storage from non-contacting measurements of bulk electrical conductivity, Canadian Journal of Soil Science 70: 527-541, 1990.

Kirkby, M. J., Hydrograph modelling strategies, in: Process in Physical and Human Geography, edited by R. Peel, M. Chisholm, and P. Haggett, Heinemann, Oxford, England: 69–90, 1975.

Kirkby, M.J., Hillslope hydrology, John Wiley and Sons Inc., New York, 389 p. 1978.

Kundzewicz, Z.W., Ecohydrology-seeking consensus on interpretation of the notion, Hydrological Sciences Journal 47(5): 799-807, 2002.

Lakshmi, V., The role of satellite remote sensing in the Prediction of Ungauged Basins, Hydrological Processes 18: 1029-1034, 2004.

McDonnell, J.J., A rationale for old water discharge through macropores in a steep, humid catchment, Water Resources Research 26(11): 2821-2832, 1990.

McDonnell, J.J., J.E. Freer, R.P. Hooper, C. Kendall, D.A. Burns, K.J. Beven, and N.E. Peters, New method developed for studying flow in hillslopes, EOS, Transactions of the American Geophysical Union 77(47): 465, 1996

McDonnell, J.J., Comment on "the changing spatial variability of subsurface flow across a hillside" by Ross Woods and Lindsay Rowe, Journal of Hydrology, New Zealand 36(1): 97-100, 1997.

McDonnell, J.J., D. Brammer, C. Kendall, N. Hjerdt, L. Rowe, M. Stewart, and R. Woods, Flow pathways on steep forested hillslopes: The tracer, tensiometer and trough approach, in Environmental Forest Science, M. Tani, editor, Kluwer Academic Publishers, 463-474, 1998.

McDonnell, J.J., and T. Tanaka, On the future of forest hydrology and biogeochemistry, Hydrological Processes 15: 2053-2055, 2001.

McGlynn, B., J.J. McDonnell, and D. Brammer, A review of the evolving perceptual model of hillslope flowpathsat the Maimai catchment, New Zealand. Journal of Hydrology 257: 1-26, 2002.

McIntosh, J., J.J. McDonnell and N.E. Peters, Tracer and hydrometric study of preferential flow in large undisturbed soil cores from the Georgia Piedmont, USA, Hydrological Processes 13: 139-155, 1999.

McNeill, J.D., Electrical conductivity of soils and rocks, Technical Note TN-5, Geonics Ltd. Mississauga, Ontario, 22p, 1980.

Meyles, E., A. Williams, L. Ternan, and J. Dowd, Runoff generation in relation to soil moisture patterns in a small Dartmoor catchment, Southwest England, Hydrological Processes 17: 251-264, 2003.

Montgomery D.R.; Dietrich W.E.; Heffner J.T., Piezometric response in shallow bedrock at CB1: Implications for runoff generation and landsliding, Water Resources Research 38(12): 101-1018, 2002.

Mosley, M.P., Streamflow generation in a forested watershed, Water Resources Research 15: 795-806, 1979.

Mosley, M.P., Subsurface flow velocities through selected forest soils, South Island, New Zealand, Journal of Hydrology 55: 65-92, 1982.

National Oceanic and Atmospheric Administration, Local climatological data, annual summary with comparative data, 1990, Atlanta, Georgia, 6 pp., Asheville, N. C., 1991.

Noguchi, S., Y. Tsuboyama, R.C. Sidle, and I. Hosoda, Subsurface runoff characteristics from a forest hillslope soil profile including macropores, Hitachi Ohta, Japan, Hydrological Processes 15: 2131-2149, 2001.

Nuttle, W.K., Eco-hydrology's past and future in focus, EOS 83(19): 205,211-212, 2002.

Nyberg, L., Spatial variability of soil water content in the covered catchment at Gardsjon, Sweden, Hydrological Processes 10: 89-103, 1996.

Onda, Y., Y. Komatsu, M. Tsujimora, and J. Fujihara, The role of subsurface flow runoff through bedrock on storm flow generation, Hydrological Processes 15: 1693-1706, 2001.

Oren, R., and D.E. Pataki, Transpiration in response to variation in microclimate and soil moisture in southeastern deciduous forests, Oecologia 127: 549-559, 2001.

Pataki D.E., and R. Oren, Species differences in stomatal control of water loss at the canopy scale in a mature bottomland deciduous forest, Advances in Water Resources 26 (12): 1267-1278, 2003.

Peters, D.L., J.M. Buttle, C.H. Taylor, and B.D. LaZerte, Runoff production in a forested, shallow soil, Canadian Shield basin, Water Resources Research 31(5): 1291-1304, 1995.

Peters, N.E., and E.B. Ratcliffe, Tracing hydrologic pathways using chloride at the Panola Mountain Research Watershed, Georgia, USA. Water, Air and Soil Pollution 105(1/2): 263-275, 1998.

Peters, N.E., R.P. Hooper, T.G. Huntington, and B.T. Aulenbach, Panola Mountain, Georgia—a water, energy, and biogeochemical budgets program site, U.S. Geological Survey Fact Sheet 162-99(4), 2000.

Peters, N.E., J.E. Freer, and B.T. Aulenbach, Hydrologic dynamics of the Panola Mountain Research Watershed, Georgia, Groundwater 41(7): 973-988, 2003.

Phillips N., B.J. Bond, N.G. McDowell, and M.G. Ryan, Canopy and hydraulic conductance in young, mature, and old Douglas-fir trees, Tree Physiology 22: 205–212, 2002.

Porporato, A., and I. Rodriquez-Iturbe, Ecohydrology-a challenging multidisciplinary research perspective, Hydrological Sciences Journal 47(5): 811-821, 2002.

Quinn, P.F., K. Beven, P. Chevallier, and O. Planchon, The prediction of hillslope flow paths for distributed modelling using digital terrain models, Hydrological Processes 5: 59–79, 1991.

Robinson, D.A., I. Lebron, S.M. Lesch, and P. Shouse, Minimizing Drift in Electrical Conductivity Measurements in High Temperature Environments using the EM-38, Soil Science Society of America Journal 68: 339-345, 2004.

Rodriguez-Iturbe, I., Eco-hydrology: A hydrologic perspective of climate-soil-vegetation dynamics, Water Resources Research 36(1): 3-9, 2000.

Roy, A., and A. Apparao, Depth of investigation in direct current methods, Geophysics 36: 943-959, 1971.

Schume, H., G. Jost, and K. Katzensteiner, Spatio-temporal analysis of the soil water content in a mixed Norway spruce (*Picea abies* (L.) Karst.)-European beech (*Fagus sylvatica* L.) stand, Geoderma 112(3-4): 273-287, 2003.

Shanley, J.B., and N.E. Peters, Preliminary observations of streamflow generation during storms in a forested Piedmont watershed using temperature as a tracer, Journal of Contaminant Hydrology 3: 349-365, 1988.

Sheets K.R., and J.M.H. Hendrickx, Noninvasive soil water content measurement using electromagnetic induction, Water Resources Research 31(10): 2401-2409, 1995.

Sherlock, M. D., and J. J. McDonnell, Spatially distributed groundwater level and soil water content measured using electromagnetic induction, Hydrological Processes 17(10): 1965-1978, 2003.

Sidle, R. Shallow groundwater fluctuations in unstable hillslopes of coastal Alaska, Zeitschrift fur Gletscherkunde und Glazialgeologie 20: 79-95, 1984.

Šimůnek, J., M. Sejna and M.Th. van Genuchten, The Hydrus-2d software package for simulating two-dimensional movement of water, heat and multiple solutes in

variably saturated media. Version 2.0, IGWMC – TPS-53, International Groundwater Modeling Center, Colorado School of Mines, Golden, Colerado, 1999.

Sivapalan, M., Process complexity at hillslope scale, process simplicity at the watershed scale: is there a connection?, Hydrological Processes 17: 1037–1041, 2003.

Sklash, M.G., M.K. Stewart, and A.J. Pearce, Storm runoff generation in humid headwater catchments: A case study of hillslope and low-order stream response, Water Resources Research 22(8): 1273-1282, 1986.

Sklash, M.G., K.J. Beven, and K. Gilman, Isotope studies of pipe flow at Plynlimon, Wales, UK, Hydrological Processes 10(7): 921-944, 1996.

Slavich, P.G., and G.H. Petterson, Estimating average rootzone salinity from electromagnetic induction (EM-38) measurements, Australian Journal of Soil Research 16: 574-582, 1980.

Stewart, M.K., and J.J. McDonnell, Modeling baseflow soil water residence times from deuterium concentrations, Water Resources Research 27(10): 2681-2694, 1991.

Sudduth, K.A., S.T. Drummond, and N.R. Kitchen, Accuracy issues in electromagnetic induction sensing of soil electrical conductivity for precision agriculture, Computers and Electronics in Agriculture 31(3): 239-264, 2001.

Sweeney, J.J., Comparison of electrical resistivity methods for investigation of groundwater conditions at a landfill site, Groundwater Monitoring Review 4: 52-59, 1984.

Tani, M., Runoff generation processes estimated from hydrological observations on a steep forested hillslope with a thin soil layer, Journal of Hydrology 200: 84-109, 1997.

Topp, G.C., J.L. Davis, and A.P. Annan, Electromagnetic determination of soil water content: Measurements in coaxial transmission lines, Water Resources Research 16: 574-582, 1980.

Topp, G.C., State of the art of measuring soil water content, Hydrological Processes 17: 2993-2996, 2003.

Torres, R., W.E. Dietrich, D.R. Montgomery, S.P. Anderson and K. Logue, Unsaturated zone processes and the hydrologic response of a steep, unchanneled catchment, Water Resources Research 34(8): 1865-1879, 1998.

Tromp-van Meerveld, H.J., M. Weiler and J.J. McDonnell, Modeling the influence of subsurface topography on the spatial and temporal variability of subsurface stormflow at the hillslope scale and streamflow at the catchment scale, European Geophysical Society, (Abstract EGU04-A-06473), 2004.

Uchida, T., K. Kosugi, and T. Mizuyama, Runoff characteristics of pipe flow and effects of pipe flow on rainfall-runoff phenomena in a mountainous watershed, Journal of Hydrology 222(1): 18-36, 1999.

Uchida, T., K. Kosugi, and T. Mizuyama, Effects of pipe flow and bedrock groundwater on runoff generation in a steep headwater catchment in Ashiu, central Japan, Water Resources Research, 10.1029/2001WR000361, 2002.

Uchida,T., Y. Asano, N. Ohte and T. Mizuyama, Seepage area and rate of bedrock groundwater discharge at a granitic unchanneled hillslope, Water Resources Research 39(1): 1018, Doi:10.1029/2002wr001298, 2003.

van Verseveld, W.J., H.J. Tromp-van Meerveld, M. Weiler and J.J. McDonnell, Modeling the influence of subsurface topography on spatial and temporal variability of subsurface stormflow. Eos Trans. AGU, 84(46), Fall Meet. Suppl., Abstract H42D-1112. 2003.

Ward, R.C., and M. Robinson, Principles of hydrology, McGraw-Hill Publishing Company, 450 p., 2000.

Welsch, D.L., C.N. Kroll, J.J. McDonnell, and D.A. Burns, Topographic controls on the chemistry of subsurface stormflow, Hydrological processes 15: 1925-1938, 2001.

Western, A. W., and R.B. Grayson, The Tarrawarra data set: Soil moisture patterns, soil characteristics, and hydrological flux measurements, Water Resources Research 34(10): 2765-2768, 1998.

Western, A. W., R.B. Grayson, G. Bloschl, G.R. Willgoose, and T.A. McMahon, Observed spatial organization of soil moisture and its relation to terrain indices, Water Resources Research 35(3): 797-810, 1999.

Western, A.W., S.-L. Zhou, R.B. Grayson, T.A. McMahon, G. Blöschl, and D.J. Wilson, Spatial correlation of soil moisture in small catchments and its relationship to dominant spatial hydrological processes, Journal of Hydrology 286 (1-4): 113-134, 2004.

Weyman, D.R., Measurement of the downslope flow in a soil, Journal of Hydrology 20: 267-288, 1973.

Whipkey, R.Z., Subsurface stormflow from forested slopes, Bull. Int. Assoc. Sci. Hydrol. 2: 74-85, 1965.

White, A.F., T.D. Dullen, M.J. Schulz, A.E. Blum, T.G. Huntington and N.E. Peters, Differential rates of feldspar weathering in granitic regoliths, Geochimica et Cosmochimica Acta 65(6): 847-869, 2001.

White, A.F., A.E. Blum, M.S. Schulz, T.G. Huntington, N.E. Peters, and D.A. Stonestrom, Chemical weathering of the Panola Granite: Solute and regolith elemental fluxes and the weathering rate of biotite, in: Hellmann, R., and S.A. Wood (ed.), Water-Rock interactions, Ore deposits, and Environmental Chemistry: A tribute to David A. Crerar, The Geochemical Society, Special Publication 7: 37-59, 2002.

Wigmosta, M.S., L. Vail, and D. P. Lettenmaier, A distributed hydrology-vegetation model for complex terrain, Water Resources Research 30: 1665-1679, 1994.

Wilson, G. V., P.M. Jardine, R.J. Luxmoore and J.R. Jones, Hydrology of a forested hillslope during storm events, Geoderma 46: 119-138, 1990.

Wilson, K.B., P. J. Hanson, and D.D. Baldocchi, Factors controlling evaporation and energy partitioning beneath a deciduous forest over an annual cycle, Agricultural and Forest Meteorology 102 (2-3): 83-103, 2000.

Wilson, D.J., A.W. Western, R.B. Grayson, A.A. Berg, M.S. Lear, M. Rodell, J.S. Famiglietti, R.A. Woods, and T.A. McMahon, Spatial distribution of soil moisture

over 6 and 30 cm depth, Mahurangi river catchment, New Zealand, Journal of Hydrology 276: 254-274, 2003.

Woods, R., and L. Rowe, The changing spatial variability of subsurface flow across a hillside, Journal of Hydrology (NZ) 35(1): 51-86, 1996.

Yeakley, J. A., W.T. Swank, L.W. Swift, G.M. Hornberger, and H.H. Shugart, Soil moisture gradients and controls on a southern Appalachian hillslope from drought through recharge, Hydrology and Earth System Sciences 2(1): 41-49, 1998.

Yu, C., W. Warrick, and M.H. Conklin, Derived functions of time domain reflectometry for soil moisture measurement, Water Resources Research 35(6): 1789-1796, 1999.

Appendices

Appendix 1: The role of variations in soil depth and bedrock micro-topography on subsurface stormflow: a virtual experiment approach

A1.1 Introduction

Lateral subsurface flow is a dominant runoff producing mechanism in many upland environments around the world (Bonell, 1998). One of the most common prerequisites for subsurface stormflow production is the development of saturation (often quite transient) at the soil-bedrock interface during events. The spatial distribution of subsurface flow is highly correlated to the accumulated area based on the bedrock topography, with sections with deepest soils (highest bedrock accumulated area) delivering most of the water (McDonnell et al., 1996; Freer et al., 1997 and 2002). Subsurface flow can also be highly non-linear (Chapter 2). There is a 55 mm precipitation threshold for significant (>1 mm) subsurface flow to occur at the Panola trenched hillslope, Georgia (Chapter 2). For rain storms smaller than 55 mm, storm total subsurface flow is almost two-orders of magnitude smaller than for storms larger than 55 mm. While threshold behavior has been shown for other sites as well (e.g. Peters et al., 1995; Tani, 1997; Noguchi et al., 2001) a clear process understanding for what is responsible for threshold behavior at the hillslope sale is lacking.

Physical (trenches, tensiometers, and wells), chemical (conservative and non-conservative solutes and nutrients), and isotopic (^{18}O and deuterium) measurements, and particular the combination of these measurements, have been very important for defining the subsurface storm flow process. However, these measurements are limited by our technological capabilities. In addition, most measurements are only at the point scale. Recent work has shown the merit of virtual experiments (Weiler and McDonnell, 2004; Cloke et al., in review). Virtual experiments are numerical experiments driven by field derived understanding in which the responses of models to varying internal states and boundary conditions provide the basis for inferences about controlling processes. One area where virtual experiments can be important is in visualizing parts of the hillslope that we cannot measure, see or conceptualize. In the case of subsurface stormflow produced via transient saturation at the soil-bedrock interface a virtual experiment approach can be very helpful for illuminating the hillslope black box. The soil-bedrock

interface is a hotspot for transient saturation, lateral flow and weathering and yet is the least well described zone on the hillslope. We used a 2-dimensional finite element model (HYDRUS-2D, Šimůnek et al., 1999) to 'see into' the soil-bedrock interface. HYDRUS-2D and earlier versions (SWMS_2D, Šimůnek et al., 1992) have been used successfully for modeling hillslope scale hydrological processes (e.g. Ritsema et al., 1996a and 1996b). Here we examine the role of bedrock topography in hillslope threshold behavior and investigate numerically the role of bedrock topography on lateral subsurface flow initiation and subsurface flow generation. Our objectives are to:

- Test if HYDRUS-2D can reproduce internal state and lateral outflow based on realistic soil data
- Examine the effects of the micro-topography of the soil-bedrock contact on watertable development and connectivity and its relation to hillslope-scale subsurface flow generation
- Understand how processes internal in the hillslope manifest themselves as thresholds at the slope base

While we do not expect the 2-dimensional model to be absolutely right and to include all the complex flow processes at our site, we do assume that if the model can reasonably reproduce observed subsurface flow at the trench and pore pressure response internal to the hillslope, then the model is 'right enough' to visualize the importance of the bedrock micro-topography and variations in soil depth on lateral subsurface flow generation. This is in keeping with the philosophy outlined in Loague and VanderKwaak (in press) where 'the aim of a model is, of course, not to reproduce reality in all its complexity but rather to capture in a vivid way what is essential to understanding some aspect of its behavior'. The model results could then be tested through measurements in the field.

A1.2 Study Site

The study hillslope is located in the Panola Mountain Research Watershed (PMRW), located 25 km southeast of Atlanta, Georgia, USA. The watershed contains a naturally regenerated second-growth forest. The catchment is 90% forested, dominated by hickory, oak, tulip poplar, and loblolly pine, and 10% partially vegetated (lichens and mosses) bedrock outcrops. The study hillslope is predominantly deciduous.

The basin relief is 56 m and slopes average 18°. The study hillslope is relatively planar and has an average slope of 13°. Soil depth on the study hillslope varies between 0 to 1.86 m, with an average of 0.63 m. The correlation length of soil depth on the study hillslope is 13 m. In general soils on the upper slope are thinner than soils on the lower slope. Soils on the study hillslope are described as light colored sandy loam soils with little textural differences. The upper 0.15 m layer is humus rich. The hillslope is underlain by the Panola Granite of granodiorite composition.

The climate is humid subtropical. Air temperature averages 15.2°C and the average monthly temperatures range from 5.5°C in January to 25.2°C in July. Annual precipitation averages 1240 mm and is distributed relatively uniformly throughout the year. During the spring and summer (April-September), rainstorms are convective (high intensity and short duration). During the remainder of the year, precipitation is dominated by synoptic weather systems (low intensity and long duration). Streamflow has a strong seasonal pattern, with the highest flows occurring during the November through March dormant season. Annual stream yield from the 41-ha catchment varies from 8 to 50% of precipitation. Average runoff ratios from the hillslope for the 1996-1998 period are 6, 10, 1 and less than 1% for the fall, winter, spring and summer respectively (Chapter 2).

A1.3 Methods

A1.3.1 Field measurements

The field based conceptual model to run our virtual experiments comes from recently completed field projects (McDonnell et al., 1996; Freer et al., 1997 and 2002; Burns et al., 1998). The measurements described below come from these sources.

The hillslope was surveyed on a 2 m grid. Depth to bedrock was measured on the same survey grid network using a 25.4 mm soil corer forced vertically through the soil profile to refusal. A small hand auger was used when soil depth was greater than 1.25 m.

A 20-m long trench was excavated down to bedrock at a midslope position approximately 30 m upslope from an ephemeral stream. The trench was divided into ten 2-m wide sections and discharge from each 2-m trench section and from five individual soil pipes was measured by routing flow through tipping-bucket gages. The number of tips was recorded every minute. Additional details of the trench and the flow-collection system are described in McDonnell et al. (1996), Freer et al. (1997 and 2002) and Burns et al. (1998).

A grid of 44 co-located recording tensiometers was installed (shallow/deep pairs) primarily on the lower half of the hillslope. The tensiometers used Honeywell wet port pressure transducers with 1 bar high flow ceramic cups. The average depth of the shallow and deep tensiometers was 0.20 m and 0.62 m below the soil surface respectively. More information on the tensiometers is given in Freer et al. (2002).

A1.3.2 Model

HYDRUS-2D (Šimůnek et al., 1999) is a two-dimensional finite element model for simulating water, heat and multiple solutes in variable saturated porous media. The program can be used to analyze water and solute movement in unsaturated, partially

saturated, or fully saturated porous media. The program solves numerically the Richards' equation for saturated-unsaturated water flow and the Fickian-based advection-dispersion equation for heat and solute transport. Observation points can be added at any node in the flow domain. Especially important for this study is that HYDRUS-2D can describe flow regions delineated by irregular boundaries, and that the code can accommodate a seepage face boundary through which water leaves the saturated part of the flow domain.

We used the measured surface and bedrock topography on a 48 m long transect on the hillslope that represents the main flow path on the hillslope to generate the mesh. The average soil depth of the transect was 0.61 m. The average soil depth of the lower 12 m of the transect was 0.75 m while the average soil depth of the upper 12 m of the transect was 0.27 m. The trench face was represented by a 'seepage face' boundary, the surface topography was represented by an 'atmospheric' boundary, the upper extent of the hillslope was represented by a 'zero-flux' boundary and the lower boundary was represented by a 'free drainage' boundary (Figure A1.1a). Observation nodes were added to the flow region at the approximate location of nine tensiometers.

The flow region was divided into five soil layers (Figure A1.1b). The top three layers represent the soil layers. The three soil layers were chosen to represent the observed decline in hydraulic conductivity and drainable porosity with depth at the study site. The lower boundary of the third soil layer represents the measured bedrock topography (and is represented by the light grey line in Figure A1.1a). The lower two layers were chosen to represent the bedrock and have a lower hydraulic conductivity and drainable porosity than the soil layers. The unsaturated soil hydraulic properties were described using the van Genuchten (1980) analytical function. All parameters for the three soil layers, except the saturated hydraulic conductivity, were estimated from the soil moisture release curves from soil cores from the hillslope. The saturated hydraulic conductivity of the soil layers and the parameters for the bedrock layers were determined by optimizing manually the observed and predicted subsurface flow for the March 6-7 1996 storm. The saturated conductivity was not allowed to vary outside a reasonable

range (10x) around the measured 0.64 m/hr vertical saturated conductivity in a large intact soil core extracted by McIntosh et al. (1999). These soil parameters were then used for all other model runs. The models were also run for a 49 mm storm on January 7 1998 to examine the effect of storm size on the results.

The March 6-7 1996 storm period to which the model was calibrated, consisted of a 49 mm storm on March 6 1996 and a 47 mm storm on March 7 1996. The maximum 1-hour rainfall intensity was 22 and 17 mm/hr for the March 6 and 7 1996 storm respectively. Less than 0.4 mm of subsurface flow was observed at the 20 m long trench during the March 6 1996 storm while 24 mm of subsurface flow was observed in response to the March 7 1996 storm. This storm was chosen for manual calibration of the model because of the complexity of the two events and because tensiometer data was available for this storm.

A1.4 Results

A1.4.1 March 6-7 1996 storm

HYDRUS-2D was able to reproduce both outflow (matrix flow) and internal pore pressures during the March 6-7 1996 storm (Figure A1.2). The model predicted the small volume of subsurface flow in response to the March 6 1996 storm and the larger volume of subsurface flow in response to the March 7 1996 storm. Modeled peak subsurface flow was delayed compared to observed peak subsurface flow, due mainly to a slower rise in modeled subsurface flow rate. The timing and magnitude of the pore pressure change during the events was also well represented (Figure A1.2b-e). HYDRUS-2D showed the wetting up and increased pore pressure during the March 6 1996 storm and positive pore pressure development during the March 7 1996 storm.

It is often assumed that lateral flow at the soil-bedrock interface will start with the initiation of localized saturation at the trench face and subsequent expansion of a saturated wedge upslope with increasing precipitation. However, positive pore pressures

and lateral flow along the soil-bedrock contact first developed on the upslope where soils are shallowest and the wetting front reached the soil-bedrock interface first (t=6, Figure A1.3). Lateral flow from the shallow upslope filled the small depressions in the bedrock topography until the water level in the depressions rose high enough for water to continue to flow downslope over the bedrock topography (t = 6-27, Figure A1.3). During the March 6 1996 storm, lateral flow occurred on the upper slope but did not reach the lower slope (t=6-24, Figure A1.3), resulting in only limited subsurface flow in response to the March 6 1996 storm. Once lateral flow occurred on the downslope, due to both locally infiltrating water and lateral subsurface flow from the upslope during the March 7 1996 storm (t=27-32, Figure A1.3), total subsurface flow increased (compare Figure A1.2 and Figure A1.3). At that point the area of positive pore pressures and lateral flow extended from the downslope boundary (trench) to the upslope such that connectivity between the lower slope and the upper slope was established and the whole hillslope contributed to subsurface flow.

After the storm, the soil and upper bedrock layers in the bedrock depressions (e.g. 6, 14 and 30 m upslope from the trench face) remained wetter than the remaining soil (Figure A1.4). Positive pore pressures were sustained in the bedrock depressions longer due to downslope impedance to drainage. In addition, the larger head in the depressions during the storm, compared to the head on the more planar hillslope sections, resulted in higher modeled infiltration rates into the bedrock in the bedrock depressions.

A1.4.2 Comparison of real and smooth bedrock topography

To determine the influence of soil depth variations on subsurface flow initiation and magnitude, we also ran the model with a smooth bedrock topography and uniform soil depth (0.61 m). Modeled subsurface flow for the transect with smooth bedrock and uniform soil depth was different from modeled subsurface flow for the mapped bedrock topography, especially for the median size (49 mm) storm (Figure A1.6a). Modeled subsurface flow response was faster compared to modeled subsurface flow for the

transect with the mapped topography (Figure A1.5a and A1.6a). Subsurface flow response to precipitation bursts during the median size storm was muted for the transect with the real bedrock topography compared to the transect with uniform soil depth and smooth bedrock topography. The development of lateral flow during the storm was very different from the development of lateral flow for the transect with the mapped bedrock topography (compare Figure A1.3 and A1.7). For the model with uniform soil depth, lateral flow started at the same time for each location on the hillslope because the wetting front reached the soil-bedrock interface at the same time because the soil depth and precipitation input were similar across the hillslope. Subsurface flow started earlier for the transect with uniform soil depth because lateral flow directly upslope from the trench started earlier because soil depth directly upslope from the trench was shallower for the transect with uniform soil depth (0.61 m) than the mapped soil depth (0.75 m for the lower 12 m of the hillslope).

We also ran the model for transects with the same average soil depth and smooth bedrock topography but with decreasing soil depth in the upslope direction. For one bedrock realization, soil depth at the downslope end of the transect was 1.5 times the average soil depth and soil depth on the upslope end was 0.5 times the average soil depth. For the other realization, soil depth at the downslope end was 1.25 times the average soil depth and the soil depth on the upslope end was 0.75 times the average soil depth. Modeled subsurface flow for these transects resembled modeled subsurface flow for the transect with mapped bedrock topography more than the model with uniform soil depth across the transect. Subsurface flow during the median size storm was muted for the transect with larger soil depth close to the trench, similar to modeled subsurface flow for the transect with the mapped bedrock topography (Figure A1.6a). Modeled peak subsurface flow rate and total subsurface flow for the transects with smooth bedrock topography and decreasing soil depth in the upslope direction were higher than modeled peak and total subsurface flow for the transect with the real bedrock topography because depression filling did not have to take place, i.e. less water was stored in bedrock pockets and more water could flow off the hillslope. In addition, less water infiltrated into the

bedrock because there were no bedrock depressions that facilitated locally increased infiltration into the bedrock.

We added a virtual non-reactive tracer to the precipitation to visualize the movement of event water into and through our study hillslope. The concentration of the virtual tracer in the hillslope prior to the storm was set to zero and the concentration of the virtual tracer in the precipitation was set to one. Modeled event-water contribution to subsurface flow was small (Figures A1.5d and A1.6d). This is in keeping with observed event water contributions to subsurface flow. The difference in observed $\delta^{18}O$ values between throughfall and soil water was less than 0.5‰ for the March 6-7 1996 storm, so an adequate hydrograph separation could not be obtained (Burns et al., 1998). During a 62 mm storm on February 2 1996, however little or no event water was present in subsurface flow (Burns et al., 1998). While the difference in subsurface flow or pore pressure for the two transects with smooth bedrock but decreasing soil depth in the upslope direction was small for the large March 6-7 1996 storm, the difference in event-water contribution for the two transects was larger (Figure A1.5d). There was a larger and earlier contribution of event water to total subsurface flow for transects with the least variation in soil depth, i.e. the shallowest soil depth directly upslope from the trench.

A1.4.3 Influence of bedrock roughness

To determine the influence of bedrock roughness on subsurface flow we also ran the model with transects of different bedrock roughness. For each location on the transect the new soil depth was calculated by multiplying the deviation of the local soil depth from the transect average soil depth by a roughness factor and adding this to the transect average soil depth (equation 1)

$$Depth_{(local\_new)} = Depth_{(average)} + \alpha\,(Depth_{(local)} - Depth_{(average)}) \qquad \textit{(Equation A1.1)}$$

where $Depth_{(local\_new)}$ is the new calculated soil depth for a location on the transect, $Depth_{(average)}$ is the average soil depth of the transect, α is the roughness factor (0.5, 1,5 and 2 in Figures A1.8 and A1.9) and $Depth_{(local)}$ is the measured soil depth at a location on the transect. When the calculated $Depth_{(local\_new)}$ was smaller than 0.02 m, $Depth_{(local\_new)}$ was set to 0.02 m.

Calculated subsurface flow, pore pressure at locations with average soil depth (8 and 24 m upslope) and tracer breakthrough were similar for the transects with different bedrock roughness for the large March 6-7 1996 storm (Figure A1.8). Peak subsurface flow and peak event-water concentration were delayed for the transect with the highest bedrock roughness (Figure A1.9a). For the median size storm subsurface flow response and tracer breakthrough were quite different Subsurface flow in response to the medium size event was most damped for the transect with the highest bedrock roughness. Event water concentrations, peak subsurface flow and rise in subsurface flow were smallest and slowest for the transects with the highest bedrock roughness. It appeared to be due to water being held up in the bedrock depressions and thus excluded from subsurface flow (Figure A1.9d). In addition, infiltration into the bedrock was larger in these depressions because the larger head of water in the depressions that increased infiltration rates into the bedrock. For the median size storm, modeled pore pressure at 8 m upslope from the trench showed a delayed second peak for the transects with the mapped bedrock topography or increased roughness (Figure A1.9c). The delayed second rise in pore pressure was not seen for transects with reduced bedrock roughness or smooth bedrock (Figures A1.6c and A1.9c). Comparison of lateral flow patterns during this storm suggests that the delayed second increase in pore pressure at 8 m upslope from the trench was due to delayed lateral flow from the upslope, i.e. water held up in depressions. Peak pore pressures during the median size storm at 24 m upslope from the trench were higher for the transect with real bedrock topography and the transect with increased bedrock roughness because of the simultaneous arrival of the local wetting front and the lateral flux from the upslope that spilled over the bedrock depression located 28 m upslope.

A1.4.4 Variations in soil depth and bedrock roughness in relation to observed threshold behavior

We modeled subsurface flow response to increasing precipitation for transects with the real bedrock topography, the smooth bedrock topography and uniform soil depth, the smooth bedrock topography with decreasing soil depth in the upslope direction such that soil depth on the downslope end of the hillslope transect was 0.5 times the hillslope average soil depth and soil depth on the upslope end of the transect was 1.5 times the hillslope average soil depth, and the transect with doubled bedrock roughness compared to the real bedrock topography. All four transects had the same transect average soil depth. The relation between total precipitation and total modeled subsurface flow did not show the sharp precipitation threshold for subsurface flow observed for this hillslope (Chapter 2) for neither of the transects (Figure A1.10). The relation between precipitation and total subsurface flow for the transect with the mapped bedrock topography resembled the observed threshold response most closely (Figure A1.10). The relation between precipitation and total subsurface flow for the transect with the smooth bedrock topography and uniform soil depth resembled least the observed precipitation threshold. For this transect subsurface flow increased more gradually (exponential) with increasing precipitation.

For the transect with the mapped bedrock topography and the transect with the doubled bedrock roughness, the relation between total precipitation and total subsurface flow appeared to consist of three domains: no subsurface flow for 0-30 mm precipitation, a linear but small increase in subsurface flow with increasing precipitation for 30-50 mm of precipitation, and a linear but larger increase in subsurface flow with increasing precipitation for storms larger than 50 mm. The small volume of subsurface flow for storms between 30-45 mm came from only a small area located directly upslope from the trench. For these storms, lateral flow from the upslope did not reach the trench. Thus only a small part of the hillslope contributed to subsurface flow, resulting in a limited subsurface flow total. For storms larger than 50 mm, lateral flow from the upslope reached the trench and the whole hillslope contributed to subsurface flow, thus resulting

in a larger increase in subsurface flow with increasing precipitation. For the transect with the mapped bedrock topography and the transect with the doubled bedrock roughness, the increase in subsurface flow with increasing precipitation after 50 mm of precipitation was 0.8 times the precipitation. This compares well with the observed increase in subsurface flow with increasing precipitation of 0.3-0.8 times the precipitation after the precipitation threshold (Chapter 2). The increase in subsurface flow with increasing precipitation was smallest for transects with rough bedrock topography because of increased losses to the bedrock due to increased infiltration in bedrock depressions where the head was largest (Figure A1.4).

A1.5 *Discussion*

A1.5.1 Role of bedrock micro-topography on subsurface flow

Our virtual experiments using HYDRUS-2D at the well studied Panola hillslope have revealed the hitherto unrecognized importance of variations in soil depth and the bedrock micro-topography on lateral subsurface stormflow. Soil depth and bedrock micro-topography also appear to be a first order control on rapidity of development of point-scale subsurface saturation development. The model results showed no saturated wedge development upslope from the trench face, as is often shown or assumed in field experiments (e.g. Whipkey, 1965; Weyman, 1973; Atkinson, 1978; Wilson et al., 1990; Buttle and Turcotte, 1999). The spatial distribution of lateral flow was very different for experiments with transects consisting of decreasing soil depth in the upslope direction and the transect with uniform soil depth (Figure A1.3 and A1.7). The difference in lateral flow development can have large effects on solute transport. Here we show the influence of bedrock topography on new-water contributions (Figure A1.5d and A1.6d). The influence of bedrock topography on total subsurface flow was larger during a median size storm than during a large storm (Figure A1.5a and A1.6a and also Figure A1.10). The main influence of the bedrock topography on subsurface flow was a result of the decrease in soil depth with upslope distance. The influence of bedrock roughness on modeled subsurface flow and event water contributions was smaller. In many catchments around

the world, soil depth decreases in an upslope direction. Thus it may be important to consider the effects of variations in soil depth and their directional trends on lateral subsurface flow.

The model results for the different transects showed a weak precipitation threshold. The model results for the transect with mapped bedrock topography or extra rough bedrock topography indicated that there were three subsurface flow responses to precipitation: no flow when total precipitation was less than 30 mm, limited subsurface flow when total storm precipitation was 30-50 mm and only a small part of the hillslope contributes to subsurface flow, and a large subsurface flow response when total precipitation was larger than 50 mm and the entire hillslope contributed to subsurface flow (Figure A1.10). Comparison of subsurface flow response for transects with different soil depth distribution and bedrock roughness indicated that a decrease in soil depth in the upslope direction and increased bedrock roughness together might be responsible for the observed sharp precipitation threshold and that precipitation thresholds are least likely to occur on sites with smooth bedrock and small variations in soil depth (open squares in Figure A1.10). In addition, the model results show that infiltration into the bedrock, facilitated by increased head in bedrock depressions, results in a smaller increase in subsurface flow with increasing precipitation after a threshold. For a model with impermeable bedrock, the increase in subsurface flow with increasing precipitation after a precipitation threshold was 1 (data not shown). This is similar to the relation between subsurface flow and precipitation after a threshold at Tatsunokuchi-yama on Honsyu Island, Japan (Tani, 1997). These model results thus suggest that the precipitation threshold depends on the soil depth variations, bedrock roughness, antecedent conditions and bedrock permeability at a site. Further more the slope of the relation between subsurface flow and precipitation after the precipitation threshold appears to be a function of bedrock permeability, and to a lesser degree, bedrock roughness.

Our virtual experiments also provide insight into the hydrologic connection between the soil and the underlying saprock/bedrock. Water content in the soil and in the

upper layers of the bedrock depressions remained higher after storms than at other locations on the hillslope due to impedance to downslope drainage and increased infiltration into the bedrock during storms due to the larger head in bedrock depressions (Figure A1.4). We hypothesize that chronic increased soil moisture at these locations could increase the weathering rates in the depressions. Deeper depressions collect more water, remain wetter for longer, increasing the potential for increased weathering, which in turn deepens the depressions further. Thus resulting in a self re-enforcing process of weathering and increased bedrock roughness. Increased bedrock roughness in turn increases infiltration into the bedrock and reduces total and peak subsurface storm flow.

A1.5.2 Limitations of a Richards equation based model

The good representation of (matrix) subsurface flow and pore pressures suggest that the model adequately represents the dominant subsurface flow processes at our site. Despite the fact that the model was only optimized to subsurface flow, the model also represented the small new-water contribution to subsurface flow well. While the model did not represent the sharp observed precipitation threshold very well, the overall resemblance to the observed relation between total storm precipitation and total subsurface flow also suggests that the model captures the internal physics of the problem.

One of the limitations of virtual experiments with a model based on the Richards equation is the exclusion of preferential flow processes in the soil. Pipe flow is an important component of total subsurface flow at this hillslope (Chapter 2). During the 1996-1998 period pipe flow from five individual soil pipes on the hillslope accounted for 42% of total subsurface flow (Chapter 2). Our virtual experiment was optimized to measured matrix subsurface flow only because fluxes calculated from pore pressure gradients (following calculations in Harr, 1977) represented the matrix flow fluxes well, but not the pipe flow fluxes (Figure A1.11). If pipe flow would have been included into the model, most likely the rise of modeled subsurface flow hydrograph would be faster, resembling the observed hydrograph more closely. Soil pipes, especially at the soil-

bedrock interface, could rapidly transmit water downslope. To allow for this rapid delivery of water in a model without soil pipes would require a large and unrealistic saturated conductivity of the soil layer at the soil-bedrock interface, which inhibits us to represent the internal hillslope response (e.g. pore pressure response) realistically.

One of the limitations of using a 2-dimensional model is the lack of a representation of 3-dimensional processes. The bedrock topography on the hillslope has a clear 3-dimensional drainage pattern (Freer et al., 2002), which would allow channeling of lateral flow over the bedrock to the main bedrock low (i.e. our selected flowpath slice). This 3-dimensional component of subsurface flow is not represented in the model.

A1.6 Conclusions

Virtual experiments using HYDRUS-2D at the well studied Panola hillslope have provided new insights into the soil-bedrock interface and its importance on subsurface flow generation. Soil depth variations have a large influence of lateral flow generation. Our virtual experiments have shown the importance of lateral flow over the bedrock on the shallower upslope slope positions and the lack of connected lateral flow on the deeper, lower slope during small-medium storms (<50 mm). The model results for the transects with real bedrock topography show that subsurface flow during median size storms (30-50 mm) is derived from only a small part on the lower hillslope. These results also show that after 50 mm of precipitation, lateral flow from the shallower upslope reaches the trench face such that the whole hillslope contributes to subsurface flow. This results in a larger increase in subsurface flow with increasing precipitation for storms larger than 50 mm. This could be a process explanation for the observed precipitation threshold for subsurface flow.

Finally model configuration decisions can determine the presence or absence of particular hillslope flow processes and, the magnitude and direction of flux (Cloke et al., 2003). If these consequences are not fully explored for any given scheme and application,

the resulting process inference may well be misleading (Cloke et al., 2003). Our virtual experiments show the potential error and misleading results involved in using smooth bedrock topography with a uniform (average) soil depth in a model when no soil depth information is available but soil depth on the real hillslope decreases with upslope distance. If a smooth bedrock topography and average soil depth are used in the model, the filling and spilling of water in and over bedrock depressions is ignored and the distribution of lateral flow is misrepresented, even though it might still be possible to re-produce the subsurface flow hydrograph with changed soil parameter values. The lack of representation of these important processes can have a large influence on modeled solute concentrations.

A1.7 Acknowledgements

We thank Brent Aulenbach for his help with data assembly and Jim Freer and Doug Burns for the initial trench construction efforts and the tensiometer data used. We would like to thank John Selker for use of the HYDRUS-2D software. This work was support by NSF grant EAR 0196381.

A1.8 References

Atkinson, T. C., Techniques for measuring subsurface flow on hillslopes, Hillslope hydrology, M. J. Kirkby Ed., Chichester, New-York, Wiley: 73-120, 1978.

Bonell, M., Selected challenges in runoff generation research in forests from the hillslope to headwater drainage basin scale, Journal of the American Water Resources Association 34(4): 765-785, 1998.

Burns, D. A., R.P. Hooper, J.J. McDonnell, J.E. Freer, C. Kendall and K. Beven, Base cation concentrations in subsurface flow from a forested hillslope: The role of flushing frequency, Water Resources Research 34(12): 3535-3544, 1998.

Buttle, J. M., and D.S. Turcotte, Runoff processes on a forested slope on the Canadian Shield, Nordic Hydrology 30: 1-20, 1999.

Cloke, H.L., J.P. Renaud, A.J. Claxton, J.J. McDonnell, M.G. Anderson, J.R. Blake and P.D. Bates, The effect of model configuration on modeled hillslope-riparian interactions. Journal of Hydrology 279: 167-181, 2003.

Cloke, H., M. Anderson, J.J. McDonnell and J. Renaud, Testing the capillary fringe groundwater ridging hypothesis of streamflow generation. Journal of Hydrology, in review.

Freer, J., J. McDonnell, K.J. Beven, D. Brammer, D. Burns, R.P. Hooper and C. Kendal, Topographic controls on subsurface stormflow at the hillslope scale for two hydrologically distinct small catchments, Hydrological Processes 11: 1347-1352, 1997.

Freer, J.E., J.J. McDonnell, K.J. Beven, N.E. Peters, D.A. Burns, R.P. Hooper, B.T. Aulenbach and C. Kendall, The role of bedrock topography on subsurface stormflow, 10.1029/2001WR000872, 2002.

Harr, R. D. Water flux in soil and subsoil on a steep forested slope, Journal of Hydrology 33: 37-58, 1977.

Loague, K., and J.E. VanderKwaak, Physics based hydrologic response simulation: Platinum bridge, 1958 Edsel, or useful tool, Hydrological Processes, in press.

McDonnell, J.J., J.E. Freer, R.P. Hooper, C. Kendall, D.A. Burns, K.J. Beven and N.E. Peters, New method developed for studying flow in hillslopes, EOS, Transactions of the American Geophysical Union 77(47): 465, 1996.

McIntosh, J., J.J. McDonnell and N.E. Peters, Tracer and hydrometric study of preferential flow in large undisturbed soil cores from the Georgia Piedmont, USA, Hydrological Processes, 13, 139-155, 1999.

Noguchi, S., Y. Tsuboyama, R.C. Sidle and I. Hosoda, Subsurface runoff characteristics from a forest hillslope soil profile including macropores, Hitachi Ohta, Japan, Hydrological Processes, 15, 2131-2149, 2001.

Peters, D.L., J.M. Buttle, C.H. Taylor, and B.D. LaZerte, Runoff production in a forested, shallow soil, Canadian Shield basin, Water Resources Research, 31(5), 1291-1304, 1995.

Ritsema, C.J., J. Stolte, K. Oostindie, E van den Elsen and P.M. van Dijk, Measuring and modelling of soil water dynamics and runoff generation in an agricultural loessial hillslope, Hydrological Processes 10: 1081-1089, 1996a.

Ritsema, C. J., K. Oostindie and J. Stolte, Evaluation of vertical and lateral flow through agricultural loessial hillslopes using a two-dimensional computer simulation model, Hydrological Processes 10: 1091-1105, 1996b.

Šimůnek, J., T. Vogel, and M.Th. van Genuchten, The SWMS_2D code for simulating water flow and solute transport in tow-dimensional variably saturated media, Version 1.1, Research Report 126, US Salinity Laboratory, Riverside, California, 169 p., 1992.

Šimůnek, J., M. Sejna, and M.Th. van Genuchten, The Hydrus-2d software package for simulating two-dimensional movement of water, heat and multiple solutes in variably saturated media. Version 2.0, IGWMC – TPS-53, International Groundwater Modeling Center, Colorado School of Mines, Golden, Colorado, 1999.

Tani, M., Runoff generation processes estimated from hydrological observations on a steep forested hillslope with a thin soil layer, Journal of Hydrology, 200, 84-109, 1997.

van Genuchten, M.Th., A closed-form equation for predicting the hydraulic conductivity of unsaturated soils, Soil Science Society of America Journal 44: 892-898, (1980).

Weiler, M. and J.J. McDonnell, Virtual experiments: A new approach for improving process conceptualization in hillslope hydrology. Journal of Hydrology, 285: 3-18, (2004).

Weyman, D.R., Measurement of the downslope flow in a soil, Journal of Hydrology 20: 267-288, 1973.

Whipkey, R.Z., Subsurface stormflow from forested slopes, Int. Ass. Sci. Hydrol. Bull. 10(2): 74-85, 1965.

Wilson, G.V., P.M. Jardine, R.J. Luxmoore and J.R. Jones, Hydrology of a forested hillslope during storm events, Geoderma 46: 119-138, 1990.

Figure A1.1 Schematic overview of the boundary conditions (a), and the distribution of the soil layers in the domain (b). The light grey line in Figure A1.1 represents the soil-bedrock interface. The transect follows the main (bedrock) flowpath on the hillslope. The vertical exaggeration is 1.5.

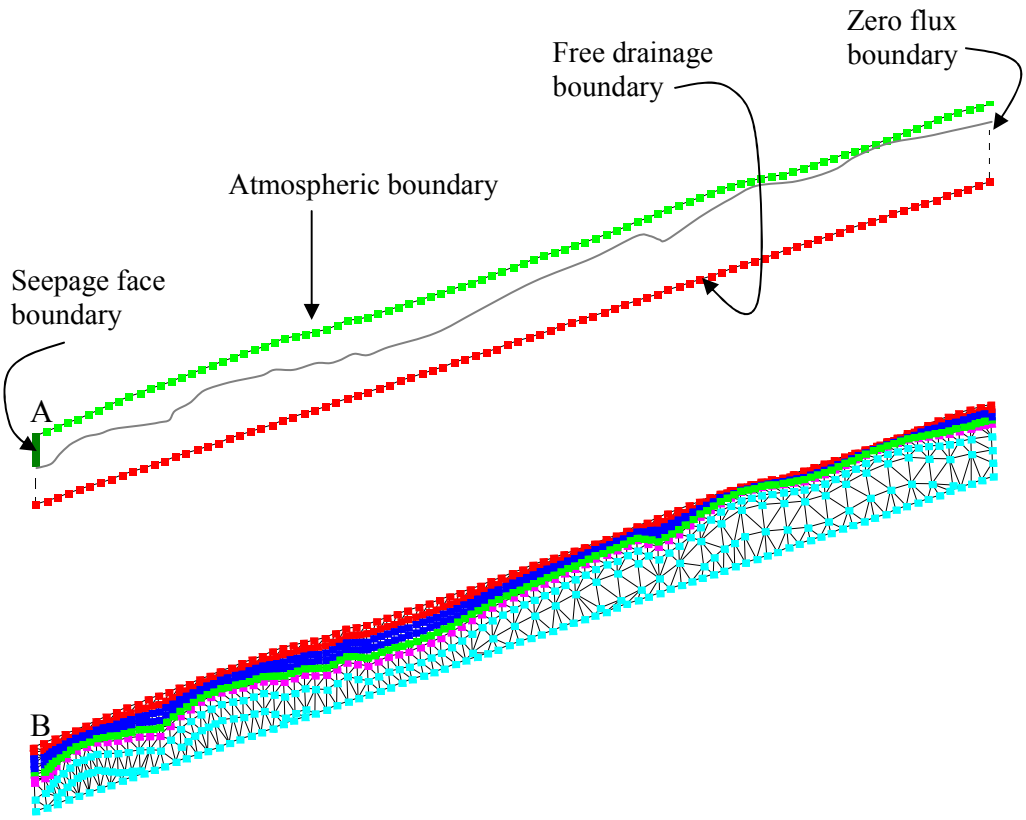

Figure A1.2 Observed and modeled (matrix) subsurface flow (a) and pore pressure in the deep tensiometers during the March 6-7 1996 storm (b-e). The light grey lines in Figure A1.1a represent the times shown in Figures A1.3 and A1.6.

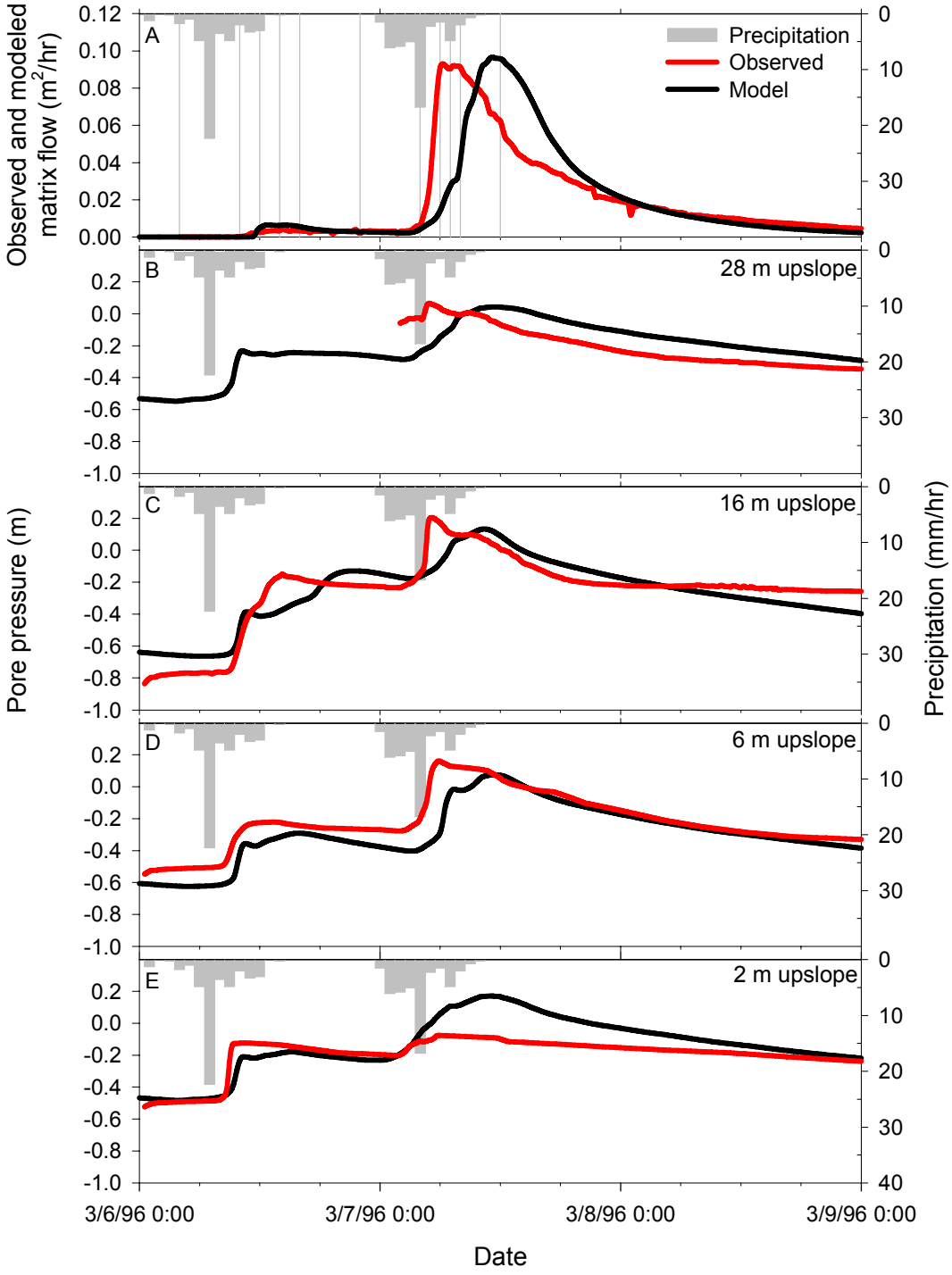

Figure A1.3 Modeled flow vectors during the March 6-7 1996 storm for the transect with mapped bedrock topography. The times are in hours after the start of precipitation and are represented as grey lines in Figure A1.2a. The vertical exaggeration is 1.5.

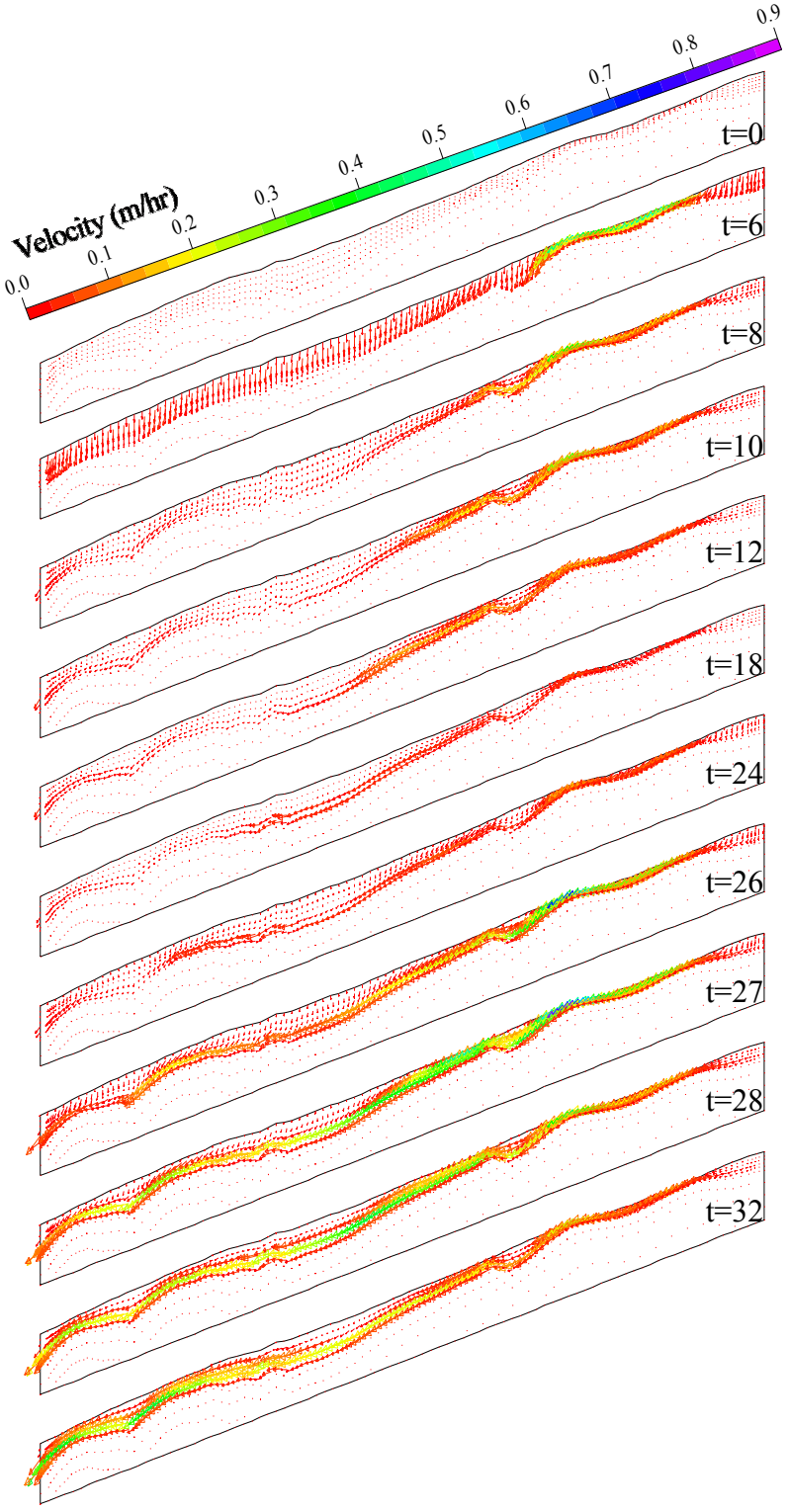

Figure A1.4 The distribution of modeled volumetric soil moisture content on 3/10/1996 18:00, 110 hours after the start of the storm.

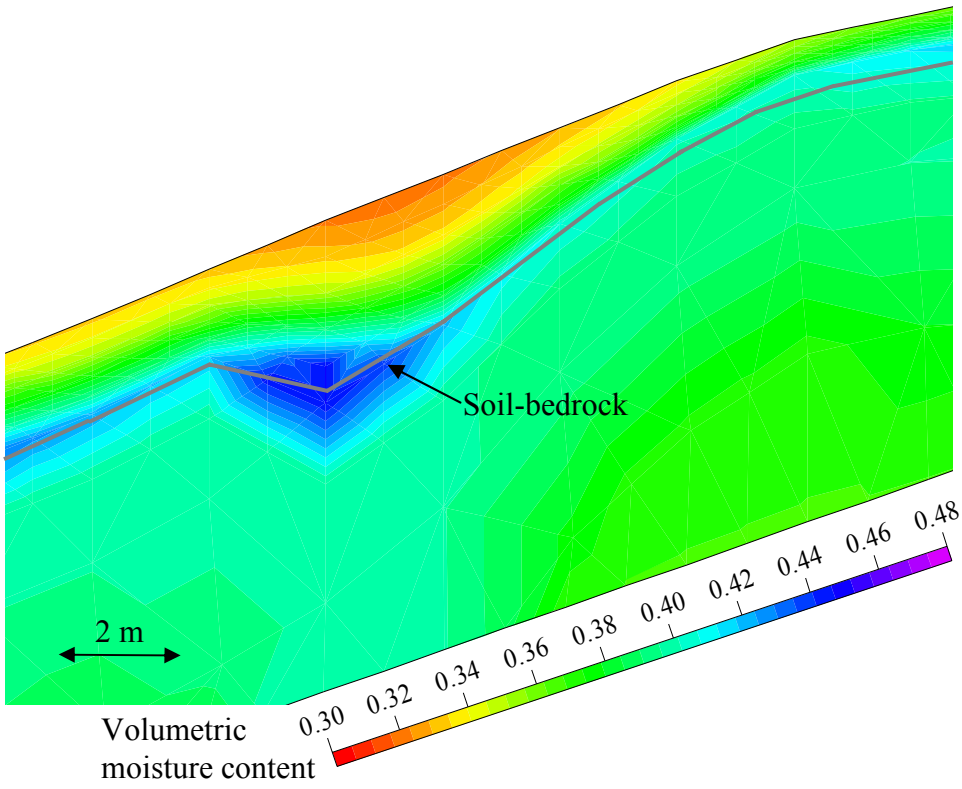

Figure A1.5 Comparison of modeled subsurface flow (a), pore pressure at 8 and 24 m upslope from the trench face (b-c) and virtual tracer concentrations in subsurface flow during the 96 mm March 6-7 1996 storm for transects with the mapped bedrock topography (black), smooth bedrock topography and uniform soil depth (blue), and smooth bedrock topography but decreasing soil depth in the upslope direction where soil depth at the downslope end of the hillslope is 1.5 times the average soil depth (pink) and where soil depth at the downslope end of the hillslope is 1.25 times the average soil depth on the hillslope (yellow) (d). The light grey lines in Figure A1.5a represent the times shown in Figures A1.3 and A1.7.

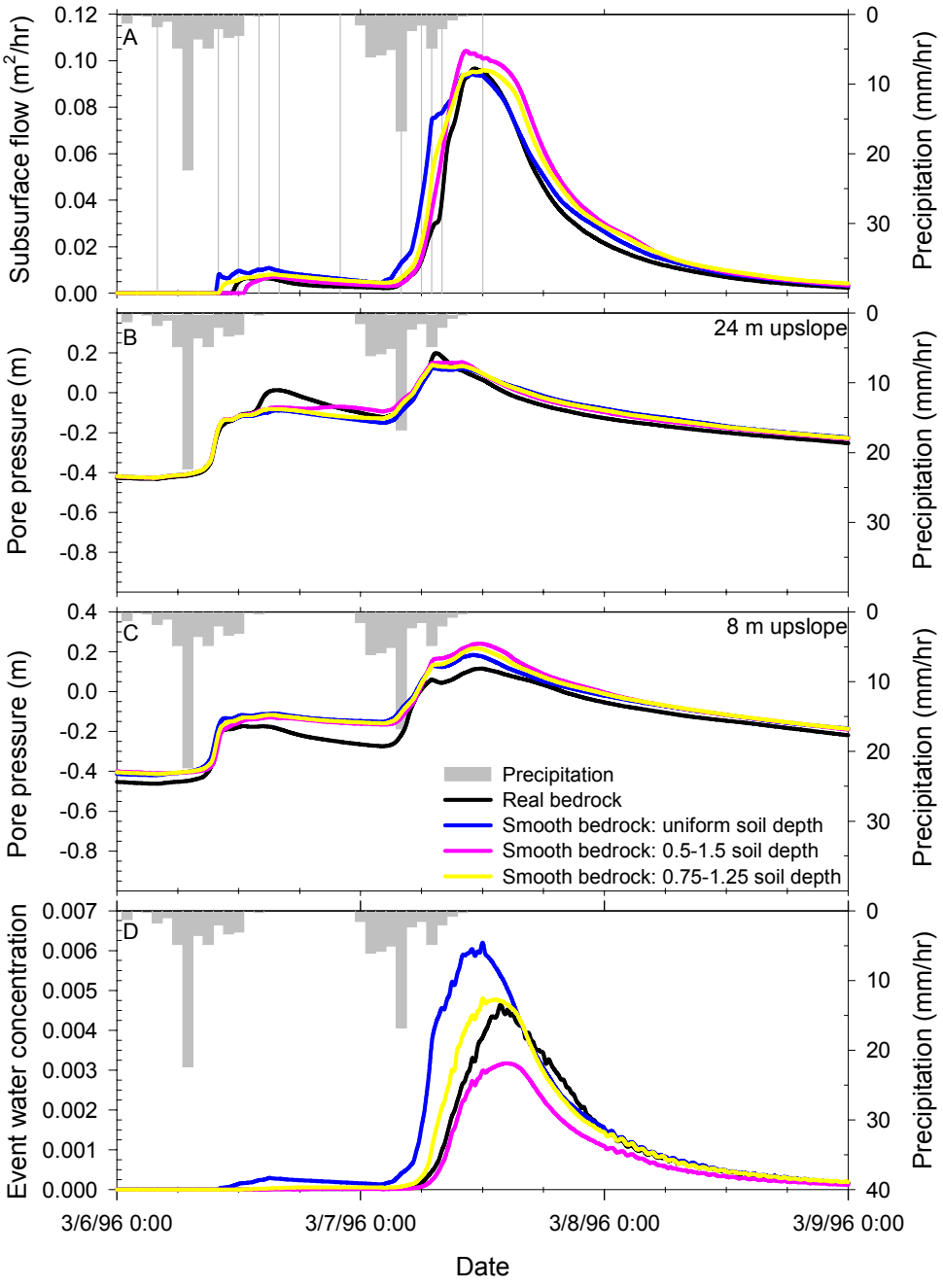

Figure A1.6 Comparison of modeled subsurface flow (a), pore pressure at 8 and 24 m upslope from the trench face (b-c) and virtual tracer concentrations in subsurface flow during the 49 mm January 6 1998 storm for transects with the mapped bedrock topography (black), smooth bedrock topography and uniform soil depth (blue), and smooth bedrock topography with decreasing soil depth in the upslope direction where soil depth at the downslope end of the hillslope is 1.5 times the average soil depth (pink) and where soil depth at the downslope end of the hillslope is 1.25 times the average soil depth on the hillslope (yellow) (d).

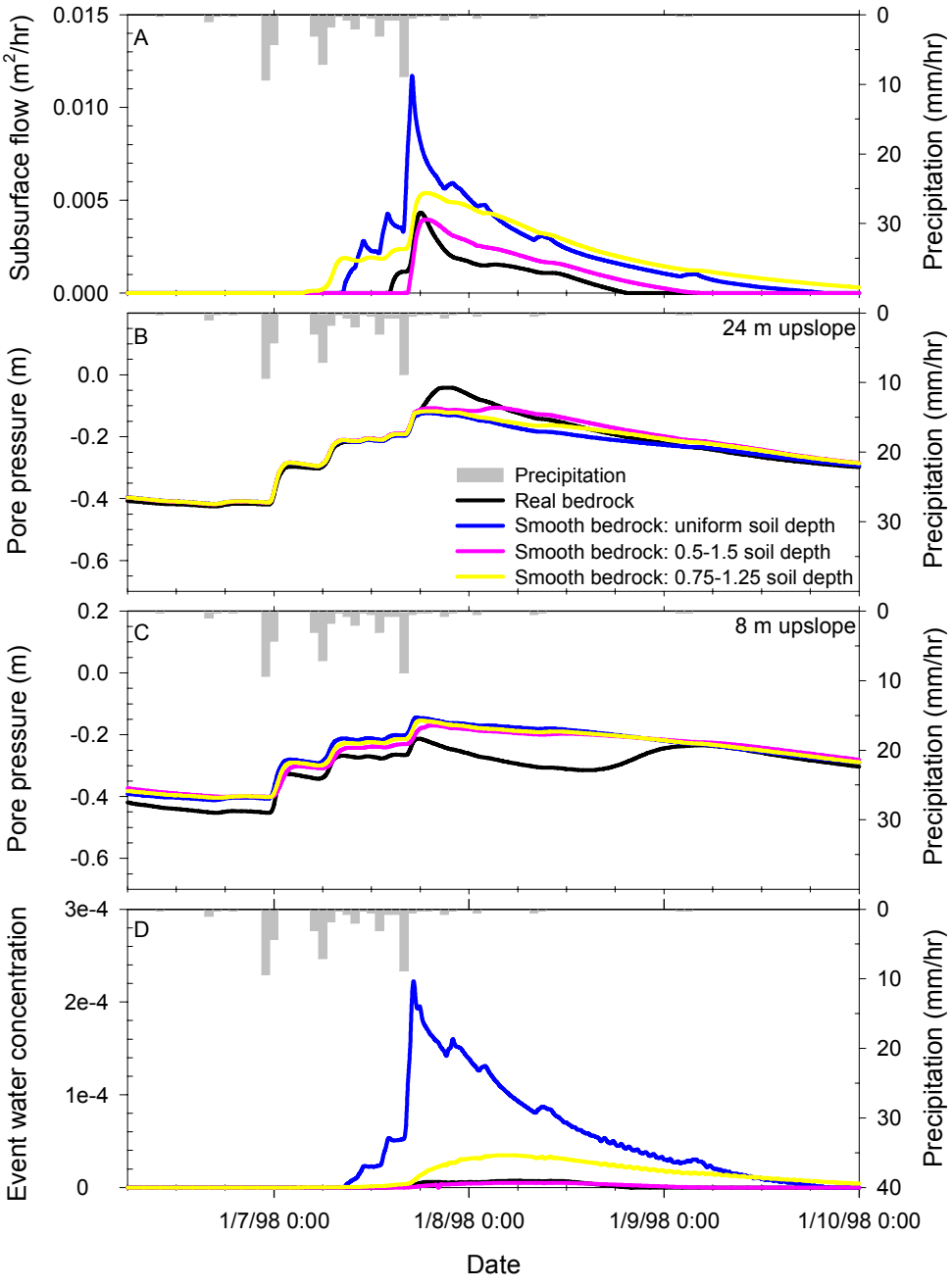

Figure A1.7 Modeled flow vectors during the March 6-7 1996 storm on a hillslope with uniform soil depth and smooth bedrock topography. The times are in hours after the start of precipitation and are represented as grey lines in Figure A1.5a. For the development of lateral flow on the transect with mapped bedrock topography and the same transect average soil depth see Figure A1.3. Note the different scale compared to Figure A1.3. The vertical exaggeration is 1.5.

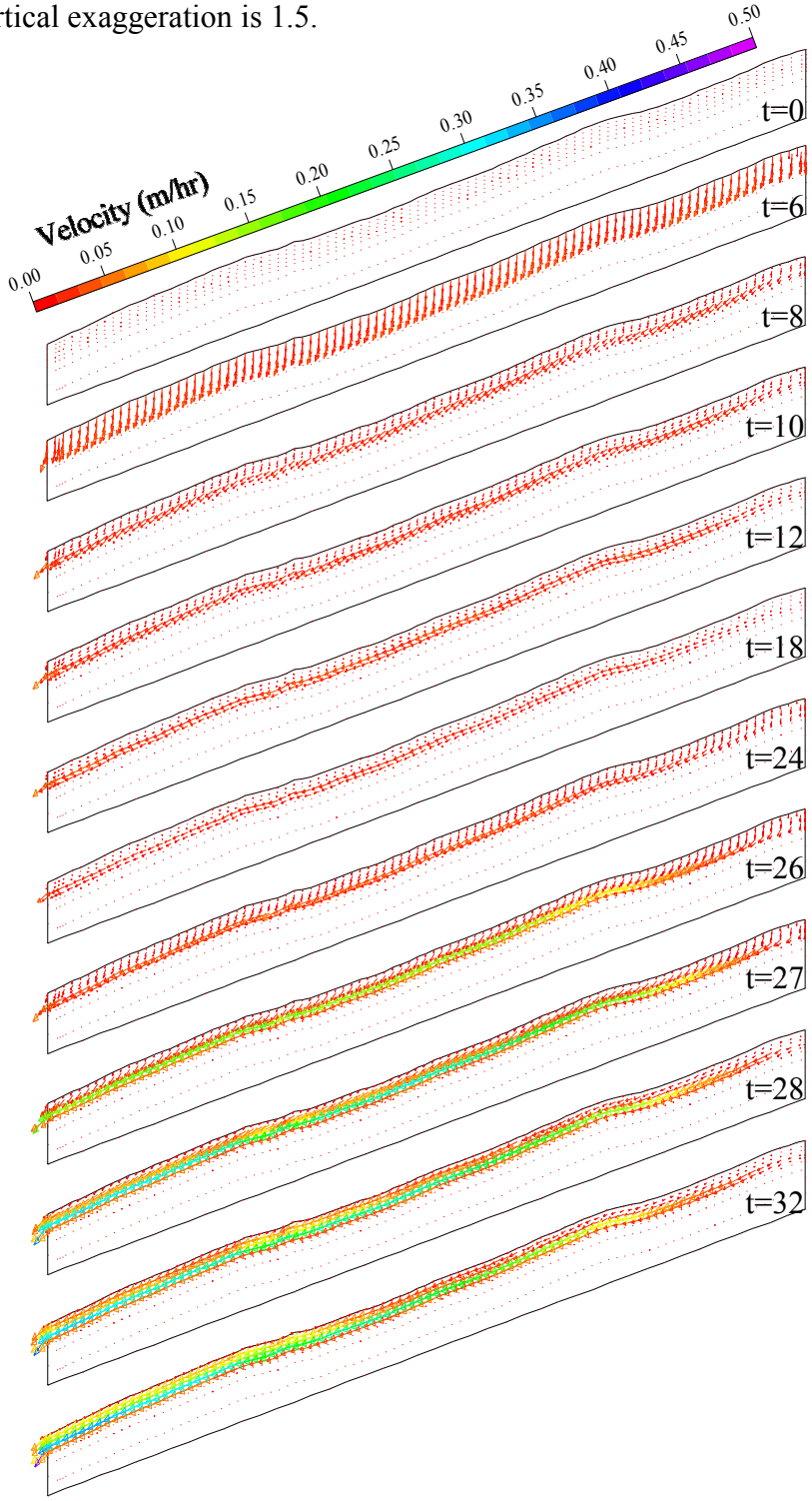

Figure A1.8 Comparison of modeled subsurface flow (a), pore pressure at 8 and 24 m upslope from the trench face (b-c) and virtual tracer concentrations subsurface flow during the 96 mm March 6-7 1996 storm for transects with the mapped bedrock topography (black), 2 times the observed bedrock roughness (yellow), 1.5 times the bedrock roughness (pink), and 0.5 times the bedrock roughness (blue) (d). The virtual tensiometers were located at the soil-bedrock interface at a location of average soil depth.

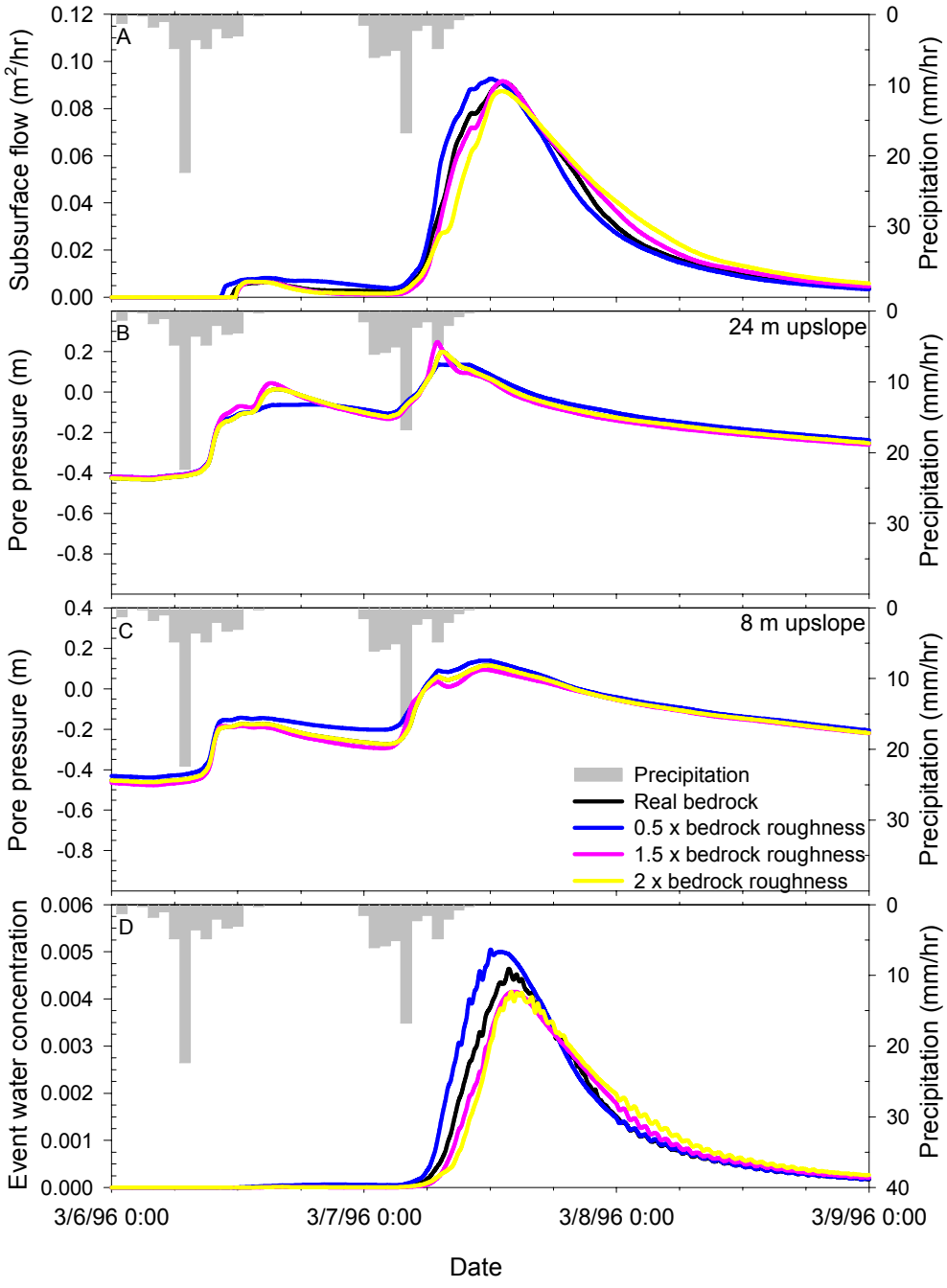

Figure A1.9 Comparison of modeled subsurface flow (a), pore pressure at 8 and 24 m upslope from the trench face (b-c) and virtual tracer concentrations subsurface flow during the 49 mm January 6 1998 storm for transects with the mapped bedrock topography (black), 2 times the observed bedrock roughness (yellow), 1.5 times the bedrock roughness (pink), and 0.5 times the bedrock roughness (blue) (d). The virtual tensiometers were located at the soil-bedrock interface at a location of average soil depth.

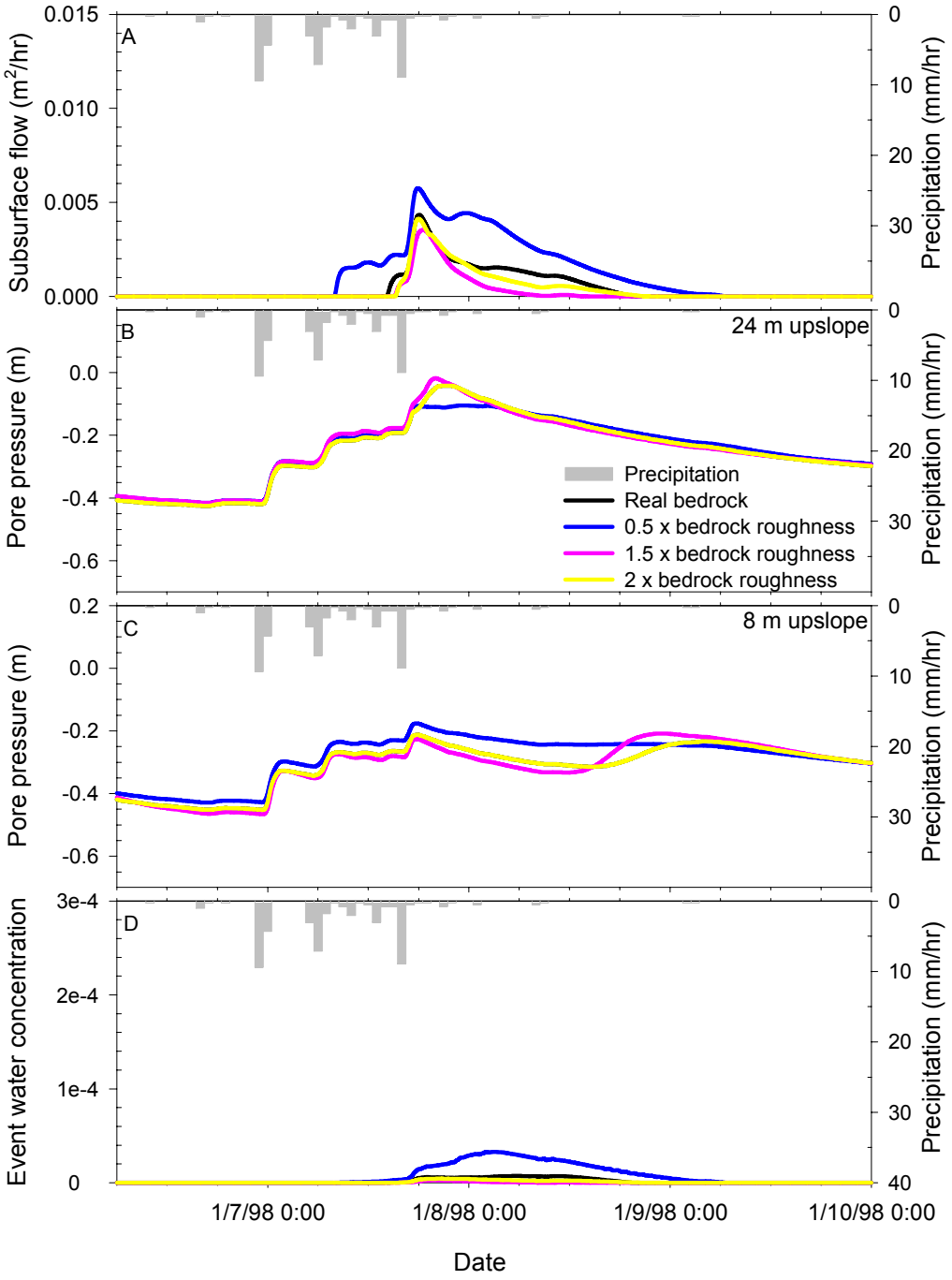

Figure A1.10 The relation between modeled total subsurface flow and total precipitation for the transects with the mapped bedrock topography (closed circles), smooth bedrock topography and uniform soil depth (open squares), smooth bedrock topography with decreasing soil depth in the upslope direction where soil depth on the upslope end of the hillslope transect is 0.5 times the hillslope average soil depth (closed triangles), and the transect with doubled bedrock roughness (open diamonds). All transects had the same hillslope average soil depth. The lines represent the three subsurface flow responses for the transect with mapped bedrock topography. Precipitation was applied at 5 mm/hr.

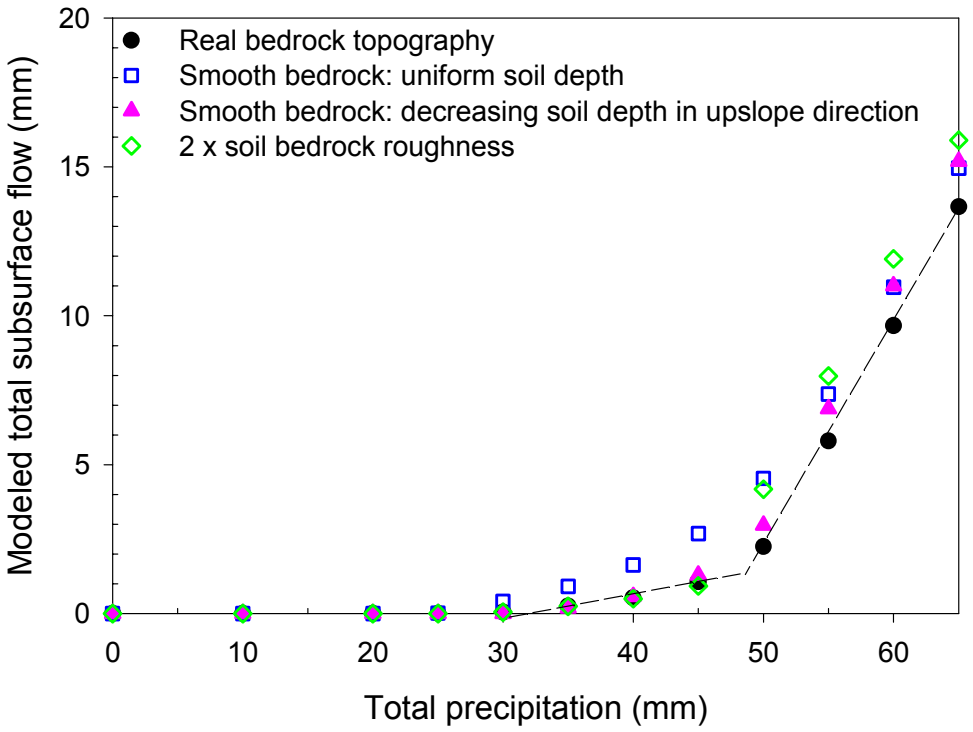

Figure A1.11 Observed matrix flow and macropore flow for a 2-m trench section and calculated subsurface flow from observed pore pressure gradients (tensiometers data).

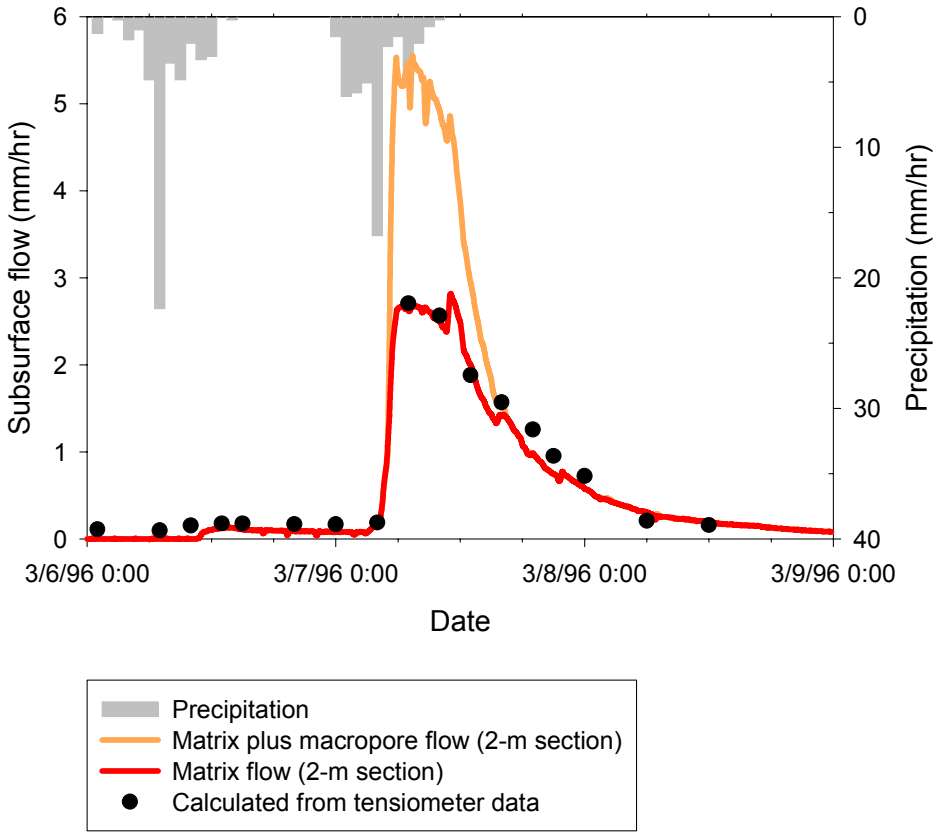

Appendix 2: Comment on: Spatial correlation of soil moisture in small catchments and its relationship to dominant spatial hydrological processes, Journal of Hydrology 286: 113-134

H.J. Tromp-van Meerveld
J.J. McDonnell

The recent paper by Western et al. (2004, Journal of Hydrology volume 286, pages 113-134) is another in a series of papers that explore the spatial patterns of soil moisture in small catchments and its relationship to their defined dominant spatial hydrological processes. These papers have influenced the field greatly and forced new examination of spatial patterns in catchment hydrology and how they can be used to better define process understanding. While we appreciate these works, and this latest paper in particular that presents results from a number of catchments in Australia and New Zealand, we worry about the implicit message in this and their other works: that indices of mapped soil moisture in the upper decimeters of the soil profile represent causally, topographically driven lateral subsurface flow. We argue that the finding that discharge varies in a strongly nonlinear way with soil moisture is a non-sequitur. In this comment we argue that soil moisture can be a passive signal between that of rainfall input and streamflow or subsurface flow output. In other words, while soil moisture may co-vary with streamflow, it is often transient saturation in the profile, at the soil-bedrock interface, or at a zone of reduced permeability in a duplex or layered soil environment that is usually the causal mechanism for lateral discharge of mobile water to the riparian zone and/or directly to the channel. This is counter to the Western et al. 2004 (page 115) main assertion that "indices of soil moisture represent topographically driven subsurface stormflow". Our motivation for writing this comment is that several recent studies have taken up the Western et al., results and begun using the soil moisture – flow path linkage as axiomatic of how hillslopes work (e.g. Meyles et al., 2003). Even more worrying is that these concepts are becoming codified into our watershed models without a level of critical assessment of whether or not these spatial patterns make functional sense.

In this comment we offer a counter argument aided with data from one of our study sites that shows how soil moisture, despite it strong correlation to flow in the stream, is of secondary importance in the generation of lateral subsurface flow. The main tenant of our argument comes from three main points that we make below: *(1) that the relation between hillslope average soil moisture and subsurface flow or stream discharge is often strong and highly nonlinear, but that (2) the relation between soil moisture*

development in time and space is not related to the development of transient saturation on the hillslope, and that (3) this transient saturation is often the causal mechanism for subsurface lateral flow to the channel.

(1) The relation between hillslope average soil moisture and subsurface flow or stream discharge is often strong and highly nonlinear

We find that flow in the stream, or in our case, flow from a hillslope is a non-linear function of hillslope average soil moisture (see Figure A2.1 for our observations during the winter and early spring period at the Panola Mountain Research Watershed (PMRW)). Subsurface flow occurs only when hillslope average soil moisture is greater than ~ 72 $\%_{Aqua\text{-}pro}$. The relation between soil moisture and subsurface flow at Panola is strikingly similar to the relation between soil moisture and streamflow at Tarrawara (Figure 3, p.2767 in Western and Grayson, 1998). Where Tarawarra is influenced by duplex soils, Panola has a saprolitic impeding layer at <1 m depth. Figure A2.1 shows how the hillslope remains relatively wet throughout the winter and spring period (until mid April) and drains quickly thereafter, similar to the two states described by Grayson et al. (1997). Soil moisture responses to precipitation are clear. During the February to early April period the hillslope drained to the same moisture level (70 $\%_{Aqua\text{-}pro}$, ~ field capacity) while it dried to lower soil moisture levels after mid April. This change corresponds at our forested site to the beginning of leaf out. While we acknowledge that the relation between hillslope average soil moisture and subsurface flow or stream discharge is often strong and highly nonlinear, we take exception to the assumption that the relation between soil moisture development in time and space is representative of mobile water movement during an event.

(2) The relation between soil moisture development in time and space is often not related to the development of transient saturation on the hillslope,

At Panola, the correlation lengths for both subsurface saturation and soil moisture appear to be very short (Figure A2.2). We admit that our grid setup at Panola for the soil moisture and subsurface saturation measurements and the small absolute number of soil moisture measurements (compared to Western et al. (1998) and Western et al. (2004)) does not allow a very precise determination of the correlation length. These comments notwithstanding, during the wet period, the locations with higher than median profile average pre-event soil moisture were relatively stable (Figure A2.3a). Pre-event soil moisture for these events was relatively similar (varying between 68-72 $\%_{Aqua\text{-}pro}$, see Figure A2.1). The spatial extent of subsurface saturation however changed with increasing storm size (Figure A2.3b). Only during the largest storms was the subsurface saturated area connected to the trench face. Clearly the locations of higher than median soil moisture and subsurface saturation did not correspond very well to each other. Subsurface saturation occurred mainly at locations with shallow soils (on the upslope) and in areas with both high bedrock contributing area and high impedance to downslope drainage near the midslope (i.e. high downslope index values) (Chapter 3), not in areas with larger than average pre-event soil moisture.

To quantify the (lack of) correlation between pre-storm soil moisture and subsurface saturation, the soil moisture measurements were re-interpolated to a new 2 by 2 m grid using linear triangulation. The logistic correlation coefficients between pre-storm soil moisture at different depths and the occurrence of subsurface saturation were very low (Table A2.1). This means that despite the strong, nonlinear relation between hillslope average soil moisture and subsurface flow, the relation between soil moisture development in time and space is often not related to the development of transient saturation on the hillslope. This is significant because this transient saturation is the causal mechanism for hillslope and stream response. Panola is not unique in this sense, numerous studies in many different hydrogeologic and climate environments have shown that transient saturation is the causal mechanism for lateral flow of mobile water on the time scale of an event (Peters et al. 1995 at Plastic Lake in Canada; Tani 1997 at the

Minamitani hillslope in Japan; McGlynn et al. 2002 for the Maimai catchment in New Zealand to name a few).

(3) Transient saturation is often the causal mechanism for subsurface lateral flow to the channel.

The storms during the winter period (wet state) all had similar pre-event soil moisture conditions (~field capacity). The measured maximum hillslope average soil moisture during the storm period was a linear function of total storm precipitation (Figure A2.4a). The area of transient saturation also increased linearly with increasing precipitation (Figure A2.4b and Chapter 3). The relation between storm total precipitation and storm total subsurface flow however was highly non-linear (Chapter 2 and Figure A2.4c) because connectivity between the subsurface saturated area to the trench occurred only during the largest storms (Figure A2.3 and Chapter 3).

Summary

While hillslope average soil moisture is strongly correlated to subsurface flow and the correlation length of both subsurface saturation and pre-event soil moisture is very short, there is a lack of correlation between the soil moisture pattern and the pattern of subsurface saturation. We show that subsurface saturation is the causal mechanism for production of lateral subsurface flow. Subsurface saturation is related to soil depth and bedrock micro-topography, not to soil moisture patterns. Thus at this planar hillslope where lateral subsurface flow is the dominant runoff mechanism and the occurrence of subsurface saturation at an impeding layer is most important for the subsurface flow generation process, the soil moisture pattern is a passive pattern, not one that actively controls flow. Subsurface flow is a due to the connection of subsurface saturated areas, which is influenced by the bedrock micro topography not pre-event soil moisture. Thus it is not the spatial soil moisture pattern or the connection of areas with high soil moisture but the connection of areas of transient saturation, which is controlled by the bedrock topography that is responsible for the occurrence of significant subsurface flow. While

soil moisture is important in that the soil on the hillslope needs to be wet enough for subsurface saturation at the soil-bedrock interface to occur, its pattern is not a first order control on the generation of lateral subsurface flow.

References

Burns, D. A., R.P. Hooper, J.J. McDonnell, J.E. Freer, C. Kendall, and K. Beven, Base cation concentrations in subsurface flow from a forested hillslope: The role of flushing frequency, Water Resources Research 34(12): 3535-3544, 1998.

Freer, J., J. McDonnell, K.J. Beven, D. Brammer, D. Burns, R.P. Hooper, and C. Kendal, Topographic controls on subsurface stormflow at the hillslope scale for two hydrologically distinct small catchments, Hydrological Processes 11: 1347-1352, 1997.

Freer, J.E., J.J. McDonnell, K.J. Beven, N.E. Peters, D.A. Burns, R.P. Hooper, B.T. Aulenbach, and C. Kendall, The role of bedrock topography on subsurface stormflow, 10.1029/2001WR000872, 2002.

Grayson, R., A.W. Western, and F.H.S. Chiew, Preferred states in spatial soil moisture patterns: Local and non-local controls, Water Resources Research 33(12): 2897-2908, 1997.

Meyles, E., A. Williams, L. Ternan, and J. Dowd (2003) Runoff generation in relation to soil moisture patterns in a small Dartmoor catchment, Southwest England, Hydrological Processes 17: 251-264.

McGlynn, B., J.J. McDonnell, and D. Brammer, A review of the evolving perceptual model of hillslope flowpathsat the Maimai catchment, New Zealand. Journal of Hydrology 257: 1-26, 2002.

Peters, D.L., J.M. Buttle, C.H. Taylor, and B.D. LaZerte, Runoff production in a forested, shallow soil, Canadian Shield basin, Water Resources Research 31(5): 1291-1304, 1995.

Tani, M., Runoff generation processes estimated from hydrological observations on a steep forested hillslope with a thin soil layer, Journal of Hydrology 200: 84-109, 1997.

Western, A. W., and R.B. Grayson, The Tarrawarra data set: Soil moisture patterns, soil characteristics, and hydrological flux measurements, Water Resources Research 34(10): 2765-2768, 1998.

Western, A.W., G. Blöschl, and R.B. Grayson, How well do indicator variograms capture the spatial connectivity of soil moisture, Hydrological Processes 12: 1851-1868, 1998.

Western, A. W., R.B. Grayson, G. Blöschl, G.R. Willgoose, and T.A. McMahon, Observed spatial organization of soil moisture and its relation to terrain indices, Water Resources Research 35(3): 797-810, 1999.

Western, A.W., S. Zhou, R.B. Grayson, T.A. McMahon, G. Blöschl, and D.J. Wilson, Spatial correlation of soil moisture in small catchments and its relation to dominant spatial hydrological processes, Journal of Hydrology 286:113-134, 2004.

Figure A2.1 The relation between subsurface flow and hillslope average soil moisture. Soil moisture was measured at 64 locations on the hillslope using the Aqua-pro sensor (Aqua-pro Sensors, Reno NV) in polycarbonate access tubes that were installed to the soil-bedrock interface. The Aqua-pro sensor is a capacitance sensor (radio frequency) that measures soil moisture on a percent scale between 0 (in air or air dried soil) and 100 (in saturated soil or water). Soil moisture was measured at 0.05 m increments to 0.3 m below the soil surface and at 0.1 m increments between 0.3 m and the soil-bedrock interface. Profile average soil moisture at a measurement location was calculated by multiplying the Aqua-pro soil moisture measurements at specific depths by the distance between the soil moisture measurements and dividing by the total soil depth at that measurement location. Hillslope average soil moisture was calculated by averaging the profile average soil moisture values from all measurement locations. Flow from the base of the hillslope was measured via a 20-m long trench excavated normal to the fall line of the slope down to bedrock at a midslope position approximately 30 m upslope from an ephemeral stream. Discharge was measured by routing flow through tipping-bucket gages. The number of tips was recorded every minute. When no subsurface flow is shown on the graph, there was no measurable subsurface flow (<0.0001 mm/day).

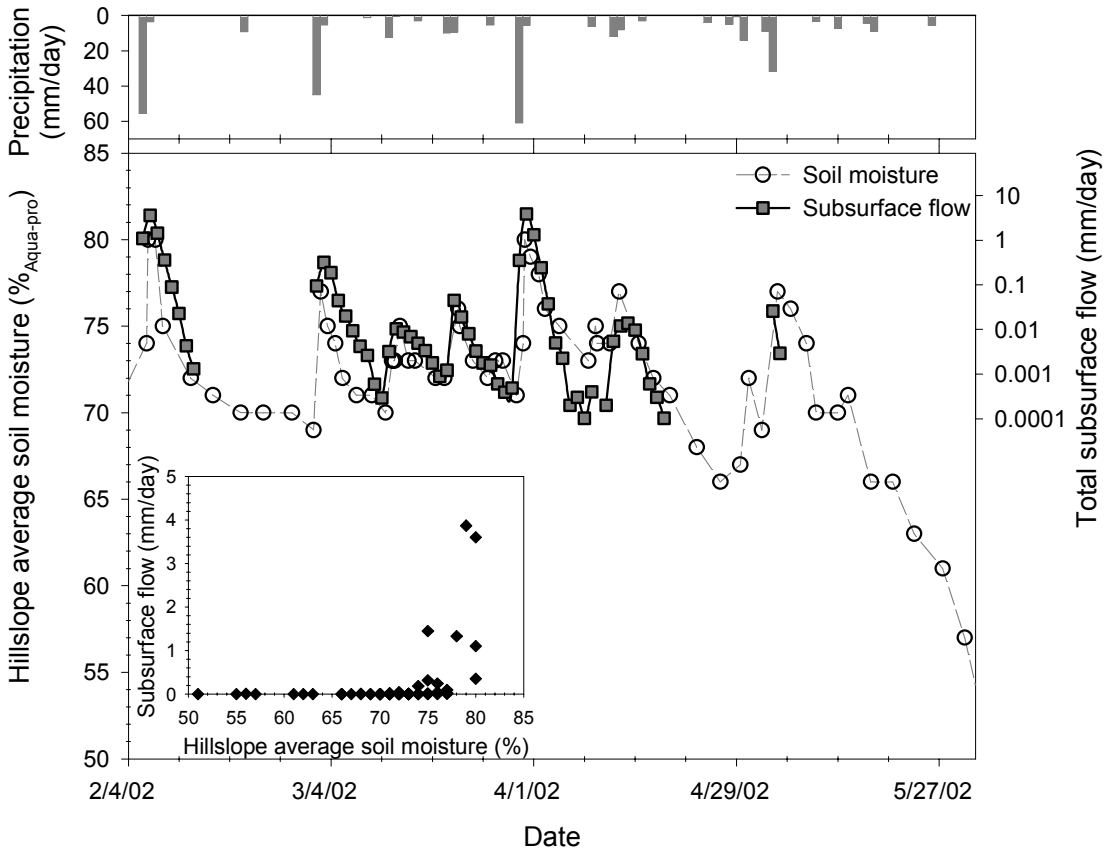

Figure A2.2 Standardized omni-directional semi-variograms of pre-event soil moisture (triangles), event soil moisture (open circles) and subsurface saturation (closed squares) for 5 storms during the 2002 study period. The delineation of the subsurface saturated areas was made via 135 crest stage gauges filled with cork dust spatially distributed across the hillslope. These 19 mm diameter PVC wells were screened over the lower 0.2 m and installed on the soil-bedrock contact. The maximum water level rise was measured after each storm during the January to August 2002 period.

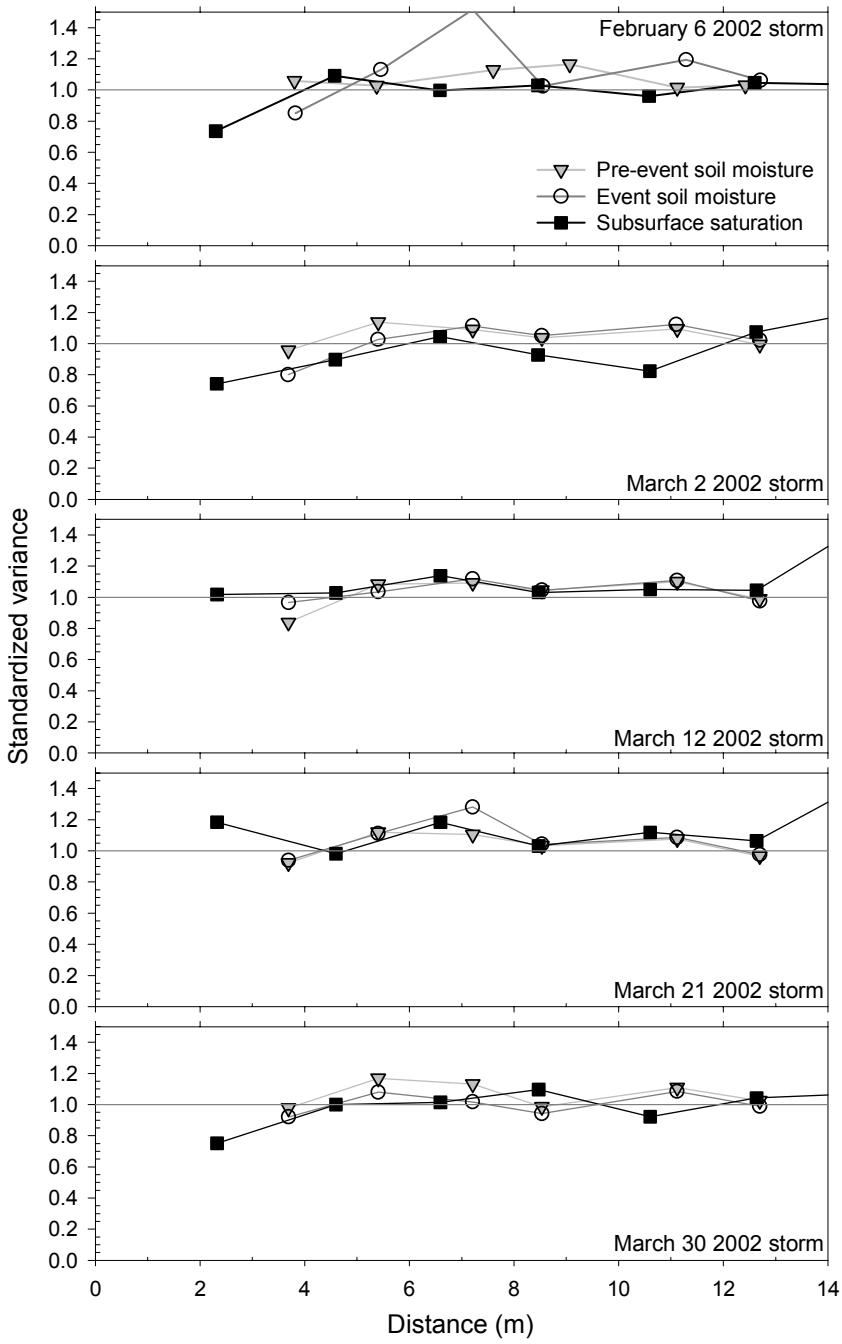

Figure A2.3 Locations of above median soil moisture (shaded area) (a) and the locations of subsurface saturation (shaded area) for five storms during the wet state during the 2002 study period (b). The standardized semi-variograms of soil moisture and subsurface saturation for these storms are shown in Figure A2.2.

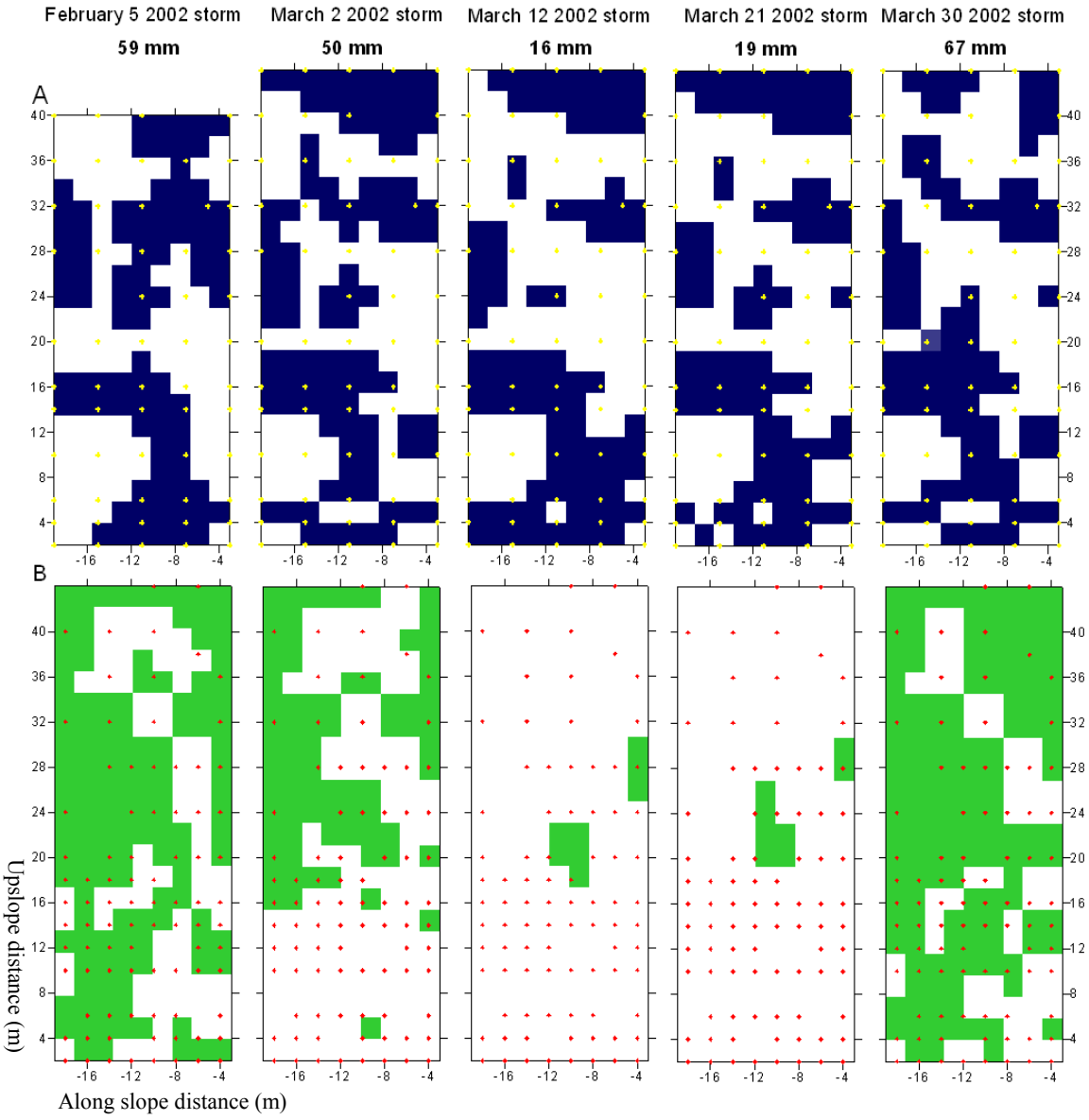

Figure A2.4 Hillslope average pre-event (triangles) and event soil moisture (circles) (a), the maximum area of transient saturation (b) and storm total subsurface flow as a function of storm total precipitation for the five storms shown in Figure A2.3 (c). The dark closed symbols in Figures A2.4b and A2.4c represent the storms shown in Figure A2.3. The light colored open symbols in Figure A2.4b and A2.4c represent other storms between January and March 2002.The 55 mm precipitation threshold shown in Figure A2.4c is from Chapter 2.

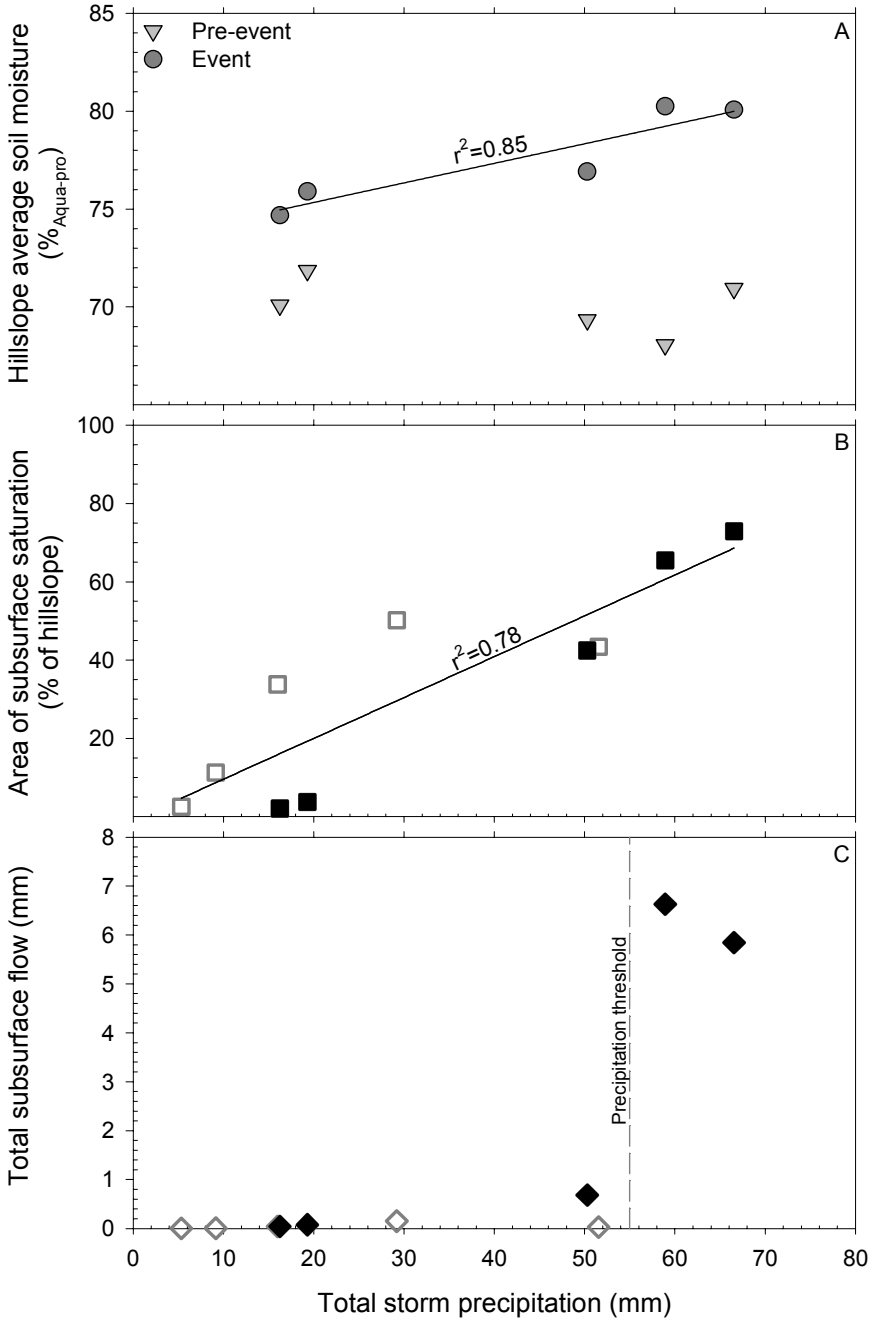

Table A2.1 The logistic R^2 between pre-event soil moisture at different depths below the surface and the occurrence of subsurface saturation for the February 6, March 2 and March 2002 storms. The small spatial extent of subsurface saturated area during the March 12 and 21 2002 storms (Figure A2.3) did not allow for an accurate determination of the logistic R^2 between soil moisture and the occurrence of subsurface saturation.

Logistic R^2	February 6 2002	March 2 2002	March 30 2002
0.05 m	0.01	0.05	0.01
0.15 m	0.00	0.00	0.00
0.30 m	0.03	0.00	0.02
0.50 m	0.02	0.06	0.03
0.70 m	0.01	0.03	0.01
At soil-bedrock contact	0.06	0.00	0.02
Profile average	0.00	0.03	0.00